Extended Born-Oppenheimer equation and the effect of external field on the nonadiabatic coupling elements

Thesis by

Biplab Sarkar

In partial fulfillment of the requirements

for the degree of

Doctor of Philosophy

Department of Chemistry

Indian Institute of Technology Guwahati

Guwahati - 781039, Assam, India

Dedicated to my Parents.

Statement

The work contained in the thesis entitled "*Extended Born-Oppenheimer equation and the effect of external field on the nonadiabatic coupling elements*" has been carried out by me under the supervision of Dr. Satrajit Adhikari, Assistant Professor, Department of Chemistry, Indian Institute of Technology Guwahati. This work has not been submitted elsewhere for the award of any degree.

(Biplab Sarkar) September 19, 2008

Department of Chemistry
Indian Institute of Technology Guwahati
Guwahati - 781039

Certificate

It is certified that the work contained in the thesis entitled "*Extended Born-Oppenheimer equation and the effect of external field on the nonadiabatic coupling elements*" by Mr. Biplab Sarkar, a Ph.D. student of the Department of Chemistry, Indian Institute of Technology Guwahati for the award of Doctor of Philosophy has been carried out under my supervision. This work has not been submitted elsewhere for the award of any degree.

(Dr. Satrajit Adhikari)
Department of Chemistry
Indian Institute of Technology Guwahati
Guwahati - 781039

Course Certificate

This is to certify that Mr. Biplab Sarkar has satisfactorily completed all the courses required for the Ph.D. degree program. These courses include :

CH 603	Supramolecular Chemistry
CH 630	A Molecular Approach to Physical Chemistry
CH 611	Bioinorganic Chemistry
CH 632	Group Theory

(Professor A. T. Khan)
Head
Department of Chemistry
Indian Institute of Technology Guwahati
Guwahati - 781039

(Dr. Anil K. Saikia)
Secretary, DPGC
Department of Chemistry
Indian Institute of Technology Guwahati
Guwahati - 781039

Acknowledgements

First and foremost I express my deep sense of gratitude to my supervisor Dr. Satrajit Adhikari for his inspiring guidance. It has been an honor and a privilege to work under his kind and invaluable supervision. His constant encouragement not only build confidence in me in pursuing the research work, but also helped me in my professional development. I shall remain indebted to him in all my future endeavor in the field of research. I also express my indebtedness to Professor Michael Baer for his collaboration with us and for his visit to IIT Guwahati. His inspiring and valuable discussions are extremely helpful for me to go into the depth of the subject. My Doctoral committee members Dr. Manabendra Ray, Professor Arun Chattopadhyay and Dr. S. B. Santra have been excellent mentors and provided a lot of encouragement over the years.

I am extremely grateful to my lab mate Dr. Panchanan Puzari, for not only his help during the entire period of my Ph.D program but also for his presence as like elder brother. It has been a great pleasure to work with him.

In the campus, my experience has been made truly memorable by Dr. Santanu Sinha, Subhabrata Das, Rupesh K. Chaubey, Dr. Sahid Hussain, Dr. Lokman H. Choudhuri, Biswa Ranjan Panda, Bachhu Rama Raju, Anirban Karmakar, Avijit Pramanik, Soumya Chatterjee, Dr. Veera Babu Rao, Ballav Moni Borah, Sonit Gogoi, Krishna Kanti Dey, Dr. Ardhendu Shekhar Patra, R. S. Swathi, Dr. S. Veluswami, Dr. Swapan K. Pandit and other students of the department. I am also grateful to Mr. Manabendra Sharma of IIT Bombay, who has helped me through his valuable suggestions time to time and also by providing necessary information in the field as and when I was in need of it. I also thank my junior lab mates Amit Kumar Paul and Subhankar Sardar for a great time at IACS, Kolkata.

My sincere gratitude is due for the Department of Chemistry, Indian Institute of Tech-

nology Guwahati, for providing me the requisite facilities and also the opportunity to work in such a wonderful place. I am also indebted to Prof. Abu Taleb Khan for his generous support and encouragement towards my research work. I express my thanks and gratitude to the staff members, Department of Chemistry, IIT Guwahati, for their support and cooperation throughout the period of my research work. I also grateful to Department of Chemistry, North-Eastern Hill University to provide me the facility to continue my research after joining the department as a lecturer.

Finally, No word can express my indebtedness to my parents; it is their blessings and support that has made me what I am today. Their love and support has made me believe in myself and I dedicate this thesis to them. I am also indebted to my brother Kaushik with whom I always share my problems and he has provided a lot of encouragement in every steps of the way. Last but not the least, I express my profound gratitude to my wife Banasri, for her endless patience to listen my complaints and frustrations. Her constant support and tremendous encouragement that had helped me a lot to make this project a success. The journey to the completion of this thesis would have been much harder without her.

Contents

Chapter 1

Introduction

The treatment of electronic transitions during a chemical reaction is one of the most important issue in the study of molecular systems. Since the molecular processes are governed by Coulombic interactions, it is well established fact that the relevant Schroedinger equation (SE), in principle, can treat those processes accurately and provide the solutions as the observable such as reactive/non-reactive cross sections or spectroscopic quantities leading to the main theoretical interest in developing numerical algorithm to solve the SE. The fundamental theoretical development by Born - Oppenheimer[1] (BO) and thereafter, Born - Huang[2] help us to pursue the quantum mechanical treatment of realistic molecular system as long as the process takes place exclusively on the ground electronic state. Indeed, the situation becomes complicated almost immediately when the excited electronic states affect the ground due the presence of so called "*nonadiabatic coupling*" (NAC),[3] i.e., the coupling among the adiabatic electronic states and thereby, further rigorous theoretical treatment is required. This adiabatic framework is formed as a result of a straightforward application of the BO treatment (not approximation) with regard to an aggregate of particles made up of fast electrons and slow nuclei.[2,4] When the electronic excitations are included in the molecular processes, the Hellmann - Feynman theorem[5,6] points out the existence of singularity in the NAC terms any where in the configuration space. These singularities arise due to the fact that electronic states become degenerate at certain points or along a line (seam) in the configuration space.[7] At this junction, we may mention that singularities dictate a crucial role in the theory of elementary particles[8] leading to vector potentials connected with the creation and annihilation of elementary particles. It may be interesting to note that the required theoretical approach to handle the singularities of NAC terms in molecular physics[9] is similar to that of used in field theory and elementary particles.

For a quite longer period, the presence of singularity in nonadiabatic coupling terms had been overlooked until Longuet-Higgins[10] and others demonstrated that such singularity destroy the single − valuedness of electronic wavefunction in many molecular systems and therefore, it is not worth to pursue dynamical calculations for the nuclei on the multi-valued diabatic potential energy surfaces (PES). Herzberg and Longuet-Higgins' (HLH)[11] corrected this deficiency by multiplying a complex phase factor,[12] known as Longuet-Higgins' phase, leading to a single valued wavefunction. This 'modification' of the electronic eigenfunctions is not an outcome of any first principle based theory but imposed in an *ad hoc* manner. In an alternative approach, Mead and Truhlar[13] introduced a vector potential in the nuclear Hamiltonian to generalize the Born-Oppenheimer equation, which is a reminiscent of the complex phase factor treatment of Herzberg and Longuet-Higgins. With these theoretical predictions, Kuppermann *et al.*[14–16] and many others[17–19] calculated integral and differential scattering cross sections of H_3 isotopic system, Adhikari *et al.*[20] evaluated the transition probabilities of a two arrangement channel pseudo Jahn-Teller model and clearly demonstrate the effect of Longuet-Higgins' phase, also known as geometric phase (GP),[13,21–23] on reactive/non-reactive transition probabilities with a demand to explore the origin of GP from first principle.

The development of any first principle based theory by including BO treatment considers the fact that slow-moving nuclei is distinguishable from fast-moving electrons in molecular systems and intends to impose the BO approximation by neglecting the effect of upper electronic state(s) on the lower with the implication − the nonadiabatic coupling elements are negligibly small. Such approximation has been assumed to be independent of the eigenspectrum of the system and thereby, the ordinary BO equations are being frequently used for calculations even for systems with large NAC terms. Even if the component of the total wavefunction on the upper electronic state(s) are negligibly small at enough low energies, the products between the singularly large NAC terms and the amplitudes of the excited state(s) wavefunctions could be finite in magnitude leading to the breakdown of BO approximation. Thus, it is a matter of contemporary research how elegantly one can handle the NAC terms instead of neglecting them forcibly. Since the definition of NAC terms appear in the adiabatic representation of SE and those terms are usually very sharp functions of nuclear coordinates with singularity in the configuration space, one may wish to perform an unitary transformation to obtain the diabatic representation of those SEs, where couplings among the electronic states are slowly varying functions of nuclear coordinates and therefore, the dynamical calculations on the diabatic PESs are numerically accurate and stable. Each of these two frameworks has its own advantages and disadvantages: The diabatic framework[24] is characterized by smooth potentials and therefore is friendly with respect to treating the nuclear Schroedinger equation, whereas the adiabatic framework, characterized by numerically rough magnitudes and becomes unfriendly. However, the adiabatic framework is well defined mathematically and robust from the physical point of view, but the diabatic framework is neither unique nor robust (because it is based on arbitrary fixed points in the configuration space).[25,26]

While developing such theories, Mead and Truhlar (MT)[27] mentioned that the consideration of the entire Hilbert space ($n = N$) to incorporate the couplings among the electronic states is indeed a trivial approach to demonstrate. In the same article,[27] they explore the Curl of the non - adiabatic coupling for any realistic description of the electronic wavefunction. A general vector field can be decomposed into longitudinal and transverse components, where the longitudinal component can be expressed as a derivative of a scalar and the transverse component by the curl of a vector. The ADT can at best remove the longitudinal component of the derivative coupling. The longitudinal and transverse components are referred to as the removable and non removable couplings.

The general characteristics of the removable and non removable components have been discussed by Kendrick, Mead and Truhlar.[28] When the energy eigenvalues are well separated, the removable and non removable couplings will be of the same order. At sufficiently low energies (well below the energy of the upper state), these coupling can be ignored in dynamics calculations due to the $1/M$ prefactor. At the close proximity of a degeneracy, only the removable coupling is singular and according to the degenerate perturbation theory, the non removable couplings are insignificant.[29] It means that the ADT angle can be obtained by integrating the derivative coupling at and around the same region. On the contrary, away from the conical intersection, the contribution from the non removable coupling appears in path dependent integrals for the ADT angles and therefore, closed line integrals of the derivative coupling[30] will not be multiples of π. The inclusion of more electronic states can reduce this problem,[31] however, greatly increases the computational cost of *ab initio* quantum chemistry and dynamical calculations.

One can separate the removable and non removable couplings by solving Poisson's equation for the ADT angle λ.[32] As there are many possible definitions for the boundary conditions on λ,[33] there is no unique solution. Moreover, the solution of Poisson's equation is computationally too expensive to be carried out for molecules of more than three atoms. Since the Born - Oppenheimer approximation implies that it is not necessary to find the best diabatic basis, one can find a diabatic basis for which the residual couplings can be neglected and such bases are referred to as quasidiabatic bases. The requirements for a quasidiabatic basis are easier to satisfy: (a) The singularity in the derivative coupling must be transformed away; (b) The residual couplings must be negligible. It is desirable for a diabatic basis to estimate the residual couplings to ensure that no spurious coupling have been incorporated. If it is necessary, the residual couplings could be perturbatively included in scattering calculations.

The question to be asked is if there exists a way to form a framework where the potentials are diabatic (and therefore smooth) and at the same time robust. The various aspects of this question were matter of discussions span over a period of more than 30 years.[7,18–20,26,33–55] The adiabatic-to-diabatic transformation (ADT) matrix, which transforms the adiabatic framework (namely, the corresponding adiabatic potentials) and yields the diabatic framework, thus forms the anticipated diabatic potentials.[35,36] This ADT matrix is calculated by solving first order differential equations along contours.[26,36] On the other hand, the transformation from adiabatic to diabatic representation of SEs for a given sub - Hilbert space is guaranteed only when the NAC terms being vector fields satisfy the so called Curl conditions. While carrying out this procedure (which satisfies the required mathematical conditions) an orthogonal ADT matrix not only replaces the adiabatic potentials but also eliminates the troublesome NAC terms and forms ordinary smooth potential-type coupling terms. Moreover, it has been shown analytically that the formulation of extended BO equations is possible only when there exists a coordinate independent ratio of the gradients for each pair of ADT/mixing angles implying zero Curls of the NAC terms. Therefore, the nature of the Curls of the NAC terms is an crucial aspect to explore in order to carry out the first principle based theoretical development on BO treatment.

Baer *et al.*[56–58] made the first attempt to pursue the first principle based BO treatment on two coupled electronic states as sub-Hilbert space, performed the adiabatic-diabatic transformation of SE and derived a new set of two coupled BO equations by grafting the effects of NAC terms into the diagonal to formulate the single surface Extended Born-Oppenheimer (EBO) equations. In an alternative approach, Varandas and Xu[54] reformulated the two state adiabatic nuclear SE by casting the NAC elements in terms of nuclear coordinate dependent electronic basis functions angle (mixing angle), found the one-to-one correspondence between mixing[54] and adiabatic-diabatic transformation (ADT)[36] angles and then, derive the single surface EBO equation in the vicinity of degeneracy. Both the formulations with two-dimensional sub-Hilbert space have the following inbuilt features: (a) The components of NAC term satisfy the Curl condition; (b) The Curl of the NAC term is zero. On the other hand, the BO treatment for any $N(\geq 3)$ state coupled BO system in the adiabatic representation of nuclear SE, the transformation from adiabatic to diabatic equations and the formulation of EBO equations has been carried out by Baer *et al.*[59] and Adhikari *et al.*[60] considering a model situation instead of including the general features of any BO system. Moreover, the formulation does not have the scope to demonstrate (a) how the Curl conditions are being satisfied $-$ a necessity to pursue adiabatic-diabatic transformation; (b) how the Curls are zeros around conical intersection(s) [CI(s)][61] $-$ a necessary condition to formulate approximate/rigorous EBO equation. In this thesis we[46,62–64] performed a generalized BO treatment of any $N \geq 3$ coupled electronic states with a detailed analysis of Curl conditions and thereby, carried out adiabatic - diabatic transformation of nuclear SE, and finally formulated an *approximate*[46,63] as well as *rigorous*[62–64] EBO equations in terms of electronic basis functions/ADT angles.

The second subject to be discussed is the interaction of an external field with a molecular system. Experimental studies related to such interactions, particularly the possibility of effecting chemical processes by laser fields, started already during the early 1980s.[65,66] At about the same time George[67,68] and co-workers were performing the first theoretical/numerical studies for atom-diatom (inelastic) collisions in relative strong laser fields. These were later extended to study the effect of laser fields on chemical exchange processes.[56,69–71] For instance, it was revealed, while considering the reaction $F+H_2 \rightarrow HF+HF$, that different photons affect in a significantly different manner the quantum yields of this reaction.[71] These somewhat sporadic studies were intensified a few years later owing to a new trend of studies aimed at revealing the relevant parameters (or conditions) to control molecular processes in laser fields.[72–74]

Recently, we have become engaged in this subject, but for a different reason: we are interested in determining to what extent an intense external field interferes and/or competes with effects due to the above-mentioned NAC terms. For this purpose we need first to develop a theoretical approach to treat systems controlled by electronic nonadiabtic coupling terms which are exposed to intense laser fields. It is important to mention that the available (perturbative) approach to treat the corresponding field-dressed SE is not really well devised to study such intense processes. According to this procedure, one uses the adiabatic field-free eigenfunctions to form the time-dependent (TD) coupling matrix that is added to the adiabatic field-free Hamiltonian.[75,76] This procedure may fail because an intense laser field is expected to excite a large number of the field-free adiabatic states, thus blowing the dimensions of matrices to numbers much too large. This situation is further aggravated by the fact that the density of molecular states increases with energy. A few years ago a different approach was presented,[77] which was also recently applied in one case.[78–80] This approach is similar to the one we employ in the field-free case but with one main difference, namely, that the above mentioned required field-dressed ADT matrix is derived along space-time contours (instead of spatial contours in the field-free case).

In the following sections the adiabatic N - electronic state coupled nuclear motion

Schroedinger equations are presented along with the NAC terms, where Hellmann-Feynmann theorem describes the general feature of those terms. The diabatic representation, the transformation from adiabatic to diabatic frameworks and the relevant curl condition, the Jahn-Teller model and the Longuet-Higgins phase and formulation of EBO equation for two-state system are also discussed.

1.1 Adiabatic Representation

In the adiabatic representation of Schroedinger equation, the total electron-nuclei Hamiltonian ($\hat{\mathbf{H}}$) that governs the motion of nuclei and electrons is usually written in the following form

$$\hat{\mathbf{H}} = \hat{\mathbf{T}}_n + \hat{\mathbf{H}}_e(\mathbf{e}, \mathbf{n}), \tag{1.1}$$

where the nuclear kinetic energy (KE) operator ($\hat{\mathbf{T}}_n$) and the eigenvalue $[u_i(\mathbf{n})]$ − eigenfunction $[\xi_i(\mathbf{e}, \mathbf{n})]$ equation for the electronic Hamiltonian $[\hat{\mathbf{H}}_e(\mathbf{e}, \mathbf{n})]$ are presented as:

$$\begin{aligned} \hat{\mathbf{T}}_n &= -\frac{\hbar^2}{2m}\sum_n \nabla_n^2, \\ \hat{\mathbf{H}}_e(\mathbf{e}, \mathbf{n})\xi_i(\mathbf{e}, \mathbf{n}) &= u_i(\mathbf{n})\xi_i(\mathbf{e}, \mathbf{n}). \end{aligned} \tag{1.2}$$

The BO expansion for the molecular wavefunction, $\Psi(\mathbf{n}, \mathbf{e})$ is given by

$$\Psi(\mathbf{n}, \mathbf{e}) = \sum_{i=1}^{N} \psi_i(\mathbf{n})\xi_i(\mathbf{e}, \mathbf{n}), \tag{1.3}$$

where $\xi_i(\mathbf{e}, \mathbf{n})$s are the electronic eigenfunctions with nuclear coordinate dependent expansion coefficients, $\psi_i(\mathbf{n})$s subsequently termed as nuclear wavefunction and the sets of nuclear and electronic coordinates are defined as $\mathbf{n}$ and $\mathbf{e}$, respectively.

Substituting the molecular wavefunction [Eq. (1.3)] and the total electron-nuclear Hamiltonian, $\hat{\mathbf{H}}$ [Eq. (1.1)] in the time-independent Schroedinger equation,

$$\hat{\mathbf{H}}\Psi(\mathbf{n}, \mathbf{e}) = E\Psi(\mathbf{n}, \mathbf{e}), \tag{1.4}$$

and performing the corresponding differentiations with respect to the nuclear coordinates and the integrations with respect to the electronic coordinates yield the explicit form of the Born-Oppenheimer system of coupled equations

$$-\frac{\hbar^2}{2m}\nabla^2\psi_k + (u_k - E)\psi_k - \frac{\hbar^2}{2m}\sum_{j=1}^{N}(2\vec{\tau}_{kj}^{(1)}\cdot\vec{\nabla} + \tau_{kj}^{(2)})\psi_k = 0; \qquad k = 1, \ldots, N \tag{1.5}$$

where $\vec{\tau}_{ij}^{(1)}$ and $\tau_{ij}^{(2)}$ are the elements of nonadiabatic coupling matrices of the first $[\vec{\boldsymbol{\tau}}^{(1)}]$ and second $[\boldsymbol{\tau}^{(2)}]$ kind, respectively.

$$\vec{\tau}_{ij}^{(1)} = \langle\xi_i(\mathbf{e},\mathbf{n})|\vec{\nabla}\xi_j(\mathbf{e},\mathbf{n})\rangle, \tag{1.6a}$$

$$\tau_{ij}^{(2)} = \langle\xi_i(\mathbf{e},\mathbf{n})|\nabla^2\xi_j(\mathbf{e},\mathbf{n})\rangle. \tag{1.6b}$$

For a given Hilbert/sub-Hilbert space, the two kinds of NAC matrices are related as:

$$\boldsymbol{\tau}^{(2)} = \vec{\boldsymbol{\tau}}^{(1)}\cdot\vec{\boldsymbol{\tau}}^{(1)} + \vec{\nabla}\vec{\boldsymbol{\tau}}^{(1)}, \tag{1.7}$$

leading to the following compact form of kinetically coupled nuclear equations:

$$-\frac{\hbar^2}{2m}\left(\vec{\nabla} + \vec{\boldsymbol{\tau}}\right)^2\Psi + (U - E)\,\Psi = 0, \tag{1.8}$$

where $\Psi(\mathbf{n})$ is a column vector that contains the nuclear functions $\{\psi_k(\mathbf{n}), k = 1, \ldots, N\}$, U is a diagonal matrix that contains the adiabatic potentials and $\boldsymbol{\tau}$ is the nonadiabatic coupling matrix. This is the nuclear SE within the adiabatic framework for a given Hilbert/sub -Hilbert space.

The transitions between the various eigenstates are governed by a dynamic coupling. This framework is expected to be efficient for dynamic studies as it applies adiabatic electronic information. The main difficulty associated with this are the nonadiabatic coupling terms as their tendency to become singular. The singularity is caused by abrupt changes of the electronic eigenvectors as a function of nuclear coordinates.

1.2 Diabatic Representation

The BO expansion in diabatic representation for the molecular wavefunction, $\Psi(\mathbf{n}, \mathbf{e})$ is given by

$$|\Psi^d(\mathbf{n}, \mathbf{e})\rangle = \sum_{i=1}^{N} \psi_i^d(\mathbf{n})|\xi_i(\mathbf{e}, \mathbf{n}_0)\rangle, \tag{1.9}$$

where $|\xi_i(\mathbf{e}, \mathbf{n}_0)\rangle$s are the electronic eigenfunctions which depends parametrically on $\mathbf{n}_0$ and $\psi_i(\mathbf{n}_0)$ is nuclear coordinate dependent expansion coefficients. $|\xi_i(\mathbf{e}, \mathbf{n}_0)\rangle$ is the eigenfunction of the Hamiltonian

$$\big(\mathbf{H}_e(\mathbf{e}, \mathbf{n}_0) - \mathbf{u}_i(\mathbf{n}_0)\big)|\xi_i(\mathbf{e}, \mathbf{n}_0)\rangle = 0 \tag{1.10}$$

where $\mathbf{u}_i(\mathbf{n}_0), i = 1, \ldots, L$ are the corresponding electronic eigenvalues as calculated for this (fixed) set of nuclear coordinates. Substituting Eqs. (1.9) and (1.10) in time-independent Schroedinger equation, $\hat{\mathbf{H}}\Psi^d(\mathbf{n}, \mathbf{e}) = E\Psi^d(\mathbf{n}, \mathbf{e})$, [recalling that the coordinates $(\mathbf{n}_0)$ are not variable] and performing the corresponding differentiations with respect to the nuclear coordinates and the integrations with respect to the electronic coordinates yeild the following expression:

$$-\Big(\frac{\hbar^2}{2m}\nabla^2 - E\Big)\psi_k^d(\mathbf{n}) + \sum_{j=1}^{N} \mathbf{V}_{kj}(\mathbf{n}, \mathbf{n}_0)\psi_k^d(\mathbf{n}) = 0 \tag{1.11}$$

where $\mathbf{V}_{kj}(\mathbf{n}, \mathbf{n}_0)$ is the (k, j) diabatic matrix element given by:

$$\mathbf{V}_{kj}(\mathbf{n}, \mathbf{n}_0) = \langle\xi_k(\mathbf{e}, \mathbf{n}_0)|\mathbf{H}_e(\mathbf{e}, \mathbf{n})|\xi_j(\mathbf{e}, \mathbf{n}_0)\rangle \tag{1.12}$$

Again, $\mathbf{H}_e(\mathbf{e}, \mathbf{n})$ *operator* is given as the sum of the electronic kinetic energy operator $\mathbf{T}_e(\mathbf{n})$ and the potential energy operator $\mathbf{U}(\mathbf{e}, \mathbf{n})$:

$$\mathbf{H}_e(\mathbf{e}, \mathbf{n}) = \mathbf{T}_e(\mathbf{n}) + \mathbf{U}(\mathbf{e}, \mathbf{n}) \tag{1.13}$$

Here $\mathbf{U}(\mathbf{e}, \mathbf{n})$ is the Coulomb field, which is governs the motion of the electron and we include also Coulomb interaction due to the fixed nuclei. A similar expression also holds for $\mathbf{H}_e(\mathbf{e},\mathbf{n}_0)$:

$$\mathbf{H}_e(\mathbf{e},\mathbf{n}_0) = \mathbf{T}_e(\mathbf{n}) + \mathbf{U}(\mathbf{e},\mathbf{n}_0) \tag{1.14}$$

Since the kinetic energy operator of the electrons does not depends on the nuclear coordinates, $\mathbf{H}_e(\mathbf{e},\mathbf{n})$ can be written in the following way:

$$\mathbf{H}_e(\mathbf{e},\mathbf{n}) = \mathbf{H}_e(\mathbf{e},\mathbf{n}_0) + \Big(\mathbf{U}(\mathbf{e},\mathbf{n}) - \mathbf{U}(\mathbf{e},\mathbf{n}_0)\Big) \tag{1.15}$$

Having this relation, we can write more explicitly the expression of $\mathbf{V}_{kj}(\mathbf{n},\mathbf{n}_0)$ as

$$\mathbf{V}_{kj}(\mathbf{n},\mathbf{n}_0) = \mathbf{v}_{kj}(\mathbf{n},\mathbf{n}_0) + \delta_{kj}\mathbf{u}_j(\mathbf{n}_0) \tag{1.16}$$

where

$$\mathbf{v}_{kj}(\mathbf{n},\mathbf{n}_0) = \langle \xi_k(\mathbf{e},\mathbf{n}_0)|\big(\mathbf{U}(\mathbf{e},\mathbf{n}) - \mathbf{U}(\mathbf{e},\mathbf{n}_0)\big)|\xi_j(\mathbf{e},\mathbf{n}_0)\rangle \tag{1.17}$$

Equation (1.11) can also be written in matrix form:

$$-\frac{\hbar^2}{2m}\vec{\nabla}^2\Psi^d + (\mathbf{V} - E)\,\Psi^d = 0, \tag{1.18}$$

Here $\mathbf{V}_{kj}(\mathbf{n},\mathbf{n}_0)$ is the diabatic potential matrix, which in contrast to $\mathbf{u}(\mathbf{n})$ in Eq. (1.8) is a full matrix. Eq. (1.18) is the Schroedinger equation within the diabatic representation.

The main difficulty here is that the nuclear dynamics is base on one single electronic basis set (calculated at $\mathbf{n}_0$). This cannot be an efficient representation because it requires a large electronic basis set producing a $\mathbf{V}$ matrix with large dimensions and large off diagonal matrix elements.

1.3 Adiabatic-to-Diabatic Transformation

The fact that the two nuclear Schroedinger equations, presented in Eq. (1.8) and (1.18), are expected to yield the same solution implies that both equations carry with them the same amount of information and therefore are related through an orthogonal transformation matrix. In order to derive this transformation matrix, we start with the adiabatic Schroedinger equation, eliminate the τ-matrix elements, and form the relevant diabatic Schroedinger equation. The newly formed diabatic Schroedinger equation and the one presented by Eq. (1.18).

We start by replacing the column vector Ψ by another column vector Φ in Eq. (1.8) where the two are related as:

$$\Psi = \mathbf{A}\Phi \tag{1.19}$$

Here $\mathbf{A}$ is a matrix of the coordinates to be determined by the requirement that the $\boldsymbol{\tau}$ matrix in Eq. (1.8) will not appear in the Schroedinger equation for Φ. To achieve that we evaluate the following expression:

$$\begin{aligned}(\nabla + \boldsymbol{\tau})^2 \mathbf{A}\Phi &= (\nabla + \boldsymbol{\tau})(\nabla + \boldsymbol{\tau})\mathbf{A}\Phi \\ &= (\nabla + \boldsymbol{\tau})\{\mathbf{A}\nabla\Phi + (\nabla\mathbf{A})\Phi + \boldsymbol{\tau}\mathbf{A}\Phi\} \\ &= \mathbf{A}\nabla^2\Phi + 2(\nabla\mathbf{A} + \boldsymbol{\tau}\mathbf{A}) \cdot \nabla\Phi + \{(\boldsymbol{\tau} + \nabla) \cdot (\nabla\mathbf{A} + \boldsymbol{\tau}\mathbf{A})\}\Phi \end{aligned} \tag{1.20}$$

Now, choosing $\mathbf{A}$ to be the solution of the following equation

$$(\nabla\mathbf{A} + \boldsymbol{\tau}\mathbf{A}) = 0 \tag{1.21}$$

the kinetic contribution to the Hamiltonian becomes

$$(\nabla + \boldsymbol{\tau})^2 \mathbf{A}\Phi = \mathbf{A}\nabla^2\Phi \tag{1.22}$$

and Eq. (1.8) takes the form

$$-\frac{\hbar^2}{2m}\mathbf{A}\nabla^2\Phi + (\mathbf{u} - E)\,\mathbf{A}\Phi = 0, \tag{1.23}$$

Multiplying by $\mathbf{A}^\dagger$ – the complex conjugate matrix of $\mathbf{A}$ – we get

$$-\frac{\hbar^2}{2m}\nabla^2\Phi + (\mathbf{W} - E)\,\Phi = 0, \tag{1.24}$$

where $\mathbf{W}$ is given by

$$\mathbf{W} = \mathbf{A}^\dagger\mathbf{u}\mathbf{A} \tag{1.25}$$

This equation [Eq. (1.24)] is the nuclear diabatic Schroedinger equation and **W** is the corresponding diabatic potential. Since **A** is the (orthogonal) transformation matrix that connects the two frameworks, it is termed the *Adiabatic-to-Diabatic Transformation matrix* or as ADT matrix.

To conclude that derivation, we state that treatment of the Schroedinger equation, whether it is done in the adiabatic or the diabatic representation, yields the same solution. In other words, the transformation from the adiabatic framework to the diabatic frameworks (or vice versa) does not affect the solution of this equation.

1.4 The Curl Condition

From basic calculus, it is known that a function of a single variable is analytic at a given interval if and only if it has well defined derivatives, to any order, at any point in that interval. In the same way, a function of several variables is analytic in a region if at any point in this region, in addition to having well defined derivatives for all variables to any order, the result of the differentiation with respect to any two variables does not depend on the order of the differentiation.

The fact that the **A** matrix fulfills Eq. (1.21) ensures the existence of derivatives to any order for any variable, at a given region in configuration space, if $\boldsymbol{\tau}$ is analytic in that region. In what follows, we have to find the conditions for a mixed differentiation of the **A** matrix elements to be independent of the order.

For that purpose, we consider the p and q components of Eq. (1.21):

$$\begin{aligned} \frac{\partial}{\partial p}A + \tau_p A &= 0, &(1.26a)\\ \frac{\partial}{\partial q}A + \tau_q A &= 0 &(1.26b)\end{aligned}$$

Differentiating the first equation with respect to q, we find

$$\begin{aligned} \frac{\partial}{\partial q}\frac{\partial}{\partial p}A + \Big(\frac{\partial}{\partial q}\tau_p\Big)A + \tau_p\frac{\partial}{\partial q}A &= 0,\\ \text{or} \quad \frac{\partial}{\partial q}\frac{\partial}{\partial p}A + \Big(\frac{\partial}{\partial q}\tau_p\Big)A - \tau_p\tau_q A &= 0 \end{aligned} \tag{1.27}$$

In the same way, we get from the second equation, the following expression:

$$\frac{\partial}{\partial p}\frac{\partial}{\partial q}A + \Big(\frac{\partial}{\partial p}\tau_q\Big)A - \tau_q\tau_p A = 0. \tag{1.28}$$

Requiring that the mixed derivative is independent of the order of the differentiation yields:

$$\Big(\frac{\partial}{\partial p}\tau_q - \frac{\partial}{\partial q}\tau_p\Big)A = (\tau_q\tau_p - \tau_p\tau_q)A \tag{1.29}$$

or (since **A** is a unitary matrix):

$$\frac{\partial}{\partial p}\tau_q - \frac{\partial}{\partial q}\tau_p = (\tau_q\tau_p - \tau_p\tau_q) = [\tau_q, \tau_p]. \tag{1.30}$$

Thus, in order for the **A** matrix to be analytic in a region, any two components of $\boldsymbol{\tau}$ have to fulfill Eq. (1.30), which is known as the Curl condition.

1.5 The nonadiabatic coupling terms and Hellmann - Feynmann theorem

We consider a diabatic potential energy matrix, **W**, and show that the relevant nonadiabatic coupling terms may become, at some points in the configuration space, singular. We assume that $\mathbf{u}_j$ and ξ_j are respectively the jth eigenvalue and eigenvector of **W**, namely:

$$\mathbf{W}|\xi_j\rangle = u_j|\xi_j\rangle \tag{1.31}$$

Next we differentiate both sides with respect to a variable s. The left hand side yields:

$$\frac{\partial}{\partial s}\Big(\mathbf{W}|\xi_j\rangle\Big) = \frac{\partial \mathbf{W}}{\partial s}|\xi_j\rangle + \mathbf{W}|\frac{\partial \xi_j}{\partial s}\rangle \tag{1.32}$$

and the right hand side yields:

$$\frac{\partial}{\partial s}\Big(u_j|\xi_j\rangle\Big) = \frac{\partial u_j}{\partial s}|\xi_j\rangle + u_j|\frac{\partial \xi_j}{\partial s}\rangle \tag{1.33}$$

Multiplying Eqs. (1.32) and (1.33) from left by ξ_k where $j \neq k$ and equating the two expression we get (recalling that $\{\xi_j\}$ is an orthogonal set):

$$\langle\xi_k|\frac{\partial \mathbf{W}}{\partial s}|\xi_j\rangle + \Big\langle\xi_k\Big|\mathbf{W}\Big|\frac{\partial \xi_j}{\partial s}\Big\rangle = \frac{\partial u_j}{\partial s}\langle\xi_k|\xi_j\rangle + u_j\Big\langle\xi_k\Big|\frac{\partial \xi_j}{\partial s}\Big\rangle \tag{1.34}$$

We know that

$$\tau_{kj}(s) = \Big\langle\xi_k\Big|\frac{\partial \xi_j}{\partial s}\Big\rangle; \qquad \Big\langle\xi_k\Big|\mathbf{W} = u_k\Big\langle\xi_k\Big|; \qquad \langle\xi_k|\xi_j\rangle = \delta_{kj}$$

We find from these expressions the relation for the nonadiabatic coupling term:

$$\tau_{kj}(s) = -\frac{\langle\xi_k|\frac{\partial \mathbf{W}}{\partial s}|\xi_j\rangle}{u_k - u_j} \tag{1.35}$$

It is noticed that singularities in the nonadiabatic coupling terms are formed whenever the system contains degenerate electronic states.

1.6 The Jahn-Teller model and Longuet-Higgins' phase

In the vicinity of a point of degeneracy between two electronic states, Jahn-Teller assumed the diabatic potentials to behave linearly as a function of the nuclear coordinates. Without loosing generality it can be assumed:

$$\mathbf{W} = k \begin{pmatrix} y & x \\ x & -y \end{pmatrix}, \tag{1.36}$$

where (x, y) are some generalized nuclear coordinates and k a force constant. The aim is to derive the eigenvalues and the eigenvectors of this potential matrix. The eigenvalues are the adiabatic potential energy states and the eigenvectors form the columns of the ADT matrix. In order to perform this derivation, we shall employ polar coordinates (q, φ), namely:

$$y = q\cos\varphi \quad \text{and} \quad x = q\sin\varphi \tag{1.37}$$

Substituting for x and y we get ϕ - independent eigenvalues of the form

$$u_1 = kq \quad \text{and} \quad u_2 = -kq \quad \text{where} \quad q = \{0, \infty\} \quad \text{and} \quad \varphi = \{0, 2\pi\} \tag{1.38}$$

As noticed from Fig. 1.1, the two surfaces u_1 and u_2 are cone-like PESs with a common apex. The corresponding eigenvectors are

$$\begin{aligned} \xi_1 &= \left(\frac{1}{\sqrt{\pi}}\cos\frac{\varphi}{2}, \frac{1}{\sqrt{\pi}}\sin\frac{\varphi}{2}\right), \\ \xi_2 &= \left(\frac{1}{\sqrt{\pi}}\sin\frac{\varphi}{2}, -\frac{1}{\sqrt{\pi}}\cos\frac{\varphi}{2}\right). \end{aligned} \tag{1.39}$$

The components of the two vectors (ξ_1, ξ_2), when multiplied by the electronic (diabatic) basis set $(|\phi_1\rangle, |\phi_2\rangle)$, form the corresponding electronic adiabatic basis set $(|\eta_1\rangle, |\eta_2\rangle)$:

$$|\eta_1\rangle = \frac{1}{\sqrt{\pi}}\cos\frac{\varphi}{2}|\phi_1\rangle + \frac{1}{\sqrt{\pi}}\sin\frac{\varphi}{2}|\phi_2\rangle,$$
$$|\eta_2\rangle = \frac{1}{\sqrt{\pi}}\sin\frac{\varphi}{2}|\phi_1\rangle - \frac{1}{\sqrt{\pi}}\cos\frac{\varphi}{2}|\phi_2\rangle. \quad (1.40)$$

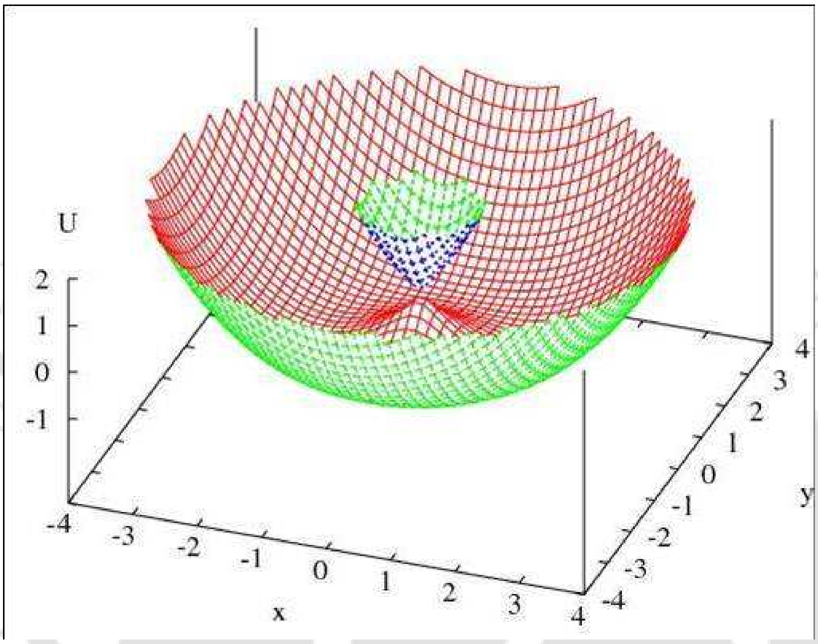

Figure 1.1: The two intersecting cones within the Jahn-Teller model.

The adiabatic functions are characterized by two interesting features: (a) they depend only on the angular coordinate (but not on the radial coordinate) and (b) they are not single-valued in configuration space because when φ is replaced by $(\varphi + 2\pi)$ $-$ a rotation which brings the adiabatic wavefunctions back to their initial position $-$ both of them change sign. This last feature, which was revealed by Longuet-Higgins,[10–12] may be, in certain cases, very crucial because multi-valued electronic eigenfunctions cause the corresponding nuclear wave functions to be multi-valued as well, a feature which has to be incorporated explicitly (through specific boundary conditions) while solving the nuclear SE. In this respect, it is important to mention that ab-initio electronic wavefunctions indeed, possess the multi-valuedness feature as describe by Longuet-Higgins.

One way to get rid of the multi-valuedness of the electronic eigenfunctions is by multiplying it by a phase factor, namely:

$$\xi_j(\varphi) = \exp(i\varphi/2)\eta_j(\varphi), \qquad j = 1, 2. \tag{1.41}$$

It is noticed that $\xi_j(\varphi), j = 1, 2$ are indeed single-valued eigenfunctions; however, instead of being real, they becomes complex.

The fact that the electronic eigenfunctions are modified as presented in Eq.(1.41) has a direct effect on the nonadiabatic coupling terms. In particular, we consider the term $\tau_{11}^{(1)}$ (which for the case of real eigenfunctions is identically zero) for the case presented in Eq. (1.41):

$$\tau_{11}^{(1)} = \langle\xi_1|\nabla\xi_1\rangle = \frac{i}{2}\nabla\varphi + \langle\eta_1|\nabla\eta_1\rangle$$

but since $\langle\eta_1|\nabla\eta_1\rangle = 0$, it follows that $\tau_{11}^{(1)}$ becomes

$$\tau_{11}^{(1)} = \frac{i}{2}\nabla\varphi \tag{1.42}$$

In the same way, we obtain

$$\tau_{11}^{(2)} = \frac{i}{2}\nabla^2\varphi - \left(\frac{1}{2}\nabla\varphi\right)^2 \tag{1.43}$$

The fact that now $\tau_{11}^{(1)}$ is not zero will affect the ordinary BO approximation. In that case the BO-SE becomes

$$-\frac{\hbar^2}{2m}\left(\nabla + \frac{i}{2}\nabla\varphi\right)^2\psi + (u - E)\psi = 0 \tag{1.44}$$

which can be considered as an extended BO approximation[22] for a case of a single isolated state expressed in terms of a complex electronic eigenfunction. This equation was interpreted for some time as the adequate SE to describe the effect of the Jahn-Teller CI which originates from the two interacting states. As it stands, it contains an effect due to an ad hoc phase related to a single (the lowest - state) electronic eigenfunction. Moreover, no prescription is given how to calculate it.

1.7 Single-surface Born-Oppenheimer equation for two - state system

We noticed that both adiabatic and diabatic framework has its advantages and disadvantages. The question to be asked is if there exists an intermediate framework that will be simple as the diabatic framework and efficient as the adiabatic one. One of the formulation proposed by Baer and Englman[57] as well as Varandas and Xu[54] to study the behavior of nuclear wave function in the vicinity of CI for two coupled electronic state of an X_3 system.

The nuclear Schroedinger equation within the adiabatic representation has the following form:

$$-\frac{\hbar^2}{2m}\nabla^2\Psi + \Big(\mathbf{u} - \frac{\hbar^2}{2m}\boldsymbol{\tau}^2 - E\Big)\Psi - \frac{\hbar^2}{2m}(2\boldsymbol{\tau}\cdot\nabla + \nabla\boldsymbol{\tau})\Psi = 0 \tag{1.45}$$

For a two-state electronic manifold (i.e., ignoring all nonadiabatic couplings to higher electronic states) the nuclear motion is described by the following coupled equations:

$$\Big(-\frac{\hbar^2}{2m}\nabla^2 + \tilde{u}_1 - E\Big)\psi_1 - \frac{\hbar^2}{2m}(2\tau\cdot\nabla + \nabla\tau)\psi_2 = 0 \tag{1.46a}$$

$$\Big(-\frac{\hbar^2}{2m}\nabla^2 + \tilde{u}_2 - E\Big)\psi_2 - \frac{\hbar^2}{2m}(2\tau\cdot\nabla + \nabla\tau)\psi_1 = 0 \tag{1.46b}$$

where $\tau \equiv \tau_{12}$ and

$$\tilde{\mathbf{u}}_j = \mathbf{u}_j - \frac{\hbar^2}{2m}\boldsymbol{\tau}^2; \qquad j = 1, 2 \tag{1.47}$$

Multiplying the second equation by the imaginary i, once adding it to the first equation and once subtracting it, two new coupled equations are formed:

$$\Big\{-\frac{\hbar^2}{2m}\nabla^2 + \tilde{u}_1 - E + i\frac{\hbar^2}{2m}(2\tau\cdot\nabla + \nabla\tau)\Big\}\psi^+ + \frac{\hbar^2}{2m}(\tilde{u}_2 - \tilde{u}_1)(\psi^+ - \psi^-) = 0 \tag{1.48a}$$

$$\Big\{-\frac{\hbar^2}{2m}\nabla^2 + \tilde{u}_1 - E - i\frac{\hbar^2}{2m}(2\tau\cdot\nabla + \nabla\tau)\Big\}\psi^- + \frac{\hbar^2}{2m}(\tilde{u}_2 - \tilde{u}_1)(\psi^+ - \psi^-) = 0 \tag{1.48b}$$

where

$$\psi^{\pm} = \psi_1 \pm i\psi_2 \tag{1.49}$$

From the above equation we get:

$$\frac{1}{2}(\psi^{+} - \psi^{-}) = i\psi_2 \tag{1.50}$$

Assuming now that the kinetic energy of the system is low enough so that the second state, u_2, is classically forbidden throughout configuration space. This implies that $\psi_2 \sim 0$ throughout configuration space and therefore the last terms in the Eq. (1.48) can be ignored and we end up with two uncoupled equation of the kind:

$$\Big\{ -\frac{\hbar^2}{2m}\nabla^2 + \tilde{u}_1 - E + i\frac{\hbar^2}{2m}\big(2\tau \cdot \nabla + \nabla\tau\big)\Big\}\psi^{\pm} = 0 \tag{1.51}$$

This is the extended Born-Oppenheimer equation which contains not only the potential energy surface but also terms responsible for topological effects.

It is now convenient to define the two real electronic wavefunctions as

$$\xi_1 = \begin{bmatrix} \cos\gamma(R) \\ -\sin\gamma(R) \end{bmatrix}, \qquad \xi_2 = \begin{bmatrix} \sin\gamma(R) \\ \cos\gamma(R) \end{bmatrix}, \tag{1.52}$$

where $\gamma(R)$ is the mixing angle and R is the nuclear internal degrees of freedom. Assuming that the electronic basis is orthonormal, it then can be shown that

$$\langle\xi_1|\nabla\xi_2\rangle = -\langle\xi_2|\nabla\xi_1\rangle = \nabla\gamma(R) \tag{1.53}$$

Similarly, we can have

$$\begin{aligned} \langle\xi_1|\nabla^2\xi_2\rangle &= -\langle\xi_2|\nabla^2\xi_1\rangle = -\nabla^2\gamma(R), \\ \langle\nabla\xi_1|\nabla\xi_1\rangle &= \langle\nabla\xi_2|\nabla\xi_2\rangle = [\nabla\gamma(R)]^2 \\ \text{and} \qquad \langle\nabla\xi_1|\nabla\xi_2\rangle &= \langle\nabla\xi_2|\nabla\xi_1\rangle = 0 \end{aligned}$$

Under this consideration one gets the following single-surface equation for the nuclear dynamics on the lower electronic state,

$$\Big\{ -\frac{\hbar^2}{2m}\{\nabla^2 - [\nabla\gamma(R)]^2\} + u_1 - E + i\frac{\hbar^2}{2m}\big[2\nabla\gamma(r)\cdot\nabla + \nabla^2\gamma(R)\big]\Big\}\psi^+ = 0 \qquad (1.54)$$

which contains the effect of the nonadiabatic coupling term.

Finally, the overview of the thesis is as follows.

In **Chapter 2** and **Chapter 3**, formulation of Born-Oppenheimer equation for three- and four- state sub-Hilbert space, respectively has been discussed. These analytically derived equations are numerically justified in **Chapter 4** and **Chapter 5** and finally in **Chapter 6** the subject discussed is the interaction of an external field with a molecular system.

References

[1] M. Born and J. R. Oppenheimer, Ann. Phys. (Leipzig) **84**, 457 (1927).

[2] M. Born and K. Huang, *Dynamical Theory of Crystal Lattices*, Oxford University Press, Oxford, 1954.

[3] S. T. Epstein, Am. J. Phys. **22**, 613 (1954).

[4] M. Born, Festchrift Goett. Nach. Math. Phys. **K1**, 1 (1951).

[5] H. Hellmann, *Einfuhrang in die Quantenchemie*, Franz Deutiche, Leipzig, Germany, 1937.

[6] R. Feynmann, Phys. Rev. **56**, 340 (1939).

[7] M. Bear and G. D. Billing, editors, *The Role of Degenerate States in Chemistry*, Wiley Interscience, Hoboken, N.J., USA, 2002.

[8] L. O'Raifeartaigh, *Dawning of Gauge Theory*, Princton University Press, Princeton, N.J., USA, 1997.

[9] R. Englman and Y. Yahalom, Adv. Chem. Phys. **124**, 197 (2002).

[10] H. C. Longuet-Higgins, Proc. R. Soc. London A **344**, 147 (1975).

[11] G. Herzberg and H. C. Longuet-Higgins, Discuss. Faraday Soc. **35**, 77 (1963).

[12] H. C. Longuet-Higgins, Adv. Spectrosc. **2**, 1429 (1961).

[13] C. A. Mead and D. G. Truhlar, J. Chem. Phys. **70**, 2284 (1979).

[14] A. Kuppermann and Y. S. M. Wu, Chem. Phys. Lett. **205**, 577 (1993).

[15] A. Kuppermann and Y. S. M. Wu, Chem. Phys. Lett. **241**, 229 (1995).

[16] A. Kuppermann and Y. S. M. Wu, Chem. Phys. Lett. **349**, 537 (2001).

[17] B. K. Kendrick and R. T. Pack, J. Chem. Phys. **104**, 7475 (1996).

[18] S. Adhikari and G. D. Billing, J. Chem. Phys. **107**, 6213 (1997).

[19] B. K. Kendrick and R. T. Pack, J. Chem. Phys. **104**, 7502 (1996).

[20] S. Adhikari and G. D. Billing, J. Chem. Phys. **111**, 40 (1999).

[21] M. V. Berry, Proc. R. Soc. London A **392**, 45 (1984).

[22] C. A. Mead, Chem. Phys. **49**, 23 (1980).

[23] Y. Aharonov and D. Bohm, Phys. Rev. **115**, 485 (1969).

[24] W. Lichten, Phys. Rev. **164**, 131 (1967).

[25] C. J. Ballhausen and A. E. Hansen, Annu. Rev. Phys. Chem. **23**, 15 (1972).

[26] M. Bear, *Beyond Born-Oppenheimer:Conical Intersections and Electronic nonadiabatic Coupling Terms*, Wiley Interscience, Hoboken, N.J., USA, 2006.

[27] C. A. Mead and D. G. Truhlar, J. Chem. Phys. **77**, 6090 (1982).

[28] B. K. Kendrick, C. A. Mead and D. G. Truhlar, Chem. Phys. **277**, 31 (2002).

[29] N. Matsunaga and D. R.Yarkony, Mol. Phys. **93**, 79 (1998).

[30] D. R.Yarkony, J. Chem. Phys. **105**, 10456 (1996).

[31] M. Baer, T. Vertesi, G. J. Halasz, A. Vivok and S. Suhai, Faraday Discuss. **127**, 337 (2004).

[32] R. G. Sadygov and D. R.Yarkony, J. Chem. Phys. **109**, 20 (1998).

[33] R. Abrol and A. Kuppermann, J. Chem. Phys. **116**, 1035 (2002).

[34] W. Domcke, D. R. Yarkony and H. Koppel, editors, *Conical Intersections: Electronic Structure, Dynamics and Spectroscopy*, World Scientific, Singapure, 2004.

[35] F. T. Smith, Phys. Rev. **179**, 111 (1969).

[36] M. Baer, Chem. Phys. Lett. **35**, 112 (1975).

[37] Z. H. Top and M. Baer, J. Chem. Phys. **66**, 1363 (1977).

[38] M. Baer, Mol. Phys. **40**, 1011 (1980).

[39] A. Alijah and M. Baer, J. Phys. Chem. A **104**, 389 (2000).

[40] R. E. Wyatt and J. Z. H. Zhang, editors, *Dynamics of Molecules and Chemical Reactions*, Dekker, New York, 1996.

[41] V. Sidis, Adv. Chem. Phys. **82**, 73 (1992).

[42] R. Baer, D. Charutz, R. Kosloff and M. Baer, J. Chem. Phys. **107**, 9141 (1996).

[43] J. C. Juanes-Marcos and S. C. Althorpe, J. Chem. Phys. **122**, 204324 (2005).

[44] P. Helvick and D. G. Truhlar, J. Chem. Phys. **96**, 2895 (1992).

[45] G. J. Tawa, S. L. Milke, D. G. Truhlar and D. W. Schwenke, J. Chem. Phys. **100**, 5751 (1994).

[46] B. Sarkar and S. Adhikari, J. Chem. Phys. **124**, 74101 (2006).

[47] P. Puzari, B. Sarkar and S. Adhikari, J. Chem. Phys. **121**, 707 (2004).

[48] B. H. Lengsfield and D. R. Yarkony, *State-selected and State-to-State Ion-Molecular Reaction Dymanics*.

[49] T. Pacher, L. S. Cederbaum and H. Köppel, Adv. Chem. Phys. **84**, 293 (1993).

[50] T. Pacher, L. S. Cederbaum and H. Köppel, J. Chem. Phys. **89**, 7367 (1988).

[51] T. Pacher, L. S. Cederbaum and H. Köppel, J. Chem. Phys. **95**, 6668 (1991).

[52] D. R.Yarkony, J. Chem. Phys. **112**, 2111 (2000).

[53] W. Domcke and G. Stock, Adv. Chem. Phys. **100**, 1 (1997).

[54] A. J. C. Varandas and Z. R. Xu, J. Chem. Phys. **112**, 2121 (2000).

[55] Z. R. Xu, M. Baer and A. J. C. Varandas, J. Chem. Phys. **112**, 2746 (2000).

[56] M. Bear, *Theories of Chemical Reaction Dynamics*, CRC Press, Boca Raton, F.L., USA, 1985.

[57] M. Baer and R. Englman, Chem. Phys. Lett. **265**, 105 (1996).

[58] M. Baer, J. Chem. Phys. **107**, 10662 (1997).

[59] M. Baer, S. H. Lin, A. Alijah, S. Adhikari and G. D. Billing, Phys. Rev. A **62**, 32506 (2000).

[60] S. Adhikari, G. D. Billing, A. Alijah, S. H. Lin and M. Baer, Phys. Rev. A **62**, 32507 (2000).

[61] R. Englman, *The Jahn-Teller Effect in Molecules and Crystals*, Wiley Interscience, New York, 1972.

[62] B. Sarkar and S. Adhikari, Int. J. Quantum Chem. , in press (2008).

[63] B. Sarkar and S. Adhikari, J. Phys. Chem. A , DOI 10.1021/jp8029709 (2008).

[64] B. Sarkar and S. Adhikari, Indian J. Phys. **81**, 925 (2007).

[65] H. P. Grieneisen, H. Xue-jing and K. L. Kompa, Chem. Phys. Lett. **82**, 411 (1981).

[66] P. Hering, P. R. Brooks, R. F. C. Jr., R. S. Judson and R. S. Lowe, Phys. Rev. Lett. **44**, 687 (1980).

[67] I. H. Zimmerman, J.-M. Yaun and T. F. George, J. Chem. Phys. **66**, 2638 (1977).

[68] T. F. George et al., *Chemical and Biochemical Applications of Lasers*, volume 4, Academic, New York, 1979.

[69] I. H. Zimmerman, M. Baer and T. F. George, J. Phys. Chem. **87**, 1478 (1983).

[70] I. Last, M. Baer, I. H. Zimmerman and T. F. George, Chem. Phys. Lett. **101**, 163 (1983).

[71] I. Last and M. Baer, J. Chem. Phys. **82**, 4954 (1985).

[72] D. J. Tannor and S. A. Rice, J. Chem. Phys. **83**, 5013 (1986).

[73] D. J. Tannor, R. Kosloff and S. A. Rice, J. Chem. Phys. **85**, 5805 (1986).

[74] D. Hammerich, R. Kosloff and M. A. Ratner, J. Chem. Phys. **97**, 6410 (1992).

[75] M. Baer, J. Phys. Chem. A **107**, 4724 (2003).

[76] M. Baer, J. Phys. Chem. A **110**, 6571 (2006).

[77] R. Baer, D. J. Kouri, M. Baer and D. K. Hoffman, J. Chem. Phys. **119**, 6998 (2003).

[78] B. Sarkar, S. Adhikari and M. Baer, J. Chem. Phys. **126**, 14106 (2006).

[79] B. Sarkar, S. Adhikari and M. Baer, J. Chem. Phys. **127**, 14301 (2007).

[80] B. Sarkar, S. Adhikari and M. Baer, J. Chem. Phys. **127**, 14302 (2007).

Chapter 2

Born-Oppenheimer equation for three-state system: Formulation

2.1 Introduction

We present[1,2] the explicit forms of the nonadiabatic coupling elements along with their Curl-Divergence equations in terms of ADT angles by considering the validity of ADT condition, $\vec{\nabla}\mathbf{A} + \vec{\boldsymbol{\tau}}\mathbf{A} = 0$, for any three state sub-Hilbert space and show the one-to-one correspondence among the ADT and mixing angles. Since the necessary condition to derive the EBO equations is the existence of a relation among the ADT angles implicating zero Curls at least around the CIs, we explore an analytical proof for the validity of such relations $\Big[\Big(\frac{\partial\theta_{ij}}{\partial p}\frac{\partial\theta_{ik}}{\partial q} - \frac{\partial\theta_{ij}}{\partial q}\frac{\partial\theta_{ik}}{\partial p}\Big) \equiv 0$, $\{p, q = x, y, z$ or $r, \theta, \phi\}$, $i, j, k = 1, 2, 3$ and $i \neq j \neq k\Big]$, among these angles considering their dependence on three nuclear coordinates. The major aim of this chapter is to perform a theoretical development on three state Born - Oppenheimer system and then, to formulate an EBO equation in terms of ADT angles and to show its' analytical differences with respect to the approximate BO equation.[1]

2.2 Theoretical developments on the Born-Oppenheimer treatment

We demonstrate[1,2] a first principles based BO treatment for any three state electronic sub-Hilbert space considering the presence of conical intersection(s) anywhere in the nuclear configuration space and formulate EBO equation in a *rigorous* manner. Since we assume these three states as either decoupled or approximately decoupled from rest of the states of a molecular system, the BO expansion[3,4] of the wavefunction for this subspace of the Hilbert space along with the total electron-nuclei Hamiltonian in the adiabatic representation are presented as:

$$\begin{aligned}
\Psi(\mathbf{n},\mathbf{e}) &= \sum_{i=1}^{3}\psi_i(\mathbf{n})\xi_i(\mathbf{e},\mathbf{n}), \\
\hat{H} &= \hat{T}_n + \hat{H}_e(\mathbf{e},\mathbf{n}), \\
\text{where} \qquad \hat{T}_n = -\frac{\hbar^2}{2m}\sum_n \nabla_n^2, &\qquad \hat{H}_e(\mathbf{e},\mathbf{n})\xi_i(\mathbf{e},\mathbf{n}) = u_i(\mathbf{n})\xi_i(\mathbf{e},\mathbf{n}),
\end{aligned} \tag{2.1}$$

where the eigenfunction $[\xi_i(\mathbf{e},\mathbf{n})]$ of the electronic Hamiltonian, $\hat{H}_e(\mathbf{e},\mathbf{n})$, is defined by the sets of nuclear ($\mathbf{n}$) and electronic ($\mathbf{e}$) coordinates with nuclear coordinate dependent eigenvalue, $u_i(\mathbf{n})$. Indeed, it is obvious to specify that $\hat{T}_n$ is the nuclear kinetic energy operator and the expansion coefficient, $\psi_i(\mathbf{n})$, shall appear as nuclear wavefunction.

The time-independent Schroedinger equation, $\hat{H}\Psi(\mathbf{n},\mathbf{e}) = E\Psi(\mathbf{n},\mathbf{e})$, for the total electron-nuclear Hamiltonian and the BO expansion of the sub-Hilbert space molecular wavefunction [Eq. (2.2)] bring the matrix representation of adiabatic nuclear SE:

$$\begin{aligned}
\sum_{j=1}^{3}(H_{ij} &- E\delta_{ij})\psi_j(\mathbf{n}) = 0, \quad i = 1,2,3, \\
H_{ii} &= -\frac{\hbar^2}{2m}(\nabla^2 + 2\vec{\tau}_{ii}^{(1)}\cdot\vec{\nabla} + \tau_{ii}^{(2)}) + u_i(\mathbf{n}), \\
H_{ij} &= -\frac{\hbar^2}{2m}(2\vec{\tau}_{ij}^{(1)}\cdot\vec{\nabla} + \tau_{ij}^{(2)}) = H_{ji}^{\dagger}, \\
\vec{\tau}_{ij}^{(1)} &= \langle\xi_i(\mathbf{e},\mathbf{n})|\vec{\nabla}\xi_j(\mathbf{e},\mathbf{n})\rangle, \qquad \tau_{ij}^{(2)} = \langle\xi_i(\mathbf{e},\mathbf{n})|\nabla^2\xi_j(\mathbf{e},\mathbf{n})\rangle, \\
&\langle\xi_i(\mathbf{e},\mathbf{n})|\xi_j(\mathbf{e},\mathbf{n})\rangle = \delta_{ij}.
\end{aligned} \tag{2.2}$$

where $\vec{\tau}_{ij}^{(1)}$ and $\tau_{ij}^{(2)}$ are the elements of nonadiabatic coupling matrices of the first $[\vec{\boldsymbol{\tau}}^{(1)}]$ and second $[\boldsymbol{\tau}^{(2)}]$ kind, respectively. Moreover, it is straight forward to show that for a given Hilbert space the matrices, $\vec{\boldsymbol{\tau}}^{(1)}$ and $\boldsymbol{\tau}^{(2)}$ are related as:

$$\boldsymbol{\tau}^{(2)} = \vec{\boldsymbol{\tau}}^{(1)} \cdot \vec{\boldsymbol{\tau}}^{(1)} + \vec{\nabla}\vec{\boldsymbol{\tau}}^{(1)} \tag{2.3}$$

and thereby, we can arrive [from Eq. (2.2)] the following compact form of kinetically coupled nuclear equations:

$$-\frac{\hbar^2}{2m}\begin{pmatrix} \vec{\nabla} & \vec{\tau}_{12} & \vec{\tau}_{13} \\ -\vec{\tau}_{12} & \vec{\nabla} & \vec{\tau}_{23} \\ -\vec{\tau}_{13} & -\vec{\tau}_{23} & \vec{\nabla} \end{pmatrix}^2 \begin{pmatrix} \psi_1 \\ \psi_2 \\ \psi_3 \end{pmatrix} + \begin{pmatrix} u_1 - E & 0 & 0 \\ 0 & u_2 - E & 0 \\ 0 & 0 & u_3 - E \end{pmatrix} \begin{pmatrix} \psi_1 \\ \psi_2 \\ \psi_3 \end{pmatrix} = 0, \tag{2.4}$$

where the NAC matrix $[\vec{\boldsymbol{\tau}}(\equiv \vec{\boldsymbol{\tau}}^{(1)})]$ is defined as,

$$\vec{\boldsymbol{\tau}} = \begin{pmatrix} 0 & \vec{\tau}_{12} & \vec{\tau}_{13} \\ -\vec{\tau}_{12} & 0 & \vec{\tau}_{23} \\ -\vec{\tau}_{13} & -\vec{\tau}_{23} & 0 \end{pmatrix}. \tag{2.5}$$

Detailed expression of adiabatic equations [Eq. (2.4)] are presented in **Appendix A**.

Since the three states constitute the sub-Hilbert space (i.e., a complete space for the present case), it is possible to transform ($\Psi = \mathbf{A}\Psi^d$) the adiabatic nuclear SE [Eq. (2.4)] to the diabatic one as below,

$$\begin{pmatrix} -\frac{\hbar^2}{2m}\nabla^2 - E & 0 & 0 \\ 0 & -\frac{\hbar^2}{2m}\nabla^2 - E & 0 \\ 0 & 0 & -\frac{\hbar^2}{2m}\nabla^2 - E \end{pmatrix} \begin{pmatrix} \psi_1^d \\ \psi_2^d \\ \psi_3^d \end{pmatrix} + \begin{pmatrix} W_{11} & W_{12} & W_{13} \\ W_{21} & W_{22} & W_{23} \\ W_{31} & W_{32} & W_{33} \end{pmatrix} \begin{pmatrix} \psi_1^d \\ \psi_2^d \\ \psi_3^d \end{pmatrix} = 0, \tag{2.6}$$

where $\mathbf{W} = \mathbf{A}^{\dagger}\mathbf{U}\mathbf{A}$ (see **Appendix A**) with $U_{ij} = u_i\delta_{ij}$, under the condition:

$$\vec{\nabla}\mathbf{A} + \vec{\tau}\mathbf{A} = 0. \tag{2.7}$$

This equation was first formulated by M. Baer,[5] and is known as Adiabatic-Diabatic Transformation (ADT) condition. In order to a obtain a meaningful solution of Eq. (2.7), we have to ensure that the chosen form of **A** matrix has the following features: (a) It is orthogonal at any point in configuration space; (b) Its' elements are cyclic functions with respect to a parameter, i.e., starting with an unit diagonal matrix, the chosen form of **A** matrix has to generate a diagonal matrix with even number (-1)s after completing the cycle.

In case of three-dimensional Hilbert space, there are nine elements in the ADT matrix (**A**). Since the model form of **A** has to be an orthogonal matrix and the ortho-normality conditions demand the fulfillment of six relations, three independent variables namely Euler like angles of rotation [$\theta_{12}(\mathbf{n})$, $\theta_{23}(\mathbf{n})$ and $\theta_{13}(\mathbf{n})$], commonly called ADT angles, are the natural requirement to construct the three state **A** matrix by taking the product of three rotation matrices, $\mathbf{A}_{12}(\theta_{12})$, $\mathbf{A}_{23}(\theta_{23})$, and $\mathbf{A}_{13}(\theta_{13})$. Let us define these three rotation matrices [$\mathbf{A}_{12}(\theta_{12})$, $\mathbf{A}_{23}(\theta_{23})$, and $\mathbf{A}_{13}(\theta_{13})$] and one of the ways of their product (**A**) as:

$$\begin{aligned}
&\mathbf{A}(\theta_{\mathbf{12}}, \theta_{\mathbf{23}}, \theta_{\mathbf{13}}) = \mathbf{A}_{12}(\theta_{12}) \cdot \mathbf{A}_{23}(\theta_{23}) \cdot \mathbf{A}_{13}(\theta_{13}) \\
&= \begin{pmatrix} \cos\theta_{12} & \sin\theta_{12} & 0 \\ -\sin\theta_{12} & \cos\theta_{12} & 0 \\ 0 & 0 & 1 \end{pmatrix} \begin{pmatrix} 1 & 0 & 0 \\ 0 & \cos\theta_{23} & \sin\theta_{23} \\ 0 & -\sin\theta_{23} & \cos\theta_{23} \end{pmatrix} \begin{pmatrix} \cos\theta_{13} & 0 & \sin\theta_{13} \\ 0 & 1 & 0 \\ -\sin\theta_{13} & 0 & \cos\theta_{13} \end{pmatrix} \\
&= \begin{pmatrix} \begin{matrix}\cos\theta_{12}\cos\theta_{13} \\ -\sin\theta_{12}\sin\theta_{13}\sin\theta_{23}\end{matrix} & \sin\theta_{12}\cos\theta_{23} & \begin{matrix}\cos\theta_{12}\sin\theta_{13} \\ +\sin\theta_{12}\cos\theta_{13}\sin\theta_{23}\end{matrix} \\ \\ \begin{matrix}-\sin\theta_{12}\cos\theta_{13} \\ -\cos\theta_{12}\sin\theta_{13}\sin\theta_{23}\end{matrix} & \cos\theta_{12}\cos\theta_{23} & \begin{matrix}-\sin\theta_{12}\sin\theta_{13} \\ +\cos\theta_{12}\cos\theta_{13}\sin\theta_{23}\end{matrix} \\ \\ -\sin\theta_{13}\cos\theta_{23} & -\sin\theta_{23} & \cos\theta_{13}\cos\theta_{23} \end{pmatrix}.
\end{aligned} \tag{2.8}$$

When we substitute the above model form of **A** matrix [Eq. (2.8)] and the anti-symmetric form of $\boldsymbol{\tau}$ matrix [Eq. (2.5)] in Eq. (2.8), the simple manipulation as performed by Top and Baer[6] and Alijah and Baer[7] leads to the following equations for ADT angles:

$$\vec{\nabla}\theta_{12} = -\vec{\tau}_{12} + \tan\theta_{23}(\vec{\tau}_{13}\cos\theta_{12} - \vec{\tau}_{23}\sin\theta_{12}), \tag{2.9a}$$

$$\vec{\nabla}\theta_{23} = -(\vec{\tau}_{13}\sin\theta_{12} + \vec{\tau}_{23}\cos\theta_{12}), \tag{2.9b}$$

$$\vec{\nabla}\theta_{13} = -\frac{1}{\cos\theta_{23}}(\vec{\tau}_{13}\cos\theta_{12} - \vec{\tau}_{23}\sin\theta_{12}), \tag{2.9c}$$

which in turn brings the explicit form of τ matrix elements in terms of ADT angles:

$$\vec{\tau}_{12} = -\vec{\nabla}\theta_{12} - \sin\theta_{23}\vec{\nabla}\theta_{13}, \tag{2.10a}$$

$$\vec{\tau}_{23} = \sin\theta_{12}\cos\theta_{23}\vec{\nabla}\theta_{13} - \cos\theta_{12}\vec{\nabla}\theta_{23}, \tag{2.10b}$$

$$\vec{\tau}_{13} = -\cos\theta_{12}\cos\theta_{23}\vec{\nabla}\theta_{13} - \sin\theta_{12}\vec{\nabla}\theta_{23}, \tag{2.10c}$$

Once the non-adiabatic coupling elements $\vec{\tau}_{12}$, $\vec{\tau}_{23}$ and $\vec{\tau}_{13}$ are evaluated by using *ab initio* calculation for a particular nuclear configuration, the solution of Eqs. (2.9) provides the ADT angles for the same nuclear configuration. On the other hand, if we have the total electron-nuclear Hamiltonian of a molecular system in the diabatic representation, one can calculate the ADT matrix by diagonalizing the **W** matrix [Eq. (2.6)] and thereby, obtain the NAC elements through Eq. (2.10).

A Curl condition[5] for each NAC element, $\vec{\tau}_{ij}$, has been derived and proved to exist for an isolated group of states (sub-Hilbert space) by considering the analyticity of the ADT matrix **A** for a pair of nuclear degrees of freedom,

$$\frac{\partial}{\partial p}\tau^q_{ij} - \frac{\partial}{\partial q}\tau^p_{ij} = (\boldsymbol{\tau}^q\boldsymbol{\tau}^p)_{ij} - (\boldsymbol{\tau}^p\boldsymbol{\tau}^q)_{ij},$$
$$\tau^p_{ij} = \langle\xi_i|\nabla_p\xi_j\rangle, \qquad \tau^q_{ij} = \langle\xi_i|\nabla_q\xi_j\rangle. \tag{2.11}$$

where p and q are in *Cartesian coordinates* with $\nabla_p = \frac{\partial}{\partial p}$ and $\nabla_q = \frac{\partial}{\partial q}$.

Thus, the explicit form of Curl equation in terms of ADT angles for each NAC element is obtained by using Eqs. (2.10) and (2.11) as below:

$$
\begin{aligned}
\text{Curl } \tau_{12}^{pq} = [\boldsymbol{\tau} \times \boldsymbol{\tau}]_{12}^{pq} &= -\cos\theta_{23}(\nabla_q\theta_{23}\nabla_p\theta_{13} - \nabla_p\theta_{23}\nabla_q\theta_{13}) && (2.12a)\\
\text{Curl } \tau_{23}^{pq} = [\boldsymbol{\tau} \times \boldsymbol{\tau}]_{23}^{pq} &= \cos\theta_{12}\cos\theta_{23}(\nabla_q\theta_{12}\nabla_p\theta_{13} - \nabla_p\theta_{12}\nabla_q\theta_{13})\\
&- \sin\theta_{12}\sin\theta_{23}(\nabla_q\theta_{23}\nabla_p\theta_{13} - \nabla_p\theta_{23}\nabla_q\theta_{13})\\
&+ \sin\theta_{12}(\nabla_q\theta_{12}\nabla_p\theta_{23} - \nabla_p\theta_{12}\nabla_q\theta_{23}) && (2.12b)\\
\text{Curl } \tau_{13}^{pq} = [\boldsymbol{\tau} \times \boldsymbol{\tau}]_{13}^{pq} &= \sin\theta_{12}\cos\theta_{23}(\nabla_q\theta_{12}\nabla_p\theta_{13} - \nabla_p\theta_{12}\nabla_q\theta_{13})\\
&+ \cos\theta_{12}\sin\theta_{23}(\nabla_q\theta_{23}\nabla_p\theta_{13} - \nabla_p\theta_{23}\nabla_q\theta_{13})\\
&- \cos\theta_{12}(\nabla_q\theta_{12}\nabla_p\theta_{23} - \nabla_p\theta_{12}\nabla_q\theta_{23}) && (2.12c)
\end{aligned}
$$

where the Divergence of $\vec{\tau}_{ij}$s [Eq. (2.10)] are given by:

$$
\begin{aligned}
\text{div } \vec{\tau}_{12} &= 2\sin\theta_{12}\cos\theta_{12}\cos^2\theta_{23}(\vec{\nabla}\theta_{13}\cdot\vec{\nabla}\theta_{13}) - 2\sin\theta_{12}\cos\theta_{12}(\vec{\nabla}\theta_{23}\cdot\vec{\nabla}\theta_{23})\\
&- 3\cos^2\theta_{12}\cos\theta_{23}(\vec{\nabla}\theta_{13}\cdot\vec{\nabla}\theta_{23}) + \sin^2\theta_{12}\cos\theta_{23}(\vec{\nabla}\theta_{13}\cdot\vec{\nabla}\theta_{23})\\
&- \sin\theta_{23}\nabla^2\theta_{13} - \nabla^2\theta_{12} && (2.13a)\\
\text{div } \vec{\tau}_{23} &= 2\sin\theta_{12}\sin\theta_{23}\cos\theta_{23}(\vec{\nabla}\theta_{13}\cdot\vec{\nabla}\theta_{13}) + 3\cos\theta_{12}\cos\theta_{23}(\vec{\nabla}\theta_{12}\cdot\vec{\nabla}\theta_{23})\\
&+ 3\sin\theta_{12}(\vec{\nabla}\theta_{12}\cdot\vec{\nabla}\theta_{23}) + \sin\theta_{12}\sin\theta_{23}(\vec{\nabla}\theta_{13}\cdot\vec{\nabla}\theta_{23})\\
&+ \sin\theta_{12}\cos\theta_{23}\nabla^2\theta_{12} - \cos\theta_{12}\nabla^2\theta_{23} && (2.13b)\\
\text{div } \vec{\tau}_{13} &= 2\sin\theta_{12}\sin\theta_{23}\cos\theta_{23}(\vec{\nabla}\theta_{12}\cdot\vec{\nabla}\theta_{12}) + 3\sin\theta_{12}\cos\theta_{23}(\vec{\nabla}\theta_{12}\cdot\vec{\nabla}\theta_{13})\\
&- 3\cos\theta_{12}(\vec{\nabla}\theta_{12}\cdot\vec{\nabla}\theta_{23}) - \cos\theta_{12}\sin\theta_{23}(\vec{\nabla}\theta_{13}\cdot\vec{\nabla}\theta_{23})\\
&- \cos\theta_{12}\cos\theta_{23}\nabla^2\theta_{13} - \sin\theta_{12}\nabla^2\theta_{23}. && (2.13c)
\end{aligned}
$$

Moreover, it is possible to show that there are altogether six (6) different ways to take the product of the three rotation matrices [$\mathbf{A}_{12}(\theta_{12})$, $\mathbf{A}_{13}(\theta_{13})$, and $\mathbf{A}_{23}(\theta_{23})$] to obtain the ADT matrix ($\mathbf{A}$):

$$
\mathbf{A} = P_n\{\mathbf{A}_{12}(\theta_{12})\cdot\mathbf{A}_{23}(\theta_{23})\cdot\mathbf{A}_{13}(\theta_{13})\}, \qquad n = 1, \ldots N!, \qquad (2.14)
$$

where P_n is the nth permutation between two rotation matrix. Indeed, it is important to note that each ADT matrix can provide similar set of differential equations for ADT angles [Eq. (2.9)], NAC elements [Eq. (2.10)] and their Curl - Divergence equations [Eqs. (2.12) and (2.13)].

Since $\vec{\nabla}\theta_{ij}$s and in general, $\nabla^2\theta_{ij}$s are non - zero around the conical intersection, the Divergence of the vector field ($\vec{\tau}_{ij}$) are non - vanishing for any arbitrary values of ADT angles and thereby, the vector field may show up non - zero Curl.[8,9] On the other hand, as a non - adiabatic coupling term of the kind, $\vec{\tau}_{ii+1}(\mathbf{n})$, associated with a $(i, i+1)$ CI with a singularity (pole) at the same CI point, decays like $\frac{1}{r}$ (where r is the distance from the CI), such vector field could be resolved into irrotational (longitudinal) and solenoidal (transverse) components.[8,9] Though the theory of electrodynamics, by definition, reminds that the Curl of longitudinal part (of vector field) is zero but Curl of transverse part may or may not, experimental observations on so-called solenoids intend to argue that if infinitely long contour lines (seams) due to conical intersection are considered as infinitesimal narrow "solenoids", seams should produce zero field outside of them but *ab initio* calculations[10,11] show the presence of non - zero $\vec{\tau}$ in the space surrounding the seams. At this junction, we may also mention about Abelian and non-Abelian magnitudes of Curl equations,[12] where it has been shown that for any two state ($N = 2$) sub-Hilbert space, the components of NAC matrices form Abelian Curl equation but for $N \geq 3$ cases, the Abelian or non-Abelian nature of Curl equation is yet to be explored.

The following section demonstrates that in order to formulate single surface EBO equation, it is necessary to find out the nature of Curl τ_{ij}^{pq}s quantitatively, at least around the point of CI, for a given sub - Hilbert space. Let us start with the matrix representation of three state adiabatic Schroedinger equation [Eq. (2.4)] as given by,

$$-\frac{\hbar^2}{2m}(\vec{\nabla} + \vec{\boldsymbol{\tau}})^2\Psi + (\mathbf{U} - E)\Psi = 0, \quad U_{ij} = u_i\delta_{ij}. \tag{2.15}$$

We wish to persue an unitary transformation on Eq. (2.15) by a matrix, $\mathbf{G}$ ($\Psi = \mathbf{G}\Phi$), such that it leads to the following form:

$$-\frac{\hbar^2}{2m}(\mathbf{G}^\dagger\vec{\nabla}\mathbf{G} + i\vec{\omega})^2\Phi + (\mathbf{V} - E)\Phi = 0, \quad \mathbf{V} = \mathbf{G}^\dagger\mathbf{U}\mathbf{G}, \quad i\vec{\omega} = \mathbf{G}^\dagger\vec{\boldsymbol{\tau}}\mathbf{G}, \tag{2.16}$$

where the eigenvalues (0 and $\pm i\vec{\omega}$) of the NAC matrix, $\vec{\boldsymbol{\tau}}$ should be vectors (including the null vector) in order to obtain physically meaningful (a scalar) Hamiltonian [Eq. (2.16)] and thereby, one can impose the BO approximation, $|\psi_1| >> |\psi_i|$, $i = 2, 3$, by considering the upper electronic states as classically closed at low enough energy, to formulate the single surface adiabatic nuclear SE (EBO).[13]

On the other hand, since the straight forward diagonalization of $\vec{\boldsymbol{\tau}}$ matrix [Eqs. (2.5) and (2.10)] gives scalar eigenvalues,

$$\omega = \pm\sqrt{\vec{\tau}_{12}\cdot\vec{\tau}_{12} + \vec{\tau}_{23}\cdot\vec{\tau}_{23} + \vec{\tau}_{13}\cdot\vec{\tau}_{13}}$$

$$= \pm\Big\{\sum_i \Big[\Big(\frac{\partial\theta_{12}}{\partial p_i}\Big)^2 + \Big(\frac{\partial\theta_{23}}{\partial p_i}\Big)^2 + \Big(\frac{\partial\theta_{13}}{\partial p_i}\Big)^2 + 2\sin\theta_{23}\Big(\frac{\partial\theta_{13}}{\partial p_i}\Big)\Big(\frac{\partial\theta_{12}}{\partial p_i}\Big)\Big]\Big\}^{\frac{1}{2}}, p_i \equiv x, y, z, \ldots. \tag{2.17}$$

but the requirement of Eq. (2.16) dictates that the eigenvalues ($\pm i\vec{\omega}$) of $\vec{\boldsymbol{\tau}}$ matrix must be vectors, the only possibility remains that the $\vec{\boldsymbol{\tau}}$ matrix could be written as the product of a vector function, $\vec{\nabla}\eta$ ($\eta \equiv \theta_{12}$ or θ_{23} or θ_{13}) and a ADT angle dependent anti - symmetric scalar matrix, $\boldsymbol{g}(\theta_{12}, \theta_{23}, \theta_{13})$. In the following paragraph, we explore to find the condition to write, $\vec{\boldsymbol{\tau}} = \vec{\nabla}\eta \cdot \boldsymbol{g}(\theta_{12}, \theta_{23}, \theta_{13})$ and present its' consequence.

The vector quantities, $\vec{\nabla}\theta_{13}$ and $\vec{\nabla}\theta_{23}$ in terms of its' Cartesian components,

$$\vec{\nabla}\theta_{13} = \vec{i}\nabla_p\theta_{13} + \vec{j}\nabla_q\theta_{13} + \cdots, \tag{2.18a}$$

$$\vec{\nabla}\theta_{23} = \vec{i}\nabla_p\theta_{23} + \vec{j}\nabla_q\theta_{23} + \cdots, \tag{2.18b}$$

are rewritten as below,

$$\vec{\nabla}\theta_{13} = \vec{i}\Big(\frac{\nabla_p\theta_{13}}{\nabla_p\theta_{12}}\Big)\nabla_p\theta_{12} + \vec{j}\Big(\frac{\nabla_q\theta_{13}}{\nabla_q\theta_{12}}\Big)\nabla_q\theta_{12} + \cdots, \tag{2.19a}$$

$$\vec{\nabla}\theta_{23} = \vec{i}\Big(\frac{\nabla_p\theta_{23}}{\nabla_p\theta_{12}}\Big)\nabla_p\theta_{12} + \vec{j}\Big(\frac{\nabla_q\theta_{23}}{\nabla_q\theta_{12}}\Big)\nabla_q\theta_{12} + \cdots, \tag{2.19b}$$

which in turn with the assumed identities, $\left(\frac{\nabla_p\theta_{13}}{\nabla_p\theta_{12}}\right) = \left(\frac{\nabla_q\theta_{13}}{\nabla_q\theta_{12}}\right)$ and $\left(\frac{\nabla_p\theta_{23}}{\nabla_p\theta_{12}}\right) = \left(\frac{\nabla_q\theta_{23}}{\nabla_q\theta_{12}}\right)$, take the following form,

$$\begin{aligned}
\vec{\nabla}\theta_{13} &= \vec{i}\Big(\frac{\nabla_p\theta_{13}}{\nabla_p\theta_{12}}\Big)\nabla_p\theta_{12} + \vec{j}\Big(\frac{\nabla_p\theta_{13}}{\nabla_p\theta_{12}}\Big)\nabla_q\theta_{12} + \cdots, \\
&= \Big(\frac{\nabla_p\theta_{13}}{\nabla_p\theta_{12}}\Big)\vec{\nabla}\theta_{12} = \Big(\frac{\nabla_q\theta_{13}}{\nabla_q\theta_{12}}\Big)\vec{\nabla}\theta_{12} = \cdots, \qquad (2.20a)\\
\vec{\nabla}\theta_{23} &= \vec{i}\Big(\frac{\nabla_p\theta_{23}}{\nabla_p\theta_{12}}\Big)\nabla_p\theta_{12} + \vec{j}\Big(\frac{\nabla_p\theta_{23}}{\nabla_p\theta_{12}}\Big)\nabla_q\theta_{12} + \cdots, \\
&= \Big(\frac{\nabla_p\theta_{23}}{\nabla_p\theta_{12}}\Big)\vec{\nabla}\theta_{12} = \Big(\frac{\nabla_q\theta_{23}}{\nabla_q\theta_{12}}\Big)\vec{\nabla}\theta_{12} = \cdots, \qquad (2.20b)
\end{aligned}$$

leading to the $\vec{\tau}$ matrix,

$$\begin{aligned}
\vec{\boldsymbol{\tau}} &= \vec{\nabla}\theta_{12}\begin{pmatrix}
0 & -1-\sin\theta_{23}\Big(\frac{\nabla_p\theta_{13}}{\nabla_p\theta_{12}}\Big) & \begin{matrix}-\sin\theta_{12}\Big(\frac{\nabla_p\theta_{23}}{\nabla_p\theta_{12}}\Big)- \\ \cos\theta_{12}\cos\theta_{23}\Big(\frac{\nabla_p\theta_{13}}{\nabla_p\theta_{12}}\Big)\end{matrix} \\
1+\sin\theta_{23}\Big(\frac{\nabla_p\theta_{13}}{\nabla_p\theta_{12}}\Big) & 0 & \begin{matrix}-\cos\theta_{12}\Big(\frac{\nabla_p\theta_{23}}{\nabla_p\theta_{12}}\Big)+ \\ \sin\theta_{12}\cos\theta_{23}\Big(\frac{\nabla_p\theta_{13}}{\nabla_p\theta_{12}}\Big)\end{matrix} \\
\begin{matrix}\sin\theta_{12}\Big(\frac{\nabla_p\theta_{23}}{\nabla_p\theta_{12}}\Big)+ \\ \cos\theta_{12}\cos\theta_{23}\Big(\frac{\nabla_p\theta_{13}}{\nabla_p\theta_{12}}\Big)\end{matrix} & \begin{matrix}\cos\theta_{12}\Big(\frac{\nabla_p\theta_{23}}{\nabla_p\theta_{12}}\Big)- \\ \sin\theta_{12}\cos\theta_{23}\Big(\frac{\nabla_p\theta_{13}}{\nabla_p\theta_{12}}\Big)\end{matrix} & 0
\end{pmatrix} \\
&= \vec{\nabla}\theta_{12}\cdot\boldsymbol{g}(\theta_{12},\theta_{23},\theta_{13}), \qquad (2.21)
\end{aligned}$$

with eigenvalues, 0, $\pm i\vec{\omega}$ and $\vec{\omega} = \vec{\nabla}\theta_{12}\Big[1+\Big(\frac{\nabla_p\theta_{13}}{\nabla_p\theta_{12}}\Big)^2+\Big(\frac{\nabla_p\theta_{23}}{\nabla_p\theta_{12}}\Big)^2+2\sin\theta_{23}\Big(\frac{\nabla_p\theta_{13}}{\nabla_p\theta_{12}}\Big)\Big]^{\frac{1}{2}}$.

In summary, Eq. (2.16) clearly demonstrates that it is possible to formulate single surface EBO equation starting from any three state sub - Hilbert space only when non - adiabatic coupling matrix can be written as a product of vector function and anti - symmetric scalar matrix. Since this product form of NAC matrix implies the identities, $\left(\frac{\nabla_p\theta_{13}}{\nabla_p\theta_{12}}\right) = \left(\frac{\nabla_q\theta_{13}}{\nabla_q\theta_{12}}\right)$, $\left(\frac{\nabla_p\theta_{23}}{\nabla_p\theta_{12}}\right) = \left(\frac{\nabla_q\theta_{23}}{\nabla_q\theta_{12}}\right)$ and $\left(\frac{\nabla_p\theta_{23}}{\nabla_p\theta_{13}}\right) = \left(\frac{\nabla_q\theta_{23}}{\nabla_q\theta_{13}}\right)$, namely, Curl $\tau_{12}^{pq} = 0$s, [see **Appendix B**] the following section explores the validity of these identities, i.e., Curl τ_{ij}^{pq}s are zero or not, at least approximately, around CI(s). At the same time, we considered the *Induced Renner-Teller model*,[14–16] a three state BO system in the diabatic representation, to numerically verify the validity of Curl equations and show zero curls at and around the degeneracy at a single point.

Though the nuclear configuration space for any three state BO sub - Hilbert space could be dependent on many nuclear degrees of freedom, we carry out further theoretical developments on Curl equations considering only three nuclear coordinates just for analytical convenience but the approach can be extendable for any number of nuclear degrees of freedom. The Cartesian components of $\vec{\nabla} \times \vec{\tau}_{12}$ along the unit vectors, $\vec{i}$, $\vec{j}$, and $\vec{k}$ are given by:

$$\text{Curl } \tau_{12}^{yz} = -\cos\theta_{23}\left[\frac{\partial\theta_{23}}{\partial y}\frac{\partial\theta_{13}}{\partial z} - \frac{\partial\theta_{23}}{\partial z}\frac{\partial\theta_{13}}{\partial y}\right], \tag{2.22a}$$

$$\text{Curl } \tau_{12}^{zx} = -\cos\theta_{23}\left[\frac{\partial\theta_{23}}{\partial x}\frac{\partial\theta_{13}}{\partial z} - \frac{\partial\theta_{23}}{\partial z}\frac{\partial\theta_{13}}{\partial x}\right], \tag{2.22b}$$

$$\text{Curl } \tau_{12}^{xy} = -\cos\theta_{23}\left[\frac{\partial\theta_{23}}{\partial x}\frac{\partial\theta_{13}}{\partial y} - \frac{\partial\theta_{23}}{\partial y}\frac{\partial\theta_{13}}{\partial x}\right], \tag{2.22c}$$

whereas it's spherical polar components along the unit vectors, $\vec{r}$, $\vec{\theta}$, and $\vec{\phi}$ are:

$$\text{Curl } \tau_{12}^{\theta\phi} = -\frac{\cos\theta_{23}}{r^2\sin\theta}\left[\frac{\partial\theta_{23}}{\partial\theta}\frac{\partial\theta_{13}}{\partial\phi} - \frac{\partial\theta_{23}}{\partial\phi}\frac{\partial\theta_{13}}{\partial\theta}\right], \tag{2.23a}$$

$$\text{Curl } \tau_{12}^{r\phi} = -\frac{\cos\theta_{23}}{r\sin\theta}\left[\frac{\partial\theta_{23}}{\partial r}\frac{\partial\theta_{13}}{\partial\phi} - \frac{\partial\theta_{23}}{\partial\phi}\frac{\partial\theta_{13}}{\partial r}\right], \tag{2.23b}$$

$$\text{Curl } \tau_{12}^{r\theta} = -\frac{\cos\theta_{23}}{r}\left[\frac{\partial\theta_{23}}{\partial r}\frac{\partial\theta_{13}}{\partial\theta} - \frac{\partial\theta_{23}}{\partial\theta}\frac{\partial\theta_{13}}{\partial r}\right]. \tag{2.23c}$$

Let us consider the ratios, $A1 = \frac{\frac{\partial\theta_{23}}{\partial\theta}}{\frac{\partial\theta_{13}}{\partial\theta}} \cdot \frac{\frac{\partial\theta_{13}}{\partial r}}{\frac{\partial\theta_{23}}{\partial r}}$ and $A2 = \frac{\frac{\partial\theta_{23}}{\partial\phi}}{\frac{\partial\theta_{13}}{\partial\phi}} \cdot \frac{\frac{\partial\theta_{13}}{\partial r}}{\frac{\partial\theta_{23}}{\partial r}}$, rewrite these quantities by using the chain rule of differentiation,

$$A1 = \frac{\dfrac{\frac{\partial\theta_{23}}{\partial\theta}}{\frac{\partial\theta_{13}}{\partial\theta}}}{\dfrac{\frac{\partial\theta_{23}}{\partial r}}{\frac{\partial\theta_{13}}{\partial r}}} = \frac{\left(1+\frac{\frac{\partial\theta_{23}}{\partial y}}{\frac{\partial\theta_{23}}{\partial x}}\cdot\frac{\frac{\partial y}{\partial\theta}}{\frac{\partial x}{\partial\theta}}+\frac{\frac{\partial\theta_{23}}{\partial z}}{\frac{\partial\theta_{23}}{\partial x}}\cdot\frac{\frac{\partial z}{\partial\theta}}{\frac{\partial x}{\partial\theta}}\right)\left(1+\frac{\frac{\partial\theta_{13}}{\partial y}}{\frac{\partial\theta_{13}}{\partial x}}\cdot\frac{\frac{\partial y}{\partial r}}{\frac{\partial x}{\partial r}}+\frac{\frac{\partial\theta_{13}}{\partial z}}{\frac{\partial\theta_{13}}{\partial x}}\cdot\frac{\frac{\partial z}{\partial r}}{\frac{\partial x}{\partial r}}\right)}{\left(1+\frac{\frac{\partial\theta_{13}}{\partial y}}{\frac{\partial\theta_{13}}{\partial x}}\cdot\frac{\frac{\partial y}{\partial\theta}}{\frac{\partial x}{\partial\theta}}+\frac{\frac{\partial\theta_{13}}{\partial z}}{\frac{\partial\theta_{13}}{\partial x}}\cdot\frac{\frac{\partial z}{\partial\theta}}{\frac{\partial x}{\partial\theta}}\right)\left(1+\frac{\frac{\partial\theta_{23}}{\partial y}}{\frac{\partial\theta_{23}}{\partial x}}\cdot\frac{\frac{\partial y}{\partial r}}{\frac{\partial x}{\partial r}}+\frac{\frac{\partial\theta_{23}}{\partial z}}{\frac{\partial\theta_{23}}{\partial x}}\cdot\frac{\frac{\partial z}{\partial r}}{\frac{\partial x}{\partial r}}\right)}, \quad (2.24)$$

$$A2 = \frac{\dfrac{\frac{\partial\theta_{23}}{\partial\phi}}{\frac{\partial\theta_{13}}{\partial\phi}}}{\dfrac{\frac{\partial\theta_{23}}{\partial r}}{\frac{\partial\theta_{13}}{\partial r}}} = \frac{\left(1+\frac{\frac{\partial\theta_{23}}{\partial y}}{\frac{\partial\theta_{23}}{\partial x}}\cdot\frac{\frac{\partial y}{\partial\phi}}{\frac{\partial x}{\partial\phi}}+\frac{\frac{\partial\theta_{23}}{\partial z}}{\frac{\partial\theta_{23}}{\partial x}}\cdot\frac{\frac{\partial z}{\partial\phi}}{\frac{\partial x}{\partial\phi}}\right)\left(1+\frac{\frac{\partial\theta_{13}}{\partial y}}{\frac{\partial\theta_{13}}{\partial x}}\cdot\frac{\frac{\partial y}{\partial r}}{\frac{\partial x}{\partial r}}+\frac{\frac{\partial\theta_{13}}{\partial z}}{\frac{\partial\theta_{13}}{\partial x}}\cdot\frac{\frac{\partial z}{\partial r}}{\frac{\partial x}{\partial r}}\right)}{\left(1+\frac{\frac{\partial\theta_{13}}{\partial y}}{\frac{\partial\theta_{13}}{\partial x}}\cdot\frac{\frac{\partial y}{\partial\phi}}{\frac{\partial x}{\partial\phi}}+\frac{\frac{\partial\theta_{13}}{\partial z}}{\frac{\partial\theta_{13}}{\partial x}}\cdot\frac{\frac{\partial z}{\partial\phi}}{\frac{\partial x}{\partial\phi}}\right)\left(1+\frac{\frac{\partial\theta_{23}}{\partial y}}{\frac{\partial\theta_{23}}{\partial x}}\cdot\frac{\frac{\partial y}{\partial r}}{\frac{\partial x}{\partial r}}+\frac{\frac{\partial\theta_{23}}{\partial z}}{\frac{\partial\theta_{23}}{\partial x}}\cdot\frac{\frac{\partial z}{\partial r}}{\frac{\partial x}{\partial r}}\right)}, \quad (2.25)$$

and intend to find their nature by using the Jacobian determinant defined around CI with the assumptions, $\frac{\frac{\partial\theta_{23}}{\partial y}}{\frac{\partial\theta_{23}}{\partial x}} \neq \frac{\frac{\partial\theta_{13}}{\partial y}}{\frac{\partial\theta_{13}}{\partial x}}$ and $\frac{\frac{\partial\theta_{23}}{\partial z}}{\frac{\partial\theta_{23}}{\partial x}} \neq \frac{\frac{\partial\theta_{13}}{\partial z}}{\frac{\partial\theta_{13}}{\partial x}}$.

The Jacobian determinant for the transformation from Cartesian to polar is given by:

$$J(r,\theta,\phi) = \begin{vmatrix} \frac{\partial x}{\partial r} & \frac{\partial y}{\partial r} & \frac{\partial z}{\partial r} \\ \frac{\partial x}{\partial\theta} & \frac{\partial y}{\partial\theta} & \frac{\partial z}{\partial\theta} \\ \frac{\partial x}{\partial\phi} & \frac{\partial y}{\partial\phi} & \frac{\partial z}{\partial\phi} \end{vmatrix} = \begin{vmatrix} \sin\theta\cos\phi & \sin\theta\sin\phi & \cos\theta \\ r\cos\theta\cos\phi & r\cos\theta\sin\phi & -r\sin\theta \\ -r\sin\theta\sin\phi & r\sin\theta\cos\phi & 0 \end{vmatrix}. \quad (2.26)$$

When the origin of the coordinate system [r =0 (x = 0, y = 0, z = 0)] coincides with the point of conical intersection, various components of the Jacobian determinant vanishes at that point (CI). It is important to note that this transformation remain valid with zero content at r = 0, along with $\frac{\partial z}{\partial\phi} = 0$ (also at $r \neq 0$), $\frac{\partial y}{\partial\phi} = r\sin\theta\cos\phi = 0$, $\frac{\partial z}{\partial\theta} = -r\sin\theta = 0$,

$\frac{\partial y}{\partial \theta} = r\cos\theta\sin\phi = 0$ and

$$\frac{\partial(x,y)}{\partial(r,\theta)} = \begin{vmatrix} \frac{\partial x}{\partial r} & \frac{\partial y}{\partial r} \\ \frac{\partial x}{\partial \theta} & \frac{\partial y}{\partial \theta} \end{vmatrix} = 0 \qquad \Rightarrow \frac{\frac{\partial y}{\partial \theta}}{\frac{\partial x}{\partial \theta}} = \frac{\frac{\partial y}{\partial r}}{\frac{\partial x}{\partial r}}, \tag{2.27a}$$

$$\frac{\partial(x,z)}{\partial(r,\theta)} = \begin{vmatrix} \frac{\partial x}{\partial r} & \frac{\partial z}{\partial r} \\ \frac{\partial x}{\partial \theta} & \frac{\partial z}{\partial \theta} \end{vmatrix} = -r\cos\theta = 0 \qquad \Rightarrow \frac{\frac{\partial z}{\partial \theta}}{\frac{\partial x}{\partial \theta}} = \frac{\frac{\partial z}{\partial r}}{\frac{\partial x}{\partial r}}, \tag{2.27b}$$

$$\frac{\partial(x,y)}{\partial(r,\phi)} = \begin{vmatrix} \frac{\partial x}{\partial r} & \frac{\partial y}{\partial r} \\ \frac{\partial x}{\partial \phi} & \frac{\partial y}{\partial \phi} \end{vmatrix} = r\sin^2\theta = 0 \qquad \Rightarrow \frac{\frac{\partial y}{\partial \phi}}{\frac{\partial x}{\partial \phi}} = \frac{\frac{\partial y}{\partial r}}{\frac{\partial x}{\partial r}}, \tag{2.27c}$$

$$\frac{\partial(x,z)}{\partial(r,\phi)} = \begin{vmatrix} \frac{\partial x}{\partial r} & \frac{\partial z}{\partial r} \\ \frac{\partial x}{\partial \phi} & \frac{\partial z}{\partial \phi} \end{vmatrix} = r\sin\theta\sin\phi\cos\phi = 0 \qquad \Rightarrow \frac{\frac{\partial z}{\partial \phi}}{\frac{\partial x}{\partial \phi}} = \frac{\frac{\partial z}{\partial r}}{\frac{\partial x}{\partial r}}. \tag{2.27d}$$

On the other hand, even if the point of conical intersection(s) is away from the origin of the coordinate system, parametric representation for the vector equation of a conical surface predicts $J(r,\theta) = 0$, $J(r,\phi) = 0$ and $J(\theta,\phi) = 0$ at the singularity (CI) (see **Appendix C**).

At $r = 0$, we substitute the Jacobian relations [Eqs. (2.27)] in both the Eqs. (2.24) and (2.25), find that, even if we have assumed $\frac{\frac{\partial \theta_{23}}{\partial y}}{\frac{\partial \theta_{23}}{\partial x}} \neq \frac{\frac{\partial \theta_{13}}{\partial y}}{\frac{\partial \theta_{13}}{\partial x}}$ and $\frac{\frac{\partial \theta_{23}}{\partial z}}{\frac{\partial \theta_{23}}{\partial x}} \neq \frac{\frac{\partial \theta_{13}}{\partial z}}{\frac{\partial \theta_{13}}{\partial x}}$, the ratios ($A1$ and $A2$) turns into unity, i.e.,

$$\frac{\frac{\partial \theta_{23}}{\partial \theta}}{\frac{\partial \theta_{23}}{\partial r}} = \frac{\frac{\partial \theta_{13}}{\partial \theta}}{\frac{\partial \theta_{13}}{\partial r}} \qquad \Rightarrow \frac{\partial \theta_{23}}{\partial r}\frac{\partial \theta_{13}}{\partial \theta} - \frac{\partial \theta_{23}}{\partial \theta}\frac{\partial \theta_{13}}{\partial r} = 0 \tag{2.28a}$$

$$\text{and} \quad \frac{\frac{\partial \theta_{23}}{\partial \phi}}{\frac{\partial \theta_{23}}{\partial r}} = \frac{\frac{\partial \theta_{13}}{\partial \phi}}{\frac{\partial \theta_{13}}{\partial r}} \qquad \Rightarrow \frac{\partial \theta_{23}}{\partial r}\frac{\partial \theta_{13}}{\partial \phi} - \frac{\partial \theta_{23}}{\partial \phi}\frac{\partial \theta_{13}}{\partial r} = 0. \tag{2.28b}$$

At $r \neq 0$, we analyze the ratios, $A1$ and $A2$, with the following two assumptions: (i) $\frac{\frac{\partial \theta_{23}}{\partial y}}{\frac{\partial \theta_{23}}{\partial x}} \neq \frac{\frac{\partial \theta_{13}}{\partial y}}{\frac{\partial \theta_{13}}{\partial x}}$ and $\frac{\frac{\partial \theta_{23}}{\partial z}}{\frac{\partial \theta_{23}}{\partial x}} \neq \frac{\frac{\partial \theta_{13}}{\partial z}}{\frac{\partial \theta_{13}}{\partial x}}$; (ii) the chosen value of r is theoretically non-zero but numerically negligible. The second assumption ($r \simeq 0$) translates the Jacobian relations as,

$$\frac{\partial(x,y)}{\partial(r,\theta)} = \begin{vmatrix} \frac{\partial x}{\partial r} & \frac{\partial y}{\partial r} \\ \frac{\partial x}{\partial \theta} & \frac{\partial y}{\partial \theta} \end{vmatrix} = 0 \qquad \Rightarrow \frac{\frac{\partial y}{\partial \theta}}{\frac{\partial x}{\partial \theta}} = \frac{\frac{\partial y}{\partial r}}{\frac{\partial x}{\partial r}}, \tag{2.29a}$$

$$\frac{\partial(x,z)}{\partial(r,\theta)} = \begin{vmatrix} \frac{\partial x}{\partial r} & \frac{\partial z}{\partial r} \\ \frac{\partial x}{\partial \theta} & \frac{\partial z}{\partial \theta} \end{vmatrix} = -r\cos\theta \simeq \epsilon \simeq 0 \qquad \Rightarrow \frac{\frac{\partial z}{\partial \theta}}{\frac{\partial x}{\partial \theta}} \simeq \frac{\frac{\partial z}{\partial r}}{\frac{\partial x}{\partial r}}, \tag{2.29b}$$

$$\frac{\partial(x,y)}{\partial(r,\phi)} = \begin{vmatrix} \frac{\partial x}{\partial r} & \frac{\partial y}{\partial r} \\ \frac{\partial x}{\partial \phi} & \frac{\partial y}{\partial \phi} \end{vmatrix} = r\sin^2\theta \simeq \epsilon \simeq 0 \qquad \Rightarrow \frac{\frac{\partial y}{\partial \phi}}{\frac{\partial x}{\partial \phi}} \simeq \frac{\frac{\partial y}{\partial r}}{\frac{\partial x}{\partial r}}, \tag{2.29c}$$

$$\frac{\partial(x,z)}{\partial(r,\phi)} = \begin{vmatrix} \frac{\partial x}{\partial r} & \frac{\partial z}{\partial r} \\ \frac{\partial x}{\partial \phi} & \frac{\partial z}{\partial \phi} \end{vmatrix} = r\sin\theta\sin\phi\cos\phi \simeq \epsilon \simeq 0 \qquad \Rightarrow \frac{\frac{\partial z}{\partial \phi}}{\frac{\partial x}{\partial \phi}} \simeq \frac{\frac{\partial z}{\partial r}}{\frac{\partial x}{\partial r}}, \tag{2.29d}$$

and thereby, approximates the ratios $A1$ and $A2$ as,

$$A1 \simeq 1 \qquad \Rightarrow \frac{\frac{\partial\theta_{23}}{\partial\theta}}{\frac{\partial\theta_{23}}{\partial r}} \simeq \frac{\frac{\partial\theta_{13}}{\partial\theta}}{\frac{\partial\theta_{13}}{\partial r}} \qquad \Rightarrow \frac{\partial\theta_{23}}{\partial r}\frac{\partial\theta_{13}}{\partial\theta} - \frac{\partial\theta_{23}}{\partial\theta}\frac{\partial\theta_{13}}{\partial r} \simeq 0, \tag{2.30a}$$

$$A2 \simeq 1 \qquad \Rightarrow \frac{\frac{\partial\theta_{23}}{\partial\phi}}{\frac{\partial\theta_{23}}{\partial r}} \simeq \frac{\frac{\partial\theta_{13}}{\partial\phi}}{\frac{\partial\theta_{13}}{\partial r}} \qquad \Rightarrow \frac{\partial\theta_{23}}{\partial r}\frac{\partial\theta_{13}}{\partial\phi} - \frac{\partial\theta_{23}}{\partial\phi}\frac{\partial\theta_{13}}{\partial r} \simeq 0. \tag{2.30b}$$

Finally, in order to analyze the first assumption we define the following ratios, $B1 = \frac{\frac{\partial\theta_{23}}{\partial y}}{\frac{\partial\theta_{13}}{\partial y}} \cdot \frac{\frac{\partial\theta_{13}}{\partial x}}{\frac{\partial\theta_{23}}{\partial x}}$ and $B2 = \frac{\frac{\partial\theta_{23}}{\partial z}}{\frac{\partial\theta_{13}}{\partial z}} \cdot \frac{\frac{\partial\theta_{13}}{\partial x}}{\frac{\partial\theta_{23}}{\partial x}}$, and express in terms of polar coordinate by using the chain rule of differentiation,

$$B1 = \frac{\frac{\frac{\partial\theta_{23}}{\partial y}}{\frac{\partial\theta_{13}}{\partial y}}}{\frac{\frac{\partial\theta_{23}}{\partial x}}{\frac{\partial\theta_{13}}{\partial x}}} = \frac{\left(1 + \frac{\frac{\partial\theta_{23}}{\partial\theta}}{\frac{\partial\theta_{23}}{\partial r}} \cdot \frac{\frac{\partial\theta}{\partial y}}{\frac{\partial r}{\partial y}} + \frac{\frac{\partial\theta_{23}}{\partial\phi}}{\frac{\partial\theta_{23}}{\partial r}} \cdot \frac{\frac{\partial\phi}{\partial y}}{\frac{\partial r}{\partial y}}\right)\left(1 + \frac{\frac{\partial\theta_{13}}{\partial\theta}}{\frac{\partial\theta_{13}}{\partial r}} \cdot \frac{\frac{\partial\theta}{\partial x}}{\frac{\partial r}{\partial x}} + \frac{\frac{\partial\theta_{13}}{\partial\phi}}{\frac{\partial\theta_{13}}{\partial r}} \cdot \frac{\frac{\partial\phi}{\partial x}}{\frac{\partial r}{\partial x}}\right)}{\left(1 + \frac{\frac{\partial\theta_{13}}{\partial\theta}}{\frac{\partial\theta_{13}}{\partial r}} \cdot \frac{\frac{\partial\theta}{\partial y}}{\frac{\partial r}{\partial y}} + \frac{\frac{\partial\theta_{13}}{\partial\phi}}{\frac{\partial\theta_{13}}{\partial r}} \cdot \frac{\frac{\partial\phi}{\partial y}}{\frac{\partial r}{\partial y}}\right)\left(1 + \frac{\frac{\partial\theta_{23}}{\partial\theta}}{\frac{\partial\theta_{23}}{\partial r}} \cdot \frac{\frac{\partial\theta}{\partial x}}{\frac{\partial r}{\partial x}} + \frac{\frac{\partial\theta_{23}}{\partial\phi}}{\frac{\partial\theta_{23}}{\partial r}} \cdot \frac{\frac{\partial\phi}{\partial x}}{\frac{\partial r}{\partial x}}\right)}, \tag{2.31}$$

$$B2 = \frac{\frac{\frac{\partial\theta_{23}}{\partial z}}{\frac{\partial\theta_{13}}{\partial z}}}{\frac{\frac{\partial\theta_{23}}{\partial x}}{\frac{\partial\theta_{13}}{\partial x}}} = \frac{\left(1 + \frac{\frac{\partial\theta_{23}}{\partial\theta}}{\frac{\partial\theta_{23}}{\partial r}} \cdot \frac{\frac{\partial\theta}{\partial z}}{\frac{\partial r}{\partial z}} + \frac{\frac{\partial\theta_{23}}{\partial\phi}}{\frac{\partial\theta_{23}}{\partial r}} \cdot \frac{\frac{\partial\phi}{\partial z}}{\frac{\partial r}{\partial z}}\right)\left(1 + \frac{\frac{\partial\theta_{13}}{\partial\theta}}{\frac{\partial\theta_{13}}{\partial r}} \cdot \frac{\frac{\partial\theta}{\partial x}}{\frac{\partial r}{\partial x}} + \frac{\frac{\partial\theta_{13}}{\partial\phi}}{\frac{\partial\theta_{13}}{\partial r}} \cdot \frac{\frac{\partial\phi}{\partial x}}{\frac{\partial r}{\partial x}}\right)}{\left(1 + \frac{\frac{\partial\theta_{13}}{\partial\theta}}{\frac{\partial\theta_{13}}{\partial r}} \cdot \frac{\frac{\partial\theta}{\partial z}}{\frac{\partial r}{\partial z}} + \frac{\frac{\partial\theta_{13}}{\partial\phi}}{\frac{\partial\theta_{13}}{\partial r}} \cdot \frac{\frac{\partial\phi}{\partial z}}{\frac{\partial r}{\partial z}}\right)\left(1 + \frac{\frac{\partial\theta_{23}}{\partial\theta}}{\frac{\partial\theta_{23}}{\partial r}} \cdot \frac{\frac{\partial\theta}{\partial x}}{\frac{\partial r}{\partial x}} + \frac{\frac{\partial\theta_{23}}{\partial\phi}}{\frac{\partial\theta_{23}}{\partial r}} \cdot \frac{\frac{\partial\phi}{\partial x}}{\frac{\partial r}{\partial x}}\right)}. \tag{2.32}$$

When Eqs. (2.30a) and (2.30b) are substituted in Eqs. (2.31) and (2.32), we obtain $B1 \simeq 1$ and $B2 \simeq 1$, i.e., $\frac{\frac{\partial\theta_{23}}{\partial y}}{\frac{\partial\theta_{23}}{\partial x}} \simeq \frac{\frac{\partial\theta_{13}}{\partial y}}{\frac{\partial\theta_{13}}{\partial x}}$ and $\frac{\frac{\partial\theta_{23}}{\partial z}}{\frac{\partial\theta_{23}}{\partial x}} \simeq \frac{\frac{\partial\theta_{13}}{\partial z}}{\frac{\partial\theta_{13}}{\partial x}}$. These outcomes contradict the first assumption whereas the second assumption cannot be wrong at $r \simeq 0$.

Thus, the quantities $\left(\frac{\partial\theta_{23}}{\partial y}\frac{\partial\theta_{13}}{\partial x} - \frac{\partial\theta_{23}}{\partial x}\frac{\partial\theta_{13}}{\partial y}\right)$, $\left(\frac{\partial\theta_{23}}{\partial z}\frac{\partial\theta_{13}}{\partial x} - \frac{\partial\theta_{23}}{\partial x}\frac{\partial\theta_{13}}{\partial z}\right)$ and $\left(\frac{\partial\theta_{23}}{\partial y}\frac{\partial\theta_{13}}{\partial z} - \frac{\partial\theta_{23}}{\partial z}\frac{\partial\theta_{13}}{\partial y}\right)$, vis - a - vis Curl τ_{12}^{pq} $(p, q \equiv x, y, z)$ or $\left(\frac{\partial\theta_{23}}{\partial\theta}\frac{\partial\theta_{13}}{\partial r} - \frac{\partial\theta_{23}}{\partial r}\frac{\partial\theta_{13}}{\partial\theta}\right)$, $\left(\frac{\partial\theta_{23}}{\partial\phi}\frac{\partial\theta_{13}}{\partial r} - \frac{\partial\theta_{23}}{\partial r}\frac{\partial\theta_{13}}{\partial\phi}\right)$ and $\left(\frac{\partial\theta_{23}}{\partial\theta}\frac{\partial\theta_{13}}{\partial\phi} - \frac{\partial\theta_{23}}{\partial\phi}\frac{\partial\theta_{13}}{\partial\theta}\right)$, vis - a - vis Curl τ_{12}^{pq} $(p, q \equiv r, \theta, \phi)$ are either identically or approximately zero around the conical intersection and similar predictions for Curl τ_{23}^{pq} and Curl τ_{13}^{pq} can also be made. Overall the proof demands that the curl of the non - adiabatic coupling elements are either identically or approximately zero **only at and around the conical intersection point(s)**. In other words, when the system is away from the conical intersection point(s), the non - removable parts of the non - adiabatic coupling terms could be important with non - zero curls.

With these implication from Curl equations, we intend to rewrite Eq. (2.16) as,

$$\begin{aligned} - & \frac{\hbar^2}{2m}\Big[(\vec{\nabla} + i\vec{\omega})^2\Phi\Big] - \frac{\hbar^2}{2m}\Big[(\mathbf{G}^\dagger\nabla^2\mathbf{G}\Phi - \nabla^2\Phi) + (i\vec{\omega}\mathbf{G}^\dagger\vec{\nabla}\mathbf{G}\Phi - i\vec{\omega}\vec{\nabla}\Phi) \\ + & (\mathbf{G}^\dagger\vec{\nabla}\mathbf{G}i\vec{\omega}\Phi - \vec{\nabla}i\vec{\omega}\Phi)\Big] + \Big[(\mathbf{V} - E)\Phi\Big] = 0, \end{aligned} \tag{2.33}$$

where $\mathbf{G}$ is the transformation matrix that diagonalizes the anti - symmetric scaler matrix $\boldsymbol{g}(\theta_{12}, \theta_{23}, \theta_{13})$ as defined in Eq. (2.21) instead of NAC matrix, $\vec{\boldsymbol{\tau}}(\theta_{12}, \theta_{23}, \theta_{13})$ as shown in Eq. (2.16). For symbolic convenience, now onwards we shall replace $\mathbf{G}^\dagger$ as $\mathbf{G}^d$ and its' element $(\mathbf{G}^\dagger)_{ij}$ as $(\mathbf{G}^d)_{ij}$ $(\equiv G_{ij}^d)$.

The *i* th BO equation can be written from the matrix equation [Eq. (2.33)] as below,

$$\begin{aligned} - & \frac{\hbar^2}{2m}\Big[(\vec{\nabla} + i\vec{\omega})^2\Phi\Big]_i - \frac{\hbar^2}{2m}\Big[\sum_k G_{ik}^d\nabla^2\psi_k - \sum_k \nabla^2(G_{ik}^d\psi_k) + \sum_k i\vec{\omega}_i G_{ik}^d\vec{\nabla}\psi_k \\ - & \sum_k i\vec{\omega}_i\vec{\nabla}(G_{ik}^d\psi_k) + \sum_{km} G_{ik}^d\vec{\nabla}(\vec{\tau}_{km}\psi_m) - \sum_{km}\vec{\nabla}(G_{ik}^d\vec{\tau}_{km}\psi_m)\Big] + \Big[(\mathbf{V} - E)\Phi\Big]_i = 0. \end{aligned} \tag{2.34}$$

We manipulate the Eq. (2.34) by considering the following aspects: (a) Since the matrix representation of the ADT ($\Phi = \mathbf{G^d}\Psi$) is given by

$$\begin{pmatrix} \phi_1 \\ \phi_2 \\ \phi_3 \end{pmatrix} = \begin{pmatrix} \frac{g_3}{\eta} & -\frac{g_2}{\eta} & \frac{g_1}{\eta} \\ -\frac{g_1 g_3 + i\eta g_2}{\sqrt{2}\lambda\eta} & \frac{g_1 g_2 - i\eta g_3}{\sqrt{2}\lambda\eta} & \frac{\lambda}{\sqrt{2}\eta} \\ \frac{-g_1 g_3 + i\eta g_2}{\sqrt{2}\lambda\eta} & \frac{g_1 g_2 + i\eta g_3}{\sqrt{2}\lambda\eta} & \frac{\eta}{\sqrt{2}\eta} \end{pmatrix} \begin{pmatrix} \psi_1 \\ \psi_2 \\ \psi_3 \end{pmatrix}, \qquad (2.35)$$

with

$$\begin{aligned} g_1 &= -1 - \sin\theta_{23}\Big(\frac{\nabla_p\theta_{13}}{\nabla_p\theta_{12}}\Big), \\ g_2 &= -\sin\theta_{12}\Big(\frac{\nabla_p\theta_{23}}{\nabla_p\theta_{12}}\Big) - \cos\theta_{12}\cos\theta_{23}\Big(\frac{\nabla_p\theta_{13}}{\nabla_p\theta_{12}}\Big), \\ g_3 &= -\cos\theta_{12}\Big(\frac{\nabla_p\theta_{23}}{\nabla_p\theta_{12}}\Big) + \sin\theta_{12}\cos\theta_{23}\Big(\frac{\nabla_p\theta_{13}}{\nabla_p\theta_{12}}\Big), \\ \lambda &= \sqrt{g_2^2 + g_3^2} = \left[\Big(\frac{\nabla_p\theta_{23}}{\nabla_p\theta_{12}}\Big)^2 + \cos^2\theta_{23}\Big(\frac{\nabla_p\theta_{13}}{\nabla_p\theta_{12}}\Big)^2\right]^{\frac{1}{2}}, \\ \eta &= \sqrt{g_1^2 + g_2^2 + g_3^2} = \left[1 + \Big(\frac{\nabla_p\theta_{13}}{\nabla_p\theta_{12}}\Big)^2 + \Big(\frac{\nabla_p\theta_{23}}{\nabla_p\theta_{12}}\Big)^2 + 2\sin\theta_{23}\Big(\frac{\nabla_p\theta_{13}}{\nabla_p\theta_{12}}\Big)\right]^{\frac{1}{2}}, \end{aligned}$$

one can have the general identity

$$\psi_k = \frac{1}{G^d_{kk}}\phi_k - \sum_{l \neq k} \frac{G^d_{kl}}{G^d_{kk}}\psi_l \qquad k, l = 1, 2, 3; \qquad (2.36)$$

(b) The product, $V\Phi$, for the ith equation can be rearranged as below,

$$(V\Phi)_i = u_1\Phi_i + \sum_{j=2}^{3} G^d_{ij}(u_j - u_1)\psi_j, \qquad i = 1, 2, 3. \qquad (2.37)$$

Finally, we substitute Eqs. (2.36) and (2.37) for $i = 1$ in the Eq. (2.34) and obtain:

$$\begin{aligned}
- & \frac{\hbar^2}{2m}(\vec{\nabla}+i\vec{\omega}_1)^2\phi_1 - \frac{\hbar^2}{2m}\Bigg[-2\Big(\frac{\vec{\nabla}G^d_{11}}{G^d_{11}}\Big)\vec{\nabla}\phi_1 + 2\Big(\frac{\vec{\nabla}G^d_{11}}{G^d_{11}}\Big)^2\phi_1 - \Big(\frac{\nabla^2 G^d_{11}}{G^d_{11}}\Big)\phi_1 \\
+ & 2(\vec{\nabla}G^d_{11})\vec{\nabla}\Big(\frac{G^d_{12}}{G^d_{11}}\psi_2 + \frac{G^d_{13}}{G^d_{11}}\psi_3\Big) + (\nabla^2 G^d_{11})\Big(\frac{G^d_{12}}{G^d_{11}}\psi_2 + \frac{G^d_{13}}{G^d_{11}}\psi_3\Big) - (\nabla^2 G^d_{12})\psi_2 - (\nabla^2 G^d_{13})\psi_3 \\
- & 2(\vec{\nabla}G^d_{12})\psi_2 - 2(\vec{\nabla}G^d_{13})\psi_3 - i\omega_1\Big(\frac{\vec{\nabla}G^d_{11}}{G^d_{11}}\Big)\phi_1 + i\omega_1(\vec{\nabla}G^d_{12})\Big(\frac{G^d_{12}}{G^d_{11}}\psi_2 + \frac{G^d_{13}}{G^d_{11}}\psi_3\Big) \\
+ & i\vec{\omega}_1(\vec{\nabla}G^d_{12})\psi_2 + i\vec{\omega}_1(\vec{\nabla}G^d_{13})\psi_3 - \Big(\frac{\vec{\nabla}G^d_{12}}{G^d_{11}}\Big)\vec{\tau}_{21}\phi_1 - \Big(\frac{\vec{\nabla}G^d_{13}}{G^d_{11}}\Big)\vec{\tau}_{31}\phi_1 \\
+ & (\vec{\nabla}G^d_{12})\vec{\tau}_{21}\Big(\frac{G^d_{12}}{G^d_{11}}\psi_2 + \frac{G^d_{13}}{G^d_{11}}\psi_3\Big) + (\vec{\nabla}G^d_{13})\vec{\tau}_{31}\Big(\frac{G^d_{12}}{G^d_{11}}\psi_2 + \frac{G^d_{13}}{G^d_{11}}\psi_3\Big) - (\vec{\nabla}G^d_{11})\vec{\tau}_{12}\psi_2 \\
- & (\vec{\nabla}G^d_{11})\vec{\tau}_{13}\psi_3\Bigg] + u_1\phi_1 + \sum_{j=2}^{3} G^d_{1j}(u_j - u_1)\psi_j - E\phi_1 = 0.
\end{aligned} \tag{2.38}$$

At this point, we are ready to impose the BO approximation, $|\psi_1| >> |\psi_i|$, $i = 2, 3$ (considering that at low enough energy, both the upper electronic states are classically closed) in the Eq. (2.38) to write the ground state EBO equation as,

$$\begin{aligned}
- & \frac{\hbar^2}{2m}(\vec{\nabla}+i\vec{\omega}_1)^2\phi_1 - \frac{\hbar^2}{2m}\Bigg[-2\Big(\frac{\vec{\nabla}G^d_{11}}{G^d_{11}}\Big)\vec{\nabla}\phi_1 + 2\Big(\frac{\vec{\nabla}G^d_{11}}{G^d_{11}}\Big)^2\phi_1 - \Big(\frac{\nabla^2 G^d_{11}}{G^d_{11}}\Big)\phi_1 \\
- & i\vec{\omega}_1\Big(\frac{\vec{\nabla}G^d_{11}}{G^d_{11}}\Big)\phi_1 - \Big(\frac{\vec{\nabla}G^d_{12}}{G^d_{11}}\Big)\vec{\tau}_{21}\phi_1 - \Big(\frac{\vec{\nabla}G^d_{13}}{G^d_{11}}\Big)\vec{\tau}_{31}\phi_1\Bigg] + (u_1 - E)\phi_1 = 0.
\end{aligned} \tag{2.39}$$

If we now introduce the approximation namely the transformation matrix **G** elements are slowly varying functions of nuclear coordinates and thereby, the matrix (**G**) commutes with the gradient operator $\vec{\nabla}$ (*ad - hoc* in nature), both Eqs. (2.33) and (2.39) lead to the following *approximate* EBO equation[1,13] for the ground electronic state:

$$-\frac{\hbar^2}{2m}(\vec{\nabla}+i\vec{\omega}_1)^2\phi_1 + (u_1 - E)\phi_1 = 0, \tag{2.40}$$

where this equation [Eq. (2.40)] with simple BO approximation becomes:

$$-\frac{\hbar^2}{2m}\nabla^2\phi_1 + (u_1 - E)\phi_1 = 0. \tag{2.41}$$

The validity of the *rigorously* formulated EBO equation [Eq. (2.39)] has been explored by performing numerical calculations on two model systems (mimicking strong non - adiabatic effects) in **Chapter 4**, while evaluating the transition probabilities on their ground electronic states. The calculated vibrational transition probabilities are compared with the exact one obtained from the diabatic equation [Eq. (2.6)]. Also, the corresponding results from *approximate* EBO equation [Eq. (2.40)] and BO approximate equation [Eq. (2.41)] are presented for comparison with diabatic [Eq. (2.6)] and *rigorous* EBO [Eq. (2.39] results.

2.3 Summary

We have carried out BO treatment and formulated *approximate/rigorous* EBO equation starting from $N = 3$ state sub - Hilbert space with single or multi CI(s) BO system. Since we assume a coupled three - state electronic BO system constitutes a sub - Hilbert space, i.e., the complete space, it is possible to transform the adiabatic nuclear SE to the diabatic one under the condition, $\vec{\nabla}\mathbf{A} + \vec{\boldsymbol{\tau}}\mathbf{A} = 0$, where the chosen form of the transformation matrix ($\mathbf{A}$) has to be orthogonal at any point in the configuration space and its' elements should be cyclic functions with respect to a parameter. Considering these natural requirements to construct such $\mathbf{A}$ matrix, we take the product of three rotation matrices (where each matrix is constituted with Euler like angle commonly called ADT angle) in six different way and substitute each of these product matrices ($\mathbf{A}$s) in the ADT condition to obtain six sets of NAC elements in terms of ADT angles. Each set of NAC elements satisfy the Curl conditions with non - zero Divergences. It appears that a particular set of NAC elements and their corresponding Curl - Divergence equations can be reassigned to any other set with proper interchange of ADT angles. In our formulation, the connectivity among the adiabatic [Eq. (2.4)], the diabatic [Eq. (2.6)] and the approximate/ rigorous EBO [Eqs. (2.39) and (2.40) equation is through the ADT matrix [Eq. (2.8)].

The actual advantage to have the explicit form of NAC elements in terms of ADT angles lies while deriving the EBO equations. It appears that the formulation of either *approximate* or *rigorous* EBO for any three state BO system is possible *only when* there exists - coordinate independent ratio of the gradients for each pair of ADT angles. The validity of such ratio implies - the Curl of the vector field, $\vec{\tau}$ is zero. In this context, the explicit form of the Curl equations in terms of ADT angles helps to explore analytically the validity of zero Curls at and around the CIs. Considering any three state BO system with three nuclear coordinates and defining the Jacobian at and around the CIs, it has been possible to show that the Curls are either identically or approximately zero around the same region of nuclear configuration space.

References

[1] B. Sarkar and S. Adhikari, J. Chem. Phys. **124**, 74101 (2006).

[2] B. Sarkar and S. Adhikari, Int. J. Quantum Chem. , in press (2008).

[3] M. Born and J. R. Oppenheimer, Ann. Phys. (Leipzig) **84**, 457 (1927).

[4] M. Born and K. Huang, *Dynamical Theory of Crystal Lattices*, Oxford University Press, Oxford, 1954.

[5] M. Baer, Chem. Phys. Lett. **35**, 112 (1975).

[6] Z. H. Top and M. Baer, J. Chem. Phys. **66**, 1363 (1977).

[7] A. Alijah and M. Baer, J. Phys. Chem. A **104**, 389 (2000).

[8] D. J. Griffiths, *Introduction to Electrodynamics*, Printice-Hall Inc., Englewood Cliffs, N.J., USA, 1989.

[9] G. B. Arfken and H. J. Weber, *Mathematical Methods for Physicists*, Acadamic Press Inc., San Diego, USA, 1995.

[10] T. Vertesi, A. Vibok, G. J. Halasz and M. Baer, J. Chem. Phys. **121**, 4000 (2004).

[11] D. R.Yarkony, J. Chem. Phys. **84**, 3206 (1986).

[12] M. Bear, *Beyond Born-Oppenheimer:Conical Intersections and Electronic nonadiabatic Coupling Terms*, Wiley Interscience, Hoboken, N.J., USA, 2006.

[13] M. Baer, S. H. Lin, A. Alijah, S. Adhikari and G. D. Billing, Phys. Rev. A **62**, 32506 (2000).

[14] H. Köppel, W. Domcke and L. S. Cederbaum, J. Chem. Phys. **74**, 2945 (1981).

[15] T. Pacher, L. S. Cederbaum and H. Köppel, Adv. Chem. Phys. **84**, 293 (1993).

[16] B. Sarkar and S. Adhikari, Indian J. Phys. **81**, 925 (2007).

Chapter 3

Born-Oppenheimer equation for four-state system: Formulation

3.1 Introduction

We demonstrate[1] the explicit forms of the nonadiabatic coupling elements in terms of ADT angles by considering the existence of ADT condition, $\vec{\nabla}\mathbf{A} + \vec{\boldsymbol{\tau}}\mathbf{A} = 0$, for any four state sub-Hilbert space. Since the NAC terms could be singular in the nuclear configuration space, it is a necessity to transform the adiabatic representation of SE to the diabatic in order to ensure accurate and stable numerical calculations but this transformation is possible only when each pair of components of the NAC terms satisfy the Curl conditions, $\frac{\partial}{\partial p}\tau^q_{ij} - \frac{\partial}{\partial q}\tau^p_{ij} = (\boldsymbol{\tau}^q\boldsymbol{\tau}^p)_{ij} - (\boldsymbol{\tau}^p\boldsymbol{\tau}^q)_{ij}$. Considering the explicit forms of the NAC terms for any four state sub-Hilbert space, we explore the analytical validity of Curl conditions. Since the necessary condition to derive the EBO equations is the existence of a relation among the ADT angles implicating zero Curls at least around the CIs, we briefly present the proof of such relations, $\left(\frac{\partial\theta_{ij}}{\partial p}\frac{\partial\theta_{ik}}{\partial q} - \frac{\partial\theta_{ij}}{\partial q}\frac{\partial\theta_{ik}}{\partial p}\right) \equiv 0$, $\{p, q = x, y, z$ or $r, \theta, \phi\}$, $i, j, k = 1, 2, 3, 4$ and $i \neq j \neq k$.

3.2 The Born-Oppenheimer treatment of a four state sub-Hilbert space

We carry out[1] the first principles based BO treatment for any four state electronic sub-Hilbert space assuming the presence of conical intersection(s) anywhere in the nuclear configuration space. Since these four states are considered as either decoupled or approximately decoupled from rest of the states of a molecular system, the BO expansion[2,3] of the wavefunction for this subspace of the Hilbert space is given by:

$$\Psi(\mathbf{n},\mathbf{e}) = \sum_{i=1}^{4} \psi_i(\mathbf{n})\xi_i(\mathbf{e},\mathbf{n}), \tag{3.1}$$

where $\xi_i(\mathbf{e},\mathbf{n})$s are the electronic eigenfunctions with nuclear coordinate dependent expansion coefficients, $\psi_i(\mathbf{n})$s subsequently termed as nuclear wavefunction and the sets of nuclear and electronic coordinates are defined as $\mathbf{n}$ and $\mathbf{e}$, respectively.

In the adiabatic representation of Schroedinger equation, the total electron-nuclei Hamiltonian ($\hat{H}$), the nuclear kinetic energy (KE) operator ($\hat{T}_n$) and the eigenvalue $[u_i(\mathbf{n})]$ − eigenfunction $[\xi_i(\mathbf{e},\mathbf{n})]$ equation for the electronic Hamiltonian $[\hat{H}_e(\mathbf{e},\mathbf{n})]$ are presented as:

$$\begin{aligned}
\hat{H} &= \hat{T}_n + \hat{H}_e(\mathbf{e},\mathbf{n}), \\
\hat{T}_n &= -\frac{\hbar^2}{2m}\sum_n \nabla_n^2, \\
\hat{H}_e(\mathbf{e},\mathbf{n})\xi_i(\mathbf{e},\mathbf{n}) &= u_i(\mathbf{n})\xi_i(\mathbf{e},\mathbf{n}).
\end{aligned} \tag{3.2}$$

The BO expansion for the sub-Hilbert space of molecular wavefunction, $\Psi(\mathbf{n},\mathbf{e})$ [Eq. (3.1)] and the total electron-nuclear Hamiltonian, $\hat{H}$ [Eq. (3.2)] are being substituted in the time-independent Schroedinger equation, $\hat{H}\Psi(\mathbf{n},\mathbf{e}) = E\Psi(\mathbf{n},\mathbf{e})$, to obtain the following matrix representation of adiabatic nuclear SE:

$$\begin{aligned}
\sum_{j=1}^{4}(H_{ij} \;\; &- \;\; E\delta_{ij})\psi_j(\mathbf{n}) = 0, \quad i = 1,2,3,4 \\
H_{ii} \;\; &= \;\; -\frac{\hbar^2}{2m}(\nabla^2 + 2\vec{\tau}_{ii}^{(1)}.\vec{\nabla} + \tau_{ii}^{(2)}) + u_i(\mathbf{n}), \\
H_{ij} \;\; &= \;\; -\frac{\hbar^2}{2m}(2\vec{\tau}_{ij}^{(1)}.\vec{\nabla} + \tau_{ij}^{(2)}) = H_{ji}^{\dagger}, \\
\vec{\tau}_{ij}^{(1)} \;\; &= \;\; \langle\xi_i(\mathbf{e},\mathbf{n})|\vec{\nabla}|\xi_j(\mathbf{e},\mathbf{n})\rangle, \quad \tau_{ij}^{(2)} = \langle\xi_i(\mathbf{e},\mathbf{n})|\nabla^2|\xi_j(\mathbf{e},\mathbf{n})\rangle, \\
&\langle\xi_i(\mathbf{e},\mathbf{n})|\xi_j(\mathbf{e},\mathbf{n})\rangle = \delta_{ij},
\end{aligned} \tag{3.3}$$

where $\vec{\tau}_{ij}^{(1)}$ and $\tau_{ij}^{(2)}$ are the elements of nonadiabatic coupling matrices of the first $[\vec{\boldsymbol{\tau}}^{(1)}]$ and second $[\boldsymbol{\tau}^{(2)}]$ kind, respectively.

For a given Hilbert/sub-Hilbert space, the two kinds of NAC matrices are related as:

$$\boldsymbol{\tau}^{(2)} = \vec{\boldsymbol{\tau}}^{(1)} \cdot \vec{\boldsymbol{\tau}}^{(1)} + \vec{\nabla}\vec{\boldsymbol{\tau}}^{(1)}, \tag{3.4}$$

leading to the following compact form of kinetically coupled nuclear equations:

$$-\frac{\hbar^2}{2m}\left(\vec{\nabla} + \vec{\tau}\right)^2 \Psi + (U - E)\,\Psi = 0, \tag{3.5}$$

where the adiabatic PES matrix elements are defined as $U_{ij} = u_i\delta_{ij}$ with the NAC matrix $[\vec{\boldsymbol{\tau}}(\equiv \vec{\boldsymbol{\tau}}^{(1)})]$ elements as,

$$\vec{\boldsymbol{\tau}} = \begin{pmatrix} 0 & \vec{\tau}_{12} & \vec{\tau}_{13} & \vec{\tau}_{14} \\ -\vec{\tau}_{12} & 0 & \vec{\tau}_{23} & \vec{\tau}_{24} \\ -\vec{\tau}_{13} & -\vec{\tau}_{23} & 0 & \vec{\tau}_{34} \\ -\vec{\tau}_{14} & -\vec{\tau}_{24} & -\vec{\tau}_{34} & 0 \end{pmatrix}. \tag{3.6}$$

Since the four states constitute the sub-Hilbert space, i.e., the complete space at present, it is possible to transform ($\Psi = \mathbf{A}\Psi^d$) the adiabatic nuclear SE [Eq. (3.5)] to the diabatic one and the diabatic matrix equations are presented as below,

$$-\frac{\hbar^2}{2m}\nabla^2\Psi^d + (W - E)\Psi^d = 0, \qquad W = A^{\dagger}UA \tag{3.7}$$

under the condition:

$$\vec{\nabla}\mathbf{A} + \vec{\tau}\mathbf{A} = 0. \tag{3.8}$$

This equation is known as Adiabatic-Diabatic Transformation (ADT) condition.[4] In order to obtain its' meaningful solution, one need to ensure that the chosen form of **A** matrix is orthogonal at any point in configuration space and its' elements are cyclic functions with respect to a parameter. At present, considering a four dimensional Hilbert space, any chosen (model) form of the ADT matrix (**A**) consisting sixteen elements has to be an orthogonal matrix with the fulfillment of twelve relations. These ortho-normality conditions demand six independent variables [$\theta_{12}(\mathbf{n})$, $\theta_{13}(\mathbf{n})$, $\theta_{14}(\mathbf{n})$, $\theta_{23}(\mathbf{n})$, $\theta_{24}(\mathbf{n})$, and $\theta_{34}(\mathbf{n})$], commonly called ADT/mixing angles, to construct the four state **A** matrix by taking the product of six rotation matrices, $\mathbf{A}_{12}(\theta_{12})$, $\mathbf{A}_{13}(\theta_{13})$, $\mathbf{A}_{14}(\theta_{14})$, $\mathbf{A}_{23}(\theta_{23})$, $\mathbf{A}_{24}(\theta_{24})$, and $\mathbf{A}_{34}(\theta_{34})$ at various ways. We define these six rotation matrices and one of the ways of their product (**A**) can be taken as:

$$\mathbf{A}(\theta_{\mathbf{34}},\theta_{\mathbf{24}},\theta_{\mathbf{14}},\theta_{\mathbf{23}},\theta_{\mathbf{13}},\theta_{\mathbf{12}}) = \mathbf{A}_{34}(\theta_{34})\cdot\mathbf{A}_{24}(\theta_{24})\cdot\mathbf{A}_{14}(\theta_{14})\cdot\mathbf{A}_{23}(\theta_{23})\cdot\mathbf{A}_{13}(\theta_{13})\cdot\mathbf{A}_{12}(\theta_{12})$$

$$= \begin{pmatrix} 1 & 0 & 0 & 0 \\ 0 & 1 & 0 & 0 \\ 0 & 0 & \cos\theta_{34} & \sin\theta_{34} \\ 0 & 0 & -\sin\theta_{34} & \cos\theta_{34} \end{pmatrix} \cdot \begin{pmatrix} 1 & 0 & 0 & 0 \\ 0 & \cos\theta_{24} & 0 & \sin\theta_{24} \\ 0 & 0 & 1 & 0 \\ 0 & -\sin\theta_{24} & 0 & \cos\theta_{24} \end{pmatrix} \cdot \begin{pmatrix} \cos\theta_{14} & 0 & 0 & \sin\theta_{14} \\ 0 & 1 & 0 & 0 \\ 0 & 0 & 1 & 0 \\ -\sin\theta_{14} & 0 & 0 & \cos\theta_{14} \end{pmatrix}$$
$$\cdot \begin{pmatrix} 1 & 0 & 0 & 0 \\ 0 & \cos\theta_{23} & \sin\theta_{23} & 0 \\ 0 & -\sin\theta_{23} & \cos\theta_{23} & 0 \\ 0 & 0 & 0 & 1 \end{pmatrix} \cdot \begin{pmatrix} \cos\theta_{13} & 0 & \sin\theta_{13} & 0 \\ 0 & 1 & 0 & 0 \\ -\sin\theta_{13} & 0 & \cos\theta_{13} & 0 \\ 0 & 0 & 0 & 1 \end{pmatrix} \cdot \begin{pmatrix} \cos\theta_{12} & \sin\theta_{12} & 0 & 0 \\ -\sin\theta_{12} & \cos\theta_{12} & 0 & 0 \\ 0 & 0 & 1 & 0 \\ 0 & 0 & 0 & 1 \end{pmatrix}$$

(3.9)

When we substitute the above model form of **A** matrix [Eq. (3.9)] and the anti-symmetric form of $\vec{\tau}$ matrix [Eq. (3.6)] in Eq. (3.8), the simple manipulation leads to the differential equations for ADT angles,[5,6] which in turn provide the explicit form of $\vec{\tau}$ matrix elements in terms of ADT angles:

$$\vec{\tau}_{12} = -\cos\theta_{13}\cos\theta_{23}\cos\theta_{14}\cos\theta_{24}\vec{\nabla}\theta_{12} - \sin\theta_{23}\cos\theta_{14}\cos\theta_{24}\vec{\nabla}\theta_{13} - \sin\theta_{24}\vec{\nabla}\theta_{14}, \tag{3.10a}$$

$$\begin{aligned}\vec{\tau}_{13} &= \cos\theta_{13}\sin\theta_{23}\cos\theta_{14}\cos\theta_{34}\vec{\nabla}\theta_{12} + \cos\theta_{13}\cos\theta_{23}\cos\theta_{14}\sin\theta_{24}\sin\theta_{34}\vec{\nabla}\theta_{12} \\ &- \cos\theta_{23}\cos\theta_{14}\cos\theta_{34}\vec{\nabla}\theta_{13} + \sin\theta_{23}\cos\theta_{14}\sin\theta_{24}\sin\theta_{34}\vec{\nabla}\theta_{13} - \cos\theta_{24}\sin\theta_{34}\vec{\nabla}\theta_{14},\end{aligned} \tag{3.10b}$$

$$\begin{aligned}\vec{\tau}_{14} &= -\cos\theta_{13}\sin\theta_{23}\cos\theta_{14}\sin\theta_{34}\vec{\nabla}\theta_{12} + \cos\theta_{13}\cos\theta_{23}\cos\theta_{14}\sin\theta_{24}\cos\theta_{34}\vec{\nabla}\theta_{12} \\ &+ \cos\theta_{23}\cos\theta_{14}\sin\theta_{34}\vec{\nabla}\theta_{13} + \sin\theta_{23}\cos\theta_{14}\sin\theta_{24}\cos\theta_{34}\vec{\nabla}\theta_{13} - \cos\theta_{24}\cos\theta_{34}\vec{\nabla}\theta_{14},\end{aligned} \tag{3.10c}$$

$$\begin{aligned}\vec{\tau}_{23} &= -\sin\theta_{13}\cos\theta_{24}\cos\theta_{34}\vec{\nabla}\theta_{12} - \cos\theta_{13}\sin\theta_{23}\sin\theta_{14}\sin\theta_{24}\cos\theta_{34}\vec{\nabla}\theta_{12} \\ &- \cos\theta_{13}\cos\theta_{23}\sin\theta_{14}\sin\theta_{34}\vec{\nabla}\theta_{12} + \cos\theta_{23}\sin\theta_{14}\sin\theta_{24}\cos\theta_{34}\vec{\nabla}\theta_{13} \\ &- \sin\theta_{23}\sin\theta_{14}\sin\theta_{34}\vec{\nabla}\theta_{13} - \cos\theta_{24}\cos\theta_{34}\vec{\nabla}\theta_{23} - \sin\theta_{34}\vec{\nabla}\theta_{24},\end{aligned} \tag{3.10d}$$

$$\begin{aligned}\vec{\tau}_{24} &= \sin\theta_{13}\cos\theta_{24}\sin\theta_{34}\vec{\nabla}\theta_{12} + \cos\theta_{13}\sin\theta_{23}\sin\theta_{14}\sin\theta_{24}\sin\theta_{34}\vec{\nabla}\theta_{12} \\ &- \cos\theta_{13}\cos\theta_{23}\sin\theta_{14}\cos\theta_{34}\vec{\nabla}\theta_{12} - \cos\theta_{23}\sin\theta_{14}\sin\theta_{24}\sin\theta_{34}\vec{\nabla}\theta_{13} \\ &- \sin\theta_{23}\sin\theta_{14}\cos\theta_{34}\vec{\nabla}\theta_{13} + \cos\theta_{24}\sin\theta_{34}\vec{\nabla}\theta_{23} - \cos\theta_{34}\vec{\nabla}\theta_{24},\end{aligned} \tag{3.10e}$$

$$\begin{aligned}\vec{\tau}_{34} &= -\sin\theta_{13}\sin\theta_{24}\vec{\nabla}\theta_{12} + \cos\theta_{13}\sin\theta_{23}\sin\theta_{14}\cos\theta_{24}\vec{\nabla}\theta_{12} \\ &- \cos\theta_{23}\sin\theta_{14}\cos\theta_{24}\vec{\nabla}\theta_{13} - \sin\theta_{24}\vec{\nabla}\theta_{23} - \vec{\nabla}\theta_{34}.\end{aligned} \tag{3.10f}$$

In an alternative manner, if we replace the so called ADT angles [$\theta_{12}(\mathbf{n})$, $\theta_{13}(\mathbf{n})$, $\theta_{14}(\mathbf{n})$, $\theta_{23}(\mathbf{n})$, $\theta_{24}(\mathbf{n})$, and $\theta_{34}(\mathbf{n})$] by electronic basis functions angles, namely, mixing angles [$\alpha(\mathbf{n})$, $\beta(\mathbf{n})$, $\gamma(\mathbf{n})$, $\lambda(\mathbf{n})$, $\delta(\mathbf{n})$, and $\eta(\mathbf{n})$] in the ADT matrix, $\mathbf{A}$ [Eq. (3.9)] and the columns of the $\mathbf{A}^\dagger$ matrix are substituted in Eq. (3.3) as electronic basis functions, we obtain the same set of equations for NAC elements [Eqs. (3.10)] as functions of mixing angles and thereby, show the one-to-one correspondence among ADT and mixing angles.

Once the nonadiabatic coupling elements $\vec{\tau}_{12}$, $\vec{\tau}_{13}$, $\vec{\tau}_{14}$, $\vec{\tau}_{23}$, $\vec{\tau}_{24}$ and $\vec{\tau}_{34}$ are evaluated by using *ab initio* calculation for a particular nuclear configuration, the solutions of Eqs. (3.10) provide the ADT angles for the same nuclear configuration and then, one can transform the adiabatic representation of Schroedinger equation with kinetic coupling, $\vec{\boldsymbol{\tau}}$ matrix among the electronic states [Eq. (3.5)] to the diabatic representation with potential coupling, namely, the **W** matrix [Eq.(3.7)] among the same states. This transformation guarantees the uniquely defined diabatic potential energy matrix in the configuration space only when the following Curl conditions of the NAC elements are valid.

A Curl condition[4] for each NAC element, $\vec{\tau}_{ij}$, has been derived and proved to exist for an isolated group of states (sub-Hilbert space) by considering the analyticity of the ADT matrix **A** for a pair of nuclear degrees of freedom,

$$\begin{aligned} \text{Curl } \tau_{ij}^{pq} = \frac{\partial}{\partial p}\tau_{ij}^{q} - \frac{\partial}{\partial q}\tau_{ij}^{p} \quad &= \quad (\boldsymbol{\tau}^{q}\boldsymbol{\tau}^{p})_{ij} - (\boldsymbol{\tau}^{p}\boldsymbol{\tau}^{q})_{ij}, \\ \tau_{ij}^{p} = \langle \xi_i | \nabla_p \xi_j \rangle, \qquad & \tau_{ij}^{q} = \langle \xi_i | \nabla_q \xi_j \rangle, \end{aligned} \tag{3.11}$$

where p and q are in *Cartesian coordinates* with $\nabla_p = \frac{\partial}{\partial p}$ and $\nabla_q = \frac{\partial}{\partial q}$.

At present, for a given four dimensional sub-Hilbert space, we demonstrate that the explicit forms of the NAC elements in terms of ADT/mixing angles satisfy the Curl conditions, i.e., the difference between the cross derivatives of any two components of a NAC element with respect to a pair of nuclear coordinates ($\frac{\partial}{\partial p}\tau_{ij}^{q} - \frac{\partial}{\partial q}\tau_{ij}^{p}$) appears to be analytically equal with the corresponding element arising from the difference of the products taken at different order between the component NAC matrices [$(\boldsymbol{\tau}^{q}\boldsymbol{\tau}^{p})_{ij} - (\boldsymbol{\tau}^{p}\boldsymbol{\tau}^{q})_{ij}$]. Since the compact expressions of the Curl and Divergence equations for the explicit forms of

NAC elements [Eqs.(3.10)] are as such lengthy, we present only two of them:

$$\begin{aligned}
\text{Curl}\ \tau_{12}^{pq} &= \sin\theta_{13}\cos\theta_{23}\cos\theta_{14}\cos\theta_{24}(\nabla_p\theta_{12}\nabla_q\theta_{13} - \nabla_q\theta_{12}\nabla_p\theta_{13}) \\
&+ \cos\theta_{13}\sin\theta_{23}\cos\theta_{14}\cos\theta_{24}(\nabla_p\theta_{12}\nabla_q\theta_{23} - \nabla_q\theta_{12}\nabla_p\theta_{23}) \\
&+ \cos\theta_{13}\cos\theta_{23}\sin\theta_{14}\cos\theta_{24}(\nabla_p\theta_{12}\nabla_q\theta_{14} - \nabla_q\theta_{12}\nabla_p\theta_{14}) \\
&+ \cos\theta_{13}\cos\theta_{23}\cos\theta_{14}\sin\theta_{24}(\nabla_p\theta_{12}\nabla_q\theta_{24} - \nabla_q\theta_{12}\nabla_p\theta_{24}) \\
&- \cos\theta_{23}\cos\theta_{14}\cos\theta_{24}(\nabla_p\theta_{13}\nabla_q\theta_{23} - \nabla_q\theta_{13}\nabla_p\theta_{23}) \\
&+ \sin\theta_{23}\sin\theta_{14}\cos\theta_{24}(\nabla_p\theta_{13}\nabla_q\theta_{14} - \nabla_q\theta_{13}\nabla_p\theta_{14}) \\
&+ \sin\theta_{23}\cos\theta_{14}\sin\theta_{24}(\nabla_p\theta_{13}\nabla_q\theta_{24} - \nabla_q\theta_{13}\nabla_p\theta_{24}) \\
&- \cos\theta_{24}(\nabla_p\theta_{14}\nabla_q\theta_{24} - \nabla_q\theta_{14}\nabla_p\theta_{24}), \qquad (3.12a)
\end{aligned}$$

$$\begin{aligned}
\text{div}\ \vec{\tau}_{12} &= -\cos\theta_{13}\cos\theta_{23}\cos\theta_{14}\cos\theta_{24}\nabla^2\theta_{12} - \sin\theta_{23}\cos\theta_{14}\cos\theta_{24}\nabla^2\theta_{13} - \sin\theta_{24}\nabla^2\theta_{14} \\
&+ \sin\theta_{13}\cos\theta_{23}\cos\theta_{14}\cos\theta_{24}\vec{\nabla}\theta_{12}\cdot\vec{\nabla}\theta_{13} + \cos\theta_{13}\sin\theta_{23}\cos\theta_{14}\cos\theta_{24}\vec{\nabla}\theta_{12}\cdot\vec{\nabla}\theta_{23} \\
&+ \cos\theta_{13}\cos\theta_{23}\sin\theta_{14}\cos\theta_{24}\vec{\nabla}\theta_{12}\cdot\vec{\nabla}\theta_{14} + \cos\theta_{13}\cos\theta_{23}\cos\theta_{14}\sin\theta_{24}\vec{\nabla}\theta_{12}\cdot\vec{\nabla}\theta_{24} \\
&- \cos\theta_{23}\cos\theta_{14}\cos\theta_{24}\vec{\nabla}\theta_{13}\cdot\vec{\nabla}\theta_{23} + \sin\theta_{13}\sin\theta_{14}\cos\theta_{24}\vec{\nabla}\theta_{13}\cdot\vec{\nabla}\theta_{14} \\
&+ \sin\theta_{13}\cos\theta_{14}\sin\theta_{24}\vec{\nabla}\theta_{13}\cdot\vec{\nabla}\theta_{24} - \cos\theta_{24}\vec{\nabla}\theta_{14}\cdot\vec{\nabla}\theta_{24}, \qquad (3.12b)
\end{aligned}$$

$$\begin{aligned}
\text{Curl}\ \tau_{34}^{pq} &= (-\cos\theta_{13}\sin\theta_{24} - \sin\theta_{13}\sin\theta_{23}\sin\theta_{14}\cos\theta_{24})(\nabla_p\theta_{12}\nabla_q\theta_{13} - \nabla_q\theta_{12}\nabla_p\theta_{13}) \\
&- (\sin\theta_{13}\cos\theta_{24} + \cos\theta_{13}\sin\theta_{23}\sin\theta_{14}\sin\theta_{24})(\nabla_p\theta_{12}\nabla_q\theta_{24} - \nabla_q\theta_{12}\nabla_p\theta_{24}) \\
&+ \cos\theta_{13}\cos\theta_{23}\sin\theta_{14}\cos\theta_{24}(\nabla_p\theta_{12}\nabla_q\theta_{23} - \nabla_q\theta_{12}\nabla_p\theta_{23}) \\
&+ \cos\theta_{13}\sin\theta_{23}\cos\theta_{14}\cos\theta_{24}(\nabla_p\theta_{12}\nabla_q\theta_{14} - \nabla_q\theta_{12}\nabla_p\theta_{14}) \\
&+ \sin\theta_{23}\sin\theta_{14}\cos\theta_{24}(\nabla_p\theta_{13}\nabla_q\theta_{23} - \nabla_q\theta_{13}\nabla_p\theta_{23}) \\
&- \cos\theta_{23}\cos\theta_{14}\cos\theta_{24}(\nabla_p\theta_{13}\nabla_q\theta_{14} - \nabla_q\theta_{13}\nabla_p\theta_{14}) \\
&+ \cos\theta_{23}\sin\theta_{14}\sin\theta_{24}(\nabla_p\theta_{13}\nabla_q\theta_{24} - \nabla_q\theta_{13}\nabla_p\theta_{24}) \\
&- \cos\theta_{24}(\nabla_p\theta_{23}\nabla_q\theta_{24} - \nabla_q\theta_{23}\nabla_p\theta_{24})
\end{aligned} \tag{3.13a}$$

$$\begin{aligned}
\text{div}\ \vec{\tau}_{34} &= \cos\theta_{13}\sin\theta_{23}\sin\theta_{14}\cos\theta_{24}\nabla^2\theta_{12} - \sin\theta_{13}\sin\theta_{24}\nabla^2\theta_{12} - \cos\theta_{23}\sin\theta_{14}\cos\theta_{24}\nabla^2\theta_{13} \\
&- \sin\theta_{24}\nabla^2\theta_{23} - \nabla^2\theta_{34} - (\sin\theta_{13}\sin\theta_{23}\sin\theta_{14}\cos\theta_{24} + \cos\theta_{13}\sin\theta_{24})\vec{\nabla}\theta_{12}\cdot\vec{\nabla}\theta_{13} \\
&+ \cos\theta_{13}\cos\theta_{23}\sin\theta_{14}\cos\theta_{24}\vec{\nabla}\theta_{12}\cdot\vec{\nabla}\theta_{23} + \cos\theta_{13}\sin\theta_{23}\cos\theta_{14}\cos\theta_{24}\vec{\nabla}\theta_{12}\cdot\vec{\nabla}\theta_{14} \\
&+ \sin\theta_{23}\sin\theta_{14}\cos\theta_{24}\vec{\nabla}\theta_{13}\cdot\vec{\nabla}\theta_{23} - \cos\theta_{13}\cos\theta_{14}\cos\theta_{24}\vec{\nabla}\theta_{13}\cdot\vec{\nabla}\theta_{14} \\
&- (\sin\theta_{13}\cos\theta_{24} + \cos\theta_{13}\sin\theta_{23}\sin\theta_{14}\sin\theta_{24})\vec{\nabla}\theta_{12}\cdot\vec{\nabla}\theta_{23} \\
&+ \cos\theta_{23}\sin\theta_{14}\sin\theta_{24}\vec{\nabla}\theta_{13}\cdot\vec{\nabla}\theta_{24} - \cos\theta_{24}\vec{\nabla}\theta_{23}\cdot\vec{\nabla}\theta_{24},
\end{aligned} \tag{3.13b}$$

and similar expressions can be evaluated for the other NAC elements.

Since $\vec{\nabla}\theta_{ij}$s and in general, $\nabla^2\theta_{ij}$s are non-zero around the conical intersection, the Divergence of the vector field ($\vec{\tau}_{ij}$) are non-vanishing for any arbitrary values of ADT/mixing angles and therefore, the vector field may show up non-zero Curl.[7,8] On the other hand, as a nonadiabatic coupling term of the kind, $\vec{\tau}_{ii+1}(\mathbf{n})$, associated with a $(i, i+1)$ CI with a singularity (pole) at the same CI point, decays like $\frac{1}{r}$ (where r is the distance from the CI), such vector field could be resolved into irrotational (longitudinal) and solenoidal (transverse) components.[7,8] Though the theory of electrodynamics, by definition, reminds that the Curl of longitudinal part (of vector field) is zero but Curl of transverse part may or may not, experimental observations on so-called solenoids intend to argue that if infinitely long contour lines (seams) due to conical intersection are considered as infinitesimal narrow "solenoids", seams should produce zero field outside of them but *ab initio* calculations[9,10] show the presence of non-zero $\vec{\tau}$ in the space surrounding the seams. Thus, the existing knowledge of the vector field ($\vec{\tau}_{ij}$) is not enough to predict about their Curls and then, the following section demonstrates that in order to perform further theoretical development like the formulation of single surface EBO equation, it is necessary to find out the nature of Curl τ_{ij}^{pq}s quantitatively, at least around the point/seam of CI, for a given sub-Hilbert space.

Since, in the adiabatic representation of SE [Eq. (3.5)], the electronic states interact through kinetic coupling terms,

$$-\frac{\hbar^2}{2m}(\vec{\nabla}+\vec{\boldsymbol{\tau}})^2\Psi + (\mathbf{U}-E)\Psi = 0, \quad U_{ij} = u_i\delta_{ij}, \tag{3.14}$$

in order to formulate the EBO equation, one need to bring the effect of the off-diagonal NAC terms to the diagonal. The convenient way of pursuing such operation is to carry out an unitary transformation on Eq. (3.14) by a matrix, $\mathbf{G}$ ($\Psi = \mathbf{G}\Phi$), such that it leads to the following form:

$$-\frac{\hbar^2}{2m}(\mathbf{G}^\dagger\vec{\nabla}\mathbf{G}+i\vec{\omega})^2\Phi + (\mathbf{V}-E)\Phi = 0, \quad \mathbf{V} = \mathbf{G}^\dagger\mathbf{U}\mathbf{G}, \quad i\vec{\omega} = \mathbf{G}^\dagger\vec{\boldsymbol{\tau}}\mathbf{G}, \tag{3.15}$$

In case of two components $\boldsymbol{\tau}$ matrix, if one of the component (e.g. $\boldsymbol{\tau}^q$, where q is the radial coordinate) appears null matrix, Eq. (3.15) can be obtained from Eq. (3.14) trivially.

The eigenvalues ($\pm i\vec{\omega}$) of the NAC matrix, $\vec{\boldsymbol{\tau}}$ should be vectors in order to obtain physically meaningful (a scalar) Hamiltonian [Eq. (3.15)] and thereby, one can impose the BO approximation, $|\psi_1| >> |\psi_i|$, $i = 2,3,4$, by considering the upper electronic states as classically closed at low enough energy, to formulate the single surface adiabatic nuclear SE (EBO).[11–14]

On the other hand, since the straight forward diagonalization of $\vec{\boldsymbol{\tau}}$ matrix [Eq. (3.6)] gives scalar eigenvalues,

$$
\begin{aligned}
i\omega &= \pm i\sqrt{\frac{A}{2} \pm \frac{1}{2}\sqrt{A^2 - 4B^2}}, \\
A &= \vec{\tau}_{12}\cdot\vec{\tau}_{12} + \vec{\tau}_{13}\cdot\vec{\tau}_{13} + \vec{\tau}_{23}\cdot\vec{\tau}_{23} + \vec{\tau}_{14}\cdot\vec{\tau}_{14} + \vec{\tau}_{24}\cdot\vec{\tau}_{24} + \vec{\tau}_{34}\cdot\vec{\tau}_{34}, \\
B &= \vec{\tau}_{14}\cdot\vec{\tau}_{23} - \vec{\tau}_{13}\cdot\vec{\tau}_{24} + \vec{\tau}_{12}\cdot\vec{\tau}_{34},
\end{aligned}
\tag{3.16}
$$

but the requirement of Eq. (3.15) dictates that the eigenvalues ($\pm i\vec{\omega}$) of $\vec{\boldsymbol{\tau}}$ matrix must be vectors, the only possibility remains that the $\vec{\boldsymbol{\tau}}$ matrix could be written as the product of a vector function, $\vec{\nabla}\eta$ ($\eta \equiv \theta_{12}$ or θ_{13} or θ_{14} or θ_{23} or θ_{24} or θ_{34}) and a ADT/mixing angle dependent anti - symmetric scalar matrix, $\boldsymbol{g}(\theta_{12}, \theta_{13}, \theta_{23}, \theta_{14}, \theta_{24}, \theta_{34})$. It is quite straight forward to find from the elements of $\vec{\boldsymbol{\tau}}$ matrix [Eq. (3.10)] that if the following identities, $\left(\frac{\nabla_p\theta_{13}}{\nabla_p\theta_{12}}\right) = \left(\frac{\nabla_q\theta_{13}}{\nabla_q\theta_{12}}\right)$, $\left(\frac{\nabla_p\theta_{14}}{\nabla_p\theta_{12}}\right) = \left(\frac{\nabla_q\theta_{14}}{\nabla_q\theta_{12}}\right)$, $\left(\frac{\nabla_p\theta_{23}}{\nabla_p\theta_{12}}\right) = \left(\frac{\nabla_q\theta_{23}}{\nabla_q\theta_{12}}\right)$, $\left(\frac{\nabla_p\theta_{24}}{\nabla_p\theta_{12}}\right) = \left(\frac{\nabla_q\theta_{24}}{\nabla_q\theta_{12}}\right)$, and $\left(\frac{\nabla_p\theta_{34}}{\nabla_p\theta_{12}}\right) = \left(\frac{\nabla_q\theta_{34}}{\nabla_q\theta_{12}}\right)$ for any pair of nuclear coordinates, namely, p and q are assumed to be true, one can write, $\vec{\boldsymbol{\tau}} = \vec{\nabla}\eta\cdot\boldsymbol{g}(\theta_{12}, \theta_{13}, \theta_{14}, \theta_{23}, \theta_{24}, \theta_{34})$, and therefore, we need to explore the validity of these identities, i.e., Curl $\tau_{ij}^{pq} = 0$s [see Eqs. (3.12a) and (3.13a)] at and around CI(s). Since we have presented the details of the proof to explore the validity of these identities in **Chapter 2**, a brief discussion only is being presented here. We consider one of the above such identities either in polar or in Cartesian coordinates, where the ADT angles are assumed to be dependent, let say, on three nuclear coordinates and find its' nature by using the Jacobian determinant for the transformation from Cartesian to polar,

$$
J(r,\theta,\phi) = \begin{vmatrix} \frac{\partial x}{\partial r} & \frac{\partial y}{\partial r} & \frac{\partial z}{\partial r} \\ \frac{\partial x}{\partial \theta} & \frac{\partial y}{\partial \theta} & \frac{\partial z}{\partial \theta} \\ \frac{\partial x}{\partial \phi} & \frac{\partial y}{\partial \phi} & \frac{\partial z}{\partial \phi} \end{vmatrix} = \begin{vmatrix} \sin\theta\cos\phi & \sin\theta\sin\phi & \cos\theta \\ r\cos\theta\cos\phi & r\cos\theta\sin\phi & -r\sin\theta \\ -r\sin\theta\sin\phi & r\sin\theta\cos\phi & 0 \end{vmatrix}
\tag{3.17}
$$

or vice versa. At this junction, we wish to remind that when the origin of the coordinate system [r =0 (x = 0, y = 0, z = 0)] coincides with the point of conical intersection, various components of the Jacobian determinant vanishes at that point (CI). It is important to note that this transformation remain valid with zero content at r = 0, along with $\frac{\partial z}{\partial \phi} = 0$ (also at $r \neq 0$), $\frac{\partial y}{\partial \phi} = r \sin\theta \cos\phi = 0$, $\frac{\partial z}{\partial \theta} = -r \sin\theta = 0$, $\frac{\partial y}{\partial \theta} = r\cos\theta \sin\phi = 0$. Even if the point of conical intersection(s) is away from the origin of the coordinate system, parametric representation for the vector equation of a conical surface predicts $J(r,\theta)$ = 0, $J(r,\phi)$ = 0 and $J(\theta,\phi)$ = 0 at the singularity (CI) (see **Appendix C**).

Since the quantities $\left(\frac{\partial\theta_{23}}{\partial y}\frac{\partial\theta_{12}}{\partial x} - \frac{\partial\theta_{23}}{\partial x}\frac{\partial\theta_{12}}{\partial y}\right)$, $\left(\frac{\partial\theta_{23}}{\partial z}\frac{\partial\theta_{12}}{\partial x} - \frac{\partial\theta_{23}}{\partial x}\frac{\partial\theta_{12}}{\partial z}\right)$ and $\left(\frac{\partial\theta_{23}}{\partial y}\frac{\partial\theta_{12}}{\partial z} - \frac{\partial\theta_{23}}{\partial z}\frac{\partial\theta_{12}}{\partial y}\right)$, or $\left(\frac{\partial\theta_{23}}{\partial \theta}\frac{\partial\theta_{12}}{\partial r} - \frac{\partial\theta_{23}}{\partial r}\frac{\partial\theta_{12}}{\partial \theta}\right)$, $\left(\frac{\partial\theta_{23}}{\partial \phi}\frac{\partial\theta_{12}}{\partial r} - \frac{\partial\theta_{23}}{\partial r}\frac{\partial\theta_{12}}{\partial \phi}\right)$ and $\left(\frac{\partial\theta_{23}}{\partial \theta}\frac{\partial\theta_{12}}{\partial \phi} - \frac{\partial\theta_{23}}{\partial \phi}\frac{\partial\theta_{12}}{\partial \theta}\right)$, appear either identically or approximately zero around the conical intersection, and similarly, such identities for the other ADT angles, vis-a-vis Curl τ_{ij}^{pq} $(p,q \equiv x,y,z)$ or Curl τ_{ij}^{pq} $(p,q \equiv r,\theta,\phi)$ can be taken either identically or approximately zero around the conical intersection, we intend to rewrite Eq. (3.15) as,

$$\begin{aligned} &- \frac{\hbar^2}{2m}\Big[(\vec{\nabla} + i\vec{\omega})^2\Phi\Big] - \frac{\hbar^2}{2m}\Big[(\mathbf{G}^\dagger\nabla^2\mathbf{G}\Phi - \nabla^2\Phi) + (i\vec{\omega}\mathbf{G}^\dagger\vec{\nabla}\mathbf{G}\Phi - i\vec{\omega}\vec{\nabla}\Phi) \\ &+ (\mathbf{G}^\dagger\vec{\nabla}\mathbf{G}i\vec{\omega}\Phi - \vec{\nabla}i\vec{\omega}\Phi)\Big] + \Big[(\mathbf{V} - E)\Phi\Big] = 0, \end{aligned} \tag{3.18}$$

where **G** is the transformation matrix that diagonalizes the anti - symmetric scalar matrix, $\boldsymbol{g}(\theta_{12},\theta_{13},\theta_{14},\theta_{23},\theta_{24},\theta_{34})$ instead of NAC matrix, $\vec{\boldsymbol{\tau}}(\theta_{12},\theta_{13},\theta_{14},\theta_{23},\theta_{24},\theta_{34})$ as shown in Eq. (3.14). For symbolic convenience, now onwards we shall replace $\mathbf{G}^\dagger$ as $\mathbf{G}^d$ and its' element $(\mathbf{G}^\dagger)_{ij}$ as $(\mathbf{G}^d)_{ij}$ $(\equiv G^d_{ij})$.

The *i* th BO equation can be written from the matrix equation [Eq. (3.18)] as below,

$$\begin{aligned} &- \frac{\hbar^2}{2m}\Big[(\vec{\nabla} + i\vec{\omega})^2\Phi\Big]_i - \frac{\hbar^2}{2m}\Big[\sum_k G^d_{ik}\nabla^2\psi_k - \sum_k \nabla^2(G^d_{ik}\psi_k) + \sum_k i\vec{\omega}_i G^d_{ik}\vec{\nabla}\psi_k \\ &- \sum_k i\vec{\omega}_i\vec{\nabla}(G^d_{ik}\psi_k) + \sum_{km} G^d_{ik}\vec{\nabla}(\vec{\tau}_{km}\psi_m) - \sum_{km}\vec{\nabla}(G^d_{ik}\vec{\tau}_{km}\psi_m)\Big] + \Big[(\mathbf{V} - E)\Phi\Big]_i = 0 \end{aligned} \tag{3.19}$$

We manipulate Eq. (3.19) by considering the following aspects: (a) Since the matrix representation of the ADT is given by

$$\Phi = \mathbf{G^d}\Psi \tag{3.20}$$

one can have the general identity

$$\psi_k = \frac{1}{G^d_{kk}}\phi_k - \sum_{l\neq k}\frac{G^d_{kl}}{G^d_{kk}}\psi_l \qquad k,l=1,2,3,4; \tag{3.21}$$

(b) The product, $V\Phi$, for the ith equation can be rearranged as below,

$$(V\Phi)_i = u_1\Phi_i + \sum_{j=2}^{4} G^d_{ij}(u_j-u_1)\psi_j, \qquad i=1,2,3,4. \tag{3.22}$$

(c) We impose the BO approximation, $|\psi_1| >> |\psi_i|$, $i=2,\ldots,4$ (considering that at low enough energy, both the upper electronic states are classically closed) in Eq. (3.19) to write the ground state EBO equation as,

$$\begin{aligned} &- \frac{\hbar^2}{2m}(\vec\nabla + i\vec\omega_1)^2\phi_1 - \frac{\hbar^2}{2m}\Big[-2\Big(\frac{\vec\nabla G^d_{11}}{G^d_{11}}\Big)\vec\nabla\phi_1 + 2\Big(\frac{\vec\nabla G^d_{11}}{G^d_{11}}\Big)^2\phi_1 - \Big(\frac{\nabla^2 G^d_{11}}{G^d_{11}}\Big)\phi_1 \\ &- i\vec\omega_1\Big(\frac{\vec\nabla G^d_{11}}{G^d_{11}}\Big)\phi_1 - \Big(\frac{\vec\nabla G^d_{12}}{G^d_{11}}\Big)\vec\tau_{21}\phi_1 - \Big(\frac{\vec\nabla G^d_{13}}{G^d_{11}}\Big)\vec\tau_{31}\phi_1 - \Big(\frac{\vec\nabla G^d_{14}}{G^d_{11}}\Big)\vec\tau_{41}\phi_1\Big] \\ &+ (u_1 - E)\phi_1 = 0. \end{aligned} \tag{3.23}$$

If we now introduce the approximation namely the transformation matrix **G** elements are slowly varying functions of nuclear coordinates and thereby, the matrix (**G**) commutes with the gradient operator $\vec\nabla$ (*ad - hoc* in nature), both Eqs. (3.18) and (3.23) lead to the following *approximate* EBO equation[13] for the ground electronic state:

$$-\frac{\hbar^2}{2m}(\vec\nabla + i\vec\omega_1)^2\phi_1 + (u_1-E)\phi_1 = 0, \tag{3.24}$$

where this equation [Eq. (3.24)] with simple BO approximation becomes:

$$-\frac{\hbar^2}{2m}\nabla^2\phi_1 + (u_1-E)\phi_1 = 0. \tag{3.25}$$

The numerical experimentation to find the condition for the existence of Eq. (3.24) has been investigated in **Chapter 5**. We solve Mathieu equation[1] for various sets of parametric values and obtain the condition to form four-state sub- Hilbert space, namely, whether the nonadiabatic coupling terms among these states satisfy zero Curl as well as Curl Condition leading to EBO equation [Eq. (3.24)].

3.2.1 The eigenvalues of NAC matrix

If the origin of the coordinate system coincides with the point of conical intersection or even if the point of conical intersection(s) is away from the origin of the coordinate system, parametric representation for the vector equation of a conical surface predicts (see **Appendix C**) the validity of the following identities: $\left(\frac{\nabla_p\theta_{13}}{\nabla_p\theta_{12}}\right) = \left(\frac{\nabla_q\theta_{13}}{\nabla_q\theta_{12}}\right)$, $\left(\frac{\nabla_p\theta_{14}}{\nabla_p\theta_{12}}\right) = \left(\frac{\nabla_q\theta_{14}}{\nabla_q\theta_{12}}\right)$, $\left(\frac{\nabla_p\theta_{23}}{\nabla_p\theta_{12}}\right) = \left(\frac{\nabla_q\theta_{23}}{\nabla_q\theta_{12}}\right)$, $\left(\frac{\nabla_p\theta_{24}}{\nabla_p\theta_{12}}\right) = \left(\frac{\nabla_q\theta_{24}}{\nabla_q\theta_{12}}\right)$, and $\left(\frac{\nabla_p\theta_{34}}{\nabla_p\theta_{12}}\right) = \left(\frac{\nabla_q\theta_{34}}{\nabla_q\theta_{12}}\right)$ for any pair of nuclear coordinates, namely, p and q, at and around the point of conical intersection. When we substitute these identities in Eq. (3.10), the nonadiabatic coupling terms takes the following form:

$$
\begin{aligned}
\vec{\tau}_{12} &= -\vec{\nabla}\theta_{12}\Big[\cos\theta_{13}\cos\theta_{23}\cos\theta_{14}\cos\theta_{24} + \sin\theta_{23}\cos\theta_{14}\cos\theta_{24}\Big(\frac{\nabla_p\theta_{13}}{\nabla_p\theta_{12}}\Big) \\
&+ \sin\theta_{24}\Big(\frac{\nabla_p\theta_{14}}{\nabla_p\theta_{12}}\Big)\Big], \qquad (3.26a) \\
\vec{\tau}_{13} &= \vec{\nabla}\theta_{12}\Big[\cos\theta_{13}\sin\theta_{23}\cos\theta_{14}\cos\theta_{34} + \cos\theta_{13}\cos\theta_{23}\cos\theta_{14}\sin\theta_{24}\sin\theta_{34} \\
&- \cos\theta_{23}\cos\theta_{14}\cos\theta_{34}\Big(\frac{\nabla_p\theta_{13}}{\nabla_p\theta_{12}}\Big) + \sin\theta_{23}\cos\theta_{14}\sin\theta_{24}\sin\theta_{34}\Big(\frac{\nabla_p\theta_{13}}{\nabla_p\theta_{12}}\Big) \\
&- \cos\theta_{24}\sin\theta_{34}\Big(\frac{\nabla_p\theta_{14}}{\nabla_p\theta_{12}}\Big)\Big], \qquad (3.26b)
\end{aligned}
$$

and similarly other NAC terms.

At this junction, we can recall Eq. (3.16) to find out the following quantities (A and B) considering the NAC elements as presented in Eqs. (3.26):

$$
\begin{aligned}
A &= \vec{\tau}_{12}\cdot\vec{\tau}_{12}+\vec{\tau}_{13}\cdot\vec{\tau}_{13}+\vec{\tau}_{23}\cdot\vec{\tau}_{23}+\vec{\tau}_{14}\cdot\vec{\tau}_{14}+\vec{\tau}_{24}\cdot\vec{\tau}_{24}+\vec{\tau}_{34}\cdot\vec{\tau}_{34},\\
&= \vec{\nabla}\theta_{12}\cdot\vec{\nabla}\theta_{12}\Big\{1+\Big(\frac{\nabla_p\theta_{13}}{\nabla_p\theta_{12}}\Big)^2+\Big(\frac{\nabla_p\theta_{23}}{\nabla_p\theta_{12}}\Big)^2+\Big(\frac{\nabla_p\theta_{14}}{\nabla_p\theta_{12}}\Big)^2+\Big(\frac{\nabla_p\theta_{24}}{\nabla_p\theta_{12}}\Big)^2+\Big(\frac{\nabla_p\theta_{34}}{\nabla_p\theta_{12}}\Big)^2\\
&+ 2\cos\theta_{23}\sin\theta_{14}\cos\theta_{24}\Big(\frac{\nabla_p\theta_{13}}{\nabla_p\theta_{12}}\Big)\Big(\frac{\nabla_p\theta_{34}}{\nabla_p\theta_{12}}\Big)+2\sin\theta_{23}\sin\theta_{14}\Big(\frac{\nabla_p\theta_{13}}{\nabla_p\theta_{12}}\Big)\Big(\frac{\nabla_p\theta_{24}}{\nabla_p\theta_{12}}\Big)\\
&+ 2\sin\theta_{24}\Big(\frac{\nabla_p\theta_{23}}{\nabla_p\theta_{12}}\Big)\Big(\frac{\nabla_p\theta_{34}}{\nabla_p\theta_{12}}\Big)+2\sin\theta_{13}\Big(\frac{\nabla_p\theta_{23}}{\nabla_p\theta_{12}}\Big)+2\cos\theta_{13}\cos\theta_{23}\sin\theta_{14}\Big(\frac{\nabla_p\theta_{24}}{\nabla_p\theta_{12}}\Big)\\
&+ 2\big(\sin\theta_{13}\sin\theta_{23}-\cos\theta_{13}\sin\theta_{23}\sin\theta_{14}\cos\theta_{24}\big)\Big(\frac{\nabla_p\theta_{34}}{\nabla_p\theta_{12}}\Big)\Big\},
\end{aligned}
\tag{3.27}
$$

$$
\begin{aligned}
B &= \vec{\tau}_{14}\cdot\vec{\tau}_{23}-\vec{\tau}_{13}\cdot\vec{\tau}_{24}+\vec{\tau}_{12}\cdot\vec{\tau}_{34},\\
&= \vec{\nabla}\theta_{12}\cdot\vec{\nabla}\theta_{12}\Big\{\Big(\frac{\nabla_p\theta_{23}}{\nabla_p\theta_{12}}\Big)\Big(\frac{\nabla_p\theta_{14}}{\nabla_p\theta_{12}}\Big)+\sin\theta_{13}\Big(\frac{\nabla_p\theta_{14}}{\nabla_p\theta_{12}}\Big)+\cos\theta_{13}\sin\theta_{23}\cos\theta_{14}\Big(\frac{\nabla_p\theta_{24}}{\nabla_p\theta_{12}}\Big)\\
&- \cos\theta_{23}\cos\theta_{14}\Big(\frac{\nabla_p\theta_{13}}{\nabla_p\theta_{12}}\Big)\Big(\frac{\nabla_p\theta_{24}}{\nabla_p\theta_{12}}\Big)+\cos\theta_{14}\cos\theta_{23}\cos\theta_{14}\cos\theta_{24}\Big(\frac{\nabla_p\theta_{34}}{\nabla_p\theta_{12}}\Big)\\
&+ \sin\theta_{23}\cos\theta_{14}\cos\theta_{24}\Big(\frac{\nabla_p\theta_{13}}{\nabla_p\theta_{12}}\Big)\Big(\frac{\nabla_p\theta_{34}}{\nabla_p\theta_{12}}\Big)+\sin\theta_{24}\frac{\nabla_p\theta_{14}}{\nabla_p\theta_{12}}\Big(\frac{\nabla_p\theta_{34}}{\nabla_p\theta_{12}}\Big)\Big\},
\end{aligned}
\tag{3.28}
$$

and thereby,

$$
\begin{aligned}
\vec{\omega}_i &= \sqrt{\frac{A}{2} \pm \frac{1}{2}\sqrt{A^2 - 4B^2}}, \\
&= \pm\vec{\nabla}\theta_{12}\Bigg[-\frac{1}{2}\Bigg\{ 1 + \Big(\frac{\nabla_p\theta_{13}}{\nabla_p\theta_{12}}\Big)^2 + \Big(\frac{\nabla_p\theta_{23}}{\nabla_p\theta_{12}}\Big)^2 + \Big(\frac{\nabla_p\theta_{14}}{\nabla_p\theta_{12}}\Big)^2 + \Big(\frac{\nabla_p\theta_{24}}{\nabla_p\theta_{12}}\Big)^2 + \Big(\frac{\nabla_p\theta_{34}}{\nabla_p\theta_{12}}\Big)^2 \\
&+ 2\cos\theta_{23}\sin\theta_{14}\cos\theta_{24}\Big(\frac{\nabla_p\theta_{13}}{\nabla_p\theta_{12}}\Big)\Big(\frac{\nabla_p\theta_{34}}{\nabla_p\theta_{12}}\Big) + 2\sin\theta_{23}\sin\theta_{14}\Big(\frac{\nabla_p\theta_{13}}{\nabla_p\theta_{12}}\Big)\Big(\frac{\nabla_p\theta_{24}}{\nabla_p\theta_{12}}\Big) \\
&+ 2\sin\theta_{24}\Big(\frac{\nabla_p\theta_{23}}{\nabla_p\theta_{12}}\Big)\Big(\frac{\nabla_p\theta_{34}}{\nabla_p\theta_{12}}\Big) + 2\sin\theta_{13}\Big(\frac{\nabla_p\theta_{23}}{\nabla_p\theta_{12}}\Big) + 2\cos\theta_{13}\cos\theta_{23}\sin\theta_{14}\Big(\frac{\nabla_p\theta_{24}}{\nabla_p\theta_{12}}\Big) \\
&+ 2\big(\sin\theta_{13}\sin\theta_{23} - \cos\theta_{13}\sin\theta_{23}\sin\theta_{14}\cos\theta_{24}\big)\Big(\frac{\nabla_p\theta_{34}}{\nabla_p\theta_{12}}\Big)\Bigg\} \\
&\pm \frac{1}{2}\Bigg\{\Big[1 + \Big(\frac{\nabla_p\theta_{13}}{\nabla_p\theta_{12}}\Big)^2 + \Big(\frac{\nabla_p\theta_{23}}{\nabla_p\theta_{12}}\Big)^2 + \Big(\frac{\nabla_p\theta_{14}}{\nabla_p\theta_{12}}\Big)^2 + \Big(\frac{\nabla_p\theta_{24}}{\nabla_p\theta_{12}}\Big)^2 + \Big(\frac{\nabla_p\theta_{34}}{\nabla_p\theta_{12}}\Big)^2 \\
&+ 2\sin\theta_{13}\Big(\frac{\nabla_p\theta_{23}}{\nabla_p\theta_{12}}\Big) + 2\big(\cos\theta_{13}\cos\theta_{23}\sin\theta_{14} + \cos\theta_{13}\sin\theta_{23}\cos\theta_{14}\big)\Big(\frac{\nabla_p\theta_{14}}{\nabla_p\theta_{12}}\Big) \\
&+ 2\big(\sin\theta_{13}\sin\theta_{23} - \cos\theta_{13}\sin\theta_{23}\sin\theta_{14}\cos\theta_{24} + \cos\theta_{13}\cos\theta_{23}\cos\theta_{14}\cos\theta_{24}\big)\Big(\frac{\nabla_p\theta_{34}}{\nabla_p\theta_{12}}\Big) \\
&+ 2\sin\theta_{13}\Big(\frac{\nabla_p\theta_{14}}{\nabla_p\theta_{12}}\Big) + 2\big(\cos\theta_{23}\sin\theta_{14}\cos\theta_{24} + \sin\theta_{23}\cos\theta_{14}\cos\theta_{24}\big)\Big(\frac{\nabla_p\theta_{13}}{\nabla_p\theta_{12}}\Big)\Big(\frac{\nabla_p\theta_{34}}{\nabla_p\theta_{12}}\Big) \\
&+ 2\big(\sin\theta_{23}\sin\theta_{14} - \cos\theta_{23}\cos\theta_{14}\big)\Big(\frac{\nabla_p\theta_{13}}{\nabla_p\theta_{12}}\Big)\Big(\frac{\nabla_p\theta_{24}}{\nabla_p\theta_{12}}\Big) + 2\sin\theta_{14}\Big(\frac{\nabla_p\theta_{23}}{\nabla_p\theta_{12}}\Big)\Big(\frac{\nabla_p\theta_{34}}{\nabla_p\theta_{12}}\Big) \\
&+ 2\Big(\frac{\nabla_p\theta_{23}}{\nabla_p\theta_{12}}\Big)\Big(\frac{\nabla_p\theta_{14}}{\nabla_p\theta_{12}}\Big) + 2\sin\theta_{24}\Big(\frac{\nabla_p\theta_{14}}{\nabla_p\theta_{12}}\Big)\Big(\frac{\nabla_p\theta_{34}}{\nabla_p\theta_{12}}\Big)\Big] \\
&\times \Big[1 + \Big(\frac{\nabla_p\theta_{13}}{\nabla_p\theta_{12}}\Big)^2 + \Big(\frac{\nabla_p\theta_{23}}{\nabla_p\theta_{12}}\Big)^2 + \Big(\frac{\nabla_p\theta_{14}}{\nabla_p\theta_{12}}\Big)^2 + \Big(\frac{\nabla_p\theta_{24}}{\nabla_p\theta_{12}}\Big)^2 + \Big(\frac{\nabla_p\theta_{34}}{\nabla_p\theta_{12}}\Big)^2 \\
&+ 2\sin\theta_{13}\Big(\frac{\nabla_p\theta_{23}}{\nabla_p\theta_{12}}\Big) + 2\big(\cos\theta_{13}\cos\theta_{23}\sin\theta_{14} - \cos\theta_{13}\sin\theta_{23}\cos\theta_{14}\big)\Big(\frac{\nabla_p\theta_{14}}{\nabla_p\theta_{12}}\Big) \\
&+ 2\big(\sin\theta_{13}\sin\theta_{23} - \cos\theta_{13}\sin\theta_{23}\sin\theta_{14}\cos\theta_{24} - \cos\theta_{13}\cos\theta_{23}\cos\theta_{14}\cos\theta_{24}\big)\Big(\frac{\nabla_p\theta_{34}}{\nabla_p\theta_{12}}\Big) \\
&- 2\sin\theta_{13}\Big(\frac{\nabla_p\theta_{14}}{\nabla_p\theta_{12}}\Big) + 2\big(\cos\theta_{23}\sin\theta_{14}\cos\theta_{24} - \sin\theta_{23}\cos\theta_{14}\cos\theta_{24}\big)\Big(\frac{\nabla_p\theta_{13}}{\nabla_p\theta_{12}}\Big)\Big(\frac{\nabla_p\theta_{34}}{\nabla_p\theta_{12}}\Big) \\
&+ 2\big(\sin\theta_{23}\sin\theta_{14} + \cos\theta_{23}\cos\theta_{14}\big)\Big(\frac{\nabla_p\theta_{13}}{\nabla_p\theta_{12}}\Big)\Big(\frac{\nabla_p\theta_{24}}{\nabla_p\theta_{12}}\Big) + 2\sin\theta_{14}\Big(\frac{\nabla_p\theta_{23}}{\nabla_p\theta_{12}}\Big)\Big(\frac{\nabla_p\theta_{34}}{\nabla_p\theta_{12}}\Big) \\
&- 2\Big(\frac{\nabla_p\theta_{23}}{\nabla_p\theta_{12}}\Big)\Big(\frac{\nabla_p\theta_{14}}{\nabla_p\theta_{12}}\Big) - 2\sin\theta_{24}\Big(\frac{\nabla_p\theta_{14}}{\nabla_p\theta_{12}}\Big)\Big(\frac{\nabla_p\theta_{34}}{\nabla_p\theta_{12}}\Big)\Big]\Bigg\}^{\frac{1}{2}}\Bigg]^{\frac{1}{2}} \qquad (3.29)
\end{aligned}
$$

3.3 Summary

We consider a four-state sub-Hilbert space as the complete one and perform a generalized BO treatment assuming the validity of adiabatic-diabatic transformation condition, $\vec{\nabla}\mathbf{A} + \vec{\tau}\mathbf{A} = 0$, where the chosen form of the transformation matrix ($\mathbf{A}$) has to be orthogonal at any point in the configuration space and its' elements should be cyclic functions with respect to a parameter. We construct the $\mathbf{A}$ matrix by taking the product of six rotation matrices (off course the product can be taken in numerous ways), substitute in the ADT condition along with generalize anti-symmetric form of the nonadiabatic coupling elements and obtain the explicit expressions of the nonadiabatic coupling elements. Since we have the analytic form of the NAC elements in terms of ADT angles, it become straight forward to formulate the explicit form of the Curl-Divergence equations for the NAC elements and show the validity of Curl equation, which ensure the adiabatic-diabatic transformation with uniquely defined diabatic PESs. Considering the Jacobian at and around the CIs, we briefly present how Curl of NAC elements could be zeros, which again ensure the formulation of EBO equation either approximate or rigorous manner. In order to justify the analytical treatment, namely, the validity of Curl condition and zero Curl for the NAC elements, we solve Mathieu equation as the model system to calculate adiabatic potential energies and nonadiabatic coupling terms. By using those NAC elements, we find that not only Curl conditions are valid but also Curls approach to zeros as the four adiabatic states intend to form a sub-Hilbert space.

References

[1] B. Sarkar and S. Adhikari, J. Phys. Chem. A , DOI 10.1021/jp8029709 (2008).

[2] M. Born and J. R. Oppenheimer, Ann. Phys. (Leipzig) **84**, 457 (1927).

[3] M. Born and K. Huang, *Dynamical Theory of Crystal Lattices*, Oxford University Press, Oxford, 1954.

[4] M. Baer, Chem. Phys. Lett. **35**, 112 (1975).

[5] Z. H. Top and M. Baer, J. Chem. Phys. **66**, 1363 (1977).

[6] A. Alijah and M. Baer, J. Phys. Chem. A **104**, 389 (2000).

[7] D. J. Griffiths, *Introduction to Electrodynamics*, Printice-Hall Inc., Englewood Cliffs, N.J., USA, 1989.

[8] G. B. Arfken and H. J. Weber, *Mathematical Methods for Physicists*, Acadamic Press Inc., San Diego, USA, 1995.

[9] T. Vertesi, A. Vibok, G. J. Halasz and M. Baer, J. Chem. Phys. **121**, 4000 (2004).

[10] D. R.Yarkony, J. Chem. Phys. **84**, 3206 (1986).

[11] M. Baer, S. H. Lin, A. Alijah, S. Adhikari and G. D. Billing, Phys. Rev. A **62**, 32506 (2000).

[12] S. Adhikari, G. D. Billing, A. Alijah, S. H. Lin and M. Baer, Phys. Rev. A **62**, 32507 (2000).

[13] B. Sarkar and S. Adhikari, J. Chem. Phys. **124**, 74101 (2006).

[14] B. Sarkar and S. Adhikari, Int. J. Quantum Chem. , in press (2008).

Chapter 4

Numerical studies of three-state sub-Hilbert space

4.1 Introduction

In this chapter, first we demonstrate[1,2] the validity of our *rigorous* EBO equation [Eq. (2.39)] and find it's necessity with respect to *approximate* EBO equation [Eq. (2.40)]. Though we obtain good agreements between the results calculated by using Eq. (2.39) and (2.40), it will be wise to use Eq. (2.39) to incorporate the contribution of the elements of **G** matrix. The results obtained from these equations are compared with so called numerically exact diabatic one [Eq. (2.6)], where calculations are performed on two different models (**Model A** and **Model B**) involving three electronic states. These models are developed by using *two nuclear coordinates only* in order to keep the simplicity of numerical calculations but not loosing the generality in terms of physical insight of the inbuilt phenomena. Secondly, we explore[3] the validity of the Curl condition, $\left[\frac{\partial}{\partial p}\tau_{ij}^{q} - \frac{\partial}{\partial q}\tau_{ij}^{p} = (\boldsymbol{\tau}^{q}\boldsymbol{\tau}^{p})_{ij} - (\boldsymbol{\tau}^{p}\boldsymbol{\tau}^{q})_{ij}\right]$, as well as zero Curls, when the three states are either degenerate at a point or approaching to form three states degeneracy at the same point, by using an *Induced Renner-Teller (RT) type model*. Since the RT model is in diabatic representation, the validity of Curl conditions are inbuilt but the outcome, the validity of zero Curls, help us to formulate the Extended Born-Oppenheimer (EBO) equation. Such EBO equation can be used to carry out accurate ground state calculation by taking into account the effect of upper PESs.

4.2 The Models and the nonadiabatic coupling elements

The nonadiabatic coupling among any three electronic states could show up single or multiple number of CI(s) at a particular or different nuclear configuration(s) space, respectively. One of the commonest possibility is the presence of two CIs, namely, the first and second electronic states may indicate a CI at a particular nuclear configuration and the second and third electronic can have another CI at different nuclear configuration. There is another possibility, not really uncommon, among the three electronic states, i.e., the CI at a single point. When the CIs are at different nuclear configuration space, they could be far apart from each other or even close enough. If they are far away from each other, effectively the 3×3 BO system translates into two 2×2 BO systems. In such situation, the matrix **G**, which diagonalizes the anti-symmetric scalar matrix $\boldsymbol{g}$, commutes with the operator $\vec{\nabla}$ and thereby, Eq. (2.40) could be considered as the *rigorous* EBO equation. On the other hand, when the system has two close enough CIs or a single CI among the three states, the **G** matrix does not commute with $\vec{\nabla}$ and Eq. (2.39) would be the *rigorous* form of the EBO equation.

4.2.1 The Model A

4.2.1.1 The nonadiabatic coupling elements and adiabatic PESs

The nonadiabatic coupling elements of the molecule C_2H is a good example to cite in connection with our following proposed **Model A** even though there are some differences also. The *ab initio*[4,5] calculations for the same molecule show that there is a CI between $2\,^2A'$ and $3\,^2A'$ states at a particular nuclear configuration and are two CIs between $3\,^2A'$ and $4\,^2A'$ states at different configuration of the nuclear space, where the spatial distributions of the NAC terms, $\vec{\tau}_{12}$, $\vec{\tau}_{13}$ and $\vec{\tau}_{23}$ depending upon the size of the circular contours dictate whether the three state problem can be resolved or not into two approximate two state systems. There are numerous molecules with similar nonadiabatic coupling profiles among the three consecutive adiabatic electronic states.

The construction of **Model A** (a 3×3 BO system) is such that it breaks up into two 2×2 BO systems when the point of CI between the first and the second states is far away from the point of CI between the second and the third states. This become possible by introducing $\vec{\tau}_{12}$ and $\vec{\tau}_{23}$ in a way that their spatial distributions either do not or have very small overlap with respect to the radial coordinate at the asymptote, where $\vec{\tau}_{13}$ is made nearly or identically zero. Such functional form of nonadiabatic terms can be incorporated by manipulating the nuclear coordinate (let say x and y) dependence of the ADT angles, $\theta_{12}(\mathbf{n})$, $\theta_{23}(\mathbf{n})$ and $\theta_{13}(\mathbf{n})$. In other words, we choose the spatial distribution of ADT angles such that $\vec{\nabla}\theta_{12} \neq 0$ and $\vec{\nabla}\theta_{23} \simeq 0$ around the first CI and $\vec{\nabla}\theta_{23} \neq 0$ and $\vec{\nabla}\theta_{12} \simeq 0$ around the second CI. Moreover, since we assume that the **Model A** do not have any conical intersection between the first and third state for the entire range, $-\infty \leq x, y \leq \infty$, the ADT angle ($\theta_{13}$) between those states for the same space is expected to be small, i.e., $\theta_{13} \simeq 0$ and $\vec{\nabla}\theta_{13} \simeq 0$. Thus, the nonadiabatic coupling elements [Eq. (2.10)] take the following form:

$$\vec{\tau}_{12} \simeq -\vec{\nabla}\theta_{12} \quad (4.1a)$$

$$\vec{\tau}_{23} \simeq -\cos\theta_{12}\vec{\nabla}\theta_{23}, \quad (4.1b)$$

$$\vec{\tau}_{13} \simeq -\sin\theta_{12}\vec{\nabla}\theta_{23}, \quad (4.1c)$$

If the CIs in **Model A** are asymptotically apart, it is quite reasonable to assume that $\cos\theta_{12} \approx 1$ and $\sin\theta_{12} \approx 0$ with $\vec{\nabla}\theta_{23} \neq 0$ and $\vec{\nabla}\theta_{12} \simeq 0$ at around the second CI and thereby, nonadiabatic coupling elements [Eq. (4.1)] are given by, $\vec{\tau}_{12} \simeq 0$, $\vec{\tau}_{23} \simeq -\vec{\nabla}\theta_{23}$ and $\vec{\tau}_{13} \simeq 0$ with Curl $\tau_{ij} \simeq 0$, whereas at around the first CI, since $\vec{\nabla}\theta_{23} \simeq 0$ and $\vec{\nabla}\theta_{12} \neq 0$, nonadiabatic coupling elements [Eq. (4.1)] appear as, $\vec{\tau}_{12} \simeq -\vec{\nabla}\theta_{12}$, $\vec{\tau}_{23} \simeq 0$ and $\vec{\tau}_{13} \simeq 0$ with Curl $\tau_{ij} \simeq 0$. Hence, both the situations altogether lead to two approximate two-state BO systems.

In summary, even if there is no conical intersection between the first and the third state, i.e., the ADT angle $\theta_{13}(\mathbf{n})$ between these two states is assumed either remain constant or zero for the entire nuclear configuration space, still it does not mean that the nonadiabatic coupling term, $\vec{\tau}_{13}$, is exactly zero since it can grow due to the spatial overlapping of the NAC terms, $\vec{\tau}_{12}$ and $\vec{\tau}_{23}$ [see Eq. (2.10)]. In order to fulfill the above expectations from **Model A**, we introduce the following three different choices of spatial distribution on the ADT angles:

(I) $\theta^1_{12}(x,y) = \frac{1}{2}\tan^{-1}(\frac{y}{x-x_0})$, $\theta^1_{23}(x,y) = \frac{1}{2}\tan^{-1}(\frac{y}{x_0-x})$ and $\theta^1_{13}(x,y) = 0$;

(II) $\theta^2_{12}(x,y) = \frac{1}{2}\tan^{-1}(\frac{y}{x-x_0}) - \frac{1}{4}\sin\Big[2\tan^{-1}(\frac{y}{x-x_0})\Big]$,
$\theta^2_{23}(x,y) = \frac{1}{2}\tan^{-1}(\frac{y}{x_0-x}) - \frac{1}{4}\sin\Big[2\tan^{-1}(\frac{y}{x_0-x})\Big]$ and $\theta^2_{13}(x,y) = 0$;

(III) $\theta^3_{12}(x,y) = \frac{1}{2}\tan^{-1}(\frac{y}{x-x_0})$, $\theta^3_{23}(x,y) = \frac{1}{2}\tan^{-1}(\frac{y}{x_0-x}) - \frac{1}{4}\sin\Big[2\tan^{-1}(\frac{y}{x_0-x})\Big]$
and $\theta^3_{13}(x,y) = 0$.

It may be noted that the choices of the functional form of these three sets of ADT angles are not quite arbitrary, particularly, the set (II) angles are the fitted ones from *ab initio* calculated data.[4] We substitute the set (II) angles in the Eq. (2.10) to obtain the spatial distributions of nonadiabatic coupling elements and display the corresponding NAC elements in Figs. 4.1a − 4.1c for various separation [$2x_0$ (= 4, 2, 0.5 Å)] between the CIs. The right inset in Fig. 4.1a shows the profile of set (II) ADT angles (θ_{12}/θ_{23}) as function of the nuclear coordinate $\theta[=\tan^{-1}(\frac{y}{x})]$, where the left inset in Figs. 4.1a − 4.1c present how the functional form of $|\tau_{13}|$ grows as $|\tau_{12}|$ and $|\tau_{23}|$ appear closer and closer. For a given separation of CIs ($2x_0$), each set of NAC terms along with the following chosen form of adiabatic PESs,

$$
\begin{aligned}
u_1(x,y) &= \frac{1}{2}\mu[\omega_0 - \tilde{\omega}_1(x)]^2 y^2 + A_1 \times f_1(x,y), \\
u_2(x,y) &= \frac{1}{2}\mu\omega_0^2 y^2 - (D_1 - A_1) \times f_1(x,y) + A_1 \times f_2(x,y) + D_1, \\
u_3(x,y) &= \frac{1}{2}\mu\omega_0^2 y^2 - (D_1 - A_1) \times f_2(x,y) + D_2, \\
\tilde{\omega}_1(x) &= \omega_1 \exp\Big[-\frac{(x-x_0)^2}{\sigma_1^2}\Big], \\
f_1(x,y) &= \exp\Big[-\frac{(x-x_0)^2 + y^2}{\sigma^2}\Big], \\
f_2(x,y) &= \exp\Big[-\frac{(x+x_0)^2 + y^2}{\sigma^2}\Big], \qquad (4.2)
\end{aligned}
$$

defines the corresponding adiabatic nuclear SE [Eq. (2.4)]. Fig. 4.2a presents those adiabatic PESs for $2x_0 = 4$ Å with the potential parameters as given by $\mu = 0.58$ amu, $A_1 = 3.0$

eV, $D_1 = 5.0$ eV, $D_2 = 10.0$ eV, $\omega_0 = 39.14 \times 10^{13}$ s^{-1}, $\omega_1 = 7.83 \times 10^{13}$ s^{-1}, $\sigma = 0.3$ Å and $\sigma_1 = 0.75$ Å, respectively.

4.2.1.2 *The diabatic and rigorous EBO equation*

Finally, each set of ADT angles as chosen in previous section are being used to construct the ADT matrix [Eq. (2.8)] and thereby, to transform the adiabatic to diabatic SE [Eq. (2.6)]. The detailed expression of adiabatic SEs and diabatic potentials for any generalized form of ADT (mixing) angles were presented in **Appendix A**. On the other hand, in order to formulate the EBO equation for **Model A**, we make use the following form of the $\boldsymbol{\tau}$ matrix by considering $\theta_{13} = 0$ in the Eq. (2.21):

$$
\begin{aligned}
\vec{\boldsymbol{\tau}} &= \vec{\nabla}\theta_{12} \begin{pmatrix} 0 & -1 & -\sin\theta_{12}\left(\frac{\nabla_p\theta_{23}}{\nabla_p\theta_{12}}\right) \\ 1 & 0 & -\cos\theta_{12}\left(\frac{\nabla_p\theta_{23}}{\nabla_p\theta_{12}}\right) \\ \sin\theta_{12}\left(\frac{\nabla_p\theta_{23}}{\nabla_p\theta_{12}}\right) & \cos\theta_{12}\left(\frac{\nabla_p\theta_{23}}{\nabla_p\theta_{12}}\right) & 0 \end{pmatrix} \\
&= \vec{\nabla}\theta_{12} \cdot \boldsymbol{g}(\theta_{12}, \theta_{13}).
\end{aligned} \tag{4.3}
$$

The eigenvalue $\pm i\vec{\omega}$ ($\vec{\omega} = \vec{\nabla}\theta_{12}\left[1 + \left(\frac{\nabla_p\theta_{23}}{\nabla_p\theta_{12}}\right)^2\right]^{\frac{1}{2}}$) and the corresponding eigenvector [$i\vec{\omega} = \vec{\nabla}\theta_{12} \cdot \mathbf{G}^{\mathrm{d}}\boldsymbol{g}(\theta_{12}, \theta_{13})\mathbf{G}$] with the following three elements,

$$
\begin{aligned}
G^d_{11} &= -\cos\theta_{12}\left(\frac{\nabla_p\theta_{23}}{\nabla_p\theta_{12}}\right) \times \left[1 + \left(\frac{\nabla_p\theta_{23}}{\nabla_p\theta_{12}}\right)^2\right]^{-\frac{1}{2}}, \\
G^d_{12} &= \sin\theta_{12}\left(\frac{\nabla_p\theta_{23}}{\nabla_p\theta_{12}}\right) \times \left[1 + \left(\frac{\nabla_p\theta_{23}}{\nabla_p\theta_{12}}\right)^2\right]^{-\frac{1}{2}}, \\
G^d_{13} &= -\left[1 + \left(\frac{\nabla_p\theta_{23}}{\nabla_p\theta_{12}}\right)^2\right]^{-\frac{1}{2}},
\end{aligned}
$$

are substituted in the Eq. (2.39) to obtain the explicit form of *rigorous* EBO equation (see **Appendix D**) for the ground state.

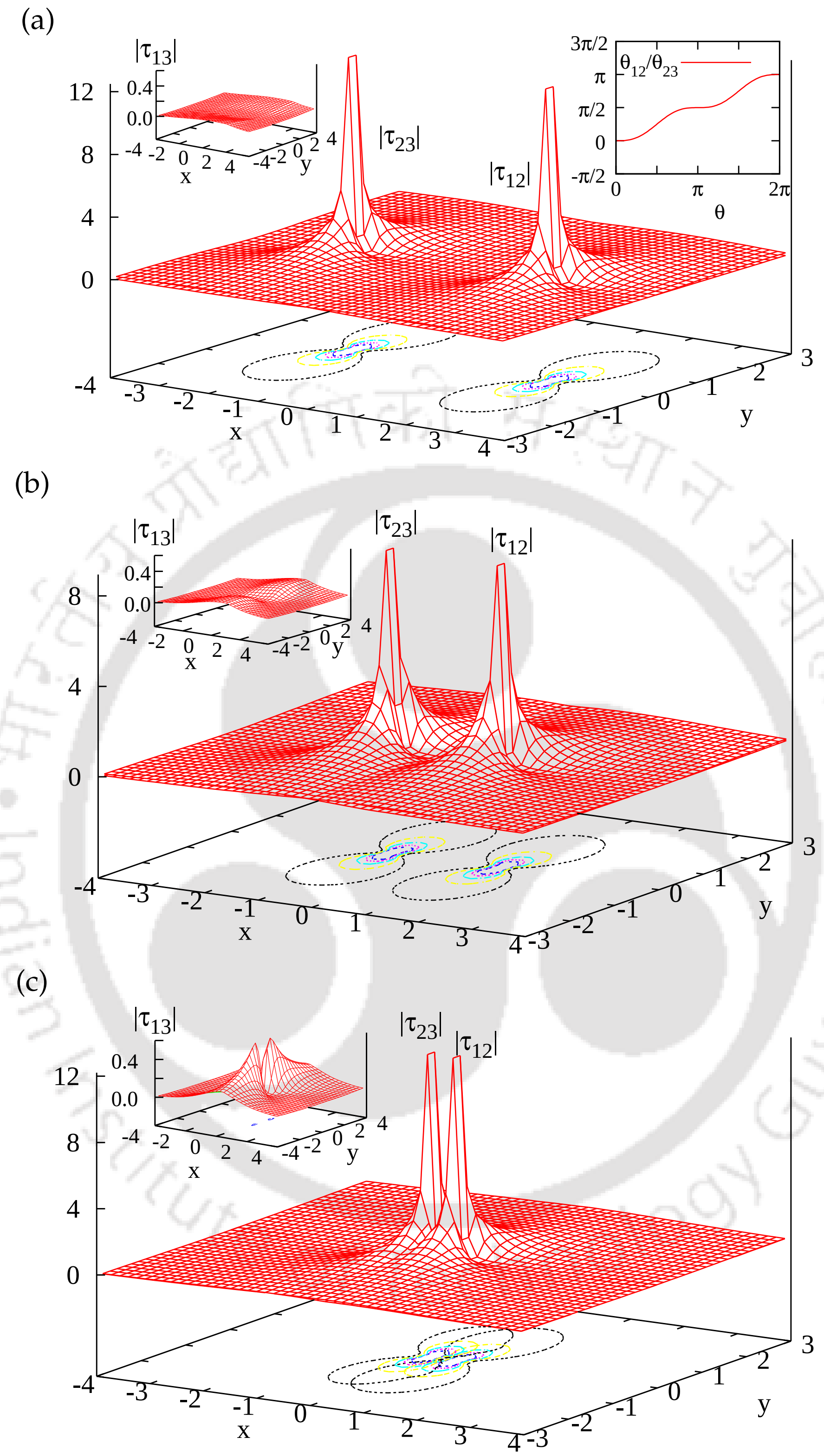

Figure 4.1: Profile of the nonadiabatic coupling elements (τ_{12} and τ_{23}) with the separation of (a) 4 Å, (b) 2 Å and (c) 0.5 Å between (1,2) and (2,3) CI considering adiabatic-to-diabatic transformation angles angles $\theta_{12}(x, y) = \theta_{23}(x, y) = \frac{1}{2}\tan^{-1}(\frac{y}{x}) - \frac{1}{4}\sin[2\tan^{-1}(\frac{y}{x})]$ and $\theta_{13}(x, y) = 0$. The inset in right of the figures show the nonadiabatic coupling element τ_{13}, while the inset on left of Fig. 4.1(a) represents the adiabatic-to-diabatic transformation angles angles.

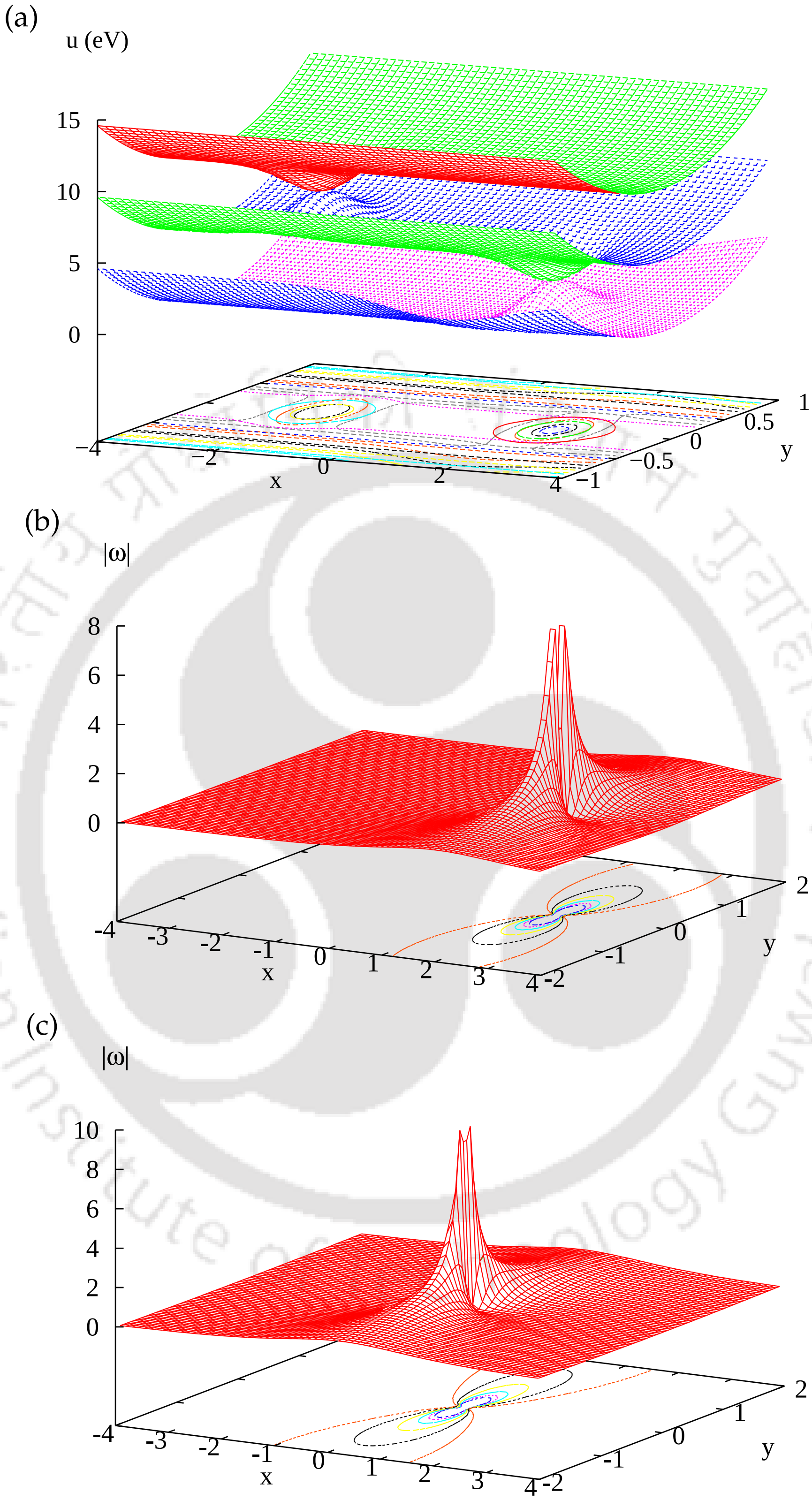

Figure 4.2: (a) The three adiabatic potential energy surfaces for Model A. The functional form of the eigenvalues ($|\omega_{II}|$) of the NAC matrix arising due to the ADT angles $\theta_{12}(x,y) = \theta_{23}(x,y) = \frac{1}{2}\tan^{-1}(\frac{y}{x}) - \frac{1}{4}\sin[2\tan^{-1}(\frac{y}{x})]$ and $\theta_{13}(x,y) = 0$ for (b) 4 Å and (c) 0.5 Å separation of CIs.

The gradient ratios of the mixing angles, θ_{12} and θ_{23} at the point (1,2) CI, $x = x_0$ for the above three sets are given by,

$$\left(\frac{\nabla_x\theta^1_{23}}{\nabla_x\theta^1_{12}}\right)\Big|_{x=x_0} = \frac{y^2}{(2x_0)^2+y^2}, \tag{4.4a}$$

$$\left(\frac{\nabla_x\theta^2_{23}}{\nabla_x\theta^2_{12}}\right)\Big|_{x=x_0} = \frac{y^2}{2[(2x_0)^2+y^2]}\left[1-\cos\left(2\tan^{-1}\frac{y}{2x_0}\right)\right], \tag{4.4b}$$

$$\left(\frac{\nabla_x\theta^3_{23}}{\nabla_x\theta^3_{12}}\right)\Big|_{x=x_0} = \frac{y^2}{(2x_0)^2+y^2}\left[1-\cos\left(2\tan^{-1}\frac{y}{2x_0}\right)\right], \tag{4.4c}$$

with the eigenvalues of the corresponding NAC matrices,

$$\vec{\omega_I} = \vec{\nabla}\theta^1_{12}\left[1+\frac{y^4}{(4x_0^2+y^2)^2}\right]^{\frac{1}{2}}, \tag{4.5a}$$

$$\vec{\omega_{II}} = \vec{\nabla}\theta^2_{12}\left\{1+\frac{y^4}{4(4x_0^2+y^2)^2}\left[1-\cos\left(2\tan^{-1}\frac{y}{2x_0}\right)\right]^2\right\}^{\frac{1}{2}}, \tag{4.5b}$$

$$\vec{\omega_{III}} = \vec{\nabla}\theta^3_{12}\left\{1+\frac{y^4}{(4x_0^2+y^2)^2}\left[1-\cos\left(2\tan^{-1}\frac{y}{2x_0}\right)\right]^2\right\}^{\frac{1}{2}}. \tag{4.5c}$$

The functional form of the eigenvalue ($|\omega|$) of the NAC matrix arising due to set (II) ADT angles are presented in Fig. 4.2b – 4.2c for the 4 Å and 0.5 Å separation of CIs, respectively.

We are now in a position to analyze the EBO equations at two extreme situations when the cis are (a) infinitely separated ($2x_0 \rightarrow \infty$) or (b) approaching to a point ($2x_0 \rightarrow 0$). Though the EBO equations of Model A are formulated with $\theta_{13}(x, y) = 0$, it is important to note that $\theta_{13}(x, y)$ may not be identically zero, particularly, when the separation between the cis is enough small. At $2x_0 \rightarrow \infty$, eigenvalues [Eq. (4.5)] of NAC matrices are, $\vec{\omega_I} = \vec{\nabla}\theta^1_{12}$, $\vec{\omega_{II}} = \vec{\nabla}\theta^2_{12}$ and $\vec{\omega_{III}} = \vec{\nabla}\theta^3_{12}$, with the following gauge invariance conditions,[6]

$$\frac{1}{2\pi}\int_0^{2\pi}\omega_I(\vec{\mathbf{n}}).d\vec{\mathbf{n}} = \frac{1}{2\pi}\int_0^{2\pi}\omega_{II}(\vec{\mathbf{n}}).d\vec{\mathbf{n}} = \frac{1}{2\pi}\int_0^{2\pi}\omega_{III}(\vec{\mathbf{n}}).d\vec{\mathbf{n}} = 0.5 \tag{4.6}$$

and the model is breakable into two 2×2 BO systems. On the other hand, at $2x_0 \rightarrow 0$, eigenvalues for the three sets are $\vec{\omega_I} = \sqrt{2}\vec{\nabla}\theta^1_{12}$, $\vec{\omega_{II}} = \sqrt{2}\vec{\nabla}\theta^2_{12}$ and $\vec{\omega_{III}} = \sqrt{5}\vec{\nabla}\theta^3_{12}$ with gauge invariance conditions,

$$\frac{1}{2\pi}\int_0^{2\pi}\omega_I(\vec{\mathbf{n}}).d\vec{\mathbf{n}} = 0.70,$$
$$\frac{1}{2\pi}\int_0^{2\pi}\omega_{II}(\vec{\mathbf{n}}).d\vec{\mathbf{n}} = 0.70,$$
$$\frac{1}{2\pi}\int_0^{2\pi}\omega_{III}(\vec{\mathbf{n}}).d\vec{\mathbf{n}} = 1.11, \tag{4.7}$$

respectively. Thus, as the separation ($2x_0$) between the cis decreases, Model A transforms towards a three state BO problem and will be faster with the set (III) - mixing angles than the other two sets.

4.2.1.3 Numerical calculations: results and discussions

We consider the product of the ground vibrational state for the harmonic mode (at the asymptote of the scattering mode) and the Gaussian wavepacket with various KE energies for the scattering mode as the initial wavefunction for the ground adiabatic state of the system. This adiabatic wavefunction is being propagated by using single surface BO approximate, approximated EBO and rigorous EBO equations as functions of time with the help of numerically accurate TDDVR[1] approach and the respective wavefunction at $t \to \infty$ is projected on the asymptotic eigenfunctions of the Hamiltonian to obtain the state - to - state vibrational transition probabilities at different energies. We perform all those dynamical calculations at total energies 1.25, 1.50 and 1.75 eV. It is important to note that all those equations (single surface BO approximate, approximated EBO and rigorous EBO equation) are derived with the assumption, namely, upper electronic states are expected to be classically closed at those energies (1.25, 1.50 and 1.75 eV) with respect to the point of first conical intersection at 3.0 eV. On the other hand, we calculate the initial diabatic wavefunctions by caring out the adiabatic - diabatic transformation [Eq. (2.8)] on the wavefunction matrix, where the first element represents the same adiabatic wavefunction for the ground state at $t = 0$. Table 4.1 $-$ 4.3 present the reactive state - to - state transition probabilities for the three sets (I) - (III), respectively. When the separation between the cis are 4 or 3 Å, transition probabilities calculated by single surface EBO equations not only follow the correct symmetry (even $\to$ odd or odd $\to$ even) but also achieve quantitative agreement with diabatic results. On the contrary, if the cis are 1 or 0.5 Å apart, there is gradual increase on even → even transitions along with even → odd transitions and some quantitative disagreement between diabatic and EBO results at all energies. As the separation between cis is decreasing, even → even transitions are growing because the model is transforming from a two to a three state BO system as predicted by gauge invariance condition. This effect is more prominent with the choice on the functional form of the set (III) - mixing angles and Table 4.3 clearly demonstrates the fact. Disagreements between diabatic and EBO results at smaller separations ($2x_0$ = 0.5 or 1.0 Å) between the cis may arise for two possible reasons: (a) EBO equation can not provide meaningful solution since the gauge invariance condition is away from half integer or integer and (b) the formulation of EBO equation considering Curl $\tau_{ij} \simeq 0$ may not be a correct approach. In order to explore the cause of disagreement between diabatic and EBO results at smaller separation of cis, we find the eigenvalues of the nonadiabatic coupling matrices constructed by using set (I)$-$ mixing angles with 4 and 0.5 Å separation of cis as

$$\vec{\omega}_I(2x_0 = 4) = \vec{\nabla}\theta^1_{12}\Big[1 + \frac{y^4}{(16 + y^2)^2}\Big]^{\frac{1}{2}}, \tag{4.8a}$$

$$\vec{\omega}_I(2x_0 = 0.5) = \vec{\nabla}\theta^1_{12}\Big[1 + \frac{y^4}{(0.25 + y^2)^2}\Big]^{\frac{1}{2}}, \tag{4.8b}$$

where the corresponding gauge invariance conditions are approximately 0.50 and 0.70, respectively. On the other hand, if we choose the functional form of mixing angles: (a) $\theta_{12} = \frac{1}{2}\tan^{-1}\frac{y}{x - x_0}$, $\theta_{23} = \frac{1}{2}\tan^{-1}\frac{y}{x + x_0}$ and $\theta_{13} = 0$ and (b) $\theta_{12} = \frac{1}{2}\tan^{-1}\frac{y}{x - x_0}$, $\theta_{23} = \frac{1}{128}\tan^{-1}\frac{y}{x + x_0}$ and $\theta_{13} = 0$ with the cis at 4.0 and 0.5 Å apart, respectively, eigenvalues of the corresponding NAC matrices are:

$$\vec{\omega}(2x_0 = 4) = \vec{\nabla}\theta^1_{12}\Big[1 + \frac{y^4}{(16 + y^2)^2}\Big]^{\frac{1}{2}}, \tag{4.9a}$$

$$\vec{\omega}(2x_0 = 0.5) = \vec{\nabla}\theta^1_{12}\Big[1 + \frac{y^4}{(16 + 64y^2)^2}\Big]^{\frac{1}{2}}, \tag{4.9b}$$

with approximately the same gauge invariance condition (0.5). Thus, diabatic and EBO results due to the cis at 0.5 Å apart with $\theta_{23} = \frac{1}{128}\tan^{-1}\frac{y}{x + x_0}$ are expected to be similar

Table 4.1: Reactive state-to-state transition probabilities when (1,2) and (2,3) conical intersections are 4 Å, 3 Å, 2 Å, 1 Å and 0.5 Å ($2x_0$) apart. The diabatic surfaces are constructed considering the mixing angles, $\theta^1_{12}(x,y) = \frac{1}{2}\tan^{-1}(\frac{y}{x-x_0})$, $\theta^1_{13}(x,y) = 0$ and $\theta^1_{23}(x,y) = \frac{1}{2}\tan^{-1}(\frac{y}{x_0-x})$. The corresponding EBOs are derived under the same condition.

$2x_0$	1.25 eV					1.50 eV					1.75 eV				
	$0 \to 0$	$0 \to 1$	$0 \to 2$	$0 \to 3$	$0 \to 4$	$0 \to 0$	$0 \to 1$	$0 \to 2$	$0 \to 3$	$0 \to 4$	$0 \to 0$	$0 \to 1$	$0 \to 2$	$0 \to 3$	$0 \to 4$
4 Å	0.0008[a]	0.0217	0.0020	0.0147	0.0007	0.0040	0.0300	0.0032	0.0412	0.0123	0.0006	0.0357	0.0075	0.0763	0.0049
	0.0005[b]	0.0274	0.0022	0.0145	0.0004	0.0008	0.0300	0.0084	0.0414	0.0021	0.0002	0.0357	0.0021	0.0761	0.0016
3 Å	0.0056	0.0490	0.0032	0.0258	0.0059	0.0007	0.0461	0.0061	0.0693	0.0032	0.0047	0.0415	0.0073	0.0851	0.0209
	0.0033	0.0492	0.0073	0.0212	0.0003	0.0004	0.0462	0.0231	0.0694	0.0010	0.0012	0.0416	0.0042	0.0851	0.0087
2 Å	0.0026	0.0514	0.0038	0.2248	0.0115	0.0044	0.0423	0.0023	0.0352	0.0010	0.0043	0.0442	0.0022	0.0357	0.0016
	0.0018	0.0515	0.0173	0.2223	0.0134	0.0042	0.0417	0.0146	0.0351	0.0010	0.0104	0.0453	0.0138	0.0357	0.0058
1 Å	0.0052	0.0850	0.0005	0.0835	0.0033	0.0010	0.0575	0.0009	0.0969	0.0031	0.0224	0.0444	0.0488	0.0526	0.0352
	0.0006	0.0850	0.0189	0.0839	0.0461	0.0232	0.0576	0.0332	0.0978	0.0258	0.0249	0.0497	0.0064	0.0675	0.0031
0.5 Å	0.0020	0.0682	0.0053	0.0252	0.0001	0.0060	0.0724	0.0015	0.0204	0.0129	0.0170	0.0347	0.0198	0.0438	0.0438
	0.0511	0.0682	0.0153	0.0154	0.0025	0.0270	0.0724	0.0430	0.0206	0.0007	0.0203	0.0345	0.0189	0.0507	0.0005

[a] EBO
[b] Diabatic

Table 4.2: Reactive state-to-state transition probabilities when (1,2) and (2,3) conical intersections are 4 Å, 3 Å, 2 Å, 1 Å and 0.5 Å ($2x_0$) apart. The diabatic surfaces are constructed considering the mixing angles, $\theta_{12}^2(x,y) = \frac{1}{2}\tan^{-1}(\frac{y}{x-x_0}) - \frac{1}{4}\sin[2\tan^{-1}(\frac{y}{x-x_0})]$, $\theta_{13}^2(x,y) = 0$, and $\theta_{23}^2(x,y) = \frac{1}{2}\tan^{-1}(\frac{y}{x_0-x}) - \frac{1}{4}\sin[2\tan^{-1}(\frac{y}{x_0-x})]$. The corresponding EBOs are derived under the same condition.

$2x_0$	1.25 eV					1.50 eV					1.75 eV				
	$0\to0$	$0\to1$	$0\to2$	$0\to3$	$0\to4$	$0\to0$	$0\to1$	$0\to2$	$0\to3$	$0\to4$	$0\to0$	$0\to1$	$0\to2$	$0\to3$	$0\to4$
4 Å	0.0025[a]	0.0500	0.0061	0.0384	0.0001	0.0021	0.0206	0.0030	0.1080	0.0204	0.0006	0.0174	0.0034	0.0885	0.0036
	0.0005[b]	0.0510	0.0006	0.0492	0.0334	0.0016	0.0216	0.0340	0.1089	0.0048	0.0000	0.0179	0.0007	0.0884	0.0004
3 Å	0.0050	0.0592	0.0039	0.0758	0.0041	0.0019	0.0427	0.0006	0.0880	0.0063	0.0002	0.0513	0.0009	0.0286	0.0003
	0.0021	0.0586	0.0224	0.0713	0.0022	0.0011	0.0428	0.0004	0.0880	0.0297	0.0003	0.0514	0.0004	0.0284	0.0002
2 Å	0.0034	0.0337	0.0000	0.0140	0.0000	0.0026	0.0366	0.0001	0.0223	0.0000	0.0022	0.0413	0.0002	0.0282	0.0001
	0.0004	0.0338	0.0031	0.0140	0.0021	0.0001	0.0366	0.0012	0.0223	0.0001	0.0002	0.0411	0.0008	0.0281	0.0002
1 Å	0.0305	0.0311	0.0001	0.0929	0.0035	0.0058	0.0485	0.0049	0.1008	0.0029	0.0081	0.0450	0.0011	0.0740	0.0163
	0.0026	0.0349	0.0008	0.0910	0.0002	0.0034	0.0480	0.0036	0.1061	0.0013	0.0057	0.0449	0.0069	0.0730	0.0005
0.5 Å	0.0012	0.0252	0.0084	0.0631	0.0005	0.0028	0.0692	0.0121	0.0694	0.0098	0.0047	0.0698	0.0011	0.0181	0.0212
	0.0104	0.0250	0.0010	0.0280	0.0139	0.0000	0.0686	0.0057	0.0539	0.0019	0.0102	0.0696	0.0282	0.1148	0.0194

[a] EBO
[b] Diabatic

Table 4.3: Reactive state-to-state transition probabilities when (1,2) and (2,3) conical intersections are 4 Å, 3 Å, 2 Å, 1 Å and 0.5 Å ($2x_0$) apart. The diabatic surfaces are constructed considering the mixing angles, $\theta^3_{12}(x,y) = \frac{1}{2}\tan^{-1}(\frac{y}{x-x_0})$, $\theta^3_{13}(x,y) = 0$ and $\theta^3_{23}(x,y) = \frac{1}{2}\tan^{-1}(\frac{y}{x_0-x}) - \frac{1}{4}\sin[2\tan^{-1}(\frac{y}{x_0-x})]$. The corresponding EBOs are derived under the same condition.

$2x_0$	1.25 eV					1.50 eV					1.75 eV				
	$0\rightarrow0$	$0\rightarrow1$	$0\rightarrow2$	$0\rightarrow3$	$0\rightarrow4$	$0\rightarrow0$	$0\rightarrow1$	$0\rightarrow2$	$0\rightarrow3$	$0\rightarrow4$	$0\rightarrow0$	$0\rightarrow1$	$0\rightarrow2$	$0\rightarrow3$	$0\rightarrow4$
4 Å	0.0009[a]	0.0247	0.0044	0.0657	0.0032	0.0015	0.0352	0.0021	0.0244	0.0049	0.0004	0.0253	0.0062	0.0635	0.0057
	0.0000[b]	0.0251	0.0008	0.0687	0.0023	0.0001	0.0352	0.0015	0.0245	0.0068	0.0108	0.0245	0.0023	0.0650	0.0017
3 Å	0.0057	0.0498	0.0036	0.0220	0.0079	0.0004	0.0491	0.0063	0.0388	0.0023	0.0017	0.0250	0.0042	0.0299	0.0057
	0.0026	0.0450	0.0043	0.0286	0.0063	0.0009	0.0488	0.0093	0.0399	0.0001	0.0000	0.0259	0.0000	0.0292	0.0003
2 Å	0.0054	0.0218	0.0007	0.0047	0.0001	0.0049	0.0355	0.0016	0.0212	0.0005	0.0043	0.0442	0.0022	0.0357	0.0016
	0.0001	0.0218	0.0003	0.0139	0.0000	0.0006	0.0355	0.0006	0.0212	0.0115	0.0024	0.0442	0.0013	0.0357	0.0038
1 Å	0.0035	0.0343	0.0023	0.1144	0.0075	0.0003	0.0281	0.0013	0.0789	0.0029	0.0029	0.0255	0.0002	0.0950	0.0176
	0.0013	0.0343	0.0026	0.1170	0.0019	0.0026	0.0281	0.0096	0.0787	0.0119	0.0004	0.0255	0.0043	0.0949	0.0046
0.5 Å	0.0117	0.0238	0.0310	0.0130	0.0028	0.0063	0.0098	0.0057	0.0538	0.0088	0.0072	0.0051	0.0040	0.0500	0.0052
	0.0211	0.0238	0.0168	0.0589	0.0034	0.0024	0.0098	0.0181	0.0578	0.0520	0.0036	0.0070	0.0030	0.0500	0.0364

[a] EBO
[b] Diabatic

Table 4.4: Comparison of reactive transition probabilities when calculations are performed on the diabatic surfaces where (1,2) and (2,3) conical intersections are separated by (a) 4 Å with the mixing angles $\theta^1_{12}(x,y) = \frac{1}{2}\tan^{-1}(\frac{y}{x-x_0})$, $\theta^1_{13}(x,y) = 0$, $\theta^1_{23}(x,y) = \frac{1}{2}\tan^{-1}(\frac{y}{x_0-x})$, and (b) 0.5 Å with the mixing angles $\theta^1_{12}(x,y) = \frac{1}{2}\tan^{-1}(\frac{y}{x-x_0})$, $\theta^1_{13}(x,y) = 0$, $\theta^1_{23}(x,y) = \frac{1}{128}\tan^{-1}(\frac{y}{x_0-x})$, whereas the corresponding EBOs are constructed under the same condition.

E(eV)	$0\rightarrow0$	$0\rightarrow1$	$0\rightarrow2$	$0\rightarrow3$	$0\rightarrow4$
1.25	0.0005[a]	0.0274	0.0022	0.0145	0.0004
	0.0083[b]	0.0287	0.0041	0.0105	0.0089
	0.0008[c]	0.0217	0.0020	0.0147	0.0007
1.50	0.0008	0.0300	0.0084	0.0414	0.0021
	0.0022	0.0309	0.0035	0.0448	0.0018
	0.0040	0.0300	0.0032	0.0412	0.0123
1.75	0.0002	0.0357	0.0021	0.0761	0.0016
	0.0040	0.0356	0.0019	0.0503	0.0000
	0.0006	0.0357	0.0075	0.0763	0.0049

[a] 4 Å
[b] 0.5 Å
[c] EBO

with those diabatic results when cis are separated by 4 Å and $\theta_{23} = \frac{1}{2}\tan^{-1}\frac{y}{x+x_0}$. We present those transition probabilities in Table 4.4 where even → odd transitions appear exclusively with reasonably good quantitative agreement. We also find the equivalent condition, $\theta_{23} = \frac{1}{72}\tan^{-1}\frac{y}{x+x_0}$ for the cis separated by 0.5 Å to reproduce the diabatic and EBO results of the BO system with $\theta_{23} = \frac{1}{2}\tan^{-1}\frac{y}{x+x_0}$ and $2x_0$ = 3 Å. Table 4.5 displays that calculated transition probabilities are qualitatively correct and quantitatively accurate. We also explore and obtain equivalent conditions between diabatic and EBO equations with the cis separated by 4 and 0.5 Å, respectively, for the set (II) as well as set (III) - mixing angles. Table 4.6 and 4.7 present that numerically calculated results are in par with our theoretical prediction. Thus, numerical calculations on Model A demonstrate that EBO equations formulated by introducing zero Curl can evaluate correct symmetry allowed transition probabilities and bring quantitative agreement with diabatic results if eigenvalues of NAC matrix are gauge invariant.

On the other hand, Table 4.8 presents the reactive state-to-state transition probabilities for the set (II) ADT angles with the separation between the CIs 4 and 0.5 Å, respectively. Calculated transition probabilities by using single surface approximated and rigorous

Table 4.5: Comparison of reactive transition probabilities when calculations are performed on the diabatic surfaces where (1,2) and (2,3) conical intersections are separated by (a) 3 Å with the mixing angles $\theta^1_{12}(x,y) = \frac{1}{2}\tan^{-1}(\frac{y}{x-x_0})$, $\theta^1_{13}(x,y) = 0$, $\theta^1_{23}(x,y) = \frac{1}{2}\tan^{-1}(\frac{y}{x_0-x})$, and (b) 0.5 Å with the mixing angles $\theta^1_{12}(x,y) = \frac{1}{2}\tan^{-1}(\frac{y}{x-x_0})$, $\theta^1_{13}(x,y) = 0$, $\theta^1_{23}(x,y) = \frac{1}{72}\tan^{-1}(\frac{y}{x_0-x})$, whereas the corresponding EBOs are constructed under the same condition.

E(eV)	$0 \to 0$	$0 \to 1$	$0 \to 2$	$0 \to 3$	$0 \to 4$
1.25	0.0033[a]	0.0492	0.0073	0.0212	0.0003
	0.0002[b]	0.0446	0.0036	0.0188	0.0013
	0.0056[c]	0.0490	0.0032	0.0258	0.0059
1.50	0.0004	0.0462	0.0231	0.0694	0.0010
	0.0028	0.0460	0.0052	0.0259	0.0018
	0.0007	0.0461	0.0061	0.0693	0.0032
1.75	0.0012	0.0416	0.0042	0.0851	0.0087
	0.0022	0.0415	0.0014	0.0519	0.0000
	0.0047	0.0415	0.0073	0.0851	0.0209

[a] 3 Å
[b] 0.5 Å
[c] EBO

EBO equations with 4 Å separation of CIs not only follow the correct symmetry (even $\to$ odd or odd $\to$ even) but also achieve quantitative agreement in comparison with diabatic results at all energies. On the other hand, when the cis are 0.5 Å apart, there is a gradual increase on even $\to$ even transitions along with even $\to$ odd transitions and some quantitative disagreement with diabatic transitions particularly at higher energies. Indeed, it is clear from Table 4.8 that single surface BO equation neither can provide correct symmetric transitions nor can calculate quantitatively accurate probabilities. Moreover, Table 4.8 shows that transition probabilities calculated by using rigorous EBO are quantitatively similar with approximated EBO ones.

4.2.2 The Model B

4.2.2.1 The nonadiabatic coupling elements and adiabatic PESs

The intention to formulate *rigorous* EBO equation [Eq. (2.39)] is to consider the effect of upper electronic states on the lower in a detailed manner, particularly, when three electronic states are strongly coupled at a point. In other words, our wish to construct such

Table 4.6: Comparison of reactive transition probabilities when calculations are performed on the diabatic surfaces where (1,2) and (2,3) conical intersections are separated by (a) 4 Å with the mixing angles $\theta^2_{12}(x,y) = \frac{1}{2}\tan^{-1}(\frac{y}{x-x_0}) - \frac{1}{4}\sin[2\tan^{-1}(\frac{y}{x-x_0})]$, $\theta^2_{13}(x,y) = 0$, $\theta^2_{23}(x,y) = \frac{1}{2}\tan^{-1}(\frac{y}{x_0-x}) - \frac{1}{4}\sin[2\tan^{-1}(\frac{y}{x_0-x})]$, and ($b$) 0.5 Å with the mixing angles $\theta^2_{12}(x,y) = \frac{1}{2}\tan^{-1}(\frac{y}{x-x_0}) - \frac{1}{4}\sin[2\tan^{-1}(\frac{y}{x-x_0})]$, $\theta^2_{13}(x,y) = 0$, $\theta^2_{23}(x,y) = \frac{1}{128}\tan^{-1}(\frac{y}{x_0-x}) - \frac{1}{256}\sin[2\tan^{-1}(\frac{y}{x_0-x})]$, whereas the corresponding EBOs are constructed under the same condition.

E(eV)	$0 \to 0$	$0 \to 1$	$0 \to 2$	$0 \to 3$	$0 \to 4$
1.25	0.0005[a]	0.0510	0.0006	0.0492	0.0334
	0.0135[b]	0.0537	0.0035	0.0397	0.0053
	0.0025[c]	0.0500	0.0061	0.0384	0.0001
1.50	0.0016	0.0216	0.0340	0.1089	0.0048
	0.0017	0.0220	0.0076	0.1031	0.0349
	0.0021	0.0206	0.0030	0.1080	0.0204
1.75	0.0000	0.0179	0.0007	0.0884	0.0004
	0.0081	0.0178	0.0204	0.0875	0.0785
	0.0006	0.0174	0.0034	0.0885	0.0036

[a] 4 Å
[b] 0.5 Å
[c] EBO

a model (**Model B**) with this kind of coupling is to explore the validity of *rigorous* EBO equation [Eq. ((2.39)] with respect to the diabatic [Eq. (2.6)] results (so called numerically exact ones) as well as to find out the necessity of *rigorous* EBO equation [Eq.(2.39)] with respect to the *approximate* EBO equation [Eq.(2.40)]. The 5×5 $\vec{\tau}$ matrix ($1\,^2A'$, $2\,^2A'$, $3\,^2A'$, $4\,^2A'$ and $5\,^2A'$) of H_3 system breaks up to 3×3 $\vec{\tau}$ matrix leading to a typical example of three state BO system. On such system, *ab-initio* calculations[7] find that $\vec{\tau}_{13}$ is relatively large and moreover, predict that the strongly overlapping $\vec{\tau}_{12}$ and $\vec{\tau}_{23}$ intersections essentially develops non-negligible value of $\vec{\tau}_{13}$, and thereby, this conical intersection among the three adiabatic states is unbreakable and coincides at a point of degeneracy.

In order to mimic the coupling of three BO states, we construct the Model B by considering: (a) ADT angles [$\theta_{12}(\mathbf{n})$, $\theta_{23}(\mathbf{n})$ and $\theta_{13}(\mathbf{n})$] defined around a point; (b) Adiabatic PESs with degeneracy at the same point. We choose the following four sets (IV) - (VII) on the functional form of ADT angles to formulate *rigorous* as well as *approximate* EBO equations and construct diabatic PESs:

Table 4.7: Comparison of reactive transition probabilities when calculations are performed on the diabatic surfaces where (1,2) and (2,3) conical intersections are separated by (*a*) 4 Å with the mixing angles $\theta^3_{12}(x,y) = \frac{1}{2}\tan^{-1}(\frac{y}{x-x_0})$, $\theta^3_{13}(x,y) = 0$, $\theta^3_{23}(x,y) = \frac{1}{2}\tan^{-1}(\frac{y}{x_0-x}) - \frac{1}{4}\sin[2\tan^{-1}(\frac{y}{x_0-x})]$, and (*b*) 0.5 Å with the mixing angles $\theta^3_{12}(x,y) = \frac{1}{2}\tan^{-1}(\frac{y}{x-x_0})$, $\theta^3_{13}(x,y) = 0$, $\theta^3_{23}(x,y) = \frac{1}{128}\tan^{-1}(\frac{y}{x_0-x}) - \frac{1}{256}\sin[2\tan^{-1}(\frac{y}{x_0-x})]$, whereas the corresponding EBOs are constructed under the same condition.

E(eV)	$0\to0$	$0\to1$	$0\to2$	$0\to3$	$0\to4$
1.25	0.0001[a]	0.0138	0.0001	0.0379	0.0000
	0.0010[b]	0.0138	0.0032	0.0171	0.0243
	0.0003[c]	0.0141	0.0007	0.0035	0.0002
1.50	0.0001	0.0352	0.0015	0.0245	0.0068
	0.0097	0.0310	0.0024	0.0111	0.0210
	0.0015	0.0352	0.0021	0.0244	0.0049
1.75	0.0108	0.0245	0.0023	0.0650	0.0017
	0.0104	0.0248	0.0095	0.0232	0.0134
	0.0004	0.0253	0.0062	0.0635	0.0057

[a] 4 Å
[b] 0.5 Å
[c] EBO

(IV) $\theta^1_{12}(x,y) = \theta^1_{13}(x,y) = \theta^1_{23}(x,y) = \frac{1}{2}\tan^{-1}(\frac{y}{x})$;

(V) $\theta^2_{12}(x,y) = \theta^2_{13}(x,y) = \theta^2_{23}(x,y) = \frac{1}{2}\tan^{-1}(\frac{y}{x}) - \frac{1}{4}\sin\left[2\tan^{-1}(\frac{y}{x})\right]$;

(VI) $\theta^3_{12}(x,y) = \frac{1}{2}\tan^{-1}(\frac{y}{x})$ and $\theta^3_{13}(x,y) = \theta^3_{23}(x,y) = \frac{1}{2}\tan^{-1}(\frac{y}{x}) - \frac{1}{4}\sin\left[2\tan^{-1}(\frac{y}{x})\right]$;

(VII) $\theta^4_{12}(x,y) = -2\sin^2\left[\frac{1}{2}\tan^{-1}(\frac{y}{x})\right]$, $\theta^4_{13}(x,y) = -\frac{1}{4}\sin\left[\tan^{-1}(\frac{y}{x})\right]$ and
$\theta^4_{23}(x,y) = \tan^{-1}(\frac{y}{x}) - \frac{1}{2}\sin\left[2\tan^{-1}(\frac{y}{x})\right]$.

Among the four sets ((IV) - (VII)) of chosen ADT angles, the functional form of set (V) angles have very similar spatial distribution with the profile of *ab-initio* calculated ADT angles for H_3 system[7] whereas the set (VII) angles were being used elsewhere to investigate any three state BO system degenerate at a point. Thus, we substitute the set (V) and (VII) ADT angles in the Eq. (2.10) to see the spatial distributions of nonadiabatic coupling elements and present in Fig. 4.3 and Fig. 4.4, respectively. The adiabatic representation of

Table 4.8: Reactive state-to-state transition probabilities when (1,2) and (2,3) conical intersections are 4 Å, and 0.5 Å ($2x_0$) apart. The diabatic surfaces are constructed considering the mixing angles, $\theta_{12}(x,y) = \frac{1}{2}\tan^{-1}(\frac{y}{x-x_0}) - \frac{1}{4}\sin[2\tan^{-1}(\frac{y}{x-x_0})]$, $\theta_{13}(x,y) = 0$, and $\theta_{23}(x,y) = \frac{1}{2}\tan^{-1}(\frac{y}{x_0-x}) - \frac{1}{4}\sin[2\tan^{-1}(\frac{y}{x_0-x})]$. The corresponding rigorous EBOs [Eq. (2.39)] and the approximated EBOs [Eq. (2.40) considering the transformation matrix commutes with the KE operator $\vec{\nabla}$ are derived under the same condition. Transition probabilities when calculations are performed on the single adiabatic surface with BO approximation [Eq. (2.41)] are also presented.

$2x_0$	1.25 eV				1.50 eV					1.75 eV				
	$0\to0$	$0\to1$	$0\to2$	$0\to3$	$0\to0$	$0\to1$	$0\to2$	$0\to3$	$0\to4$	$0\to0$	$0\to1$	$0\to2$	$0\to3$	$0\to4$
4 Å	0.0005[a]	0.0510	0.0006	0.0492	0.0016	0.0216	0.0340	0.1089	0.0048	0.0000	0.0179	0.0007	0.0884	0.0004
	0.0063[b]	0.0502	0.0010	0.0301	0.0045	0.0210	0.0069	0.1423	0.0045	0.0009	0.0175	0.0003	0.1000	0.0023
	0.0025[c]	0.0500	0.0061	0.0384	0.0021	0.0206	0.0030	0.1080	0.0204	0.0006	0.0174	0.0034	0.0885	0.0036
	0.0390[d]	0.0000	0.0619	0.0000	0.0600	0.0000	0.0939	0.0000	0.0138	0.0430	0.0000	0.0190	0.0000	0.1691
0.5 Å	0.0104	0.0250	0.0010	0.0280	0.0000	0.0686	0.0057	0.0539	0.0019	0.0102	0.0696	0.0282	0.1148	0.0194
	0.0002	0.0251	0.0042	0.0734	0.0017	0.0695	0.0036	0.0770	0.0056	0.0050	0.0698	0.0057	0.0190	0.0026
	0.0012	0.0252	0.0084	0.0631	0.0028	0.0692	0.0121	0.0694	0.0098	0.0047	0.0698	0.0011	0.0181	0.0212
	0.0390	0.0000	0.0619	0.0000	0.0600	0.0000	0.0939	0.0000	0.0138	0.0430	0.0000	0.0190	0.0000	0.1691

[a] Diabatic
[b] rigorous EBO
[c] approximated EBO
[d] BO Approx.

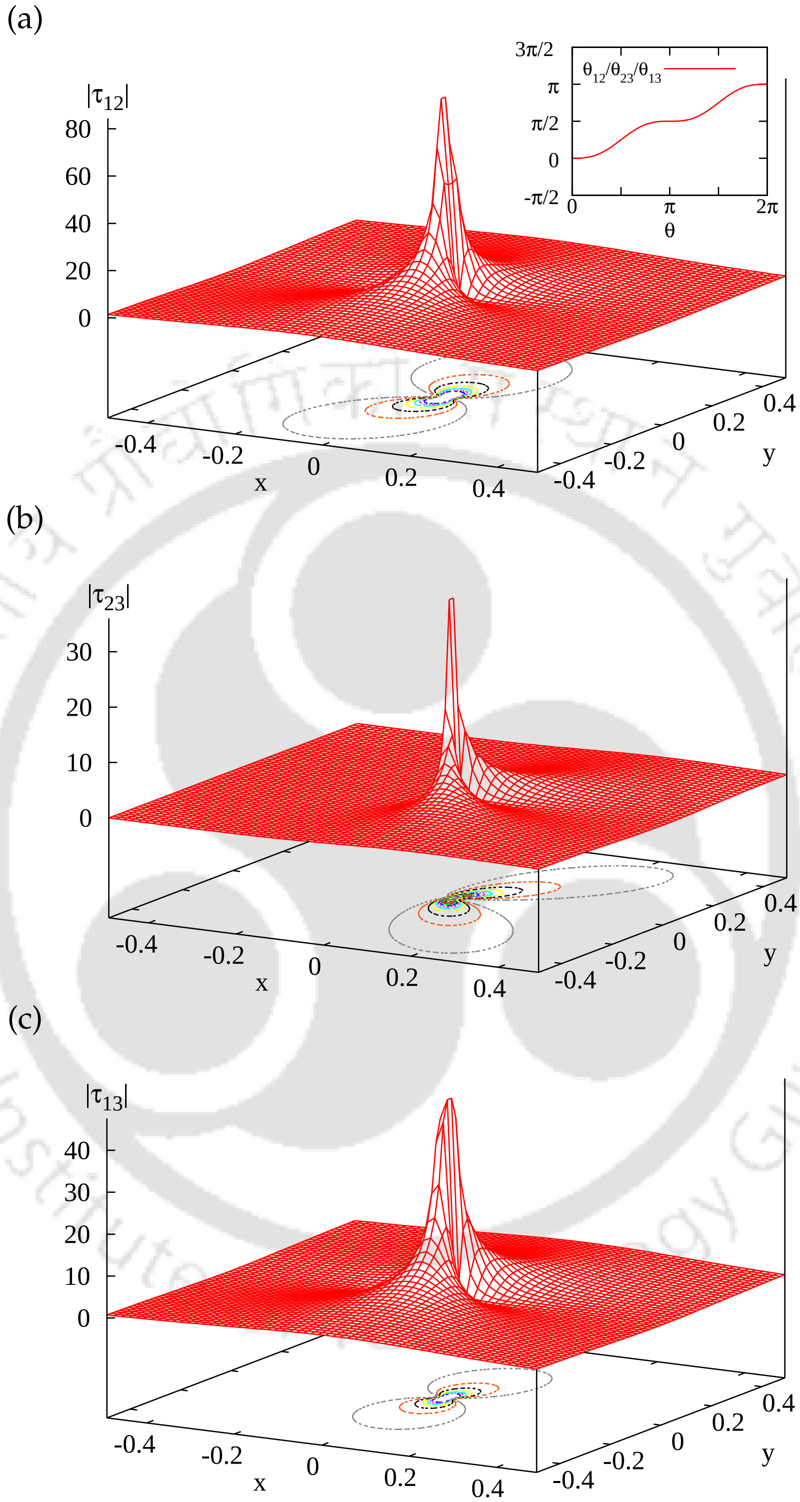

Figure 4.3: Profile of the nonadiabatic coupling elements, (a) τ_{12}, (b) τ_{23} and (c) τ_{13} for the adiabatic - to - diabatic transformation angles angles $\theta_{12}(x,y) = \theta_{13}(x,y) = \theta_{23}(x,y) = \frac{1}{2}\tan^{-1}(\frac{y}{x}) - \frac{1}{4}\sin[2\tan^{-1}(\frac{y}{x})]$ when the conical intersections are situated at a point. The inset on left of Fig. 4.3(a) represents the corresponding adiabatic-to-diabatic transformation angles angles.

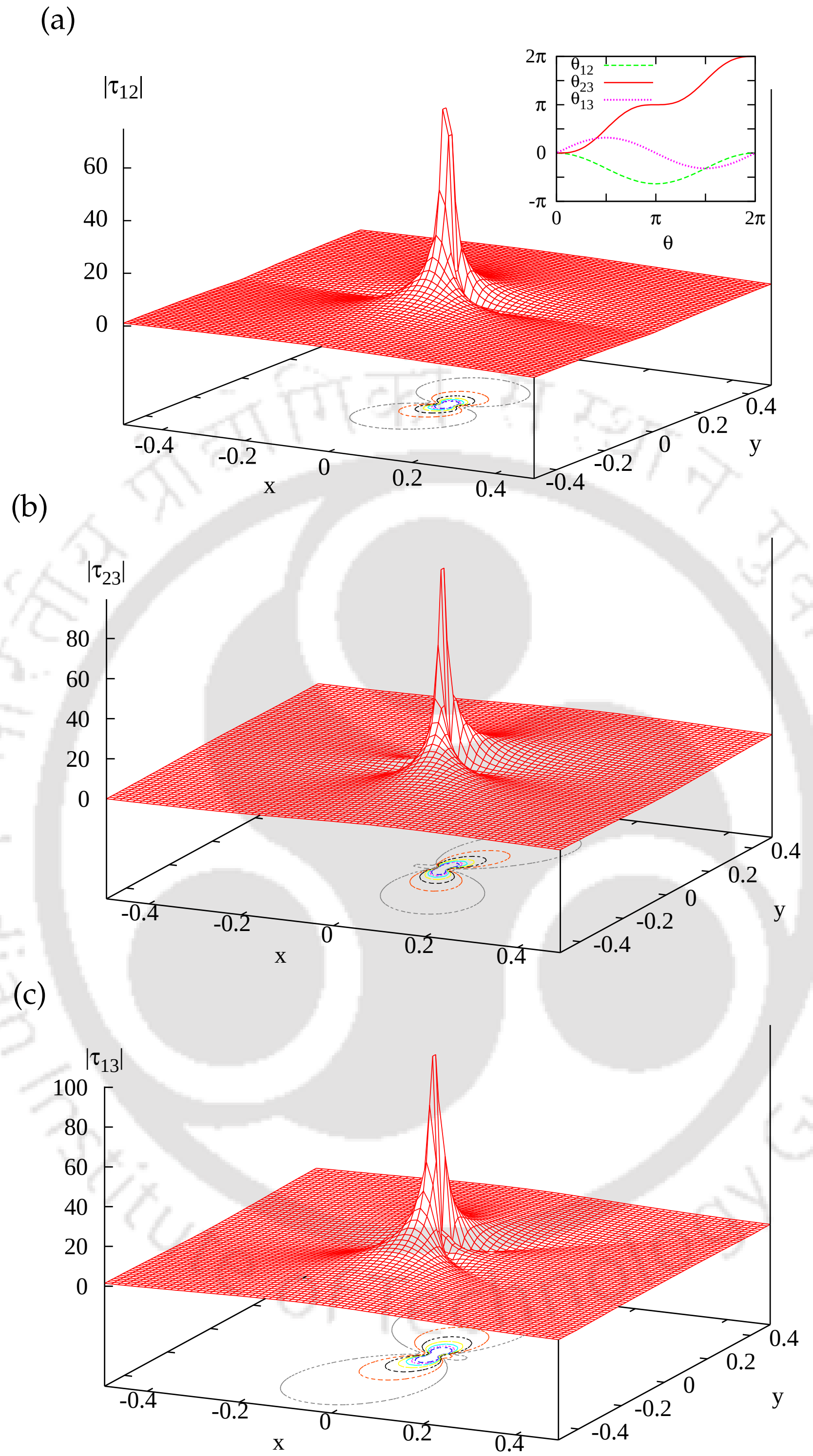

Figure 4.4: Profile of the nonadiabatic coupling elements, (a) τ_{12}, (b) τ_{23} and (c) τ_{13} for the adiabatic - to - diabatic transformation angles angles $\theta_{12}(x,y) = -2\sin^2[\frac{1}{2}\tan^{-1}(\frac{y}{x})]$, $\theta_{13}(x,y) = -\frac{1}{4}\sin[\tan^{-1}(\frac{y}{x})]$, $\theta_{23}(x,y) = \tan^{-1}(\frac{y}{x}) - \frac{1}{2}\sin[2\tan^{-1}(\frac{y}{x})]$ when the conical intersections are situated at a point. The inset on left of Fig. 4.4(a) represents the corresponding adiabatic - to - diabatic transformation angles angles.

SE is thus constituted with each set of NAC terms along with the following chosen form of adiabatic PESs,

$$
\begin{aligned}
u_1(x,y) &= \frac{1}{2}\mu[\omega_0 - \tilde{\omega}_1(x)]^2 y^2 + A_1 \times f(x,y) \\
u_2(x,y) &= \frac{1}{2}\mu\omega_0^2 y^2 - (D_1 - A_1) \times f(x,y) + D_1 \\
u_3(x,y) &= \frac{1}{2}\mu\omega_0^2 y^2 - (D_2 - A_1) \times f(x,y) + D_2 \\
\tilde{\omega}_1(x) &= \omega_1 \exp\left[(-\frac{x}{\sigma_1})^2\right] \\
f(x,y) &= \exp\left[-\frac{x^2+y^2}{\sigma^2}\right]
\end{aligned}
\tag{4.10}
$$

where the point of conical intersection is at x=0 and y=0 [see Fig. 4.5a] and potential parameters are same as Model A.

4.2.2.2 *The diabatic and rigorous EBO equation*

In a similar manner, each set of ADT angles [set (IV)-(VII)] constructs the ADT matrix [Eq. (2.8)] leading to the transformation from adiabatic [Eq. (2.4)] to diabatic [Eq. (2.6)] SE, where the generalized expressions for adiabatic and diabatic SE were presented in *Appendix A*. It may be noted that the transformation matrices, $\mathbf{A}(\theta_{12}, \theta_{23}, \theta_{13})$s [see Eqs.(2.8) and (2.14)] being developed by using the above choices of the four sets [set (IV)-(VII)] of ADT angles do not change their sign while completing a cycle, where the ADT angles are functions of $\theta[= \tan^{-1}(\frac{y}{x})]$ in various ways within the configuration space, $0 \leq \theta \leq 2\pi$. Moreover, the transformation matrix, $\mathbf{A}$ [Eq. (2.8) or (2.14)] under the ADT condition, $\vec{\nabla}\mathbf{A} + \vec{\boldsymbol{\tau}}\mathbf{A} = 0$, provides the explicit form of $\vec{\boldsymbol{\tau}}$ [Eq. (2.10)] matrix elements in terms of any arbitrary but analytic functional form of ADT angles. In other words, if the columns of the orthogonal matrix, $\mathbf{A}^{\dagger}$, are considered as electronic basis functions and are substituted in the adiabatic SE, the explicit form of $\vec{\boldsymbol{\tau}}$ matrix elements appear in terms of mixing angles and satisfy the same ADT condition. Both these aspects ensure uniquely defined diabatic potential matrix in configuration space, i.e., the topological matrix, $\mathbf{D} = \exp(\int_0^{2\pi} \vec{\boldsymbol{\tau}} \cdot d\vec{\mathbf{n}})$, derived from ADT condition, should be the unit matrix. The explicit expression of $\mathbf{D}$ is formulated by using the **G** matrix as,

$$\mathbf{D} = \prod_{k=0}^{M} \mathbf{G}(\mathbf{n}_k)\mathbf{E}(\mathbf{n}_k)\mathbf{G}^{\dagger}(\mathbf{n}_k), \tag{4.11}$$

where $\{\mathbf{n}_k, k = 0, 1, \cdots, M\}$ is a series of points along the contour (the last point $\mathbf{n}_k$ is identical with $\mathbf{n}_0$), $\mathbf{G}(\mathbf{n}_k)$ is the transformation matrix that diagonalizes $g(\mathbf{n}_k)$ and $\mathbf{E}(\mathbf{n}_k)$ is a diagonal matrix. The form of the matrix, $\mathbf{G}^{\dagger}(\mathbf{n}_k)$ is shown in Eq. (2.35) and the diagonal elements of $\mathbf{E}(\mathbf{n}_k)$ are given by, $\mathbf{E}_j(\mathbf{n}_k) = \exp[-i \int_{n_{k-1}}^{n_k} \vec{\omega}_j(\mathbf{n}) \cdot d\vec{\mathbf{n}}]$. While performing numerical calculations to evaluate **D** matrix by using the four sets of ADT angles, it appears that in all cases, the matrix is unit one and the typical values of the **D** elements for the set (V) ADT angles are obtained as:

$$\mathbf{D} = \begin{pmatrix} 1.000235 & 0.000000 & 0.000202 \\ 0.000000 & 1.000322 & 0.000000 \\ -0.000498 & 0.000000 & 1.000127 \end{pmatrix}.$$

Considering the conical intersection of a three states BO system is at a point and introducing zero Curl τ_{ij} around the same point, the general form of nonadiabatic coupling matrix is given by Eq. (2.21) and thereby, the eigenvalues of the NAC matrices for the four sets ((IV) - (VII)) of ADT angles appear as,

$$\vec{\omega}_{IV} = \vec{\nabla}\theta_{12}^{1}\sqrt{3 + 2\sin\theta_{12}^{1}}, \tag{4.12a}$$

$$\vec{\omega}_{V} = \vec{\nabla}\theta_{12}^{2}\sqrt{3 + 2\sin\theta_{12}^{2}}, \tag{4.12b}$$

$$\vec{\omega}_{VI} = \vec{\nabla}\theta_{12}^{3}\sqrt{1 + 2(1 - \cos 4\theta_{12}^{3})^2 + 2(1 - \cos 4\theta_{12}^{3})\sin(\theta_{12}^{3} - \frac{1}{4}\sin 4\theta_{12}^{3})}, \tag{4.12c}$$

$$\vec{\omega}_{VII} = \vec{\nabla}\theta_{12}^{4}\sqrt{1 + \frac{q + 4p^2}{p} + 4\sqrt{p}\sin(\sqrt{p})}, \quad q = (1 + \theta_{12}^{4})^2, \ \ p = 1 - q, \tag{4.12d}$$

where the functional form of the eigenvalues ($|\omega|$) of the NAC matrix arising from set (V) and (VII) ADT angles are displayed in Fig. 4.5b and 4.5c, respectively. The above eigenvalue and the corresponding eigenvector with the following three elements,

$$
\begin{aligned}
G^d_{11} = \frac{g_3}{\eta} &= \left[-\cos\theta_{12}\Big(\frac{\nabla_p\theta_{23}}{\nabla_p\theta_{12}}\Big) + \sin\theta_{12}\cos\theta_{23}\Big(\frac{\nabla_p\theta_{13}}{\nabla_p\theta_{12}}\Big)\right] \\
&\times \left[1 + \left(\frac{\nabla_p\theta_{13}}{\nabla_p\theta_{12}}\right)^2 + \left(\frac{\nabla_p\theta_{23}}{\nabla_p\theta_{12}}\right)^2 + 2\sin\theta_{23}\left(\frac{\nabla_p\theta_{13}}{\nabla_p\theta_{12}}\right)\right]^{-\frac{1}{2}}, \\
G^d_{12} = -\frac{g_2}{\eta} &= \left[\sin\theta_{12}\Big(\frac{\nabla_p\theta_{23}}{\nabla_p\theta_{12}}\Big) + \cos\theta_{12}\cos\theta_{23}\Big(\frac{\nabla_p\theta_{13}}{\nabla_p\theta_{12}}\Big)\right] \\
&\times \left[1 + \left(\frac{\nabla_p\theta_{13}}{\nabla_p\theta_{12}}\right)^2 + \left(\frac{\nabla_p\theta_{23}}{\nabla_p\theta_{12}}\right)^2 + 2\sin\theta_{23}\left(\frac{\nabla_p\theta_{13}}{\nabla_p\theta_{12}}\right)\right]^{-\frac{1}{2}}, \\
G^d_{13} = \frac{g_1}{\eta} &= \left[-1 - \sin\theta_{23}\Big(\frac{\nabla_p\theta_{13}}{\nabla_p\theta_{12}}\Big)\right]\left[1 + \left(\frac{\nabla_p\theta_{13}}{\nabla_p\theta_{12}}\right)^2 + \left(\frac{\nabla_p\theta_{23}}{\nabla_p\theta_{12}}\right)^2 + 2\sin\theta_{23}\left(\frac{\nabla_p\theta_{13}}{\nabla_p\theta_{12}}\right)\right]^{-\frac{1}{2}}
\end{aligned}
$$

are substituted in the Eq. (2.39) to obtain the explicit form of *rigorous* EBO equation (see **Appendix D**) for the ground state. On the other hand, the necessity of *rigorous* EBO equation [Eq. (2.39] with respect to *approximate* EBO equation [Eq. (2.40] may be predicted from the following gauge invariance,

$$
\begin{aligned}
\Gamma_{IV} &= \frac{1}{2\pi}\int_0^{2\pi} \vec{\omega}_{VIII}(\mathbf{n}).d\vec{\mathbf{n}} = 1.030761, \\
\Gamma_{V} &= \frac{1}{2\pi}\int_0^{2\pi} \vec{\omega}_{IX}(\mathbf{n}).d\vec{\mathbf{n}} = 1.030776, \\
\Gamma_{VI} &= \frac{1}{2\pi}\int_0^{2\pi} \vec{\omega}_{X}(\mathbf{n}).d\vec{\mathbf{n}} = 1.057193, \\
\Gamma_{VII} &= \frac{1}{2\pi}\int_0^{2\pi} \vec{\omega}_{XI}(\mathbf{n}).d\vec{\mathbf{n}} = 1.090524.
\end{aligned} \tag{4.13}
$$

Since, for all four sets of ADT angles, the eigenvalues of the associated $\vec{\tau}$ matrix approximately obey the gauge invariance condition, namely unity, we expect both *rigorous* and *approximate* EBO equation can provide meaningful solutions and at the same time, the *rigorous* EBO equation may not show up much advantage over the approximate one. The general form of these gauge invariance integrals [Eq. (4.13)] along the integrands as defined in Eq. (4.12) are the so called *incomplete elliptic integral of the second kind* and their nature is generic as long as the functional forms of the ADT angles are analytic. This implies that when three electronic states are coupled, the nonadiabatic effect of the upper

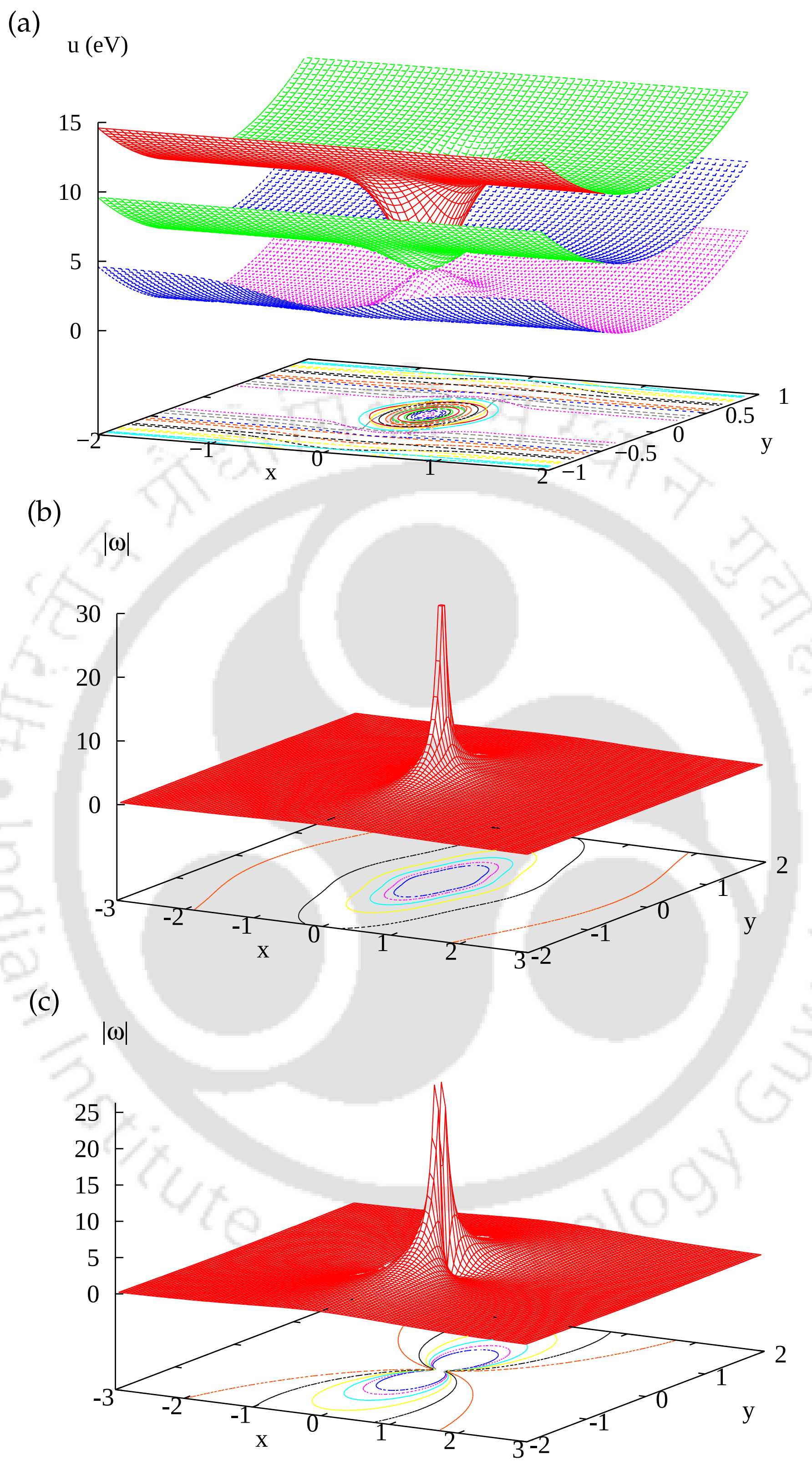

Figure 4.5: (a) The three adiabatic potential energy surfaces for Model B. The functional form of the eigenvalues ($|\omega|$) of the NAC matrix arising due to the mixing angles (b) $\theta_{12}(x,y) = \theta_{23}(x,y) = \frac{1}{2}\tan^{-1}(\frac{y}{x}) - \frac{1}{4}\sin[2\tan^{-1}(\frac{y}{x})]$ and $\theta_{13}(x,y) = 0$ (c) $\theta_{12}(x,y) = -2\sin^2[\frac{1}{2}\tan^{-1}(\frac{y}{x})]$, $\theta_{13}(x,y) = -\frac{1}{4}\sin[\tan^{-1}(\frac{y}{x})]$, $\theta_{23}(x,y) = \tan^{-1}(\frac{y}{x}) - \frac{1}{2}\sin[2\tan^{-1}(\frac{y}{x})]$ when the conical intersections are situated at a point.

states on the ground is equivalent to a potential developed due to an elliptic motion of the nuclei around the point of conical intersection.

4.2.2.3 Numerical calculations: results and discussions

We initialize the ground adiabatic wavefunction with different initial KE as described in case of **Model A**, propagate the wavefunction and then, project the function at $t \rightarrow \infty$ on the asymptotic eigenfunctions of the Hamiltonian to calculate state - to - state vibrational transition probabilities. Since the point of conical intersection among the three states is at 3.0 eV, it is expected that the upper electronic states are classically closed with respect to the ground at total energies 1.25, 1.50 and 1.75 eV and thereby, the formulated *approximate* and *rigorous* EBO equations should provide transition probabilities with enough accuracy. Table II - V present the reactive state - to - state transition probabilities for the four sets (IV) - (VII) of ADT angles, respectively, where the first row displays the diabatic results, the second and third rows show the transition probabilities calculated by *rigorous* and *approximate* EBO equation, respectively with BO approximate results on the fourth row. As such, BO approximate results have very little quantitative agreement with diabatic ones. On the other hand, both *rigorous* and *approximate* EBO equations calculate accurate transition probabilities but those probabilities have similar level of agreement with respect to numerically exact diabatic results. In other words, all these Tables demonstrate that there is as such no clear advantage of *rigorous* EBO equation over the *approximate* EBO one.

4.2.3 Summary

We have chosen various sets of ADT angles to define the corresponding NAC terms and thereby, to mimic two situations of any three state BO system, namely, (a) the point of CI between the first and the second state is away from the CI between the second and third (**Model A**) and (b) the point of CI among the three state is at a particular nuclear configuration (**Model B**). For both the models with different choices of ADT angles, we have formulated the *approximate* and *rigorous* EBO equations by imposing zero Curl conditions. The validity as well as necessity of *rigorous* EBO equation with respect to the *approximate* ones for both the Models (constituted with two nuclear coordinates) have been explored

Table 4.9: Reactive state-to-state transition probabilities when all the conical intersections situated at a point. Diabatic surfaces are constructed considering the mixing angles, $\theta_{12}(x,y) = \theta_{13}(x,y) = \theta_{23}(x,y) = \frac{1}{2}\tan^{-1}(\frac{y}{x})$. The corresponding generalized EBOs [Eq. (2.39)] and the approximated EBOs [Eq. (2.40)] considering the transformation matrix commutes with the KE operator $\vec{\nabla}$ are derived under the same condition. Transition probabilities when calculations are performed on the single adiabatic surface with BO approximation [Eq. (2.41)] are also presented.

E(eV)	$0 \to 0$	$0 \to 1$	$0 \to 2$	$0 \to 3$	$0 \to 4$	$0 \to 5$
1.25	0.0227[a]	0.0000	0.0677	0.0000		
	0.0232[b]	0.0083	0.0742	0.0017		
	0.0228[c]	0.0035	0.0727	0.0131		
	0.0390[d]	0.0000	0.0619	0.0000		
1.50	0.0314	0.0000	0.0391	0.0000	0.0905	0.0000
	0.0314	0.0093	0.0793	0.0055	0.0594	0.0058
	0.0384	0.0030	0.0704	0.0017	0.0898	0.0060
	0.0600	0.0000	0.0939	0.0000	0.0138	0.0000
1.75	0.0250	0.0000	0.0562	0.0000	0.1280	0.0000
	0.0280	0.0099	0.0499	0.0008	0.1231	0.0098
	0.0251	0.0006	0.0590	0.0012	0.1388	0.0179
	0.0430	0.0000	0.0190	0.0000	0.1691	0.0000

[a] Diabatic
[b] rigorous EBO
[c] approximated EBO
[d] BO Approx.

by performing numerical calculations. Transition probabilities calculated by using diabatic, *approximate* and *rigorous* EBO equations have good agreement among each other but as such *rigorous* EBO results could not show up clear advantage over the *approximate* one.

4.3 The Induced Renner-Teller Type model

Degenerate electronic states are the typical examples for the cause of failure of adiabatic (BO) approximation. In the case of linear molecules, the coupling among the vibrational modes of degenerate electronic states is known as Renner-Teller (RT) effect.[8] Such effect commonly arises due to an isolated Π states of a molecule, namely, those Π states show negligible interaction with other electronic states. This situation corresponds the well

Table 4.10: Reactive state-to-state transition probabilities when the conical intersections situated at a point. Diabatic surfaces are constructed considering the mixing angles, $\theta_{12}(x,y) = \theta_{13}(x,y) = \theta_{23}(x,y) = \frac{1}{2}\tan^{-1}(\frac{y}{x}) - \frac{1}{4}\sin[2\tan^{-1}(\frac{y}{x})]$. The corresponding generalized EBOs [Eq. (2.39)] and the approximated EBOs [Eq. (2.40)] considering the transformation matrix commutes with the KE operator $\vec{\nabla}$ are derived under the same condition. Transition probabilities when calculations are performed on the single adiabatic surface with BO approximation [Eq. (2.41)] are also presented.

E(eV)	$0 \rightarrow 0$	$0 \rightarrow 1$	$0 \rightarrow 2$	$0 \rightarrow 3$	$0 \rightarrow 4$	$0 \rightarrow 5$
1.25	0.0123[a]	0.0000	0.0782	0.0000		
	0.0125[b]	0.0089	0.0608	0.0073		
	0.0123[c]	0.0001	0.0745	0.0549		
	0.0390[d]	0.0000	0.0619	0.0000		
1.50	0.0255	0.0000	0.0668	0.0000	0.0677	0.0000
	0.0269	0.0012	0.0438	0.0026	0.0827	0.0042
	0.0261	0.0075	0.0651	0.0118	0.0386	0.0029
	0.0600	0.0000	0.0939	0.0000	0.0138	0.0000
1.75	0.0509	0.0000	0.0270	0.0000	0.0433	0.0000
	0.0498	0.0073	0.0284	0.0085	0.0266	0.0081
	0.0509	0.0077	0.0304	0.0315	0.0023	0.0189
	0.0430	0.0000	0.0190	0.0000	0.1691	0.0000

[a] Diabatic
[b] rigorous EBO
[c] approximated EBO
[d] BO Approx.

- known RT case of two interacting (Π) states through vibronic coupling with quadratic terms. On the other hand, the interaction between the Π states can be induced by a Σ state through a bending mode with linear coupling terms and thereby, demonstrate induced RT effect.[9,10]

We consider two nuclear coordinates: the bending amplitude is denoted by a dimensionless normal coordinate, ρ and ϕ is the vibrational azimuthal angle with respect to an arbitrary reference plane. These two coordinates can be termed as polar coordinates and related with Cartesian: $x = \rho\cos\phi$ and $y = \rho\sin\phi$. In the diabatic representation (more precisely, crude adiabatic basis), we locate the system at the reference geometry given by $\rho = 0$ and $\phi = 0$ (i.e., $x = 0$ and $y = 0$). When the nuclear vibration is assumed harmonic, the electronic Hamiltonian takes the following form after considering symmetry of the

Table 4.11: Reactive state-to-state transition probabilities when the conical intersections situated at a point. Diabatic surfaces are constructed considering the mixing angles, $\theta_{12}(x,y) = \frac{1}{2}\tan^{-1}(\frac{y}{x})$, $\theta_{13}(x,y) = \theta_{23}(x,y) = \frac{1}{2}\tan^{-1}(\frac{y}{x}) - \frac{1}{4}\sin[2\tan^{-1}(\frac{y}{x})]$. The corresponding generalized EBOs [Eq. (2.39)] and the approximated EBOs [Eq. (2.40)] considering the transformation matrix commutes with the KE operator $\vec{\nabla}$ are derived under the same condition. Transition probabilities when calculations are performed on the single adiabatic surface with BO approximation [Eq. (2.41)] are also presented.

E(eV)	$0\rightarrow0$	$0\rightarrow1$	$0\rightarrow2$	$0\rightarrow3$	$0\rightarrow4$	$0\rightarrow5$
1.25	0.0112[a]	0.0000	0.0642	0.0000		
	0.0112[b]	0.0089	0.0683	0.0205		
	0.0112[c]	0.0009	0.0669	0.0323		
	0.0390[d]	0.0000	0.0619	0.0000		
1.50	0.0296	0.0000	0.0497	0.0000	0.0745	0.0000
	0.0256	0.0096	0.0513	0.0002	0.1444	0.0084
	0.0257	0.0036	0.0495	0.0003	0.1985	0.0008
	0.0600	0.0000	0.0939	0.0000	0.0138	0.0000
1.75	0.0417	0.0000	0.0534	0.0000	0.1101	0.0000
	0.0425	0.0099	0.0535	0.0087	0.1734	0.0128
	0.0418	0.0067	0.0535	0.0051	0.2131	0.0280
	0.0430	0.0000	0.0190	0.0000	0.1691	0.0000

[a] Diabatic
[b] rigorous EBO
[c] approximated EBO
[d] BO Approx.

problem (RT system) within the first order expansion in ρ:

$$\mathbf{H}_e^{\epsilon} = \begin{pmatrix} E_{\Pi} + \frac{1}{2}\omega\rho^2 & 0 & \lambda\rho\exp(i\phi) \\ 0 & E_{\Pi} + \frac{1}{2}\omega\rho^2 & \lambda\rho\exp(-i\phi) \\ \lambda\rho\exp(i\phi) & \lambda\rho\exp(i\phi) & E_{\Sigma} + \frac{1}{2}\omega\rho^2 \end{pmatrix}, \tag{4.14}$$

where the frequency of the harmonic potential is ω, E_{Π} and E_{Σ} are the energies of the Π and Σ states at the equilibrium geometry and λ is a coupling constant.

The electronic Hamiltonian [Eq. (4.14)] under the following unitary transformation,

$$\mathbf{U}_{\epsilon} = \frac{1}{\sqrt{2}} \begin{pmatrix} 1 & -i & 0 \\ 1 & i & 0 \\ 0 & 0 & \sqrt{2} \end{pmatrix}, \tag{4.15}$$

Table 4.12: Reactive state-to-state transition probabilities when the conical intersections situated at a point. Diabatic surfaces are constructed considering the mixing angles, $\theta_{12}(x,y) = -2\sin^2[\frac{1}{2}\tan^{-1}(\frac{y}{x})]$, $\theta_{13}(x,y) = -\frac{1}{4}\sin[\tan^{-1}(\frac{y}{x})]$, $\theta_{23}(x,y) = \tan^{-1}(\frac{y}{x}) - \frac{1}{2}\sin[2\tan^{-1}(\frac{y}{x})]$. The corresponding generalized EBOs [Eq. (2.39)] and the approximated EBOs [Eq. (2.40)] considering the transformation matrix commutes with the KE operator $\vec{\nabla}$ are derived under the same condition. Transition probabilities when calculations are performed on the single adiabatic surface with BO approximation [Eq. (2.41)] are also presented.

E(eV)	$0\rightarrow 0$	$0\rightarrow 1$	$0\rightarrow 2$	$0\rightarrow 3$	$0\rightarrow 4$	$0\rightarrow 5$
1.25	0.0275[a]	0.0000	0.0156	0.0000		
	0.0272[b]	0.0050	0.0158	0.0070		
	0.0275[c]	0.0001	0.0144	0.0042		
	0.0390[d]	0.0000	0.0619	0.0000		
1.50	0.0371	0.0000	0.0077	0.0000	0.0356	0.0000
	0.0372	0.0012	0.0200	0.0098	0.0177	0.0143
	0.0371	0.0002	0.0065	0.0078	0.0255	0.0059
	0.0600	0.0000	0.0939	0.0000	0.0138	0.0000
1.75	0.0237	0.0000	0.0208	0.0000	0.1400	0.0000
	0.0244	0.0033	0.0101	0.0190	0.1099	0.0159
	0.0238	0.0010	0.0178	0.0294	0.0884	0.0523
	0.0430	0.0000	0.0190	0.0000	0.1691	0.0000

[a] Diabatic
[b] rigorous EBO
[c] approximated EBO
[d] BO Approx.

takes the following form in polar coordinates ρ and ϕ:

$$\mathbf{H}_e = \mathbf{U}_\epsilon^\dagger \mathbf{H}_e^\epsilon \mathbf{U}_\epsilon = \begin{pmatrix} E_\Pi + \frac{1}{2}\omega\rho^2 & 0 & \sqrt{2}\lambda\rho\cos\phi \\ 0 & E_\Pi + \frac{1}{2}\omega\rho^2 & -\sqrt{2}\lambda\rho\sin\phi \\ \sqrt{2}\lambda\rho\cos\phi & -\sqrt{2}\lambda\rho\sin\phi & E_\Sigma + \frac{1}{2}\omega\rho^2 \end{pmatrix}, \tag{4.16}$$

where the kinetic energy operator of the nuclear motion is:

$$\hat{T}_N = -\frac{\omega}{2}\Big(\frac{1}{\rho}\frac{\partial}{\partial\rho}\rho\frac{\partial}{\partial\rho} + \frac{1}{\rho^2}\frac{\partial^2}{\partial\phi^2}\Big). \tag{4.17}$$

4.3.1 The nonadiabatic coupling elements and their Curl-Divergence equations

We obtain the analytic form of the NAC terms by analyzing the eigenvectors of the potentially coupled diabatic Hamiltonian ($\mathbf{H_e}$)[Eq.(4.16)] matrix:

$$\mathbf{S} = \begin{pmatrix} \sin\phi & w_+\cos\phi & w_-\cos\phi \\ \cos\phi & -w_+\sin\phi & -w_-\sin\phi \\ 0 & -w_- & w_+ \end{pmatrix}, \tag{4.18}$$

with $w_\pm = \frac{1}{\sqrt{2}}\left\{\frac{\left[(E_\Sigma-E_\Pi)^2+8\lambda^2\rho^2\right]^{1/2} \pm (E_\Sigma-E_\Pi)}{\left[(E_\Sigma-E_\Pi)^2+8\lambda^2\rho^2\right]^{1/2}}\right\}^{1/2}$, $\rho^2 = x^2+y^2$ and $\Delta = \frac{1}{2}\big(E_\Sigma - E_\Pi\big)$, i.e., the energy gap parameter between the Π and Σ states.

The matrix S diagonalize the matrix $\mathbf{H}_e$ as

$$\mathbf{S}^\dagger\mathbf{H}_e\mathbf{S} = \mathbf{V} = \begin{pmatrix} V_\Pi & 0 & 0 \\ 0 & V_- & 0 \\ 0 & 0 & V_+ \end{pmatrix}, \tag{4.19}$$

where the adiabatic potential energy surfaces are given by:

$$V_\Pi = E_\Pi + \frac{1}{2}\omega\rho^2 \tag{4.20}$$

$$V_\pm = \frac{1}{2}(E_\Sigma + E_\Pi) + \frac{1}{2}\omega\rho^2 \pm \sqrt{\left[\frac{1}{2}(E_\Sigma - E_\Pi\right]^2 + 2\lambda^2\rho^2}. \tag{4.21}$$

Figs. 4.6 present adiabatic PESs as functions of the nuclear coordinate, ρ only (because surfaces are independent of ϕ) for various parametric values of the energy gap, 2Δ and coupling parameter, λ. Though the polar radius, ρ, is defined either for positive or with negative values, figures are plotted for both values just in order to keep better views. For any non-zero values of the gap, 2Δ, both the Π states show degeneracy at $\rho = 0$ but split at $\rho \neq 0$ gradually with increasing values of λ. On the other hand, as the gap decreases, the adiabatic surfaces tend to form degeneracy at a point.

Considering the definition of nonadiabatic coupling elements of the first kind [Eq.

(2.2)], the derivative couplings among the electronic states can be calculated as

$$\mathbf{S}^{\dagger}\nabla\mathbf{S} = \begin{pmatrix} 0 & -w_+\nabla\phi & -w_-\nabla\phi \\ w_+\nabla\phi & 0 & w_+\nabla w_- - w_-\nabla w_+ \\ w_-\nabla\phi & -w_+\nabla w_- + w_-\nabla w_+ & 0 \end{pmatrix}, \tag{4.22}$$

where analytical forms of the ρ and ϕ components (τ^{ρ} and τ^{ϕ}) of the NAC elements are:

$$\begin{aligned} \tau^{\rho} &= \begin{pmatrix} 0 & -w_+\nabla_\rho\phi & -w_-\nabla_\rho\phi \\ w_+\nabla_\rho\phi & 0 & w_+\nabla_\rho w_- - w_-\nabla_\rho w_+ \\ w_-\nabla_\rho\phi & -w_+\nabla_\rho w_- + w_-\nabla_\rho w_+ & 0 \end{pmatrix} \\ &= \begin{pmatrix} 0 & 0 & 0 \\ 0 & 0 & w_+\nabla_\rho w_- - w_-\nabla_\rho w_+ \\ 0 & -w_+\nabla_\rho w_- + w_-\nabla_\rho w_+ & 0 \end{pmatrix} \\ &= \begin{pmatrix} 0 & 0 & 0 \\ 0 & 0 & \frac{1}{\sqrt{2}}\frac{\Delta\lambda}{(\Delta^2+2\lambda^2\rho^2)} \\ 0 & -\frac{1}{\sqrt{2}}\frac{\Delta\lambda}{(\Delta^2+2\lambda^2\rho^2)} & 0 \end{pmatrix} \end{aligned} \tag{4.23}$$

and

$$\begin{aligned} \tau^{\phi} &= \frac{1}{\rho}\begin{pmatrix} 0 & -w_+\nabla_\phi\phi & -w_-\nabla_\phi\phi \\ w_+\nabla_\phi\phi & 0 & w_+\nabla_\phi w_- - w_-\nabla_\phi w_+ \\ w_-\nabla_\phi\phi & -w_+\nabla_\phi w_- + w_-\nabla_\phi w_+ & 0 \end{pmatrix} \\ &= \frac{1}{\rho}\begin{pmatrix} 0 & -w_+ & -w_- \\ w_+ & 0 & 0 \\ w_- & 0 & 0 \end{pmatrix} \\ &= \frac{1}{\rho}\begin{pmatrix} 0 & -\frac{1}{\sqrt{2}}\left[1+\frac{\Delta}{\sqrt{\Delta^2+2\lambda^2\rho^2}}\right]^{\frac{1}{2}} & -\frac{1}{\sqrt{2}}\left[1-\frac{\Delta}{\sqrt{\Delta^2+2\lambda^2\rho^2}}\right]^{\frac{1}{2}} \\ \frac{1}{\sqrt{2}}\left[1+\frac{\Delta}{\sqrt{\Delta^2+2\lambda^2\rho^2}}\right]^{\frac{1}{2}} & 0 & 0 \\ \frac{1}{\sqrt{2}}\left[1-\frac{\Delta}{\sqrt{\Delta^2+2\lambda^2\rho^2}}\right]^{\frac{1}{2}} & 0 & 0 \end{pmatrix}, \end{aligned} \tag{4.24}$$

respectively.

It is important to note that all the NAC elements, both their ρ or ϕ components, are independent of the nuclear coordinate, ϕ but depends on ρ along with the parameters, Δ and λ. It appears that if the ϕ components of the NAC terms are non - zero, invariably its' ρ components are zeros and vice versa, i.e., $\tau_{12}^{\phi} \neq 0$, $\tau_{12}^{\rho} = 0$, $\tau_{13}^{\phi} \neq 0$, $\tau_{13}^{\rho} = 0$, $\tau_{23}^{\phi} = 0$, and $\tau_{23}^{\rho} \neq 0$. Moreover, each NAC element shows singularity, namely, the denominator approaches to zero in a faster manner than the numerator, at $\rho \to 0$ under the condition $\Delta = \alpha + \rho^n$ with $\alpha = 0$ and $n = 1$. Figs. 4.7 display the non -zero components of the NAC elements as functions of ρ for various values of Δ and λ.

The Curl-Divergence equations for NAC elements are given by:

$$\text{Curl}\,\tau = \frac{1}{\rho}(\frac{\partial}{\partial\rho}\tau'_\phi - \frac{\partial}{\partial\phi}\tau_\rho) = \frac{1}{\rho}(\tau_\rho\tau'_\phi - \tau'_\phi\tau_\rho) \qquad \tau'_\phi = \rho\tau_\phi \tag{4.25}$$

$$= \frac{1}{\rho}\begin{pmatrix} 0 & -\nabla_\rho w_+ & -\nabla_\rho w_- \\ \nabla_\rho w_+ & 0 & 0 \\ \nabla_\rho w_- & 0 & 0 \end{pmatrix}$$

$$= \begin{pmatrix} 0 & \frac{\Delta\lambda^2}{\sqrt{2}(\Delta^2+2\lambda^2\rho^2)^{3/2}} \times \left[1 + \frac{\Delta}{\sqrt{\Delta^2+2\lambda^2\rho^2}}\right]^{\frac{1}{2}} & -\frac{\Delta\lambda^2}{\sqrt{2}(\Delta^2+2\lambda^2\rho^2)^{3/2}} \times \left[1 - \frac{\Delta}{\sqrt{\Delta^2+2\lambda^2\rho^2}}\right]^{\frac{1}{2}} \\ \frac{\Delta\lambda^2}{\sqrt{2}(\Delta^2+2\lambda^2\rho^2)^{3/2}} \times \left[1 + \frac{\Delta}{\sqrt{\Delta^2+2\lambda^2\rho^2}}\right]^{\frac{1}{2}} & 0 & 0 \\ -\frac{\Delta\lambda^2}{\sqrt{2}(\Delta^2+2\lambda^2\rho^2)^{3/2}} \times \left[1 - \frac{\Delta}{\sqrt{\Delta^2+2\lambda^2\rho^2}}\right]^{\frac{1}{2}} & 0 & 0 \end{pmatrix} \tag{4.26}$$

and

$$\text{Div}\,\tau = \begin{pmatrix} 0 & 0 & 0 \\ 0 & 0 & w_+\nabla_\rho^2 w_- - w_-\nabla_\rho^2 w_+ \\ 0 & -(w_+\nabla_\rho^2 w_- - w_-\nabla_\rho^2 w_+) & 0 \end{pmatrix}$$

$$= \begin{pmatrix} 0 & 0 & 0 \\ 0 & 0 & -\frac{2\sqrt{2}\Delta\lambda^3\rho}{(\Delta^2+2\lambda^2\rho^2)^2} \\ 0 & -\frac{2\sqrt{2}\Delta\lambda^3\rho}{(\Delta^2+2\lambda^2\rho^2)^2} & 0 \end{pmatrix} \tag{4.27}$$

Figs. 4.8 present the Curl of NAC terms as functions of ρ for three different values of the parameters, Δ and λ. It is quite clear that as the gap between the Π and Σ state, Δ, and the force constant, λ, decreases, Curls of all the NAC elements approach to zero as functions of ρ. The analytical expressions of Curls of the NAC elements demonstrate that the Curls are zeros, namely, the numerator of the Curls approaches to zero in a faster manner than the denominator at $\rho \to 0$ under the condition $\Delta = \alpha + \rho^n$ with $\alpha = 0$ and $n = 4$. Since τ_{12}^{ϕ} and τ_{13}^{ϕ} are independent of ϕ and the corresponding ρ components, τ_{12}^{ρ} and τ_{13}^{ρ} are zeros, the calculated divergence of these two elements are expected to be zeros. On the other hand, we find that the ϕ component of the NAC element, τ_{23}^{ϕ} is zero but its' ρ component, τ_{23}^{ρ} is non-zero and therefore, the element shows non -zero divergence as shown in Fig. 4.9.

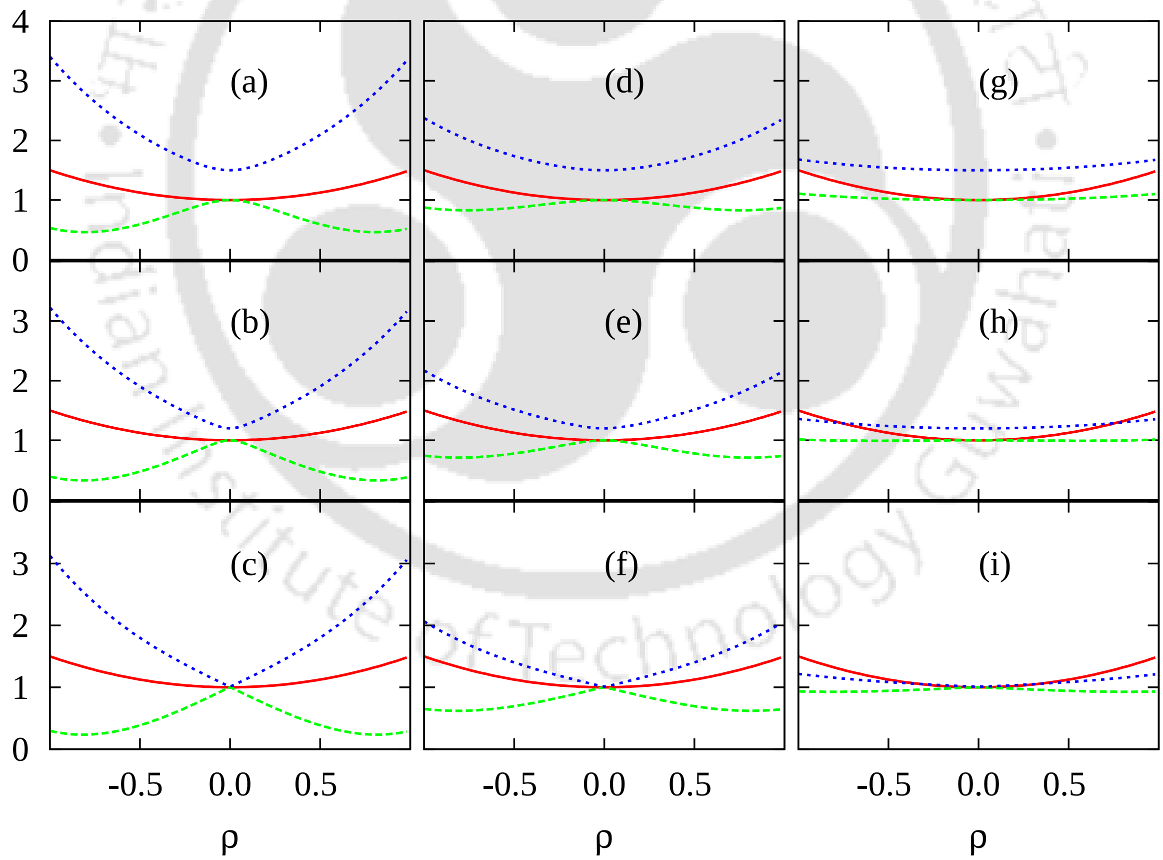

Figure 4.6: The three adiabatic potential energy curves as a function of ρ where (a), (b) and (c) are for λ =1.0, $\omega = 1.0$ with Δ values 0.5, 0.2 and 0.01, respectively. Figs. 1(d), (e) and (f) are for λ =0.5, $\omega = 1.0$ with Δ values 0.5, 0.2 and 0.01, respectively. Figs. 1(g), (h) and (i) are for λ =0.1, $\omega = 1.0$ with Δ values 0.5, 0.2 and 0.01, respectively.

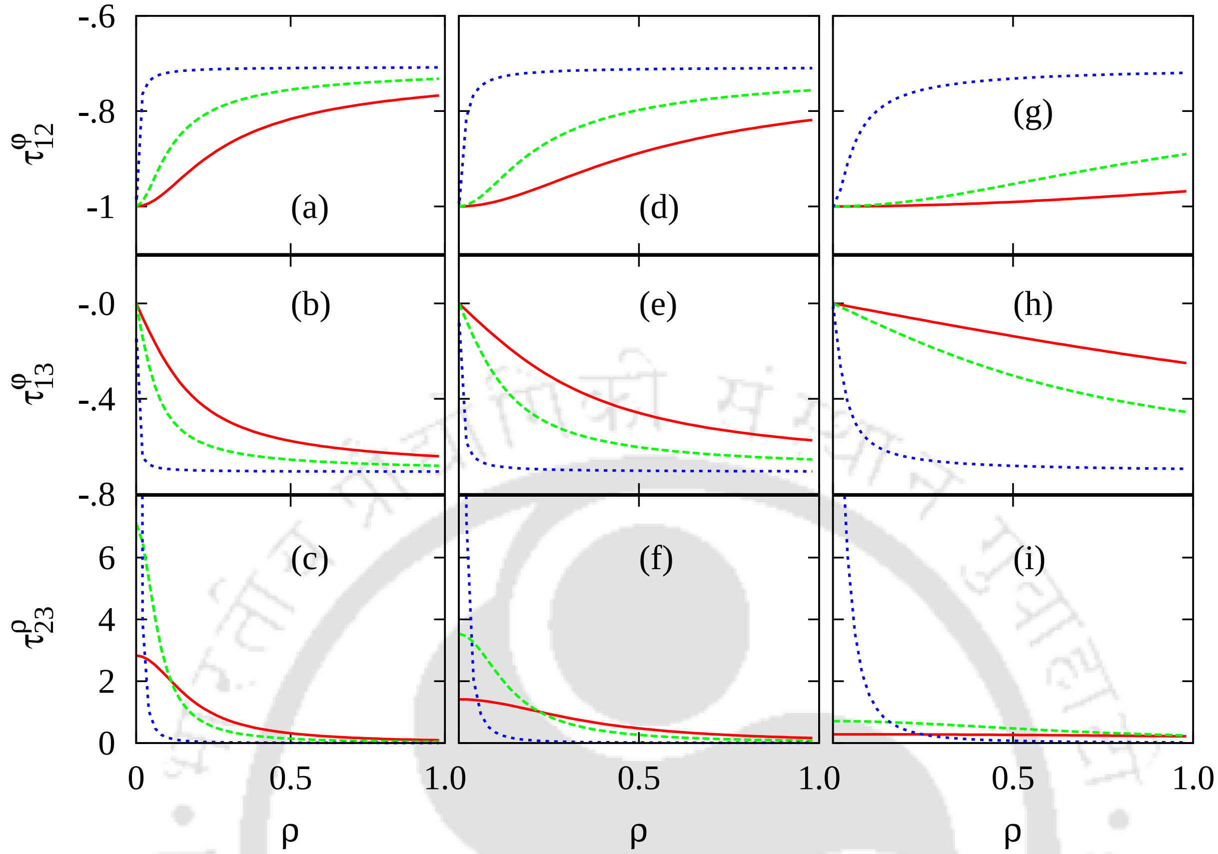

Figure 4.7: The components of the nonadiabtic coupling elements as a function of ρ where (a), (b) and (c) are the three NAC terms (τ^{ϕ}_{12}, τ^{ϕ}_{13}, and τ^{ρ}_{23}) for $\omega = 1.0$, λ=1.0 with $\Delta = 0.5$ (dot), $\Delta = 0.2$ (dash) and $\Delta = 0.01$ (line). Figs. (d), (e) and (f) are for λ=0.5, Figs. (g), (h) and (i) are for λ=0.1, respectively.

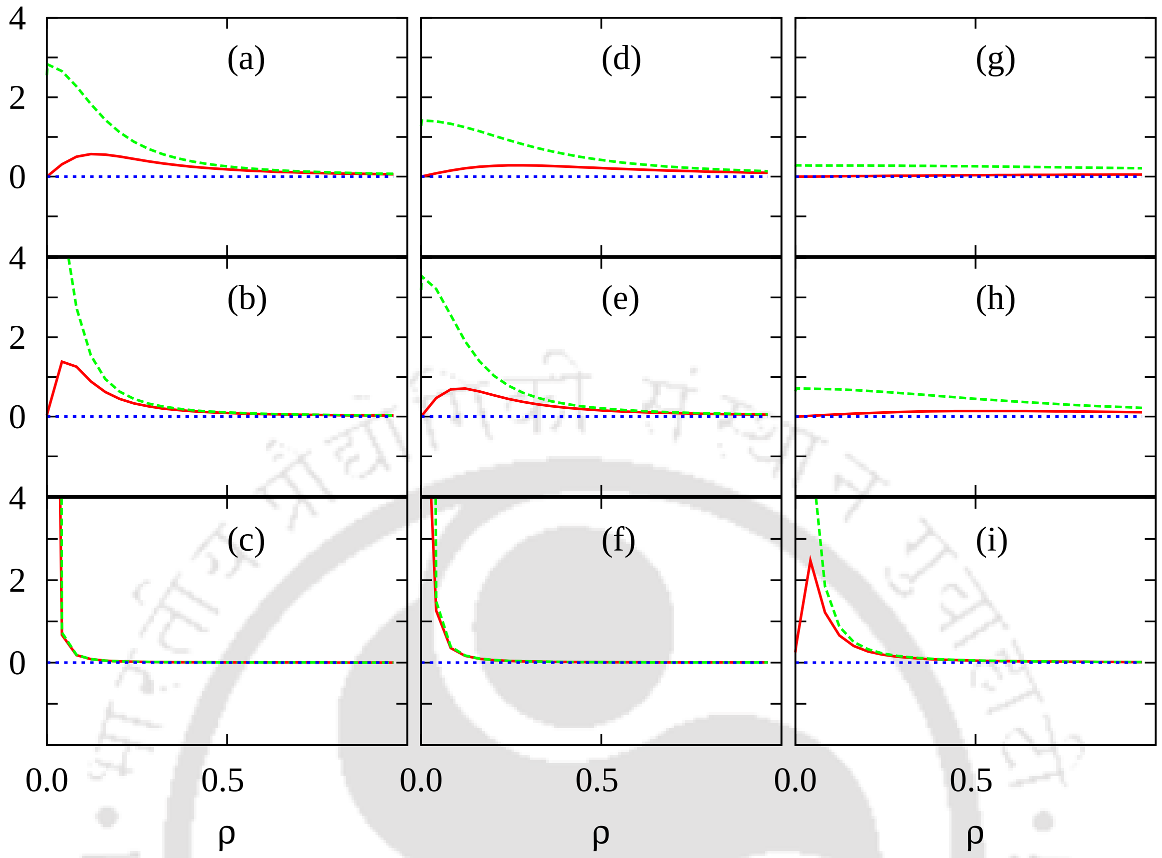

Figure 4.8: The three Curl components of the NAC terms (Curl τ_{12} (line), Curl τ_{13} (dash), and Curl τ_{23} (dot)) as a function of ρ where (a), (b) and (c) are for λ =1.0, $\omega = 1.0$ with Δ values 0.5, 0.2 and 0.01, respectively. Figs. (d), (e) and (f) are for λ =0.5, $\omega = 1.0$ with Δ values 0.5, 0.2 and 0.01, respectively. Figs. (g), (h) and (i) are for λ =0.1, $\omega = 1.0$ with Δ values 0.5, 0.2 and 0.01, respectively.

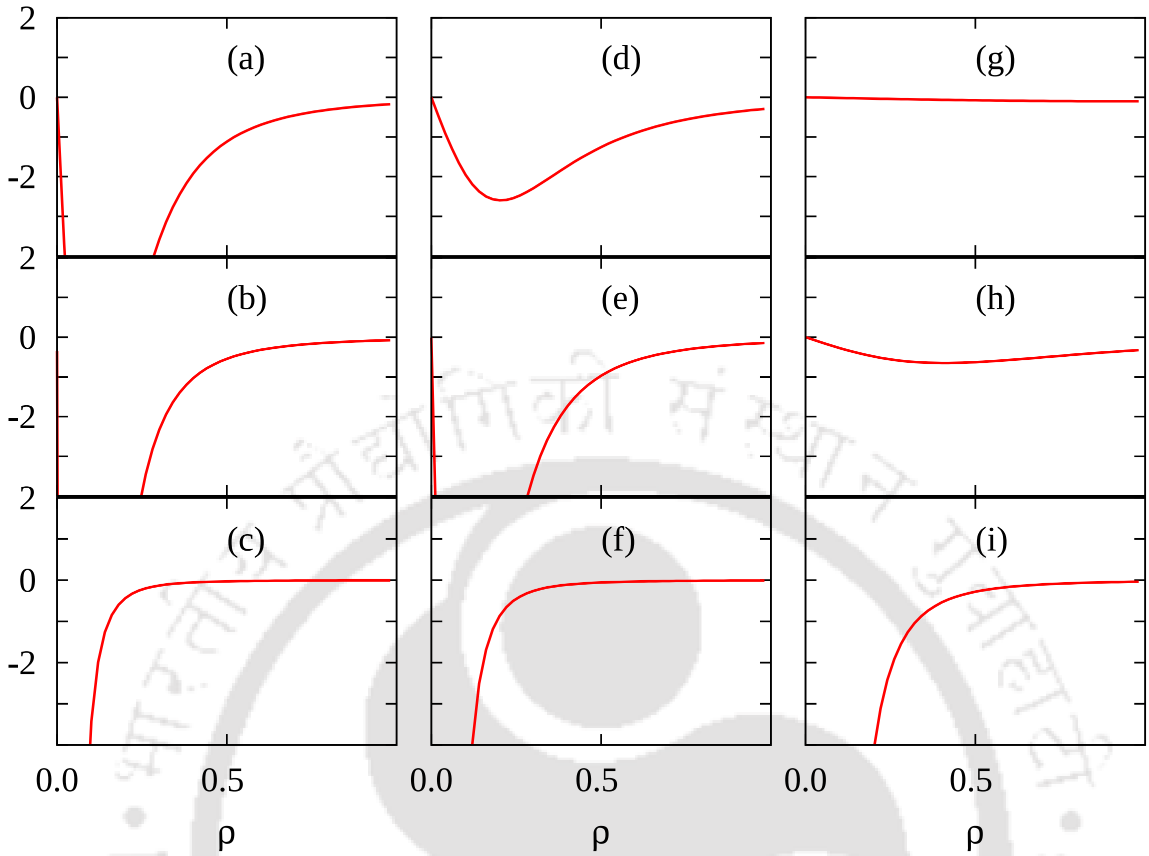

Figure 4.9: The divergence of the NAC terms (div τ_{23}) as a function of ρ where (a), (b) and (c) are for λ =1.0, $\omega = 1.0$ with Δ values 0.5, 0.2 and 0.01, respectively. Figs. (d), (e) and (f) are for λ =0.5, $\omega = 1.0$ with Δ values 0.5, 0.2 and 0.01, respectively. Figs. (g), (h) and (i) are for λ =0.1, $\omega = 1.0$ with Δ values 0.5, 0.2 and 0.01, respectively.

4.3.2 The NAC elements at three state degeneracy and formulation of Extended Born-Oppenheimer equation

When the gap, Δ, between the Π and Σ states is negligibly small or even at zero, the NAC matrices become:

$$\tau^{\rho} = \begin{pmatrix} 0 & 0 & 0 \\ 0 & 0 & 0 \\ 0 & 0 & 0 \end{pmatrix}; \quad \tau^{\phi} = \frac{1}{\rho}\begin{pmatrix} 0 & -\frac{1}{\sqrt{2}} & -\frac{1}{\sqrt{2}} \\ \frac{1}{\sqrt{2}} & 0 & 0 \\ \frac{1}{\sqrt{2}} & 0 & 0 \end{pmatrix}, \tag{4.28}$$

or in Cartesian coordinates:

$$\tau^{x} = \nabla_x\phi \begin{pmatrix} 0 & \frac{1}{\sqrt{2}} & \frac{1}{\sqrt{2}} \\ -\frac{1}{\sqrt{2}} & 0 & 0 \\ -\frac{1}{\sqrt{2}} & 0 & 0 \end{pmatrix}; \quad \tau^{y} = \nabla_y\phi \begin{pmatrix} 0 & \frac{1}{\sqrt{2}} & \frac{1}{\sqrt{2}} \\ -\frac{1}{\sqrt{2}} & 0 & 0 \\ -\frac{1}{\sqrt{2}} & 0 & 0 \end{pmatrix}. \tag{4.29}$$

Since the components of the NAC matrices commute with each other at the three state degenerate point, the total NAC matrix can be written as the product of a vector function and a scalar matrix, a condition to formulate EBO equation. The eigenvalues of the scalar matrix are 0 and $\pm i$ with eigenvector matrix (G):

$$G = \begin{pmatrix} \sqrt{2} & -\frac{1}{2}i & -\frac{1}{2}i \\ -\sqrt{2} & \frac{1}{2}i & \frac{1}{2}i \\ 0 & -\frac{1}{\sqrt{2}} & \frac{1}{\sqrt{2}} \end{pmatrix} \tag{4.30}$$

Since the matrix G is constant at the point of degeneracy, it obviously commute with the operator $\vec{\nabla}$ in Eq. (2.39) and therefore, the EBO equation [Eq. (2.40)] takes the following form in Cartesian coordinates:

$$-\frac{\hbar^2}{2m}\Big\{(\nabla_x + i\nabla_x\phi)^2 + (\nabla_y + i\nabla_y\phi)^2\Big\}\Phi_1 + (E_{\Pi} + \frac{1}{2}\omega(x^2+y^2) - E)\Phi_1 = 0. \tag{4.31}$$

$$\Longrightarrow -\frac{\hbar^2}{2m}\Big\{\Big(\nabla_x - i\frac{y}{x^2+y^2}\Big)^2 + \Big(\nabla_y + i\frac{x}{x^2+y^2}\Big)^2\Big\}\Phi_1 + \big(E_\Pi + \frac{1}{2}\omega(x^2+y^2) - E\big)\Phi_1 = 0. \quad (4.32)$$

4.3.3 Summary

Considering any three-state sub-Hilbert space as the complete one, we briefly present the generalized BO treatment assuming the validity of adiabatic-diabatic transformation condition, $\vec{\nabla}\mathbf{A} + \vec{\tau}\mathbf{A} = 0$, where the chosen form of the transformation matrix (**A**) has to be orthogonal at any point in the configuration space and its' elements should be cyclic functions with respect to a parameter. We demonstrate how (a) the **A** matrix can be constructed by taking the product of six rotation matrices, (b) the same transformation matrix **A** under the ADT condition can provide the explicit expressions of the NAC terms, and (c) the explicit form of Curl-Divergence equations for those NAC terms can be derived. The validity of Curl equation to ensure the ADT transformation leading to uniquely defined diabatic PESs and the proof of zero Curl at and around CI(s), a necessary condition to formulate EBO equation, are being presented. In order to justify these theoretical advancements, we start with a diabatic Hamiltonian known as induced Renner-Teller type model, analytically calculate the electronic basis functions, nonadiabatic coupling elements, and their Curl and divergence equations. The nature of all these quantities are investigated at the situation of three state degeneracy or when those states are approaching to form three state degeneracy. Finally, we present the analytical form of EBO equation for a three state degeneracy at a point.

References

[1] B. Sarkar and S. Adhikari, J. Chem. Phys. **124**, 74101 (2006).

[2] B. Sarkar and S. Adhikari, Int. J. Quantum Chem. , in press (2008).

[3] B. Sarkar and S. Adhikari, Indian J. Phys. **81**, 925 (2007).

[4] A. M. Mebel, A. Yahalom, R. Englman and M. Baer, J. Chem. Phys. **115**, 3573 (2001).

[5] A. M. Mebel, G. J. Halasz, A. Vibok, A. Alijah and M. Baer, J. Chem. Phys. **117**, 991 (2002).

[6] M. Baer, S. H. Lin, A. Alijah, S. Adhikari and G. D. Billing, Phys. Rev. A **62**, 32506 (2000).

[7] G. J. Halasz, A. M. M. A. Vibok and M. Baer, J. Chem. Phys. **118**, 3052 (2003).

[8] C. Jungen and A. J. Merer, *Molecular Spectroscopy: Modern Research*, volume 2, Academic Press Inc., N.Y., USA.

[9] H. Köppel, W. Domcke and L. S. Cederbaum, J. Chem. Phys. **74**, 2945 (1981).

[10] T. Pacher, L. S. Cederbaum and H. Köppel, Adv. Chem. Phys. **84**, 293 (1993).

Chapter 5

Numerical studies of four-state sub-Hilbert space

5.1 Introduction

In the following sections,[1] we explore the validity of Curl condition $\left[\frac{\partial}{\partial p}\tau_{ij}^{q} - \frac{\partial}{\partial q}\tau_{ij}^{p} = (\boldsymbol{\tau}^{q}\boldsymbol{\tau}^{p})_{ij} - (\boldsymbol{\tau}^{p}\boldsymbol{\tau}^{q})_{ij}\right]$, as well as the identities $\left[\left(\frac{\partial\theta_{ij}}{\partial p}\frac{\partial\theta_{ik}}{\partial q} - \frac{\partial\theta_{ij}}{\partial q}\frac{\partial\theta_{ik}}{\partial p}\right) \equiv 0, \{p, q = x, y, z \text{ or } r, \theta, \phi\}, i, j, k = 1, 2, 3, 4 \text{ and } i \neq j \neq k\right]$, leading to zero Curl along the seam of the CI for a four state sub-Hilbert space by employing the Mathieu equation.[2–7] At this junction, we remind: (a) The validity of Curl condition [Eqs. (3.12a) and (3.13a)] implies that the adiabatic-diabatic transformation can provide uniquely defined diabatic PESs, on which stable and accurate numerical calculations can be performed; (b) The zero Curls bring the Extended Born-Oppenheimer (EBO) equation and then, one can carry out accurate calculation on the ground state EBO equation by taking into account the effect of upper PESs. The calculated NAC terms by employing Mathieu equation, provides an immense scope to explore the above two important aspects.

5.2 The Mathieu equation as the model system

The electronic SE to be considered is written for one electronic (circular) coordinate, θ, and is expressed in terms of two nuclear coordinates, ϕ and q:

$$\left(-\frac{1}{2}E_{el}\frac{\partial^2}{\partial\theta^2} - G(q,\phi)\cos(2\theta-\phi) - u_j(q,\phi)\right)\xi_j(\theta|q,\phi) = 0 \tag{5.1}$$

where E_{el} is a characteristic electronic quantity, $G(q,\phi)$ is the nuclear-electronic interaction coefficient, and $u_j(q,\phi)$ and $\xi_j(\theta|q,\phi)$ are the jth eigenvalue and eigenfunction, respectively, which parametrically depend on the nuclear coordinates. Equation (5.1) is recognized as the well-known Mathieu equation. For the degenerate systems, we consider the above symmetrical system where the degeneracy is at the origin, but for a non symmetrical system[2] where the degeneracy is shifted to some point in configuration space, one have to consider the following extended Mathieu equation.

$$\left\{-E_{el}\frac{\partial^2}{\partial\theta^2} - k\Big[(q\cos\phi - a)\cos 2\theta + (q\sin\phi - b)\sin 2\theta\Big] - u_j(q,\phi)\right\}\xi_j(\theta|q,\phi) = 0 \tag{5.2}$$

As can be seen the interaction due to the nuclear motion at the point (a,b) is zero which means that the degeneracy of the electronic states is left at this point. The difference between the two is with respect to the location of CI. In the first model the CI is located at the origin and in the later, it is located at some point (a,b) in the nuclear configuration space.

For the present study, we solve the symmetric case [Eq.(5.1)] and assume $G(q,\phi)$ to be independent of ϕ and linearly dependent on q, namely, equal to kq with k as a given constant. This choice of the interaction term has several advantages: (1) It form singular NAC elements (or degenerate eigenvalues) along the coordinate q only; (2) The eigenvalues of Eq. (5.1) depend on q but are independent of ϕ; (3) The eigenvectors are functions of ϕ and q, and their nature is such that the resulting NAC elements are ϕ independent but varies with q only.

To solve the Mathieu equation, we expand the $\xi_j(\theta|q,\phi)$ eigenfunctions in the Fourier series. We select the following two families of solutions:[8]

$$ce_{2n+1}(z,-x) = \sum_{m=0}^{\infty} A_{2m+1}^{2n+1}(-x)\cos(2m+1)z$$
$$se_{2n+1}(z,-x) = \sum_{m=0}^{\infty} B_{2m+1}^{2n+1}(-x)\sin(2m+1)z \quad (5.3)$$

where z is given as:

$$z = \theta - \frac{\phi}{2} \quad (5.4)$$

Here, the cosine series stands for the $\xi_j(\theta|q,\phi)$ functions with odd j values and the sine function for those with the even j values.

It is well-known that the geometrical series, as presented in Eqs. (5.3) and (5.4), does not converge at a point close to the real axis. This feature may effect the rate of convergence for points on the real axis and therefore, the convergence in each case was treated with care. In this respect it is important to mention that we have included 200 bases in each case to guarantee the convergence though the required convergence arrives within 50 bases.

5.3 Numerical calculations: results and discussions

5.3.1 Non - adiabatic coupling elements

Since we choose the nuclear - electronic interaction coefficient, $G(q,\phi)$ (=kq), as independent of the nuclear coordinate ϕ, the adiabatic potential energies being the solutions of Mathieu equation are dependent only on the coordinate q. We present the first four adiabatic PESs (u_1, u_2, u_3 and u_4) as functions of q in Figs. 5.1 for a fixed $k = 0.2$ with various E_{el} = (a) 0.05, (b) 0.04, (c) 0.03,(d) 0.02, and (e) 0.01, where in Figs. 5.2 for a particular E_{el} = 0.01 with different k = (a) 0.20, (b) 0.15, (c) 0.10, (d) 0.05, and (e) 0.04. The solutions of Mathieu equation are such that adiabatic PESs show pairwise degeneracy, namely, between u_1 and u_2 and then, between u_3 and u_4 up to different values of q depending on the constants, E_{el} and k. In Figs. 5.1a $-$ 5.1e, for a fixed value of $k(=0.2)$ and gradually decreasing values of E_{el}, both u_1 and u_2 come closer and closer to the set u_3 and u_4 but each individual set (Set I: u_1 and u_2 and Set II: u_3 and u_4) loses its' degeneracy at different but smaller values of q. On the other hand, Figs. 5.2a $-$ 5.2e display that for a fixed value of E_{el} with higher to lower values of k, the degeneracy within the individual set sustains more as functions of q. In summary, as the value of E_{el} decreases, each set of adiabatic states loses its degeneracy [Figs. 5.1a to 5.1e], but as the value k decreases, the same degeneracy increases [Figs. 5.2a to 5.2e].

Figures 5.3 present the ϕ component of the non - adiabatic coupling terms, (a) τ_{12}^{ϕ}, (b) τ_{13}^{ϕ}, (c) τ_{14}^{ϕ}, (d) τ_{23}^{ϕ}, (e) τ_{24}^{ϕ}, and (f) τ_{34}^{ϕ} and Figs. 5.4 display the q components, (a) τ_{12}^{q}, (b) τ_{13}^{q}, (c) τ_{14}^{q}, (d) τ_{23}^{q}, (e) τ_{24}^{q}, and (f) τ_{34}^{q} as functions of q for various values of E_{el} (=0.05, 0.04, 0.03, 0.02 and 0.01) and a fixed k (= 0.2). It is clear from the figures that as the E_{el} value decreases, both the ϕ as well as q components of the NAC terms undergo more and more changes as the functions of q indicating increasingly stronger interaction among the adiabatic states. On the contrary, Figs. 5.5 present the ϕ component of the NAC terms, (a) τ_{12}^{ϕ}, (b) τ_{13}^{ϕ}, (c) τ_{14}^{ϕ}, (d) τ_{23}^{ϕ}, (e) τ_{24}^{ϕ}, and (f) τ_{34}^{ϕ} and Figs 5.6 display the q components, (a) τ_{12}^{q}, (b) τ_{13}^{q}, (c) τ_{14}^{q}, (d) τ_{23}^{q}, (e) τ_{24}^{q}, and (f) τ_{34}^{q} as functions of q with different values of k (=0.20, 0.15, 0.10, 0.05, 0.04) and a fixed E_{el} (= 0.01). It is again quite evident from the figures that as the k value decreases with a fixed E_{el}, both the ϕ and the q components of the non - adiabatic coupling terms show less and less changes as the functions of q leading to gradually lower interaction among the adiabatic states. Thus, as the value of E_{el} increases, the interaction among the adiabatic states through NAC terms decreases, but as the value k increases, the interaction elements among the same states increase.

Figures 5.3 - 5.6 demonstrate two interesting features: (a) If the ϕ component of a NAC element shows non - zero magnitude, invariably its' q component appears zero or the vice versa as functions of the nuclear coordinate, q. This feature of NAC terms obtained as the solution of Mathieu equation is being endorsed from the calculated divergence of the same NAC terms. Figures 5.7a - 5.7b display the divergence of the NAC elements as functions of q for two different set of parametric values of E_{el} and k, where the NAC elements with non - zero ϕ component show zero divergence but with non - zero q component presents non - zero divergence as expected from electrodynamics. (b) The choices of the parameters, E_{el} and k, are such that the four adiabatic states are interacting with each other, where all the NAC elements show non - zero values except $\vec{\tau}_{14}$ and $\vec{\tau}_{23}$ only at $q = 0$. More precisely, since either q or ϕ component of NAC elements are non - zero, it will be interesting to see how the Curl of the NAC elements behave as functions of q for various chosen values of the parameters, E_{el} and k.

Figures 5.8 present the Curls of the NAC elements calculated by using the equation, $C_{ij} = (\boldsymbol{\tau}^{\phi}\boldsymbol{\tau}^{q})_{ij} - (\boldsymbol{\tau}^{q}\boldsymbol{\tau}^{\phi})_{ij}$, Figures 5.9 display the same quantities evaluated by using the equation, $Z_{ij} = \frac{\partial}{\partial q}\tau^{\phi}_{ij} - \frac{\partial}{\partial \phi}\tau^{q}_{ij}$ and Figures 5.10 demonstrate their difference, $F_{ij} = C_{ij} - Z_{ij}$, known as Yang - Mills field elements as functions of q for various values of the parameter, E_{el} (= 0.05, 0.04, 0.03, 0.02 and 0.01) with a fixed k (= 0.2). In a similar manner, Figs. 5.11, 5.12 and 5.13 demonstrate the elements of the matrices, C_{ij}, Z_{ij}, and F_{ij}, respectively as functions of q for various values of the parameter, k (= 0.20, 0.15, 0.10, 0.05, and 0.04) with a fixed E_{el} (= 0.01). Figures 5.8 and Figures 5.9 clearly indicate that as the E_{el} values decreases for a fixed k, the Curls of the non - adiabatic coupling elements deviates more from zeros since the individual sets of states loses degeneracy due to the increasingly stronger interaction among themselves. Figures 5.11 and Figures 5.12 demonstrate the same feature but in other way, i.e., for a fixed E_{el} with decreasing values of k, the Curls of the non - adiabatic coupling terms approach to zeros due to the lower interaction among the sets. In summary, Figures 5.8, 5.9, 5.11, and 5.12 tell that as the adiabatic states intend to form a sub - Hilbert space, the Curls of the NAC terms lead to zeros. On the other hand, Figures 5.10 and 5.13 present the validity of Curl conditions, namely, as these four adiabatic states form a subspace, the Curl conditions remain satisfied leading to zero Yang - Mills field, otherwise such conditions are also deviating like Curls. In other words, we find when Curls of the NAC terms are approaching to zeros for a set of parametric values, Yang - Mills field elements are also showing the same trend. On the contrary, when the NAC elements among the first four state tend to show zero Curls and zero Curl conditions (Yang - Mills fields) for a set of parametric values (e.g., k = 0.04 and E_{el} = 0.01), the nearest neighbour NAC elements of the complimentary space appear to vanish for the same set of parameters leading to four state sub - Hilbert space. Figure 5.14 presents the nearest neighbour non zero NAC elements (τ^{ϕ}_{16}, τ^{ϕ}_{25}, τ^{q}_{15}, and τ^{q}_{26}) as functions of q for a fixed E_{el} = 0.01 with different k = 0.20, 0.15, 0.10, 0.05, and 0.04. The figure indicates that all the NAC elements gradually vanish as the k value decreases. Figure 5.15 demonstrates the relative magnitude of the sub - space and the complimentary space NAC elements when the first four states is decoupled from the rest (i.e., k = 0.04 and E_{el} = 0.01).

Since the solution of Mathieu equation shows conical intersections due to degeneracies at q=0, the nature of the non - adiabatic coupling terms close to $q \rightarrow 0$ are important to investigate. Figs. 5.8 - 5.9 as well as Figs. 5.11 - 5.12 clearly indicate that if Curls deviate from zero for various chosen values of k and E_{el}, it happens prominently well within $q < 0.25$. At $k = 0.2$, $E_{el} = 0.04$ and $k = 0.04$, $E_{el} = 0.01$, Figs. 5.8 - 5.13 demonstrate that the Curls and Curl Conditions are *around zeros* for those values of q with the ratio, $x(=\frac{kq}{E_{el}}) < 1$, leading to form a four state sub - Hilbert space. In more specific terms, since the validity of curl condition ($F = C - Z = 0$) ensures the existence of sub - Hilbert space, we have calculated the Yang - Mills field (F) elements for various chosen values of k and q with fixed E_{el} and presented those elements in the Table 5.1. It is clear from the table that as the value of x become lower and lower ($<< 1$), the magnitude of the F elements tend to *virtually zero* forming a four state sub - Hilbert space but in all practical purpose of numerical calculation, even $x < 1$ situation may be considered (see Table 5.1) as sub - Hilbert space. Therefore, the solution of Mathieu equation for the parametric space with $x << 1$ not only mimic a realistic molecular system but also shows the existence or presence of a four state sub - Hilbert space.

Table 5.1: The elements of the Matrix F ($F = C - Z$) for different values of k and q at $E_{el} = 0.01$.

k	$x(q = 0.1)$	F_{12}	F_{14}	F_{23}	F_{34}
0.08	0.8	-0.000054	-0.001348	0.001996	-0.050028
0.04	0.4	-0.000003	-0.000188	0.000229	-0.012502
0.02	0.2	0.000000	-0.000025	0.000027	-0.003125
0.01	0.1	0.000000	-0.000003	0.000003	-0.000781
0.005	0.05	0.000000	0.000000	0.000000	-0.000195
	$x(q = 0.3)$				
0.08	2.4	-0.001097	-0.007698	0.021465	-0.150657
0.04	1.2	-0.000087	-0.001355	0.002412	-0.037544
0.02	0.6	-0.000006	-0.000200	0.000269	-0.009378
0.01	0.3	0.000000	-0.000027	0.000032	-0.002344
0.005	0.15	0.000000	-0.000004	0.000004	-0.000586

5.3.2 Adiabatic - Diabatic Transformation (ADT) angle

When we substitute the model form of **A** matrix [Eq. 3.9] and the anti - symmetric form of $\vec{\boldsymbol{\tau}}$ matrix [Eq. 3.10] in the ADT equation ($\nabla\mathbf{A}+\boldsymbol{\tau}\mathbf{A}=0$), the simple manipulation leads to the following differential equations for the ADT angles,

$$\begin{aligned}
\vec{\nabla}\theta_{12} &= -\frac{1}{\cos\theta_{13}\cos\theta_{14}}\Big[\cos\theta_{23}\Big\{\vec{\tau}_{12}\cos\theta_{24}-\sin\theta_{24}\big(\vec{\tau}_{13}\sin\theta_{34}+\vec{\tau}_{14}\cos\theta_{34}\big)\Big\} \\
&- \sin\theta_{23}\big(\vec{\tau}_{13}\cos\theta_{34}-\vec{\tau}_{14}\sin\theta_{34}\big)\Big] &(5.5a)\\
\vec{\nabla}\theta_{13} &= -\frac{1}{\cos\theta_{14}}\Big[\sin\theta_{23}\Big\{\vec{\tau}_{12}\cos\theta_{24}-\sin\theta_{24}\big(\vec{\tau}_{13}\sin\theta_{34}+\vec{\tau}_{14}\cos\theta_{34}\big)\Big\} \\
&+ \cos\theta_{23}\big(\vec{\tau}_{13}\cos\theta_{34}-\vec{\tau}_{14}\sin\theta_{34}\big)\Big] &(5.5b)\\
\vec{\nabla}\theta_{23} &= \frac{1}{\cos\theta_{14}}\Big(\tan\theta_{13}\Big[\cos\theta_{23}\Big\{\vec{\tau}_{12}\cos\theta_{24}-\sin\theta_{24}\big(\vec{\tau}_{13}\sin\theta_{34}+\vec{\tau}_{14}\cos\theta_{34}\big)\Big\} \\
&- \sin\theta_{23}\big(\vec{\tau}_{13}\cos\theta_{34}-\vec{\tau}_{14}\sin\theta_{34}\big)\Big]\Big)+\frac{1}{\cos\theta_{24}}\Big\{\tan\theta_{14}\sin\theta_{24}\big(\vec{\tau}_{13}\cos\theta_{34}-\vec{\tau}_{14}\sin\theta_{34}\big) \\
&- \big(\vec{\tau}_{23}\cos\theta_{34}-\vec{\tau}_{24}\sin\theta_{34}\big)\Big\} &(5.5c)\\
\vec{\nabla}\theta_{14} &= -\vec{\tau}_{12}\sin\theta_{24}-\cos\theta_{24}\big(\vec{\tau}_{13}\sin\theta_{34}+\vec{\tau}_{14}\cos\theta_{34}\big) &(5.5d)\\
\vec{\nabla}\theta_{24} &= \tan\theta_{14}\Big\{\vec{\tau}_{12}\cos\theta_{24}-\sin\theta_{24}\big(\vec{\tau}_{13}\sin\theta_{34}+\vec{\tau}_{14}\cos\theta_{34}\big)\Big\} \\
&- \big(\vec{\tau}_{23}\sin\theta_{34}-\vec{\tau}_{24}\cos\theta_{34}\big) &(5.5e)\\
\vec{\nabla}\theta_{34} &= \frac{1}{\cos\theta_{24}}\Big\{\tan\theta_{14}\big(\vec{\tau}_{13}\cos\theta_{34}-\vec{\tau}_{14}\sin\theta_{34}\big)+\sin\theta_{24}\big(\vec{\tau}_{23}\cos\theta_{34}-\vec{\tau}_{24}\sin\theta_{34}\big) \\
&- \vec{\tau}_{34}\cos\theta_{24}\Big\}. &(5.5f)
\end{aligned}$$

Numerically calculated τ^q and τ^ϕ matrix elements as presented in previous section (section 5.3.1) are substituted in the q and ϕ components of the above differential equations and solved those coupled differential equations to obtain six ADT angles as functions of q and ϕ. While solving those differential equation, we initialize all the ADT angles to zeros at $q=0$ and $\phi=0$. Figures 5.16 demonstrates that at $q\to 0$, the ADT angles start with zeros at $\phi=0$ and end up with integral multiple of π at $\phi=2\pi$, whereas at $q\neq 0$, the ADT angles oftenly move away from zero to a particular value even at $\phi=0$ and take the same magnitude (either with plus or minus sign) at $\phi=2\pi$ such that the ADT angles at $\phi = 0$ and $\phi = 2\pi$ satisfy the single - valuedness of ADT matrix. The same figure shows the ADT angles both for E=0.01 and k=0.2 as well as E=0.01 and k=0.04 cases. At this junction, we are in a position to calculate the identities (the differences of the product of the cross derivatives) as defined in the curl equation [Eq. 3.12a] and later used while formulating EBO equation (see the discussion below Eq. 3.16). Figures 5.17 presents few such identities as functions of q and ϕ for the above two cases, namely, E=0.01 and k=0.2, and E=0.01 and k=0.04. It is quite clear that at E=0.01 and k=0.04, the identities are either zeros or varying very little around zeros as functions of q and ϕ leading to zero Curls, whereas at E=0.01 and k=0.2, the same identities are showing substantially larger values essentially indicating non - zero Curls.

Finally, as the representative four states intend to form a sub - Hilbert space for a set or sets of parametric values, Curls and Yang - Mills fields of the NAC terms tend to zeros leading to the validity of the adiabatic equation [Eq. 3.15] and the extended BO equations [Eq. 3.23]. In other word, the formulation of Eq. 3.23 from Eq. 3.14 is *only possible* if the sub - space is complete vis -a -vis NAC terms are Curl free. At this junction, we wish to remind that Curl free NAC terms imply the commutation among the components of the NAC terms (i.e., the rhs of Eq. 3.11):

$$\left[\boldsymbol{\tau}^{\phi}, \boldsymbol{\tau}^{q}\right] = 0 \tag{5.6}$$

as well as the validity of the following identities [Eq. 3.12a and Eq. 3.13a]:

$$\nabla_p \theta_{ij} \nabla_q \theta_{jk} - \nabla_q \theta_{ij} \nabla_q \theta_{jk} = 0, \; \{i \neq j \neq k\} = 1, 2, 3. \tag{5.7}$$

Since we know that when two operators commute with each other, they will have a common eigenfunction (**G**) [Eq. 3.15], i.e., **G** diagonalizes both the components of $\vec{\boldsymbol{\tau}}$ matrix with eigenvalues $\pm i\vec{\omega}$. In this article, we just explore the condition to find out such sub - Hilbert space, where beyond BO equation [Eqs. 3.15 and 3.23] could be valid and required calculations can be carried out.

5.4 Summary

In order to justify the analytical treatment, namely, the validity of Curl condition and zero Curl for the NAC elements, we solve Mathieu equation as the model system to calculate adiabatic potential energies and nonadiabatic coupling terms. By using those NAC elements, we find that not only Curl conditions are valid but also Curls approach to zeros as the four adiabatic states intend to form a sub - Hilbert space. We explore the condition to find out such sub - Hilbert space, where beyond BO equation [Eq. (3.23) and (3.24)] could be valid and required calculations can be carried out.

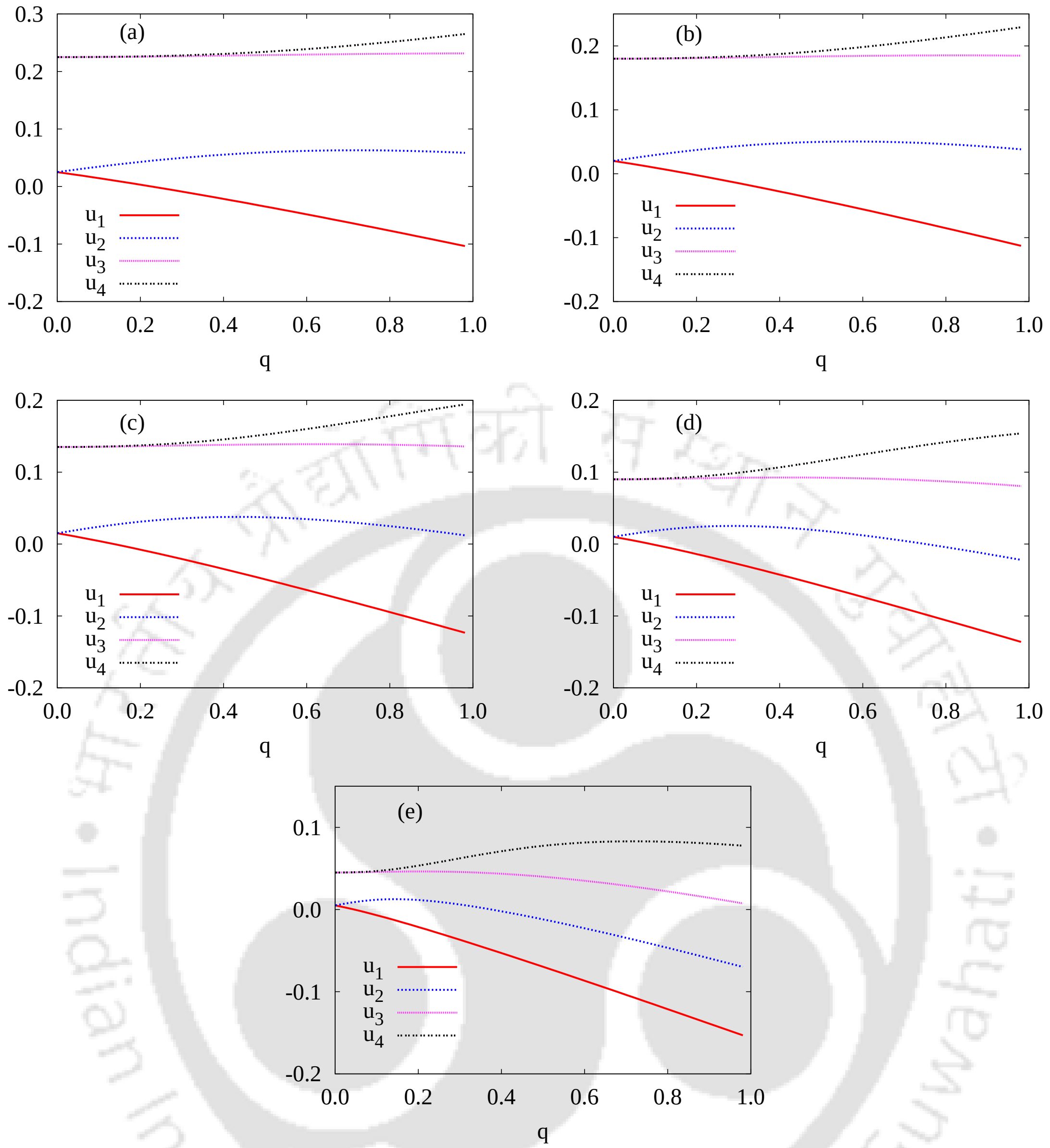

Figure 5.1: The first four adiabatic potential where $k = 0.2$ and (a) $E_{el} = 0.05$, (b) $E_{el} = 0.04$, (c) $E_{el} = 0.03$, (d) $E_{el} = 0.02$, and (e) $E_{el} = 0.01$.

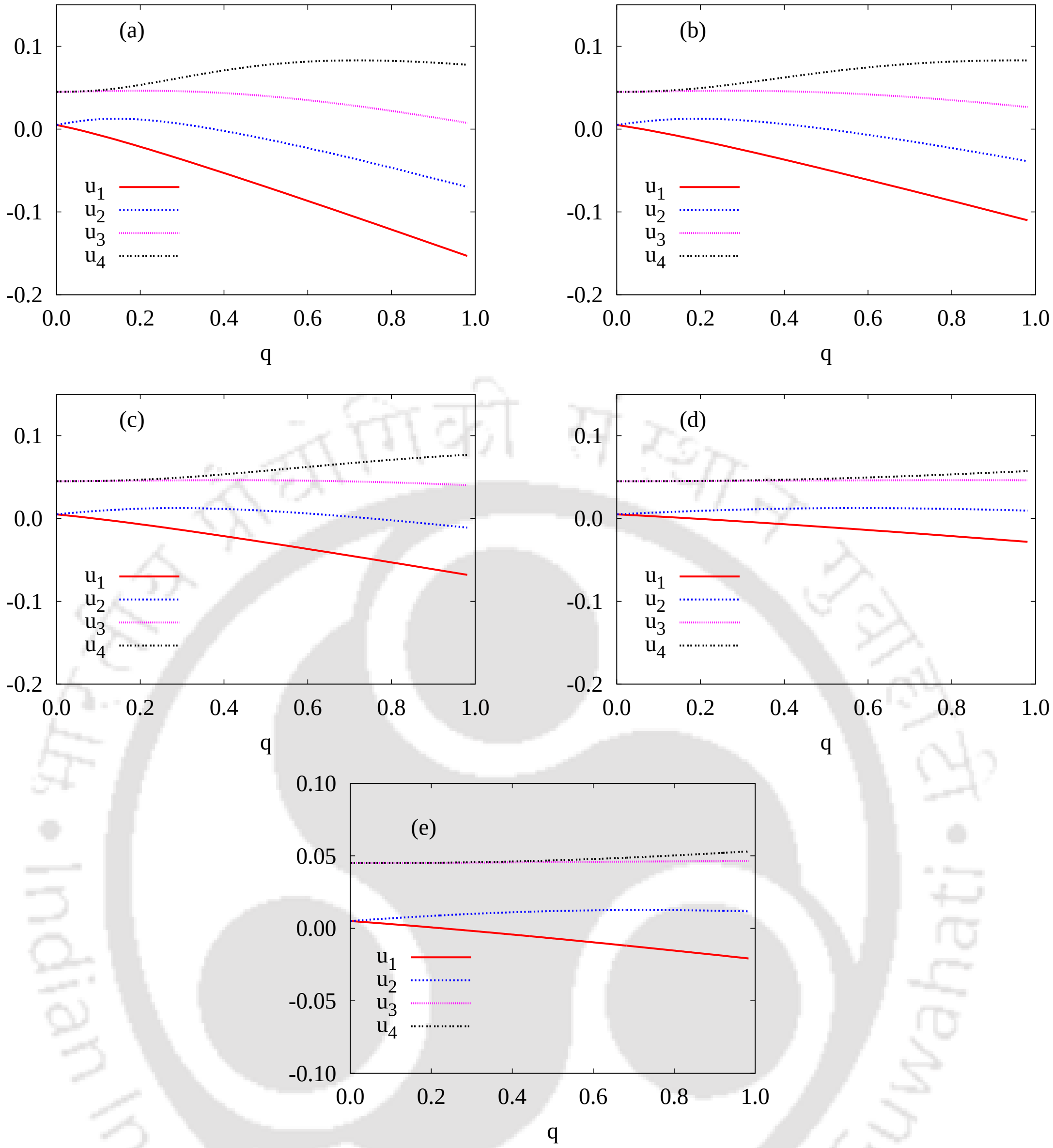

Figure 5.2: The first four adiabatic potential where $E_{el} = 0.01$ and (a) $k = 0.20$, (b) $k = 0.15$, (c) $k = 0.10$, (d) $k = 0.05$, and (e) $k = 0.04$.

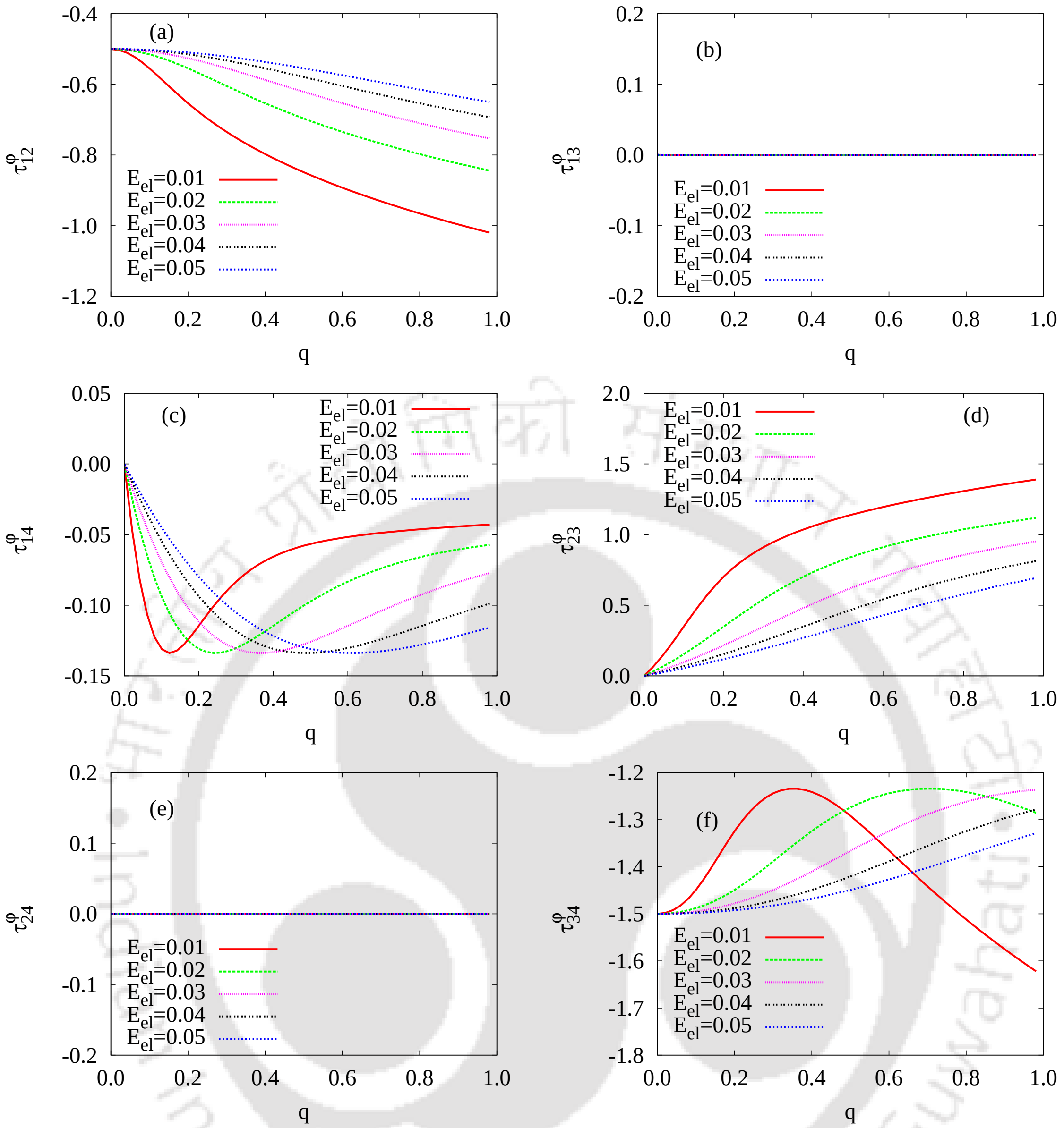

Figure 5.3: The ϕ components of non-adiabatic coupling elements: (a) τ_{12}^{ϕ} , (b) τ_{13}^{ϕ}, (c) τ_{14}^{ϕ}, (d) τ_{23}^{ϕ}, (e) τ_{24}^{ϕ} and (f) τ_{34}^{ϕ} as a function of q with different E_{el} where $k = 0.2$.

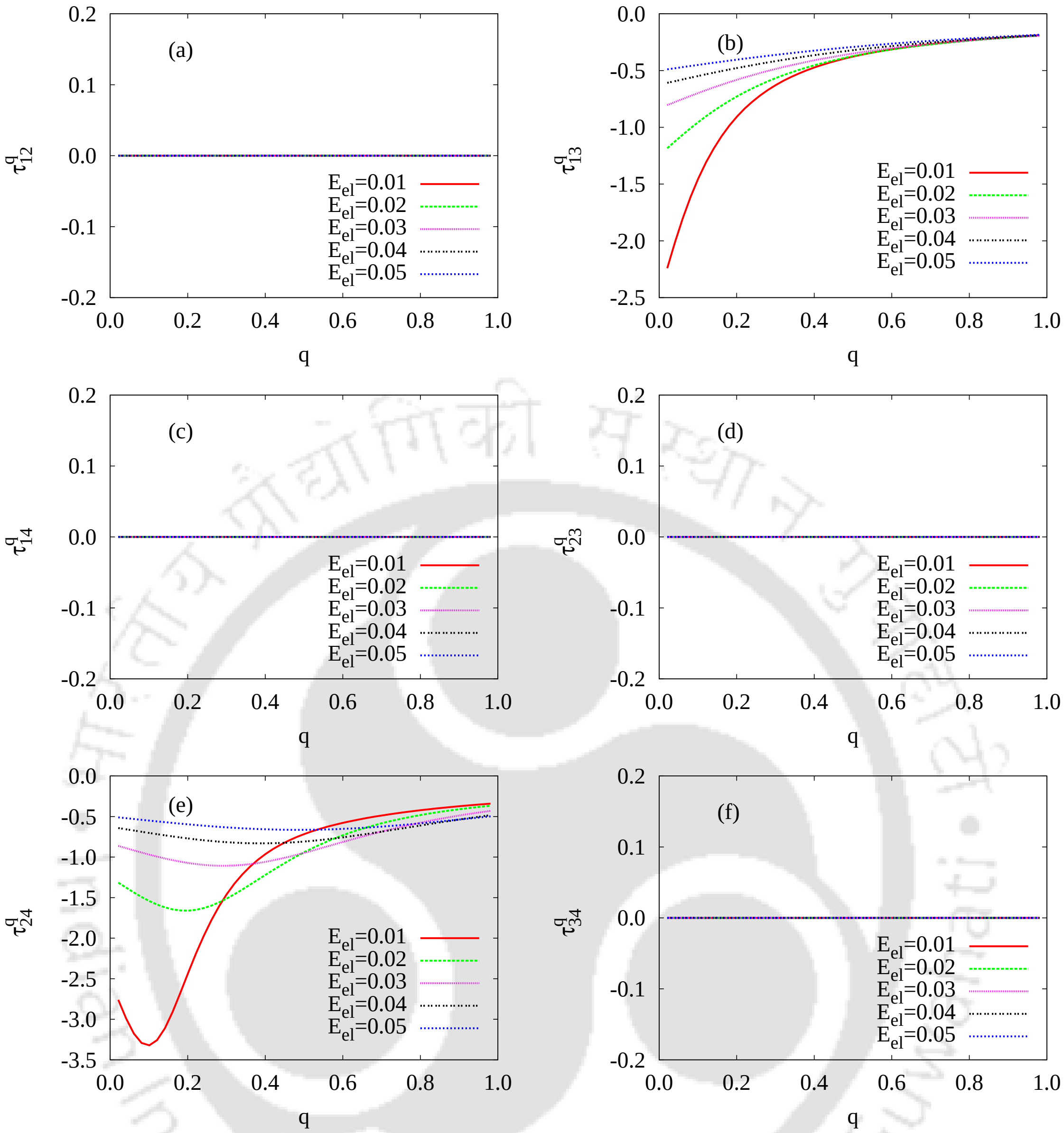

Figure 5.4: The q components of non-adiabatic coupling elements: (a) τ^q_{12} , (b) τ^q_{13}, (c) τ^q_{14}, (d) τ^q_{23}, (e) τ^q_{24} and (f) τ^q_{34} as a function of q with different E_{el} where $k = 0.2$.

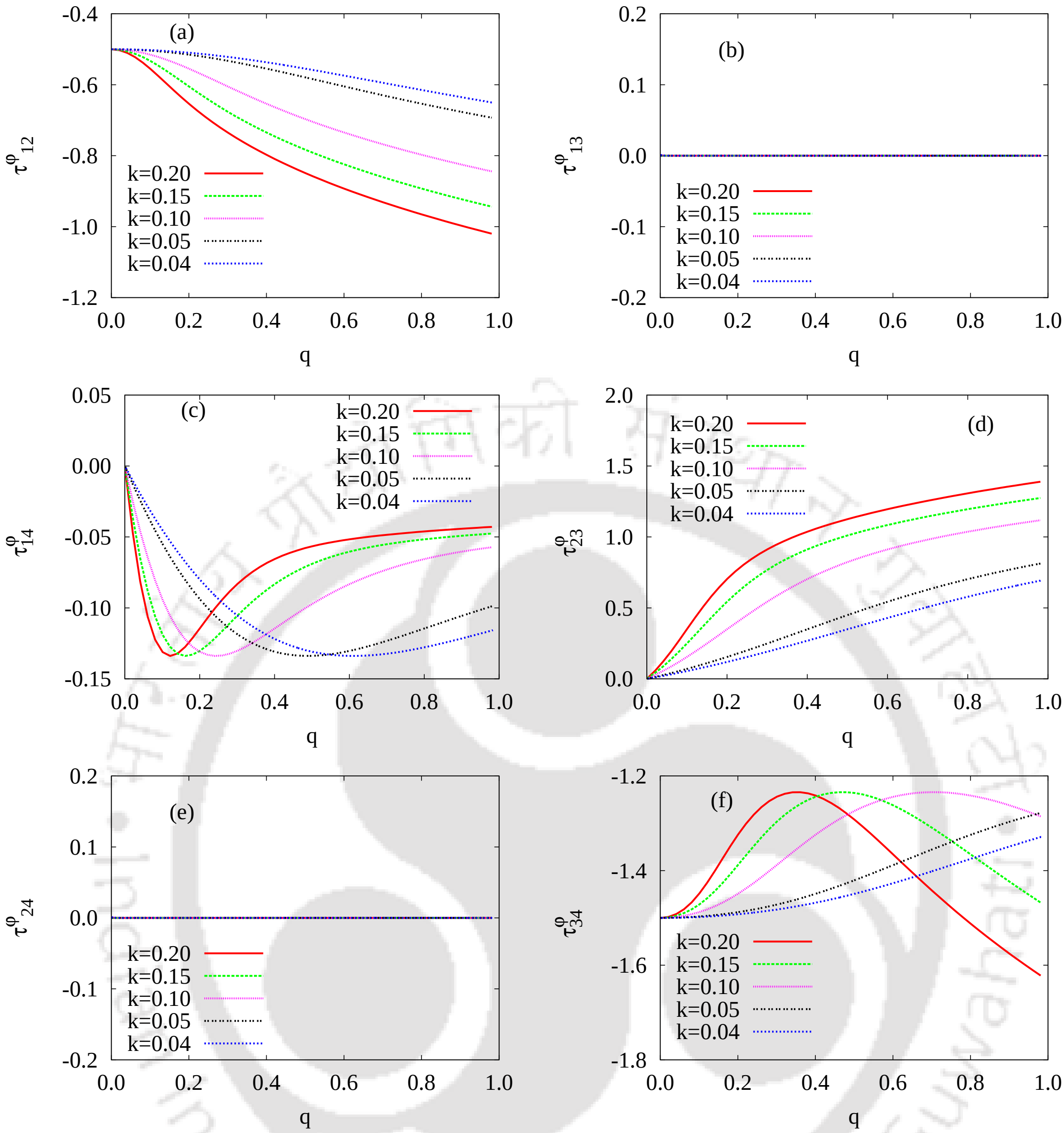

Figure 5.5: The ϕ components of non-adiabatic coupling elements: (a) τ_{12}^{ϕ} , (b) τ_{13}^{ϕ}, (c) τ_{14}^{ϕ}, (d) τ_{23}^{ϕ}, (e) τ_{24}^{ϕ} and (f) τ_{34}^{ϕ} as a function of q with different k where $E_{el} = 0.01$.

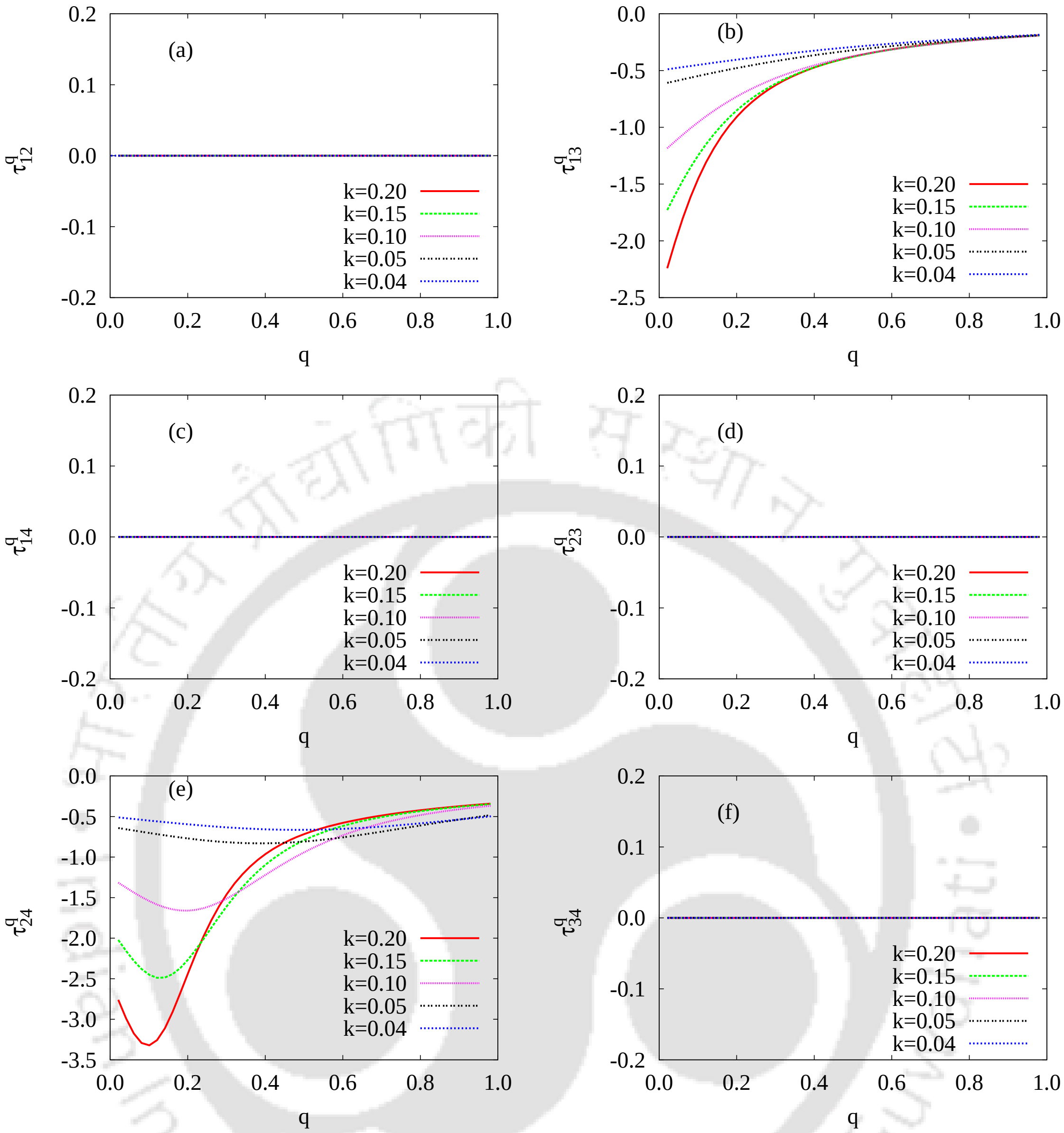

Figure 5.6: The q components of non-adiabatic coupling elements: (a) τ_{12}^q , (b) τ_{13}^q, (c) τ_{14}^q, (d) τ_{23}^q, (e) τ_{24}^q and (f) τ_{34}^q as a function of q with different k where $E_{el} = 0.01$.

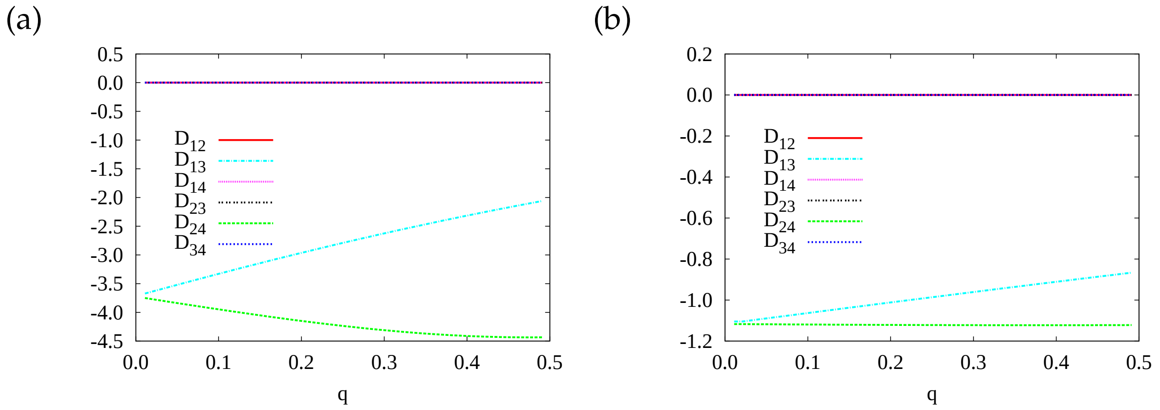

Figure 5.7: Divergence of the non-adiabatic coupling elements as a function of q where (a) $E_{el} = 0.05$, $k = 0.20$, and (b) $E_{el} = 0.01$, $k = 0.04$.

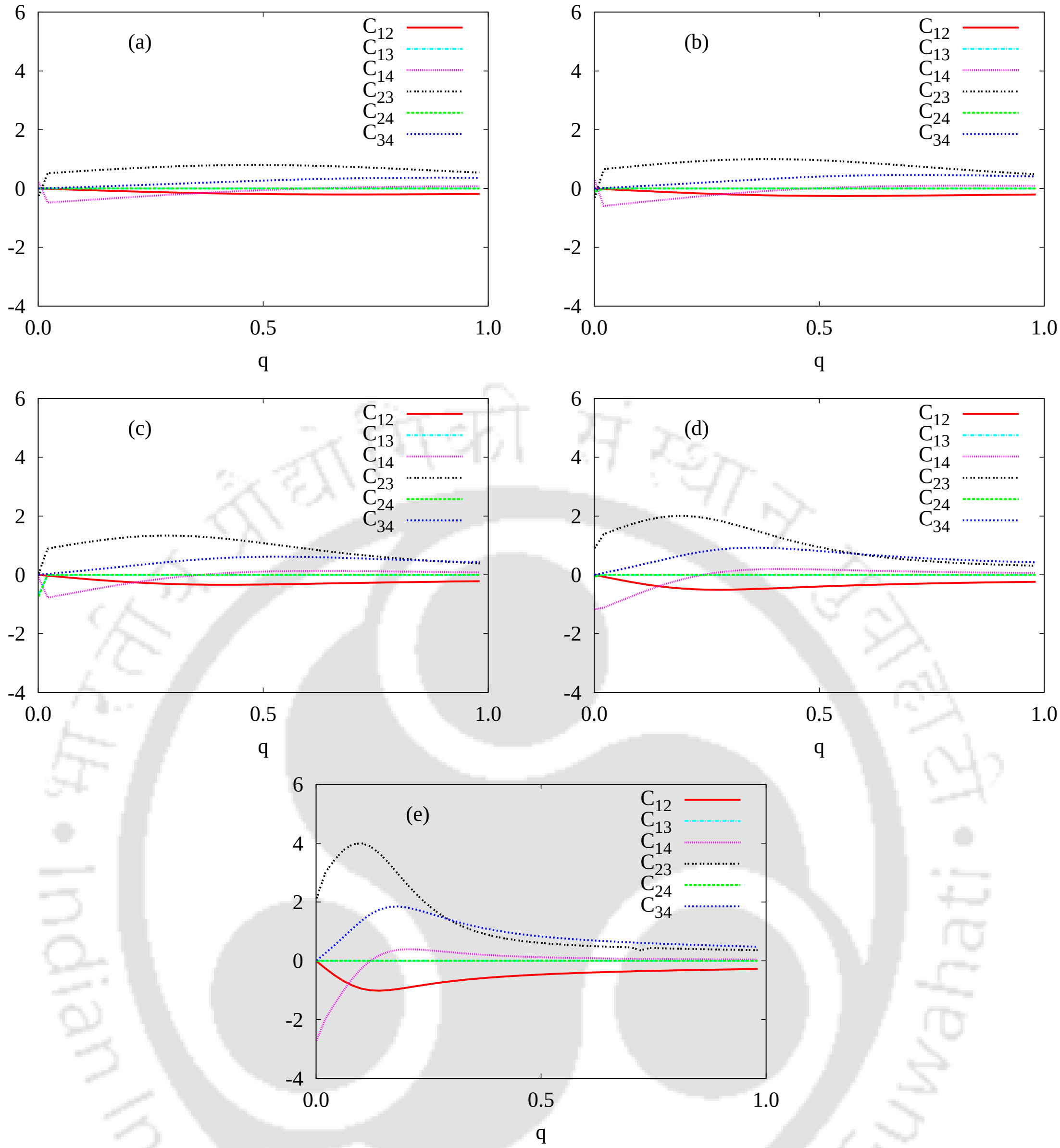

Figure 5.8: Curls of the non-adiabatic coupling elements calculated by using the equation, $C_{ij} = (\boldsymbol{\tau}^{\phi}\boldsymbol{\tau}^{q})_{ij} - (\boldsymbol{\tau}^{q}\boldsymbol{\tau}^{\phi})_{ij}$ as a function of q where $k = 0.2$ and (a) $E_{el} = 0.05$, (b) $E_{el} = 0.04$, (c) $E_{el} = 0.03$, (d) $E_{el} = 0.02$, and (e) $E_{el} = 0.01$.

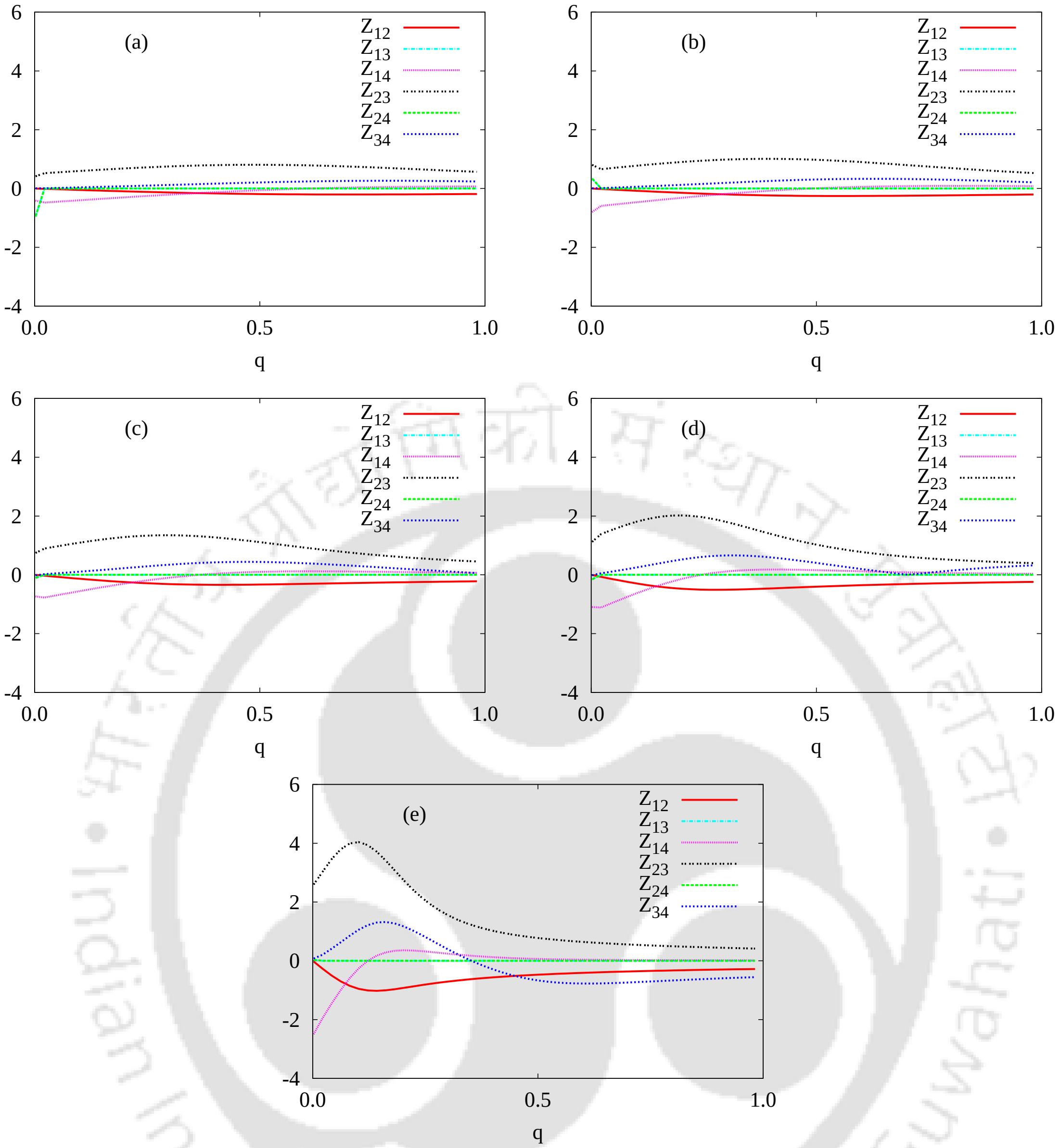

Figure 5.9: Curls of the non-adiabatic coupling elements calculated by using the equation, $Z_{ij} = \frac{\partial}{\partial \phi}\tau_{ij}^{q} - \frac{\partial}{\partial q}\tau_{ij}^{\phi}$ as a function of q where $k = 0.2$ and (a) $E_{el} = 0.05$, (b) $E_{el} = 0.04$, (c) $E_{el} = 0.03$, (d) $E_{el} = 0.02$, and (e) $E_{el} = 0.01$.

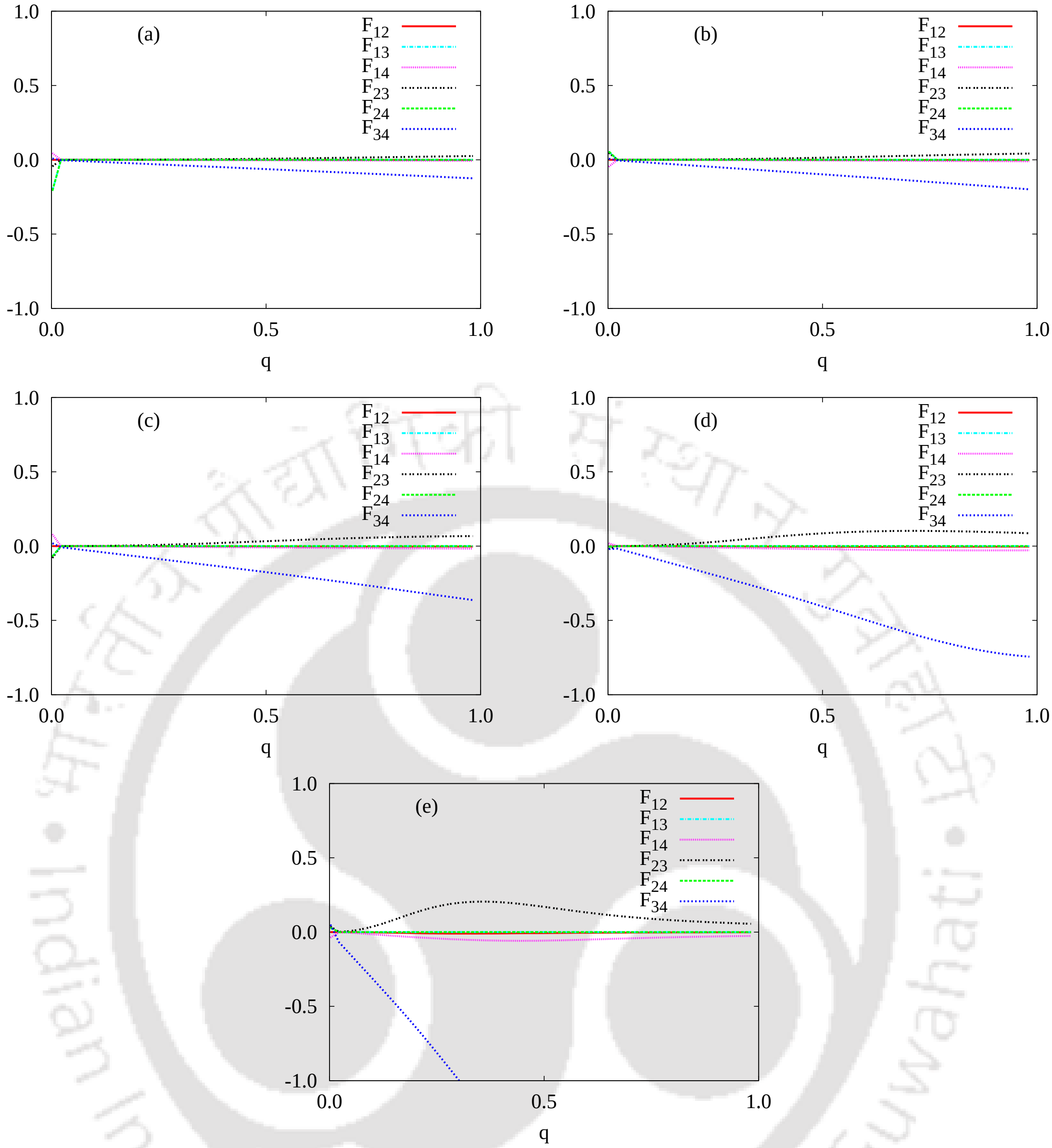

Figure 5.10: Off diagonal elements of the Matrix F ($F = C - Z$) as a function of q where $k = 0.2$ and (a) $E_{el} = 0.05$, (b) $E_{el} = 0.04$, (c) $E_{el} = 0.03$, (d) $E_{el} = 0.02$, and (e) $E_{el} = 0.01$.

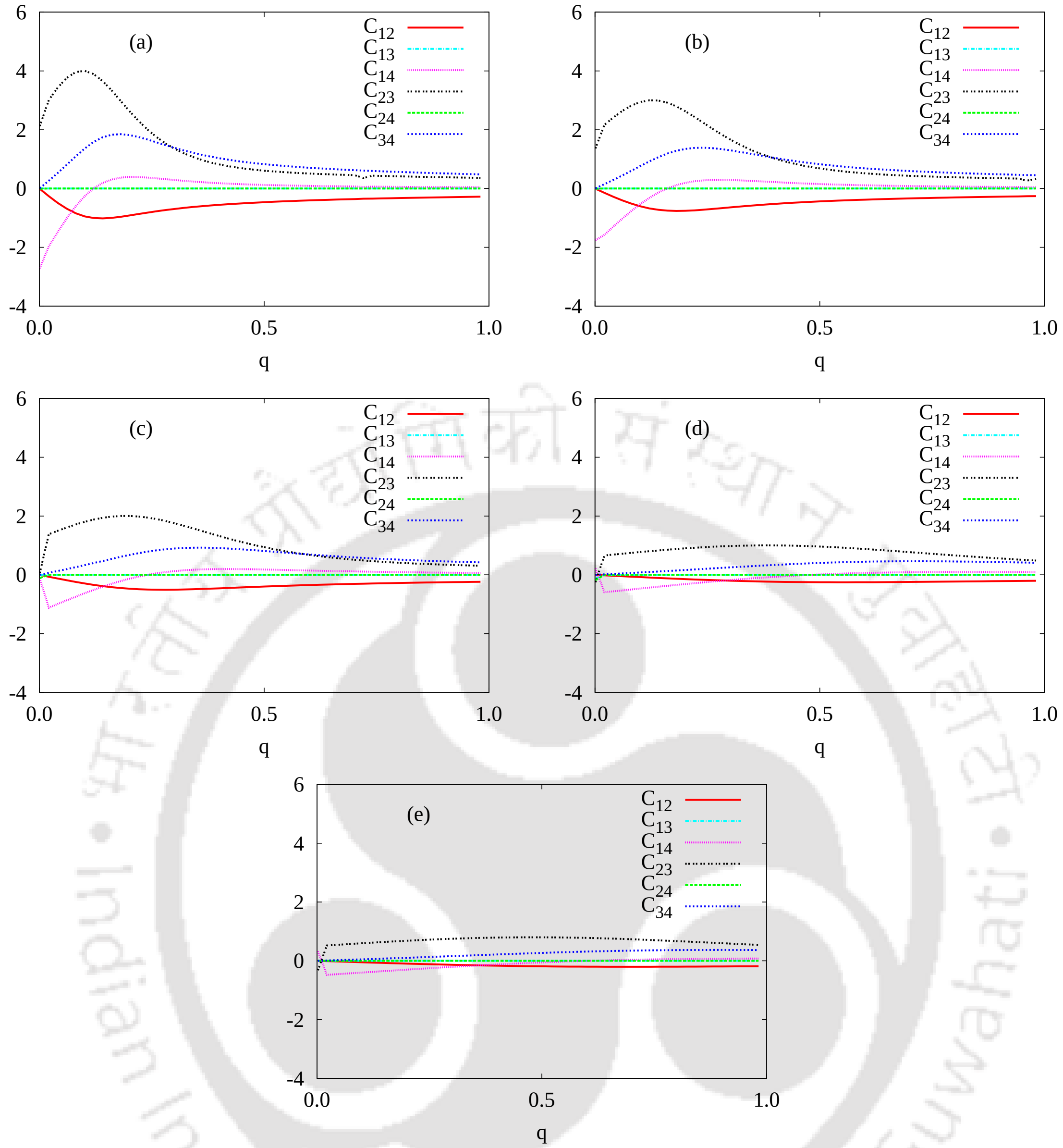

Figure 5.11: Curls of the non-adiabatic coupling elements calculated by using the equation, $C_{ij} = (\boldsymbol{\tau}^{\phi}\boldsymbol{\tau}^{q})_{ij} - (\boldsymbol{\tau}^{q}\boldsymbol{\tau}^{\phi})_{ij}$ as a function of q where $E_{el} = 0.01$ and (a) $k = 0.20$, (b) $k = 0.15$, (c) $k = 0.10$, (d) $k = 0.05$, and (e) $k = 0.04$.

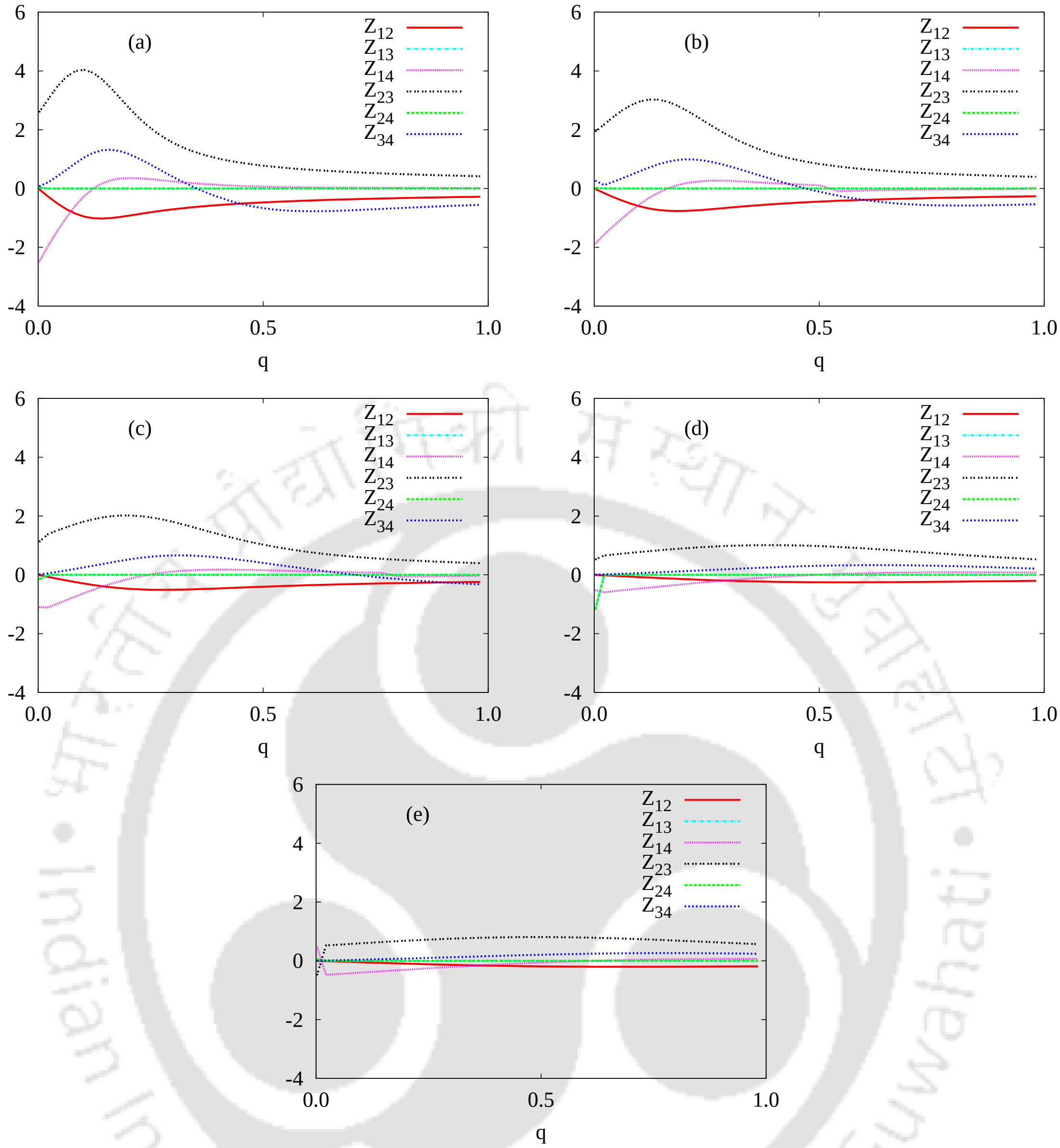

Figure 5.12: Curls of the non-adiabatic coupling elements calculated by using the equation, $Z_{ij} = \frac{\partial}{\partial \phi}\tau_{ij}^{q} - \frac{\partial}{\partial q}\tau_{ij}^{\phi}$ as a function of q where $E_{el} = 0.01$ and (a) $k = 0.20$, (b) $k = 0.15$, (c) $k = 0.10$, (d) $k = 0.05$, and (e) $k = 0.04$.

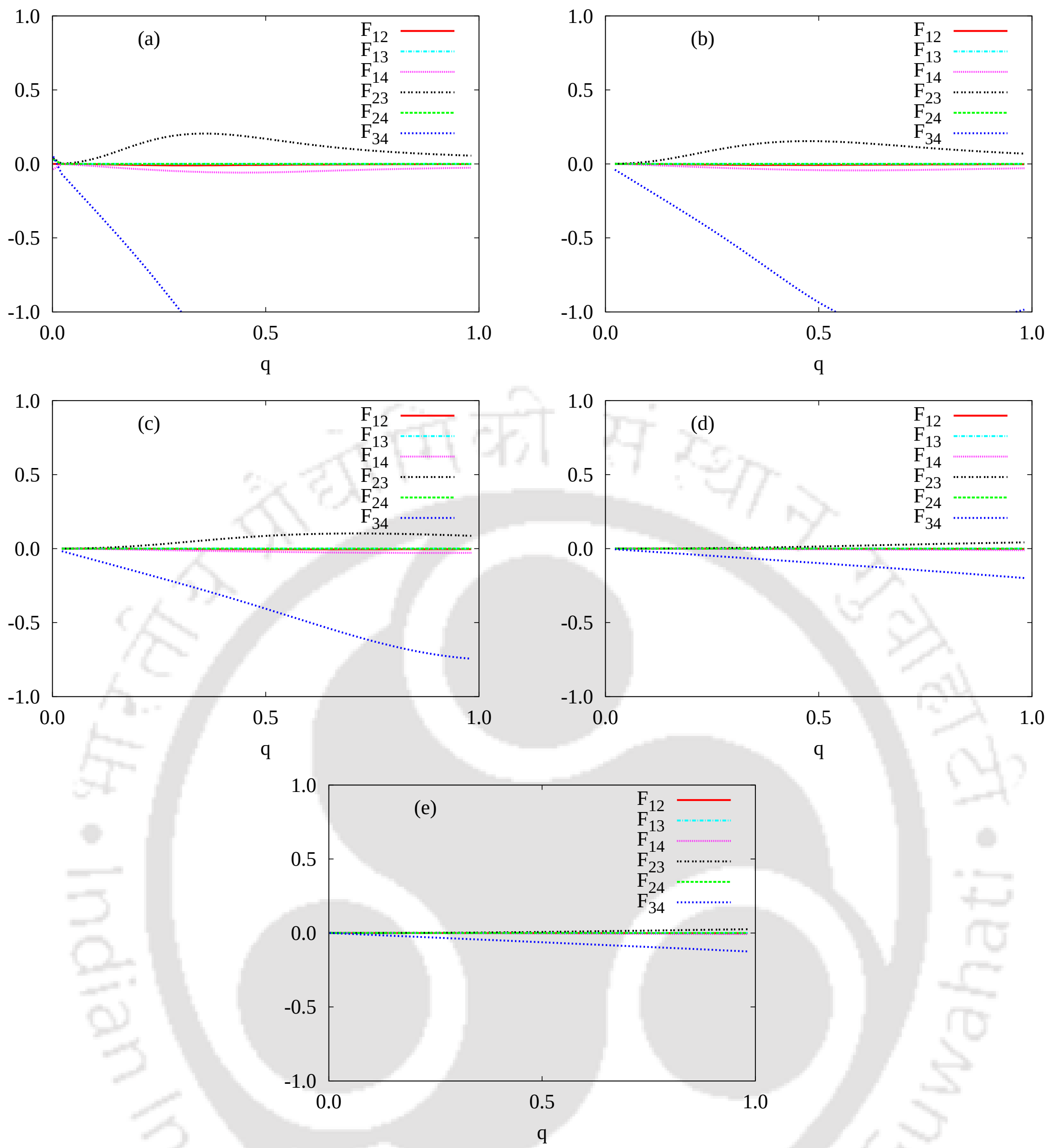

Figure 5.13: Off diagonal elements of the Matrix F ($F = C - Z$) as a function of q where $E_{el} = 0.01$ and (a) $k = 0.20$, (b) $k = 0.15$, (c) $k = 0.10$, (d) $k = 0.05$, and (e) $k = 0.04$.

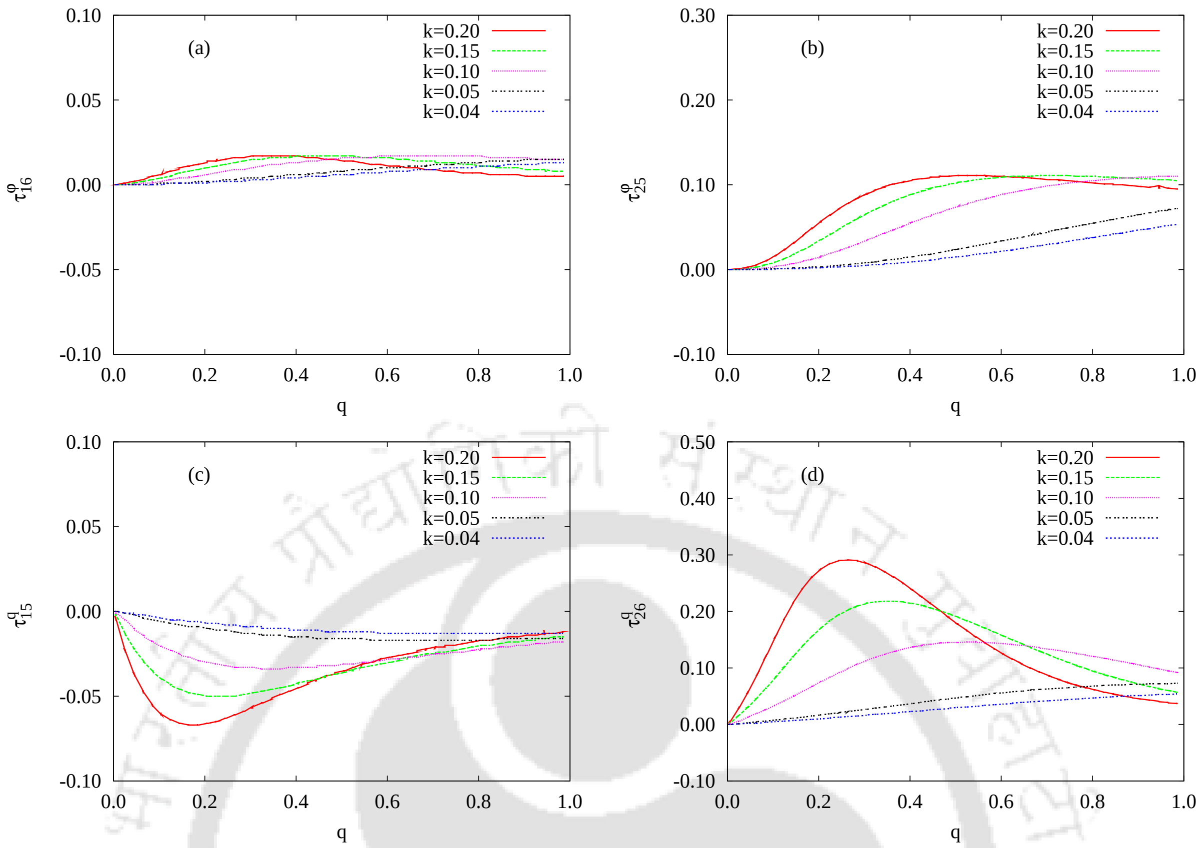

Figure 5.14: The ϕ and q components of nonadiabatic coupling elements in the complimentary space: (a) τ^{ϕ}_{16} , (b) τ^{ϕ}_{25}, (c) τ^{q}_{15}, (d) τ^{q}_{26} as a function of q with different k where $E_{el} = 0.01$.

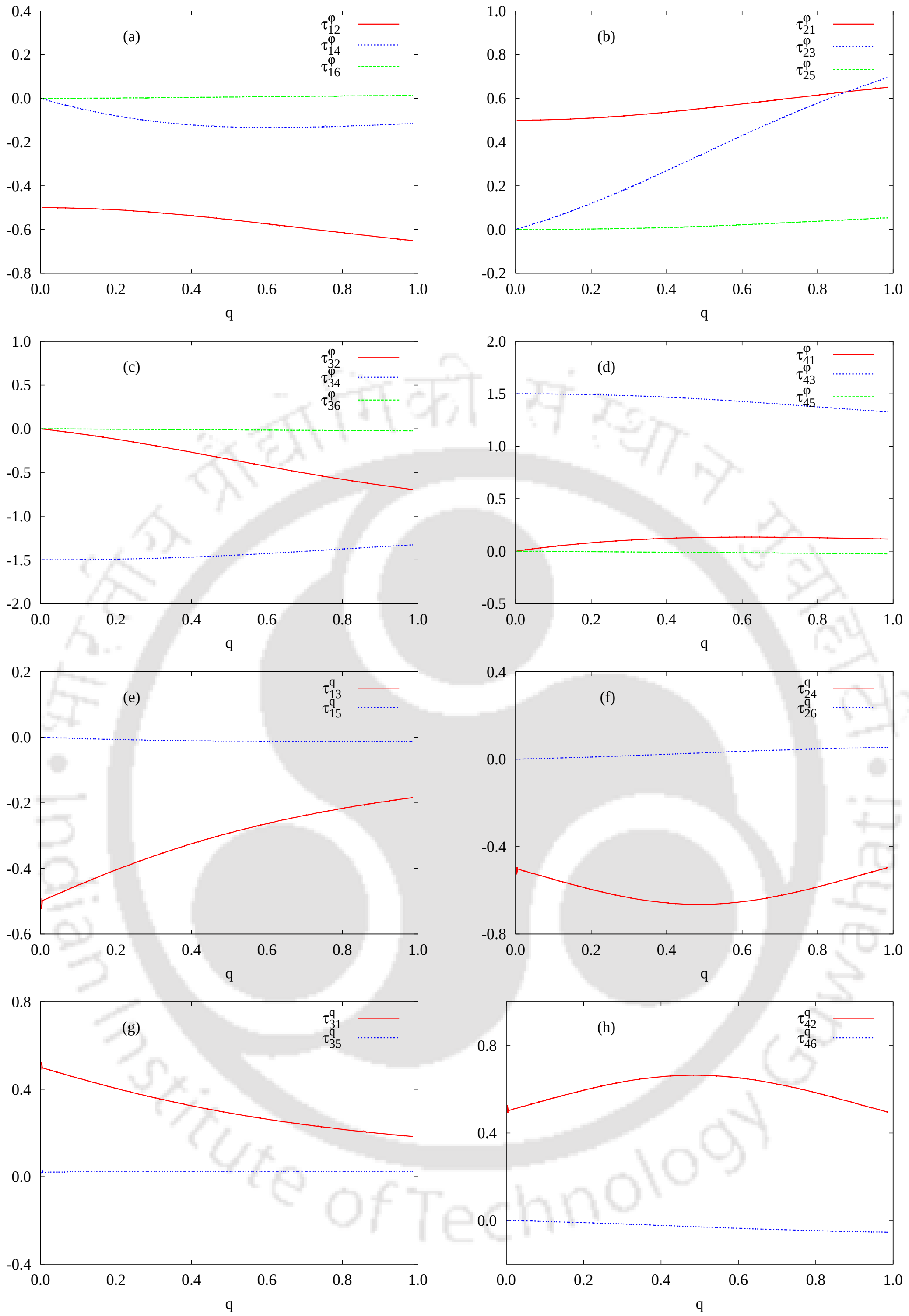

Figure 5.15: The ϕ and q components of nonadiabatic coupling elements of the four - state sub - space are compared with the corresponding components of the complimentary space elements: (a) τ^{ϕ}_{12}, τ^{ϕ}_{14} and τ^{ϕ}_{16}; (b) τ^{ϕ}_{21}, τ^{ϕ}_{23} and τ^{ϕ}_{25}; (c) τ^{ϕ}_{32}, τ^{ϕ}_{34} and τ^{ϕ}_{36}; (d) τ^{ϕ}_{41}, τ^{ϕ}_{43} and τ^{ϕ}_{45}; (e) τ^{q}_{13}, τ^{q}_{15} ; (f) τ^{q}_{24}, τ^{q}_{26} ; (g) τ^{q}_{31}, τ^{q}_{35} ; (h) τ^{q}_{42}, τ^{q}_{46} , as a function of q where $k = 0.04$ and $E_{el} = 0.01$.

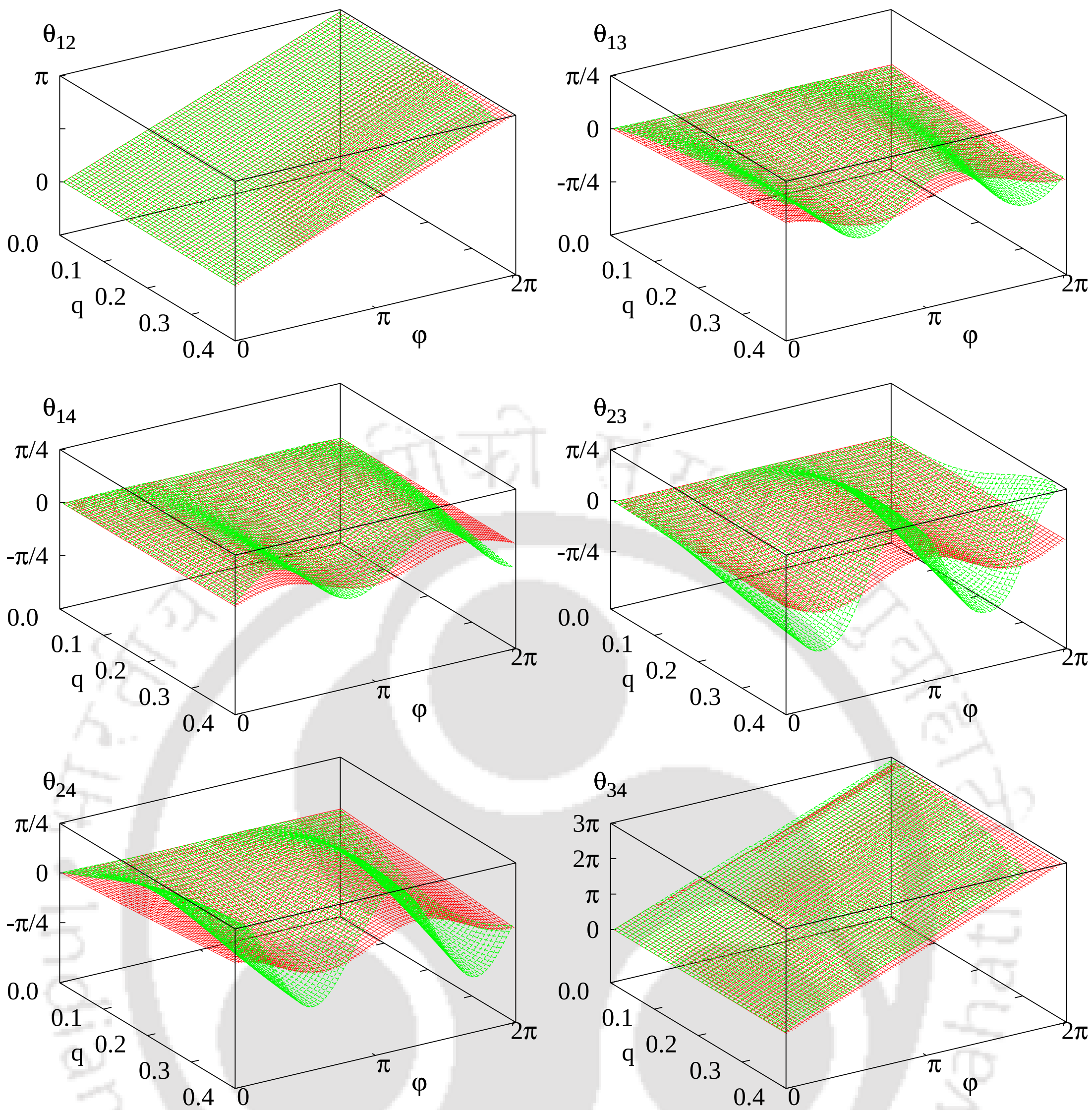

Figure 5.16: The adiabatic-to-diabatic transformation angles as a function of q and ϕ where $E_{el} = 0.01$, $k = 0.2$ (green) and $E_{el} = 0.01$, $k = 0.04$ (red), respectively.

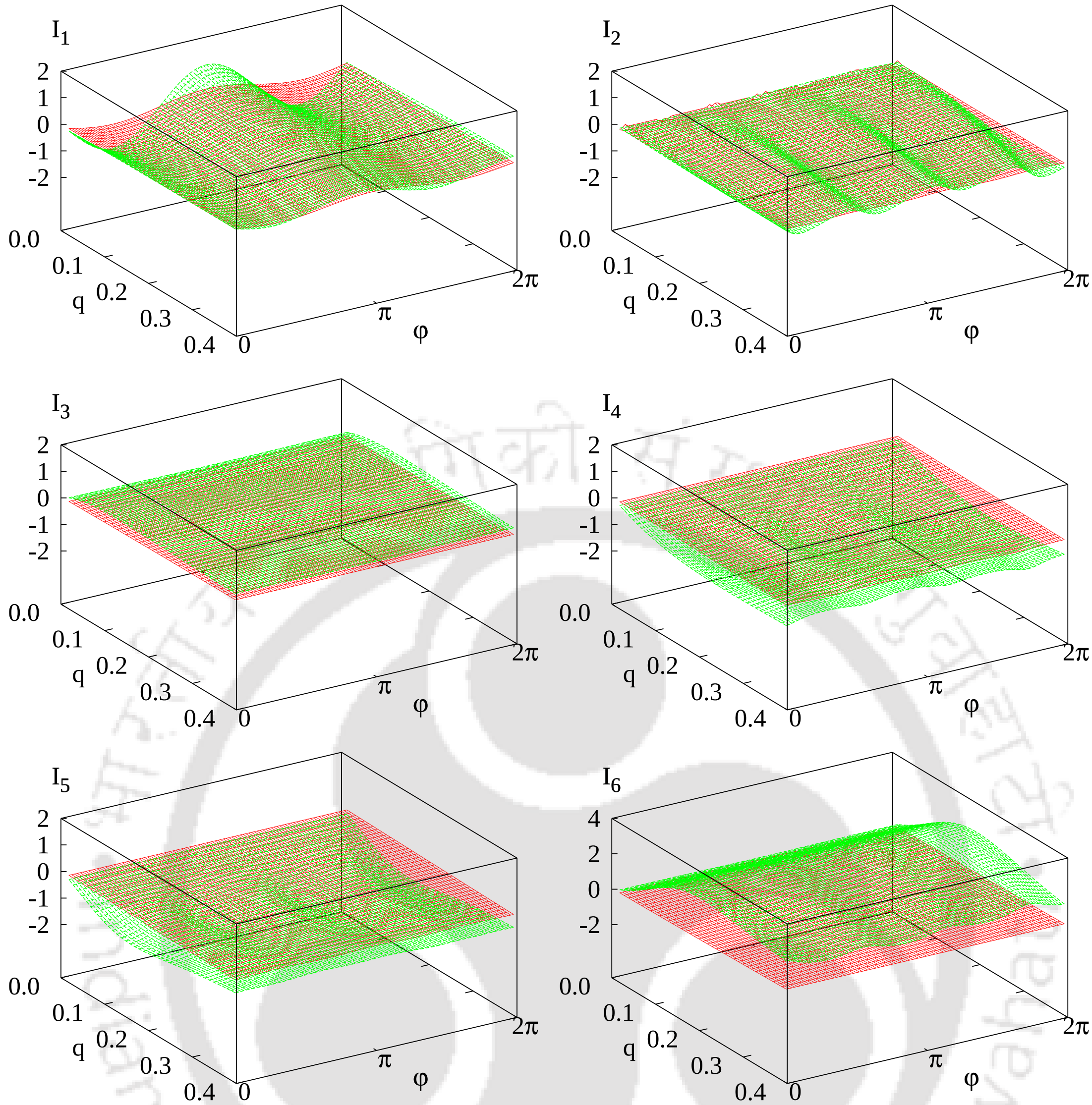

Figure 5.17: The identities (the differences of the product of the cross derivatives with respect to q and ϕ) for each pair of ADT angles as a function of q and ϕ where $E_{el} = 0.01$, $k = 0.2$ (green) and $E_{el} = 0.01$, $k = 0.04$ (red), respectively. Here $I_1 = (\nabla_q\theta_{12}\nabla_\phi\theta_{14} - \nabla_\phi\theta_{12}\nabla_q\theta_{14})$, $I_2 = (\nabla_q\theta_{12}\nabla_\phi\theta_{34} - \nabla_\phi\theta_{12}\nabla_q\theta_{34})$, $I_3 = (\nabla_q\theta_{13}\nabla_\phi\theta_{14} - \nabla_\phi\theta_{13}\nabla_q\theta_{14})$, $I_4 = (\nabla_q\theta_{13}\nabla_\phi\theta_{23} - \nabla_\phi\theta_{13}\nabla_q\theta_{23})$, $I_5 = (\nabla_q\theta_{14}\nabla_\phi\theta_{24} - \nabla_\phi\theta_{14}\nabla_q\theta_{24})$, $I_6 = (\nabla_q\theta_{23}\nabla_\phi\theta_{24} - \nabla_\phi\theta_{23}\nabla_q\theta_{24})$.

References

[1] B. Sarkar and S. Adhikari, J. Phys. Chem. A , DOI 10.1021/jp8029709 (2008).

[2] M. Baer, A. Yahalom and R. Englman, J. Chem. Phys. **109**, 6550 (1998).

[3] M. Bear, *Beyond Born-Oppenheimer:Conical Intersections and Electronic nonadiabatic Coupling Terms*, Wiley Interscience, Hoboken, N.J., USA, 2006.

[4] R. Englman, A. Yahalom and M. Baer, Int. J. Quantum Chem. **90**, 266 (2002).

[5] T. Vertesi et al., J. Phys. Chem. A **107**, 7189 (2003).

[6] M. Baer, T. Vertesi, G. J. Halasz, A. Vivok and S. Suhai, Faraday Discuss. **127**, 337 (2004).

[7] M. Baer, Phys. Rep. **358**, 75 (2002).

[8] N. W. MacLachlan, *Theory and Applcation of Mathieu Functions*, Clarendon, Oxford, 1947.

Chapter 6

The effect of external field on the nonadiabatic coupling elements

6.1 Introduction

We study a molecular system (based on the Mathieu equation)[1-6] interacting with an intense, short-pulsed *electric* field. The strength of the field is measured by the number (L) of electronic states that become populated during this process. Introducing space-time contours we discuss a rigorous way to form N coupled Schroedinger equations where $N < L$, which maintains the effects due to the remaining $(L - N)$ populated states. It is shown that whereas the size of L is unlimited, the main requirement concerning N is that the original group of N field-free states forms a Hilbert subspace in the spacial region of interest.

6.2 The Schrödinger Equation

We showed that a numerical study of an interaction between a molecular system and an intense electromagnetic field is based on three ingredients: (1) the electronic field-dressed Hamiltonian, (2) the field-free manifold, and (3) the matrix $\boldsymbol{\omega}(s,t)$, which is responsible for the transformation from the field-free to the field-dressed frameworks.[7]

6.2.1 The field-dressed Hamiltonian

We start with the total wave function $\tilde{\mathbf{\Psi}}(s_e|s,t)$ (s_e stands for the collection of electronic coordinates), which describes the spatial distribution of the nuclei and the electrons and is assumed to be the solution of the following TD-SE:

$$i\hbar\frac{\partial\tilde{\mathbf{\Psi}}}{\partial t} = \left(-\frac{\hbar^2}{2\mu}\nabla^2 + \mathbf{H}_e\right)\tilde{\mathbf{\Psi}} \tag{6.1}$$

Here, ∇ is the grad operator for the (mass-scaled) nuclear coordinates, μ is the characteristic nuclear mass of the system, and $\mathbf{H}_e$ is the electronic Hamiltonian which for time $t \leq 0$ is time independent (TID), namely, $\mathbf{H}_e = \mathbf{H}_e(s_e|s)$, but for $t \geq 0$ becomes TD so that $\mathbf{H}_e = \mathbf{H}_e(s_e|s,t)$.

Following the BO approach, the $\tilde{\mathbf{\Psi}}$ wavefunction is expanded in terms of a dressed electronic basis set,

$$\tilde{\mathbf{\Psi}}(s_e|s,t) = \xi^T(s_e|s,t)\tilde{\psi}(s,t), \tag{6.2}$$

where $\xi(s_e|s,t)$ is a column vector (so that $\xi^T(s_e|s,t)$ is the corresponding row vector) that contains the dressed basis functions. In what follows we assume these functions to be a solution of the following TD eigenfunction problem:

$$i\hbar\frac{\partial|\xi_j(s_e|s,t)|}{\partial t} = \mathbf{H}_e(s_e|s,t)\xi_j(s_e|s,t), \qquad j = \{1, N\}, \tag{6.3}$$

where N is the number of functions needed to achieve converged results.

In what follows $\mathbf{H}_e(s_e|s,t)$ is assumed to contain the interaction potential formed by the field

$$\mathbf{H}_e(s_e|s,t) = \mathbf{H}_{e0}(s_e|s) + U_E(s_e|s,t) \tag{6.4}$$

Here, $\mathbf{H}_{e0}(s_e|s)(= \mathbf{H}_e(s_e|s))$ is the unperturbed field-free Hamiltonian and $U_E(s_e|s,t)$ is the interaction formed by the field.

To continue we introduce the electromagnetic field and assume it to interact only with the electrons (in other words, we ignore the interaction of the field with nuclei). For simplicity we consider only the electric component $\mathbf{E}(s_e|s,t)$, and since its interaction with the nuclei is ignored, we have **E**=$\mathbf{E}(s_e|t)$. Assuming that the electric interaction is formed by one single electron, its potential is given by the following line integral in the electronic space:[7–9]

$$U_E(s_e|t) = -\frac{e}{\hbar}\int_{\Gamma_e} \mathbf{ds}'_e \cdot \mathbf{E}(s_e|t), \tag{6.5}$$

where e is the electronic charge and Γ_e is the corresponding electronic contour.

6.2.2 The field-free and the field-dressed framework

we present first the theory related to the field-free framework and then extend it to include the field-dressed framework.

6.2.2.1 *The field-free NAC terms and the corresponding diabatic potentials*

In this section we briefly review the theory related to the field-free NAC terms and the corresponding diabatic potential matrices. We start with the BO NAC terms, $\boldsymbol{\tau}_{ji}(s)$, defined as

$$\boldsymbol{\tau}_{ji}(s) = \langle \xi_{0j}|\nabla\xi_{0i}\rangle, \qquad i,j = \{1,L\} \tag{6.6}$$

where $\xi_{k0}(s_e|s), k(=j,i)$, are the adiabatic BO eigenfunctions and ∇ is the grad operator defined with respect to the mass scaled nuclear coordinates s.

Assuming that the L eigenfunctions in Eq. (6.6) form a Hilbert subspace, the nuclear BO-SE can be shown to be of the form

$$-\frac{\hbar^2}{2\mu}(\nabla+\boldsymbol{\tau})^2\boldsymbol{\Psi} + (\mathbf{u}+E)\boldsymbol{\Psi} = 0 \tag{6.7}$$

where $\boldsymbol{\tau}(s)$ is an antisymmetric matrix which contains the NAC terms [and is sometimes also mentioned as the nonadiabatic coupling matrix (NACM)] defined in Eq. (6.6), **u**[=**u**(s)] is a diagonal matrix that contains the nuclear (BO) adiabatic potential energy surfaces, $\mathbf{\Psi}$ is a column vector that contains the nuclear wave functions to be solved, E is the energy, and μ is the mass of the system.

The next subject is related to the ADT. As mentioned earlier, the aim of the diabatization is to eliminate the unpleasant singular NAC elements from Eq. (6.7) (and replace the spiky adiabatic potentials by smoother potentials), and for this purpose we perform the following transformation:

$$\mathbf{\Psi} = \mathbf{A}\mathbf{\Psi} \tag{6.8}$$

Substituting Eq. (6.8) in Eq. (6.7), performing the usual algebra, and demanding the elimination of the $\boldsymbol{\tau}$ matrix yields the following first order differential equation for the ADT matrix $\mathbf{A}$:

$$\nabla\mathbf{A} + \boldsymbol{\tau}\mathbf{A} = 0 \tag{6.9}$$

Equation (6.9) has to be solved along contours in configuration space. The solution of Eq. (6.9) is given in the form of an exponentiated line integral,

$$\mathbf{A}(s|\Gamma_s) = \wp \exp\left\{-\int_0^s \boldsymbol{\tau}(s'|\Gamma_s)\cdot ds'\right\}, \tag{6.10}$$

where Γ_s is a contour, $\wp$ is a path ordering operator which reminds us that the exponentiated line integral has to be performed in a given order, and the dot stands for the scalar product.

6.2.2.2 *The field-dressed NAC elements and the corresponding diabatic potentials*

Employing Eqs. (6.1) − (6.3), it was shown that the SE for the field-dressed nuclear functions $\tilde{\mathbf{\Psi}}(s)$ is[10]

$$i\hbar\frac{\partial\tilde{\mathbf{\Psi}}}{\partial t} = -\frac{\hbar^2}{2\mu}\left(\nabla + \tilde{\boldsymbol{\tau}}\right)^2\tilde{\mathbf{\Psi}} \tag{6.11}$$

where $\tilde{\boldsymbol{\tau}}$ is the field-dressed NACM given in the form

$$\tilde{\boldsymbol{\tau}} = \boldsymbol{\omega}^\dagger\boldsymbol{\tau}\boldsymbol{\omega} + \boldsymbol{\omega}^\dagger\nabla\boldsymbol{\omega} \tag{6.12}$$

Here, $\boldsymbol{\omega}(s,t)$ is the matrix responsible for the transformation from the field-free manifold to the field-dressed manifold. Our next step is to express the adiabatic nuclear functions in terms of the corresponding diabatic functions [as is done in the field-free case, see Eq. (6.8)], and for this purpose we employ the relevant field-dressed ADT matrix $\tilde{\mathbf{A}}(s,t)$. This transformation yields the following diabatic field-dressed SE:

$$i\hbar\frac{\partial\tilde{\boldsymbol{\Phi}}}{\partial t} = \left(-\frac{\hbar^2}{2\mu}\nabla^2 + \tilde{\mathbf{W}}\right)\tilde{\boldsymbol{\Phi}} \tag{6.13}$$

where $\tilde{\mathbf{W}}$ is the corresponding field-dressed diabatic potential matrix

$$\tilde{\mathbf{W}} = \tilde{\mathbf{A}}^{\dagger}\tilde{\tilde{\mathbf{H}}}\tilde{\mathbf{A}} \tag{6.14}$$

Here, $\tilde{\tilde{\mathbf{H}}}(\mathbf{s},\mathbf{t})$ is the relevant (quasiadiabatic) potential matrix and $\tilde{\mathbf{A}}(s,t)$ is the field-dressed ADT matrix.

The quasiadiabatic potential matrix, $\tilde{\tilde{\mathbf{H}}}(\mathbf{s},\mathbf{t})$ is given in the form

$$\tilde{\tilde{\mathbf{H}}} = \boldsymbol{\omega}^{\dagger}\tilde{\mathbf{H}}\boldsymbol{\omega} \tag{6.15}$$

where $\boldsymbol{\omega}(s,t)$ was mentioned earlier and $\tilde{\mathbf{H}}(s,t)$ is the matrix representation of the field-dressed Hamiltonian in Eq. (6.4), namely,

$$\tilde{\mathbf{H}}_{mk}(s,t) = \langle\xi_{0m}(s_e|s)|\mathbf{H}_e(s_e|s,t)|\xi_{0k}(s_e|s)\rangle. \tag{6.16}$$

The field-dressed potential matrix $\tilde{\mathbf{W}}(s,t)$, in Eq. (6.14), plays the same role as the field-free potential matrix $\mathbf{W}$(s). Since the field is turned on only at $t > 0$, the two matrices are identical for $t \le 0$ [the matrix $\boldsymbol{\omega}(s,t \le 0)$ is the unit matrix and the matrix $\tilde{\tilde{\mathbf{H}}}(\mathbf{s},\mathbf{t} \le \mathbf{0})$ is identical to $\mathbf{u}(s)$ so that due to Eqs. (6.4), (6.15), and (6.16) we also get that $\tilde{\tilde{\mathbf{H}}}(s,t \le 0) \equiv \mathbf{u}(s)$]. However for $t > 0$, $\boldsymbol{\omega}(s,t)$ is no longer a unit matrix, $\tilde{\mathbf{H}}(s,t)$ is no longer diagonal, and consequently $\tilde{\tilde{\mathbf{H}}}(\mathbf{s},\mathbf{t})$ differs from $\mathbf{u}(s)$ which causes $\tilde{\mathbf{W}}(s,t)$ to differ from $\mathbf{W}(s)$.

The field-dressed ADT matrix, $\tilde{\mathbf{A}}(s,t)$ is just like in the field-free case the field-dressed ADT matrix satisfies first order differential equations which, in the present case, are of the form

$$\nabla \tilde{\mathbf{A}} + \tilde{\boldsymbol{\tau}} \tilde{\mathbf{A}} = 0, \tag{6.17a}$$

$$i\hbar \frac{\partial \tilde{\mathbf{A}}}{\partial t} + \tilde{\tilde{\mathbf{H}}} \tilde{\mathbf{A}} = 0, \tag{6.17b}$$

where $\tilde{\boldsymbol{\tau}}$ and $\tilde{\tilde{\mathbf{H}}}$ were introduced earlier [see Eqs. (6.12) and (6.15) respectively]. Equation (6.17a) is defined with respect to the spatial coordinates and Eq. (6.17b) is defined with respect to the temporal coordinate. Equations (6.17) have to be solved along space-time contours Γ_{st}. Their solution can be written, schematically, as an exponentiated space-time line integral

$$\tilde{\mathbf{A}}(z|\Gamma_{st}) = \wp \exp \left\{ - \int_{z_0}^{z} \tilde{\tilde{\boldsymbol{\tau}}}(z'|\Gamma_{st}) \cdot dz' \right\}, \tag{6.18}$$

where $\wp$, as before, is an ordering operator, z is a space-time coordinate defined either as $z = s$ or as $z = (-i/\hbar)t$ (as the case may be), the dot stands for the corresponding scalar product, and $\tilde{\tilde{\boldsymbol{\tau}}}$ is the (extended) space-time NACM defined as

$$\tilde{\tilde{\boldsymbol{\tau}}} = (\tilde{\boldsymbol{\tau}}, \tilde{\tilde{\mathbf{H}}}). \tag{6.19}$$

A more explicit form for Eq. (6.18) is

$$\tilde{\mathbf{A}}(s, t|\Gamma_{st}) = \wp \prod_{n=1}^{M} \exp \left\{ - \int_{s_{n-1}}^{s_n} \tilde{\boldsymbol{\tau}}(s, t_n) \cdot ds \right\} \times \exp \left\{ \frac{i}{\hbar} \int_{t_{n-1}}^{t_n} \tilde{\tilde{\mathbf{H}}}(s_{n-1}, t) \cdot dt \right\}, \tag{6.20}$$

where M is the number of (s, t) segments along the space-time contour Γ_{st}. Equation (6.20) is used to calculate $\tilde{\mathbf{A}}(s, t)$ along a given space-time contour.

6.2.3 The transformation matrix, $\boldsymbol{\omega}(s,t)$

In order to solve Eq. (6.1) we expand each of the functions, $\xi_j(s_e|s,t); j=\{1,N\}$ in terms of the TID basis set functions $\xi_{0k}(s_e|s)(\equiv \xi_k(s_e|s,t=0)), k=\{1,L\}$,

$$|\xi_j(s_e|s,t)\rangle = \sum_{k=1}^{L} |\xi_{0k}(s_e|s)\rangle \boldsymbol{\omega}_{kj}(s,t), \qquad j=\{1,N\}, \tag{6.21}$$

where $\boldsymbol{\omega}(s,t)$ is an $N\times L$ rectangular matrix which contains the expansion coefficients. Usually, one expects a matrix of the type $\boldsymbol{\omega}(s,t)$ to be a square matrix. However, we intend to show that $\boldsymbol{\omega}(s,t)$ can also be assumed to be a rectangular matrix and that this feature has certain advantages.

Substituting Eq. (6.21) in Eq. (6.1) and recalling Eq. (6.3) yield the following set of equations for the $\boldsymbol{\omega}$ elements,

$$i\hbar \frac{\partial \boldsymbol{\omega}_{mj}(s,t)}{\partial t} = \sum_{k=1}^{L} \tilde{\mathbf{H}}_{mk}(s,t)\boldsymbol{\omega}_{kj}(s,t), \qquad m=\{1,L\}, \qquad j=\{1,N\}, \tag{6.22}$$

where $\tilde{\mathbf{H}}_{mk}(s,t)$ is given by

$$\tilde{\mathbf{H}}_{mk}(s,t) = \mathbf{U}_{mk}(s,t) + \mathbf{u}_k(s)\delta_{mk} \tag{6.23}$$

In this expression the elements of the (square $L\times L$) matrix $\mathbf{U}(s,t)$ are due to the perturbation $\mathbf{U}_E(s_e|s,t)$ [see Eq. (6.5)]. Thus,

$$\mathbf{U}_{mk}(s,t) = \langle \xi_{0m}(s_e|s)|\mathbf{U}_E(s_e|s,t)|\xi_{0k}(s_e|s)\rangle. \tag{6.24}$$

For the purpose of further studies we rewrite Eq. (6.22) in a matrix form,

$$i\hbar \frac{\partial \boldsymbol{\omega}(s,t)}{\partial t} = \tilde{\mathbf{H}}(s,t)\boldsymbol{\omega}(s,t). \tag{6.25}$$

Besides being ordinary expansion coefficients, the $\boldsymbol{\omega}$ - elements along the various columns are associated with the transition probabilities for the excitation process caused by the field at a given time and for a given nuclear configuration. Thus, if to solve the elements of the jth column we apply the initial conditions $(0, 0, \ldots, 1, 0, \ldots, 0)$ (which is a vector of zeros with 1 located at the jth position), then, consequently, the magnitude $P_{kj}(s,t) = \boldsymbol{\omega}_{kj}(s,t)|^2$ is the probability (Copenhagen interpretation) to find the molecule at time t in the kth (electronic) state when at time $t = 0$ it was in the jth state. With this interpretation it is well understood that in this process only a limited number of states get populated.

6.3 The Hilbert Subspace

6.3.1 The field-free Hilbert subspace

We consider a group of N states (out of an infinite Hilbert space), and for the sake of convenience we assume them to be the N lowest states a limitation that can be easily removed.

The breakup of the Hilbert space is based on the features that characterize the above-mentioned N states and are related to the NAC elements, namely,

$$|\boldsymbol{\tau}_{jk}| \cong O(\epsilon) \quad \text{for} \quad j \leq N, \quad k > N. \tag{6.26}$$

Here, ϵ is a relatively small number. In other words, the NAC elements between states that belong to the group and those outside the group are all assumed to be negligibly small. This implies that the $\boldsymbol{\tau}$ matrix has the following form:

$$\boldsymbol{\tau} = \begin{pmatrix} 0 & \tau_{12} & \tau_{13} & \dots & \tau_{1N} & & & & & \\ -\tau_{12} & 0 & \tau_{23} & \dots & \tau_{2N} & & & & & \\ -\tau_{13} & -\tau_{23} & 0 & \dots & \tau_{3N} & & & O(\epsilon) & & \\ \dots & \dots & \dots & 0 & \dots & & & & & \\ -\tau_{1N} & -\tau_{2N} & -\tau_{3N} & \dots & 0 & & & & & \\ & & & & & 0 & \tau_{N+1N+2} & \tau_{N+1N+3} & \dots & \dots \\ & & & & & -\tau_{N+1N+2} & 0 & \tau_{N+2N+3} & \dots & \dots \\ & & O(\epsilon) & & & -\tau_{N+1N+3} & -\tau_{N+2N+3} & 0 & \dots & \dots \\ & & & & & \dots & \dots & \dots & 0 & \dots \\ & & & & & \dots & \dots & \dots & \dots & 0 \end{pmatrix} \quad (6.27)$$

If this breakup takes place at every point in a given region, we define the N states as a Hilbert subspace in this region. The main difficulty with this definition is that no absolute sensible measure is given for the allowed magnitudes of the various ε's. All we can say is that "ε is a relatively small number," but this statement has no meaning in practical applications. Nevertheless, the situation described by Eq. (6.26) is the basic assumption of the theory in the presented perspective.

In numerical applications the decision whether a group of states forms a Hilbert subspace is not deducted from Eq. (6.26) but is determined by a much more sensitive mathematical tool, namely, the topological matrix **D**.

The **D** matrix is closely related to the ADT matrix **A** introduced in previous section and presented in Eq. (6.10) as an exponentiated line integral. Whereas the **A** matrix is defined for an open contour, the **D** matrix, which is similar to the **A** matrix, is defined for a closed contour Γ_s, namely,

$$\mathbf{D}(\Gamma_s) = \wp \exp\left\{ -\oint_{\Gamma_s} ds \cdot \boldsymbol{\tau}(s|\Gamma_s) \right\}. \quad (6.28)$$

The important feature that characterizes the matrix $\mathbf{D}(\Gamma_s)$ is that it becomes *diagonal* whenever the group of N states forms a Hilbert subspace as defined above. Since the **D** matrix is a unitary matrix, it contains (in case of real eigenfunctions) along its diagonal ± 1. The number of the (-1)s and their location along the diagonal reveal information regarding the number of CI points (i.e., degeneracy points) and their positions in a given region. Moreover, calculating the **D** matrix along different contours in the region of interest, one can unambiguously determine the number of CI points in that region[11].

6.3.2 The field-dressed Hilbert subspace

When discussing a field-dressed system, we may face the question whether the numerical tools to study the topological effects related to a field-free molecular system can be extended to treat field-dressed systems. We discussed first the spatial components of field-dressed NACM [see Eq. (6.12)] and then extended this issue to include the temporal component [see Eq. (6.19). Having the full space-time NACM available, we formed the corresponding first order space-time differential equations [see Eq. (6.17)] which are to be solved to yield the field-dressed ADT matrix [see Eq. (6.20)] as well as the corresponding topological matrix $\mathbf{D}(\Gamma_s)$ which is solved in a similar way, but for a closed contour.

The aim of the forthcoming analysis is to show that the various features of the field-free **D** matrix are maintained in case of the field-dressed system as well. In order to show that, we proceed in two steps: (1) First, we consider a simplified situation, namely, a region made up of two coordinates a spatial coordinate R and a temporal coordinate t [see Fig. 6.1a], and prove that this $(R-t)$ region cannot contain any singularities. (2) This fact is then used to show that adding the t coordinate to a spatial region [see Fig. 6.1b] does not affect the features of the spatial **D** matrix.

We start by considering a given $R-t$ region, Λ_{Rt}, and introduce the following closed contour, Rt:

$$\Gamma_{Rt} \equiv (R_0, t_0) \rightarrow (R_0 + \Delta R, t_0) \rightarrow (R_0 + \Delta R, t_0 + \Delta t) \rightarrow (R_0, t_0 + \Delta t) \rightarrow (R_0, t_0). \quad (6.29)$$

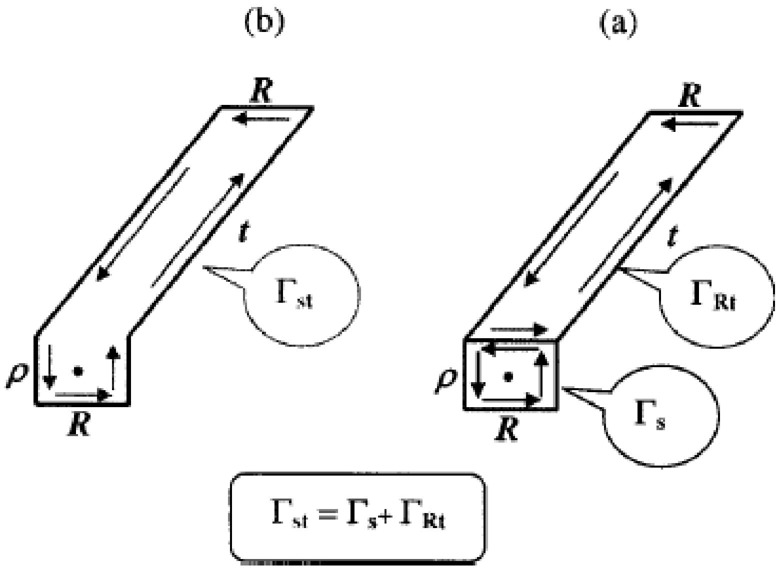

Figure 6.1: Space-time region. (a) The closed Γ_{st} presented as a sum of two closed contours: $\Gamma_{st} = \Gamma_s + \Gamma_{Rt}$, where both Γ_s and Γ_{st} are closed contours. The first is a "pure" spatial closed contour (that forms a spacial region), and the second is a space-time contour (that forms space-time region). (b) The closed space-time contour Γ_{st} (follow the arrow) made up of two space coordinates R and ρ and one time coordinate t. The dot stands for a degeneracy point (or point of conical intersection) located in the spatial region (no degeneracy point can be found in the space-time region).

The relevant expression for the integration along a closed contour is given by,

$$\Delta\tilde{\mathbf{A}} = \oint_{\Gamma_{Rt}} dz' \cdot \tilde{\tilde{\boldsymbol{\tau}}}(z')\tilde{\mathbf{A}}(z'). \qquad (6.30)$$

Here, z stands for the two-component vector (R, t) and the dot for the corresponding scalar product. It is known that if both ΔR and Δt are small enough, then the value of $\Delta\tilde{\mathbf{A}}$ is given, approximately, in the form

$$\Delta\tilde{\mathbf{A}}(R,t) = \tilde{\mathbf{A}}(R,t)\mathbf{F}_{Rt}(R,t)\Delta R\Delta t, \qquad (6.31)$$

where $\mathbf{F}_{Rt}$ is the relevant (non-Abelian) curl,

$$\mathbf{F}_{Rt}(R,t) = i\hbar\frac{\partial\tilde{\boldsymbol{\tau}}_R}{\partial t} - \frac{\partial\tilde{\tilde{\mathbf{H}}}}{\partial R} + [\tilde{\tilde{\mathbf{H}}}, \tilde{\boldsymbol{\tau}}_R] \qquad (6.32)$$

[$\tilde{\tilde{\mathbf{H}}}$ is defined in Eq. (6.15)]. It is known that the condition for not having singularities in that region is that any integration in that region, as given in Eq. (6.31), is zero. Consequently, in order for $\Delta\tilde{\mathbf{A}} = 0$ to be fulfilled inside the region defined by Γ_{Rt}, the curl condition $\mathbf{F}_{Rt} = 0$ has to be satisfied at every point in that region. Indeed, $\mathbf{F}_{Rt} = 0$ for any $\tilde{\boldsymbol{\tau}}$ and $\tilde{\tilde{\mathbf{H}}}$ that satisfy Eqs. (6.12) and (6.15), respectively.

It is important to emphasize that the space-time curl condition $\mathbf{F}_{Rt} = 0$ is satisfied for any dimension whether or not the group of states forms a Hilbert subspace or whether or not $N = L$ (namely, whether or not $\boldsymbol{\omega}$ is a square matrix).[8,9] Although the proof is given for an essentially infinitesimal region it can be extended to any finite region.[12]

Corollary: *A space-time region formed by an open spatial contour does not contain singularities.*

Next, we discuss the relevant $\tilde{\mathbf{D}}$ matrix. The $\tilde{\mathbf{A}}$ matrix fulfills an integral equation along a given space-time contour, Γ_{Rt}, which is schematically written as

$$\tilde{\mathbf{A}}(z|z_0, \Gamma_{Rt}) = \tilde{\mathbf{A}}(z_0) - \int_{z_0}^{z} dz' \cdot \tilde{\tilde{\boldsymbol{\tau}}}(z'|\Gamma_{Rt})\tilde{\mathbf{A}}(z|z_0, \Gamma_{Rt}). \tag{6.33}$$

Consequently, the equation for the $\tilde{\mathbf{D}}$ matrix (which is closely related to the corresponding $\tilde{\mathbf{A}}$ matrix calculated at the end point of the closed space-time contour) takes the form

$$\tilde{\mathbf{D}}(\Gamma_{Rt}) = \mathbf{I} - \oint_{\Gamma_{Rt}} dz' \cdot \tilde{\tilde{\boldsymbol{\tau}}}(z'|\Gamma_{Rt})\tilde{\mathbf{A}}(z|z_0, \Gamma_{Rt}), \tag{6.34}$$

where $\mathbf{I}$ is the unit matrix. Since, as discussed above, the line integral itself is identically zero [see Eqs. (6.30) (6.32)], we obtain

$$\tilde{\mathbf{D}}(\Gamma_{Rt}) = \mathbf{I}, \tag{6.35}$$

or, in other words, the $\tilde{\mathbf{D}}$ matrix is the unit matrix.

Next, we consider a closed space-time contour Γ_{st}, as given in Fig. 6.1b. It is seen that this contour can be presented in terms of a closed spatial contour, Γ_s, and a closed space-time contour, Γ_{st} (where its spatial segments do not add up to form a closed spatial contour). Accordingly, this contour can be written as

$$\Gamma_{st} = \Gamma_s + \Gamma_{Rt} \tag{6.36}$$

Next, employing, along Γ_{st}, the relevant integral equation for the $\tilde{\mathbf{D}}$ matrix, we obtain

$$\tilde{\mathbf{D}}(\Gamma_{st}) = \mathbf{I} - \oint_{\Gamma_{st}} dz' \cdot \tilde{\tilde{\boldsymbol{\tau}}}(z'|\Gamma_{st})\tilde{\mathbf{A}}(z|z_0, \Gamma_{st}), \tag{6.37}$$

which, following Eq. (6.36), can be written as

$$\tilde{\mathbf{D}}(\Gamma_{st}) = \mathbf{I} - \oint_{\Gamma_s} dz' \cdot \tilde{\tilde{\boldsymbol{\tau}}}(z'|\Gamma_s)\tilde{\mathbf{A}}(z|z_0, \Gamma_s) - \oint_{\Gamma_{Rt}} dz' \cdot \tilde{\tilde{\boldsymbol{\tau}}}(z'|\Gamma_{Rt})\tilde{\mathbf{A}}(z|z_0, \Gamma_{Rt}). \tag{6.38}$$

However, according to a previous analysis, the third term in Eq (6.38) is identically zero. In addition, it can be seen that the first two terms in Eq. (6.38) form the spatial matrix $\mathbf{D}(\Gamma_s)$.

In other words, we established the fact that the $\tilde{\mathbf{D}}$ matrix for a space-time region formed by a closed space-time contour Γ_{st} is identical to the spatial D matrix formed by the spatial segments that from the closed spatial contour Γ_s, namely,

$$\tilde{\mathbf{D}}(\Gamma_{st}) = \tilde{\mathbf{D}}(\Gamma_s). \tag{6.39}$$

The conclusions due to these findings are summarized in the next corollary.

Corollary. *If a closed space-time region contains singularities they have to be located in the closed spatial region only.*

6.3.3 The square case: $N = L$

From the analysis carried out in the previous sections we see that, just like in the field-free case, the treatment of field- dressed systems requires considering groups of states that form a Hilbert subspace. In the previous section we showed that if a group of N field-free states forms a Hilbert subspace in a given region, the corresponding field-dressed states also form a Hilbert subspace in the corresponding space-time region. This statement applies whether N is equal to L or differs from L. In general, we expect $N < L$ or, in case of intense fields, eventually $N \ll L$. In the present section we discuss the characteristic features of the square case, namely, the case when $N = L$.[4]

The square case is of special interest because Eqs. (6.17) can be solved analytically. We recall that since all the matrices (namely, $\boldsymbol{\tau}$, $\boldsymbol{\omega}$, $\tilde{\mathbf{H}}_e$, $\tilde{\boldsymbol{\tau}}$, $\tilde{\tilde{\mathbf{H}}}_\mathbf{e}$, and $\tilde{\mathbf{A}}$) mentioned in Eqs. (6.17) are of dimension $N \times N$, the unknown matrix $\tilde{\mathbf{A}}$ can be presented as a product of two N-dimensional matrices,

$$\tilde{\mathbf{A}}(s,t) = \boldsymbol{\omega}^\dagger(s,t)\mathbf{B}, \tag{6.40}$$

where $\boldsymbol{\omega}$ is introduced in Eqs. (6.21) and (6.25), but $\mathbf{B}$ is to be determined. Substituting Eq. (6.40) in Eq. (6.17a) and recalling the definition of $\tilde{\boldsymbol{\tau}}$ [see Eq.(6.12)], we get, following a few algebraic operations, that $\mathbf{B}$ is a solution of the first order (field-free) vectorial equation

$$\nabla\mathbf{B} + \boldsymbol{\tau}(s)\mathbf{B} = 0 \tag{6.41}$$

Thus, $\mathbf{B} = \mathbf{B}(s)$. Comparing Eq. (6.41) with Eq. (6.9) it is noticed that $\mathbf{B}(s)$ and the field-free ADT matrix $\mathbf{A}(s)$ are solutions of the same equation. If both are solved for the same boundary conditions, the two solutions are identical or, in other words, Eq. (6.40) can be rewritten as

$$\tilde{\mathbf{A}}(s,t) = \boldsymbol{\omega}^\dagger(s,t)\mathbf{A}(s). \tag{6.42}$$

However, Eq. (6.42) has also to satisfy Eq. (6.17b). To check that we substitute Eq. (6.42) in Eq. (6.17b) and recalling Eq. (6.15), we find that this substitution leads to the first order equation for $\boldsymbol{\omega}$, as given in Eq. (6.25). Equation (6.42) implies that in the case of $L = N$ the space-time ADT matrix $\tilde{\mathbf{A}}(s,t)$ is written as a product of the matrix $\boldsymbol{\omega}^\dagger(s,t)$ and the field-free ADT matrix $\mathbf{A}(s)$.

This simplified expression for $\tilde{\mathbf{A}}$ can now be used to derive the corresponding field-dressed diabatic potential matrix. Thus, substituting Eq. (6.42) in Eq. (6.14) yields the following diabatic potential:

$$\tilde{\mathbf{W}}(s,t)(\equiv \mathbf{W}(s,t)) = \mathbf{A}^{\dagger}(s)\tilde{\mathbf{H}}(s,t)\mathbf{A}(s). \tag{6.43}$$

For the case of the perturbative framework the diabatization yields an identical potential matrix $\mathbf{W}(s,t)$ as given in Eq. (6.43).

Corollary. *When the general (nonperturbative) approach is carried out for $N = L$, the resulting diabatic potential matrix is identical to the one obtained within the simplified perturbative approach.*

6.4 The Mathieu Equation

The numerical treatment of the above three mentioned matrces, $\tilde{\mathbf{A}}$, $\tilde{\mathbf{D}}$, and $\boldsymbol{\omega}$, is carried out for a model system based on Mathieu equation.[1-6,11]

The Mathieu Equation [see also **Chapter 5**] to be applied in this study is of the form

$$\left(-\frac{1}{2}E_{el}\frac{\partial^2}{\partial\theta_e^2} - G(q,\phi)\cos(2\theta_e-\phi) - u_j(q,\phi)\right)\xi_j(\theta_e|q,\phi) = 0 \tag{6.44}$$

where E_{el} is a characteristic electronic quantity, $G(q,\phi)$ is the nuclear-electronic interaction coefficient, and $u_j(q,\phi)$ and $\xi_j(\theta_e|q,\phi)$ are the jth eigenvalue and eigenfunction, respectively, which parametrically depend on the nuclear coordinates. The solution of Mathieu equation can be obtained by expanding the $\xi_j(\theta_e|q,\phi)$ eigenfunctions in the Fourier series with the following two series of solutions:

$$\begin{aligned}\xi_j^{(c)}(\theta_e|q,\phi) &= \sum_{m=0}^{\infty} A_{2m+1}^{j}(q)\cos(2m+1)(\theta_e-\phi/2)\\ \xi_j^{(s)}(\theta_e|q,\phi) &= \sum_{m=0}^{\infty} A_{2m+1}^{j}(q)\sin(2m+1)(\theta_e-\phi/2)\end{aligned} \tag{6.45}$$

where the upper indices c and s label cosine and sine respectively.

For the present study the angular NAC terms form, at $q\sim 0$, the following nonadiabatic coupling matrix:

$$\boldsymbol{\tau}_{\phi}(q \sim 0|N) = \begin{pmatrix} 0 & \boldsymbol{\tau}_{12}^{\phi} & 0 & 0 & 0 \\ -\boldsymbol{\tau}_{12}^{\phi} & 0 & 0 & 0 & 0 \\ 0 & 0 & 0 & \boldsymbol{\tau}_{34}^{\phi} & 0 \\ 0 & 0 & -\boldsymbol{\tau}_{34}^{\phi} & 0 & 0 \\ 0 & 0 & 0 & 0 & 0 \end{pmatrix} \tag{6.46}$$

It is important to emphasize that all degeneracy points (i.e., points of CIs) produced by the Mathieu equations are located at $q = 0$. Consequently, line integrals for contours that surround the point $q = 0$ (and follow circles with radii, q, small enough) detect these degeneracy points by producing odd multiples of π and these which do not surround it are zero.

6.5 The External Electric Field

The external field is assumed to be dependent on time and on spatial coordinates. In general the field may depend on both the electronic coordinates, i.e., (q_e, θ_e), and on the nuclear coordinates, namely, (q, ϕ). However, in the present study, we let it depend only on the electronic coordinates.

6.5.1 The (electronic) potential

We have to present explicitly the electric field in order to calculate the corresponding electric potential as given in Eq. (6.5). It is noticed that such a calculation requires the introduction of contours in the electronic space. Since the model is defined in terms of a single electronic coordinate, i.e., θ_e, it is quite natural to assume the (closed) contour Γ_e to be a circle defined in terms of the electronic polar coordinates q_e, θ_e. Consequently, the electric potential due to this field is given in the form of a line integral along an open electronic, circular, contour:

$$U_E(\theta_e, q_e|x, \phi, t) = -\frac{e}{\hbar}\int_0^{\theta_e} \mathbf{E}_{\theta_e}(\tilde{\theta}_e, q_e|x, \phi, t)d\tilde{\theta}_e \tag{6.47}$$

where it is assumed that $ds_e = q_e d\theta_e$ and the two nuclear coordinates x and ϕ as well as the time t are parameters. To simplify our treatment we assume that the electric field does not depend on the nuclear coordinates (x, ϕ).

Since **E** is an external field formed outside the molecular region **E** has to fulfill, with respect to the electronic coordinates (as well as with respect to the atomic coordinate), the two equations: curl **E**=0 and div **E**=0. Consequently, a possible choice for the two planar components of E is

$$E_{x_e}(x_e, y_e, t) = -x_e \tilde{E}(t)$$
$$E_{y_e}(x_e, y_e, t) = y_e \tilde{E}(t) \tag{6.48}$$

With this choice it can be shown that the angular component of the field is

$$E_\theta(\theta_e, q_e|t) = q_e \tilde{E}(t)\sin(2\theta_e) \tag{6.49}$$

substituting Eq (6.49) in Eq (6.47) and recalling that $U_E(s_e, t) \equiv U_(\theta_e, q_e|t)$ yields the result

$$U_(\theta_e, q_e|t) = -\frac{e}{\hbar} q_e \tilde{E}(t)\cos(2\theta_e) \tag{6.50}$$

As for the shape of the intense electric pulse we write it as

$$\tilde{E}(t) = E_0 g(t) \tag{6.51}$$

where $g(t)$ is assumed to be the normal distribution

$$g(t) = \exp\left(-\frac{(t-t_0)^2}{2\sigma_t^2}\right). \tag{6.52}$$

In what follows we assume short pulses so that σ_t, the magnitude responsible for the width of the normal distribution, is narrow enough (immaterial of the value of t_0) to guarantee that at both ends of the time interval, namely, $t = 0, T$, we have $\tilde{E}(t) \sim 0$.

6.5.2 The nuclear dressed-field potential

Having introduced explicitly the electronic potential due to the external field we are in position to write the nuclear field-dressed Hamiltonian as

$$\tilde{\mathbf{H}}(x, \phi|t) = \mathbf{u}(x, \phi) + E(t)\mathbf{M}(x, \phi) \quad (6.53)$$

where $\mathbf{u}(x, \phi)$ is a diagonal matrix that contains eigenvalues of Eq. (6.2), $E(t)$ is related to the field intensity and is given in the form:

$$E(t) = E_0 \exp\left(-\frac{(t-t_0)^2}{2\sigma_t^2}\right) \quad (6.54)$$

and $M(x, \phi)$ is the dipole-moment matrix that contains the following elements:

$$\mathbf{M}_{mk}(x, \phi) = -\langle \xi_{0m}(\theta_e|x, \phi)|\cos 2\theta_e|\xi_{0k}(\theta_e|x, \phi)\rangle \quad (6.55)$$

Comparing Eq. (6.53) with Eqs. (6.23) and (6.24) it is noticed that $\mathbf{U}(x, \phi|t) \equiv E(t)\mathbf{M}(x, \phi)$ and therefore Eq. (6.53) can also be written as

$$\tilde{\mathbf{H}}(x, \phi|t) = \mathbf{u}(x) + \mathbf{U}(x, \phi|t) \quad (6.56)$$

In other words, the dependence of the field dressed potentials is due to the dipole moment matrix elements only.

6.5.3 Derivation of closed space-time contours for intense short-pulsed electric fields

In the present study we treat highly intense pulsed fields that operate for a short time, i.e., a time that corresponds to a fraction of a molecular vibration. Since this study is carried out for a model we employ unitless magnitudes only.

The main purpose of the present study is to probe numerically to what extent an $N < L$ case is capable to yield a diagonal $\tilde{\mathbf{D}}$ matrix. It is true that we proved, step-by-step, that not only in the case of $N = L$ but also in the case of $N < L$ we can guarantee that if N satisfies certain conditions the calculated $\tilde{\mathbf{D}}$ matrices are diagonal (and in this way secure the single valuedness of the resulting diabatic potentials). In the present section we elaborate on the contours to be used for the numerical study.

The $\tilde{\mathbf{D}}$ matrices have to be calculated along closed space-time contours. Therefore the first difficulty that needs to be resolved is to reveal a characteristic space-time contour along which $\tilde{\mathbf{D}}$ matrices have to be calculated. To achieve this aim we suggest, employing a semiclassical approach, to form a connection between the spatial coordinates and time.

To explain the idea we consider a diatomic molecule vibrating along a given interval R. Next an external field is turned on while the molecule is at the point R_{in} and is turned off again while the molecule reaches the point R_{fi}. We assumed the temporal pulse to form a normal distribution. Next we require that this pulse forms also a normal distribution along R, namely,

$$E(R) = E_0 \exp\left(-\frac{(R-R_0)^2}{2\sigma_R^2}\right) \tag{6.57}$$

where R_0 is a point in the range $R_{in} < R_0 < R_{fi}$ and σ_R is the corresponding spatial width of the pulse. Such a requirement is satisfied if R and t are linearly related, namely,

$$R = \eta t \tag{6.58}$$

Consequently, also the two sets of parameters that define the two distributions are related linearly: $\sigma_R = \eta\sigma_t$ and $R_0 = \eta t_0$.

The advantage in using Eq. (6.58) is not only because it transforms a normal distribution in time to become a normal distribution in space but also because it defines a line that may become a segment, Γ_{Rt}, for a (closed) space-time contour,

$$\begin{aligned} \Gamma_{Rt} &= \lim_{\Delta R, \Delta t \to 0} \Big\{ (R=0, t=0) \\ &\rightarrow (R=0, t=\Delta t) \\ &\rightarrow (R=\Delta R, t=\Delta t) \rightarrow \ldots \Big\} \end{aligned} \tag{6.59}$$

where due to Eq. (6.58) we have $\Delta R = \eta \Delta t$. Moreover this line may be considered as an element in a group of contours that covers the whole space-time region of interest by just varying a single parameter, η (see Fig. 6.2). Among other possibilities, assuming $\eta = 0$ we get the t axis and assuming $\eta = \infty$ we get the R axis.

Returning now to the model where the nuclear coordinate is the angle ϕ instead of R. As a result, Eq. (6.58) is replaced by

$$\phi = \eta t \tag{6.60}$$

and form the corresponding normal distribution of the field along the ϕ axis as given in Eq (6.57)

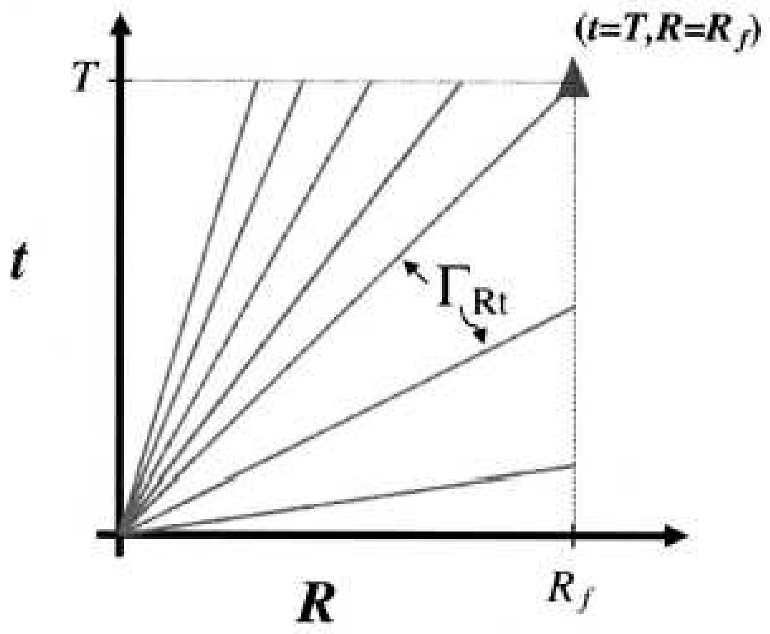

Figure 6.2: Space-time contours formed by the equation $\phi = \eta t$ covering the $\phi - t$ plane. These contours are general and can be used for solving the adiabatic-to-diabatic transformation matrix.

For the purpose of the present study we apply only one contour of this type and for reasons of convenience we choose the one formed by $\eta = 1$, which is a straight line that connects the initial point $t = 0, \phi = 0$ with the final point $t = T, \phi = T$

According to the theory, the selected contour has to fulfill two additional conditions: (1) It has to be a closed contour, in the spatial region, that surrounds the degeneracy points of interest. (2) At the same time it has also to be a closed contour in the corresponding space-time region. For instance, the contour Γ_{st} in Fig. 6.1b satisfies both conditions: the contour by itself is closed in the space-time region and its spatial component Γ_s is a spatial closed contour [see Fig 6.1a]. Consequently, the segment, $\Gamma_{\phi,t}$ defined as $\{(t = 0, \phi = 0) \to (t = T, \phi = T)\}$ has to be modified so that it becomes a closed spatial contour Γ_ϕ and then add another segment that completes it to become a closed contour $\Gamma_{\phi-t}$ in the $\phi - t$ plane. To form the closed spatial contour the range for has to be and for that to happen it is enough to assume that $T = 2\pi$. Next, in order to close the space-time contour we need to add a second segment, Γ_t namely, $\{(t = T, \phi = 2\pi) \to (t = 0, \phi = 2\pi)\}$ which is a segment along the negative time axis. The closed space-time contour $\Gamma_{\phi-t} = \Gamma_{\phi t} + \Gamma_t$, in the $\phi - t$ plane, is presented in Fig. 6.3.

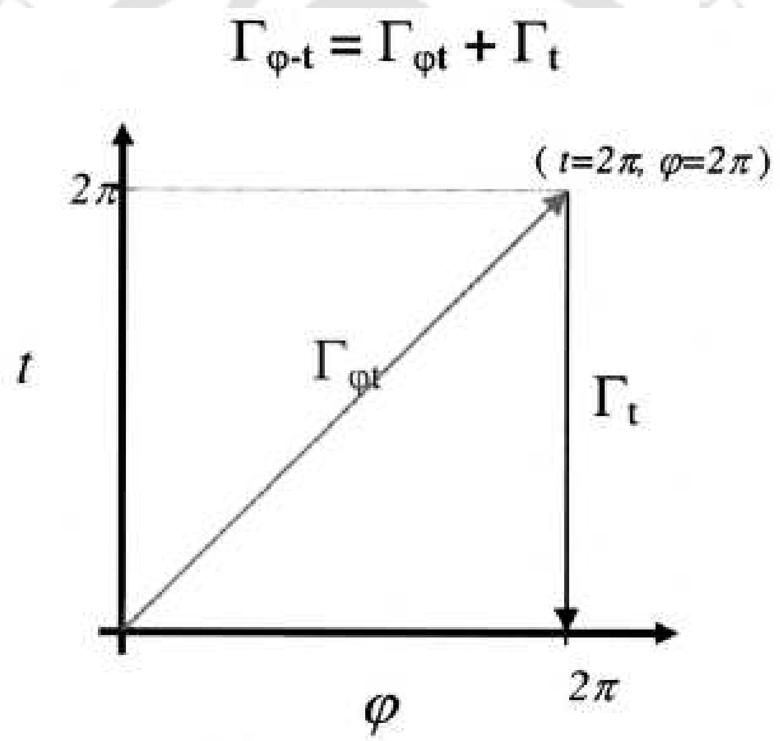

Figure 6.3: A closed space-time contours $\Gamma_{\phi-t}$, made up of two linear segments: the first, $\Gamma_{\phi t}$, that connects the initial point $(t = 0, \phi = 0)$ with the intermediate point $(t = 2\pi, \phi = 2\pi)$ and the second, Γ_t, that connects the initial point $(t = 2\pi, \phi = 2\pi)$ with the intermediate point $(t = 0, \phi = 2\pi)$.

We considered space-time contours by choosing a linear dependence between ϕ and t. This choice may look as a special case, but, in fact, it can be considered as a legitimate possibility (out of many other possibilities) to derive the diabatic potentials later applied to solve the nuclear SE.

6.6 Numerical Results

6.6.1 Introductory comments

Following the discussion of the previous section we introduce a new independent variable, y, defined as a variable along the segment $\Gamma_{\phi t}$ (see Fig. 6.3):

$$y = \sqrt{\phi^2 + t^2} \tag{6.61}$$

where ϕ and t are related according to Eq. (6.60). In the case of $\eta = 1$ we get that

$$y = \sqrt{2}\phi \tag{6.62}$$

In what follows some of the results are presented as a function of y only (and therefore for an open contour). However, other parts of the results in particular, the elements of the ADT matrix, $\tilde{A}(\phi, t|\Gamma_{\phi-t})$ have to be presented along a closed $y - t$ contour. Since the interval of y, namely, $\{0, 2\pi\sqrt{2}\}$ is not a closed contour we close the contour by adding the segment that connects $(t = T, \phi = 2\pi)$ with $(t = 0, \phi = 2\pi)$ as is seen in Fig. 6.3. To present these results the relevant figures (Figs. 6.4 - 6.6) are divided into two parts: On the left hand side (lhs) we show the results as a function of y along the $\{0, 2\pi\sqrt{2}\}$ interval and on the right hand side (rhs) we show the results as a function of t along the interval $t = T$ to $t = 0$.

Another magnitude to be mentioned is x. All the results to be reported in this study are obtained for $x = 1.183$. For this value of x the field-free $\boldsymbol{\tau}_\phi$ matrix breaks, up along the diagonal, into a series of two-dimensional blocks as can be seen in Eq. (6.45). This means that the values for N that guarantee that the $\mathbf{D}$ matrices and therefore also the $\tilde{\mathbf{D}}$ matrices are diagonal matrices are the even ones, namely, $N = 2, 4, \ldots$

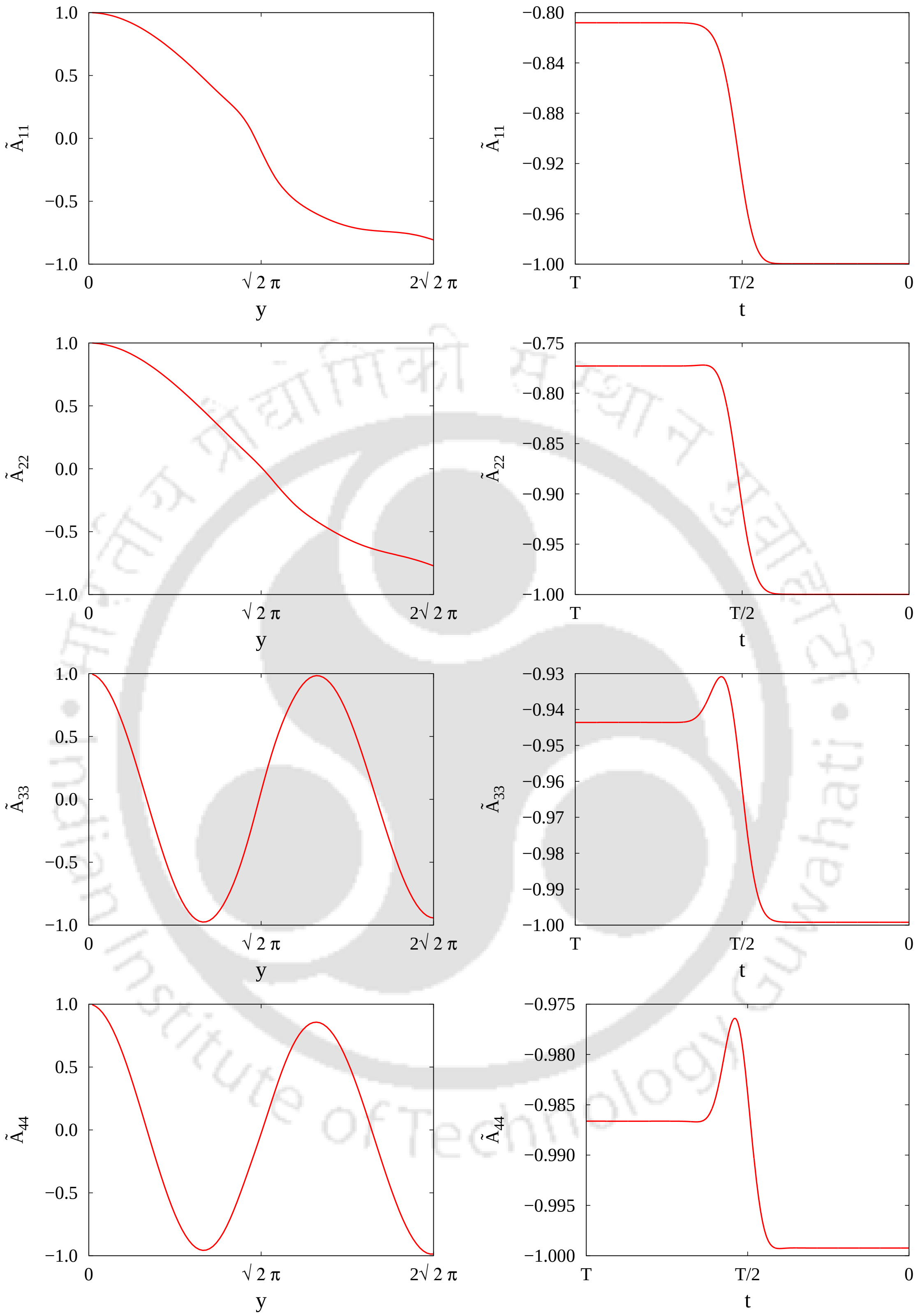

Figure 6.4: The diagonal elements of the matrix $\tilde{\mathbf{A}}$ as calculated along the closed space-time contour $\Gamma_{\phi-t}$ (see Fig 6.3). In the figure the four diagonal elements are presented $\tilde{\mathbf{A}}_{jj}, j = \{1, 4\}$ as calculated for E_0=1.5, $\sigma_\phi = 0.349$ rad, N=4, and L=6. On the lhs of each figure the matrix elements are presented as a function of y along $\Gamma_{\phi t}$ and, on the rhs, this presentation is continued as a function of t, along Γ_t.

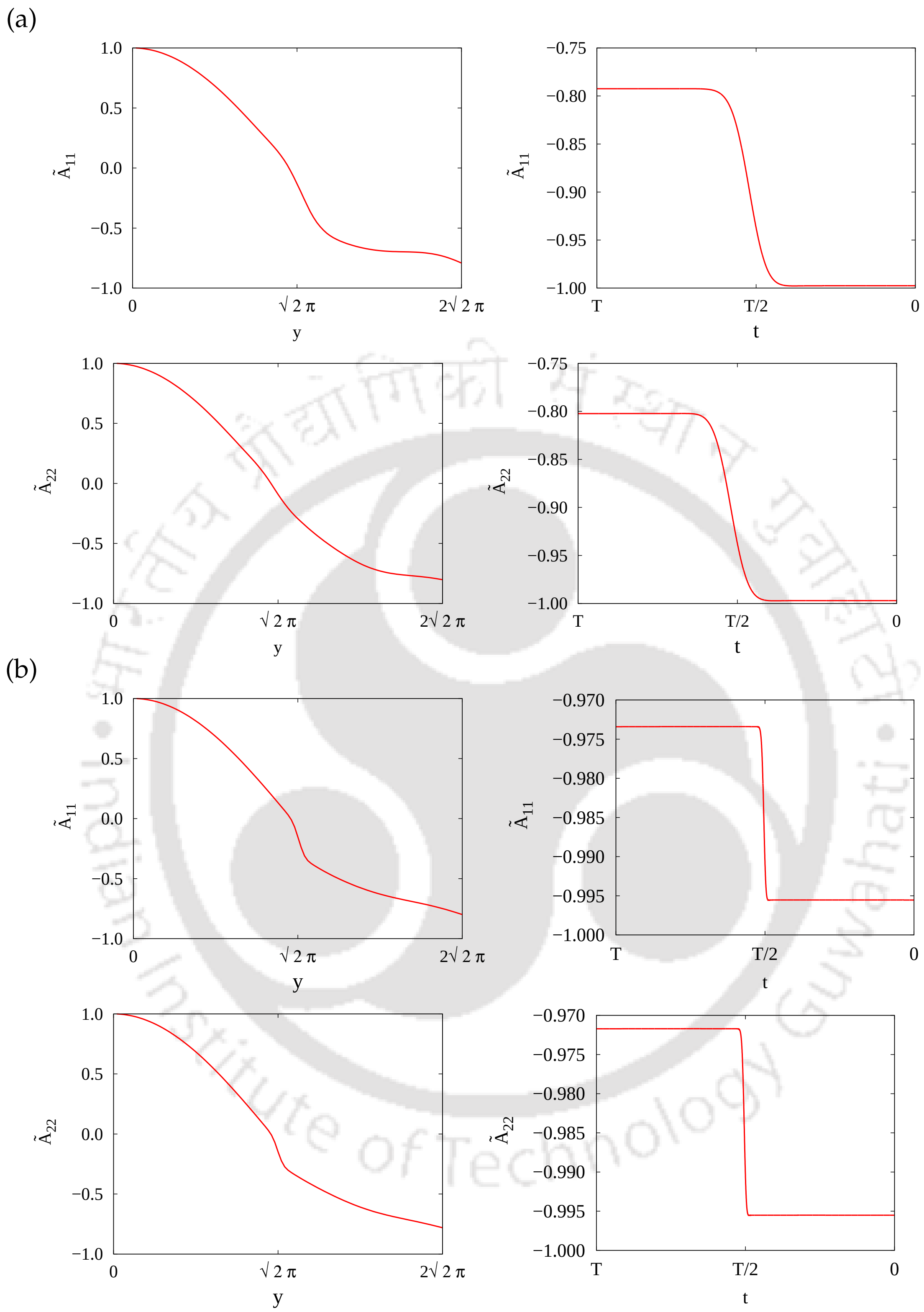

Figure 6.5: The diagonal elements of the matrix $\tilde{\mathbf{A}}$ as calculated along the closed space-time contour $\Gamma_{\phi-t}$ (see Fig 6.3). In the figure two different situations are presented: (a) In the first situation the diagonal elements $\tilde{\mathbf{A}}_{jj}, j = \{1, 2\}$ as calculated for E_0=1.5, $\sigma_\phi = 0.350$ rad, N=2, and L=4. (b) In the second situation the diagonal elements $\tilde{\mathbf{A}}_{jj}, j = \{1, 2\}$ as calculated for E_0=4, $\sigma_\phi = 0.087$ rad, N=2, and L=6. On the lhs of each figure the matrix elements are presented as a function of y along $\Gamma_{\phi t}$ and, on the rhs, this presentation is continued as a function of t, along Γ_t.

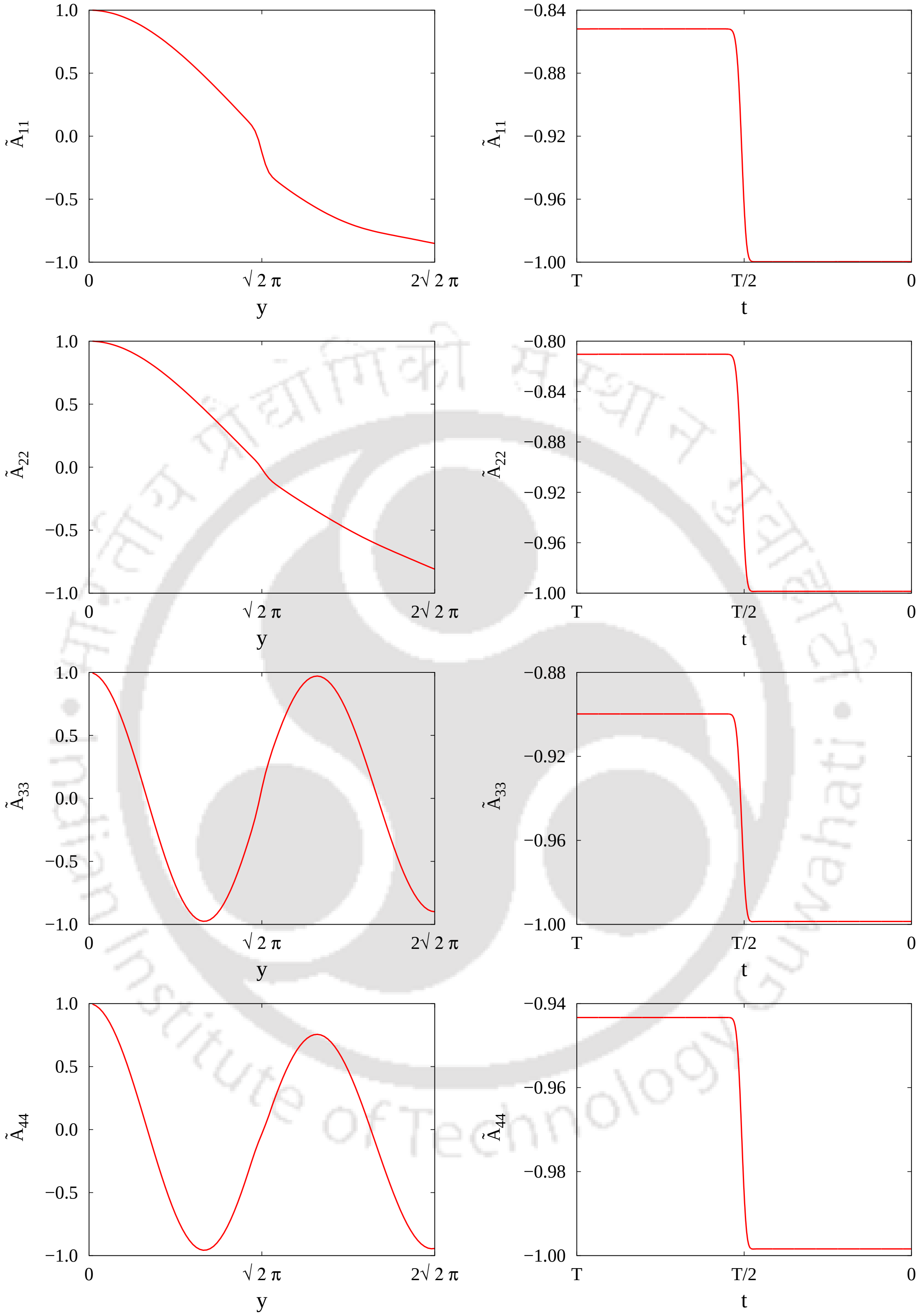

Figure 6.6: The diagonal elements of the matrix $\tilde{\mathbf{A}}$ as calculated along the closed space-time contour $\Gamma_{\phi-t}$ (see Fig 6.3). In the figure the four diagonal elements are presented $\tilde{\mathbf{A}}_{jj}, j = \{1, 4\}$ as calculated for E_0=4, $\sigma_\phi = 0.087$ rad, N=4, and L=8. On the lhs of each figure the matrix elements are presented as a function of y along $\Gamma_{\phi t}$ and, on the rhs, this presentation is continued as a function of t, along Γ_t.

6.6.2 Numerical treatment of the ω matrix and the corresponding electronic transition probabilities P

The equations to be solved re

$$i\hbar\frac{\partial\bar{\omega}_{jm}}{\partial t} = \sum_{k=1}^{L} Z_{mk}(t|x,\phi)\bar{\omega}_{jk}(t|x,\phi) \qquad m=\{1,L\} \qquad j=\{1,N\} \tag{6.63}$$

where

$$Z_{mk}(t|x,\phi) = \mathbf{U}_{mk}(x,\phi|t)\left\{\left[\exp\left(\frac{i}{\hbar}\int_0^t [\tilde{\mathbf{H}}_{mm}(t|x,\phi) - \tilde{\mathbf{H}}_{kk}(t|x,\phi)]dt\right) - \delta_{km}\right]\right\} \tag{6.64}$$

Here $\tilde{\mathbf{H}}(t|x,\phi)$ was introduced earlier. To obtain Eq. (6.63) we performed the following transformation:

$$\boldsymbol{\omega}_{kj}(t|q,\phi) = \exp\left\{\left(-\frac{i}{\hbar}\int_0^t [\tilde{\mathbf{H}}_{kk}(t|q,\phi)dt\right)\right\}\bar{\omega}_{kj}(t|q,\phi), \qquad k=\{1,L\} \qquad j=\{1,N\} \tag{6.65}$$

The details related to the solution of the first order differential equation for the $\boldsymbol{\omega}$ matrix are given in **Appendix E**.

It is important to realize that the diagonal elements of the matrix Z as defined in Eq. (6.64) are zero, a fact that enhances the convergence rate during the propagation of the solutions. The N sets of L equations in Eq. (6.63) are solved for N different sets of initial conditions where the jth set is solved for the vector $(0,0,\ldots,1,0,\ldots,0)$ with the "1" standing at the jth location.

To perform these calculations we freeze both x and ϕ and solve for the time dependence along time range $T = 2\pi$. Since the elements of the $\boldsymbol{\omega}$- matrix are complex numbers we concentrate only on their norms. This introduces the probability matrix P with the elements P_{kj} defined as

$$P_{kj}(\phi,t) = |\boldsymbol{\omega}_{kj}(\phi,t)|^2 \tag{6.66}$$

These matrix elements are also interpreted as the transition probabilities, due to the external field, from the initial state j to the final state k, for the assigned time and nuclear configuration.

In Fig. 6.7 first column of these matrix elements are presented as a function of t for $N = L = 4$ case at $E_0 = 20$, $x = 1.1$ a.u. and $\phi = 45^o$. The result indicate that a field of a given intensity is capable of directly exciting the molecular model to its fourth level.

In Figs. 6.8 - 6.10 some of these elements $P_{kj}(y)$ are presented [not as a function of ϕ and t but as a function of y], calculated along the line $\phi = t$. In Fig. 6.8 results for $E_0 = 1.5$ are presented as calculated for $\sigma = 0.350$ rad, $L = 4$, and the initial state $j = 2$. In panels transition probabilities P_{k2} for the four lower states, $k = 1, 4$ are shown, respectively. In Fig. 6.9 similar results for $E_0 = 4$ are presented, as calculated for $\sigma = 0.174$ rad, $L = 4$, and the initial state $j = 2$. In the four panels transition probabilities P_{k2} for the four lower states, $k = \{1, 4\}$, are shown respectively. Similar results are presented in Fig.6.10 for $L = 6$ and the initial state $j = 4$. In the six panels transition probabilities P_{k4} for the six lower states, $k = \{1, 4\}$, are shown respectively. The issue we are interested to discuss now is related to the distinction between N and L. According to our approach we decide on N which, also, means solving N nuclear SEs and then include all the necessary elements, L, along each of the N columns of the matrix.

In the first example see Fig. 6.8 we decide that $N = 2$. If we apply the perturbative approach then the number of elements in each column of the $\boldsymbol{\omega}$ matrix has to be $L(= N) = 2$. If we apply our approach we might decide on any number L but from Fig. 6.8 it can be seen that it is sufficient to assume $L = 4$ because the probabilities P_{k2} for $k > 4$ are negligible small. Thus, by choosing the perturbative approach we miss the third and the fourth matrix elements which account for more than 10% of the transition probabilities along the considered contour [the sum of the probabilities $P_{32}(y) + P_{42}(y) = 10\% - 15\%$]

The situation worsens for the perturbative approach in the second example because now the two missing elements of the P matrix account for almost 50% of the transition probability see Fig. 6.9. However, employing our approach and assuming $N = 2$ and $L = 4$ we find that the missing elements of P the fifth, sixth, etc. account for, only, of the probability.

One may think that by increasing N from $N = 2$ to $N = 4$ may cover for the mishaps of the perturbative approach as encountered in the previous cases. In this case the per-

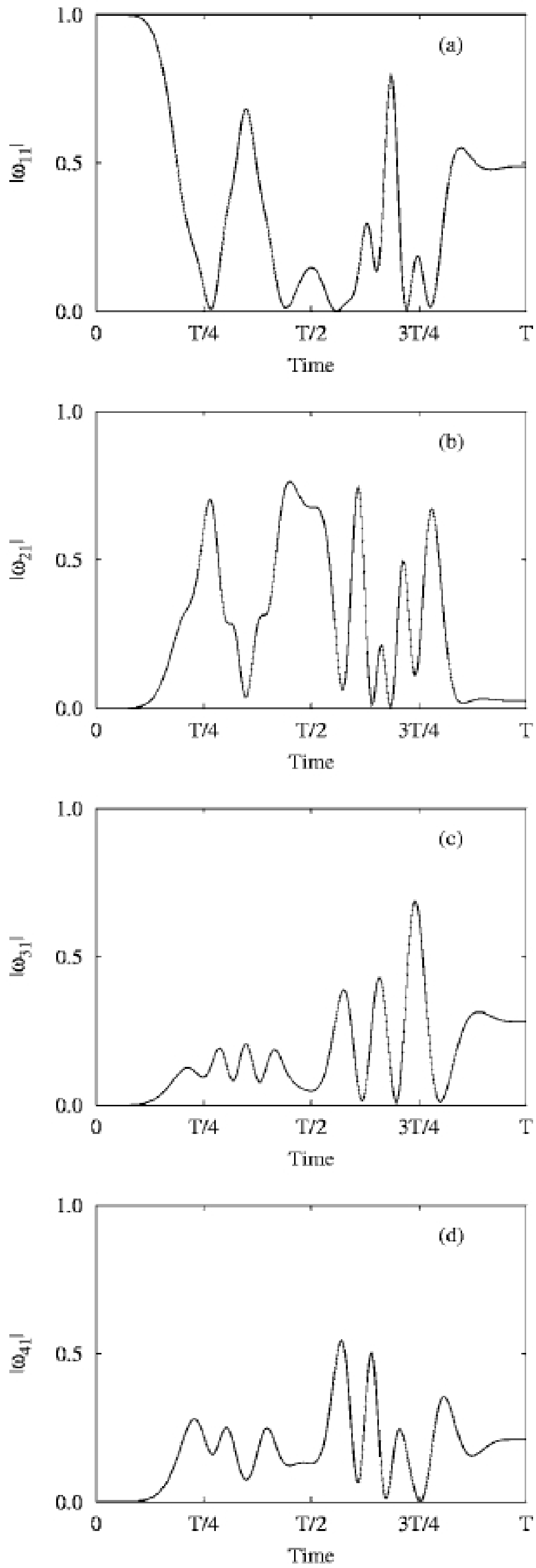

Figure 6.7: $\omega_{j1}(\phi, x|t)$, as a function of T for j=1,2,3,4, E_0=20, $\sigma_\phi = 45^o$ rad and L=4.

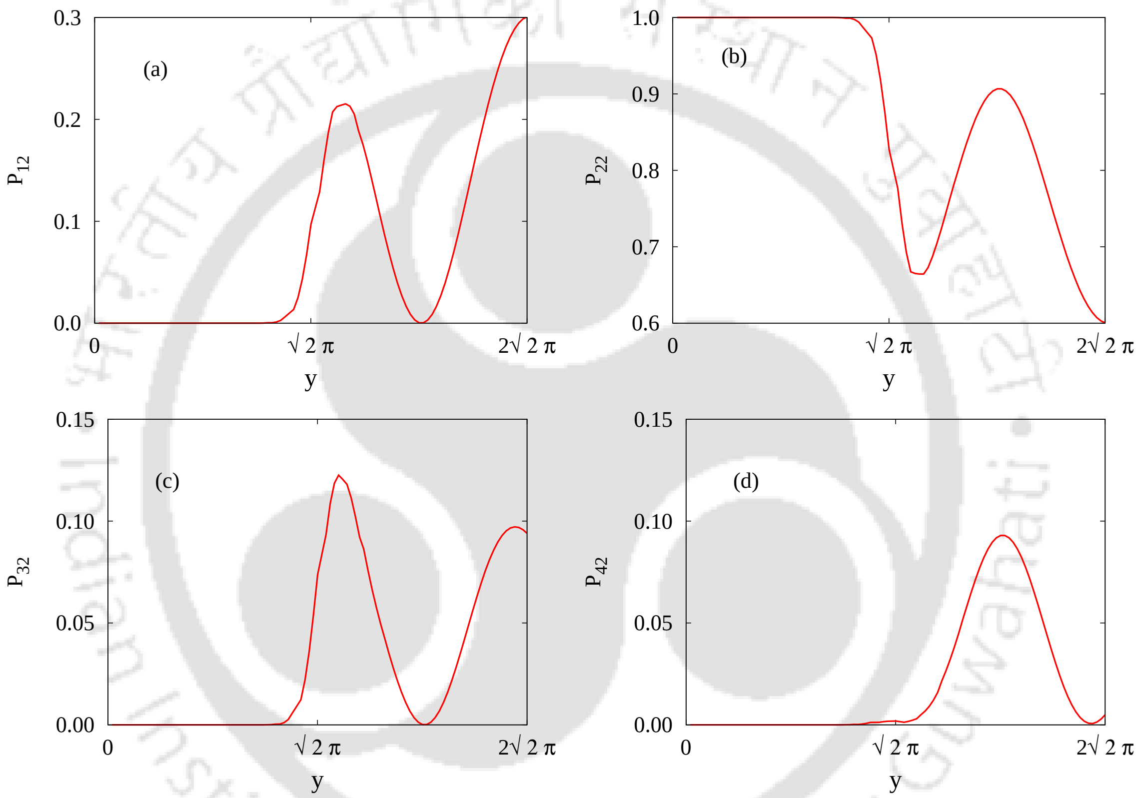

Figure 6.8: Electronic transition probabilities, $P_{k2}(y) = |\omega_{k2}(y)|^2$, as a function of y calculated along the line $\Gamma_{\phi t}$. Results are shown for j=2 (the initial state), E_0=1.5, $\sigma_\phi = 0.350$ rad and L=4. The curves in the panels (a)-(d) are calculated for $k = \{1, 4\}$

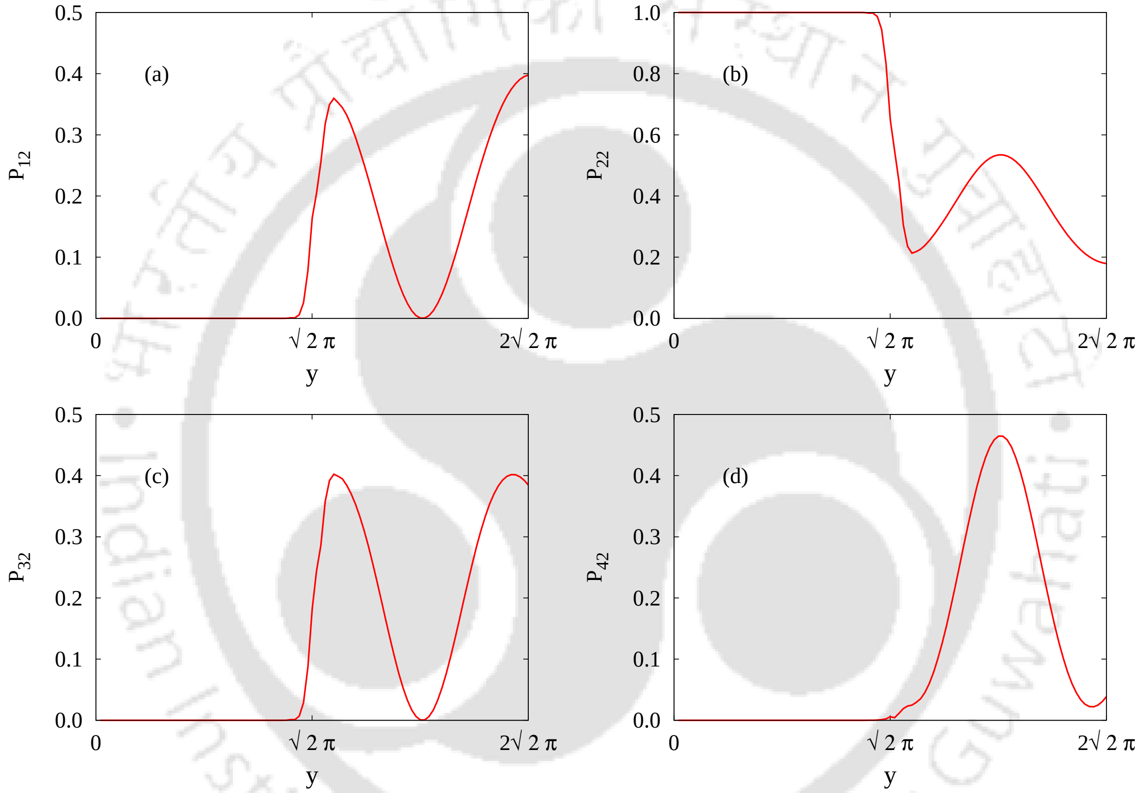

Figure 6.9: Electronic transition probabilities, $P_{k2}(y) = |\omega_{k2}(y)|^2$, as a function of y calculated along the line $\Gamma_{\phi t}$. Results are shown for j=2 (the initial state), E_0=4, $\sigma_\phi = 0.174$ rad and L=4. The curves in the panels (a)-(d) are calculated for $k = \{1, 4\}$.

turbative approach leads to $L = 4$. In Fig. 6.10 we show the probabilities for $L = 6$ as calculated for $j = 4$ and it is noticed that now the missing fifth and the sixth elements along the fourth column of the P matrix still account for more than 10% of the transition probability. According to our approach we may assume that $N = 4$ but $L = 6$ and by doing that we keep all the necessary elements of the P and of the $\boldsymbol{\omega}$ matrix.

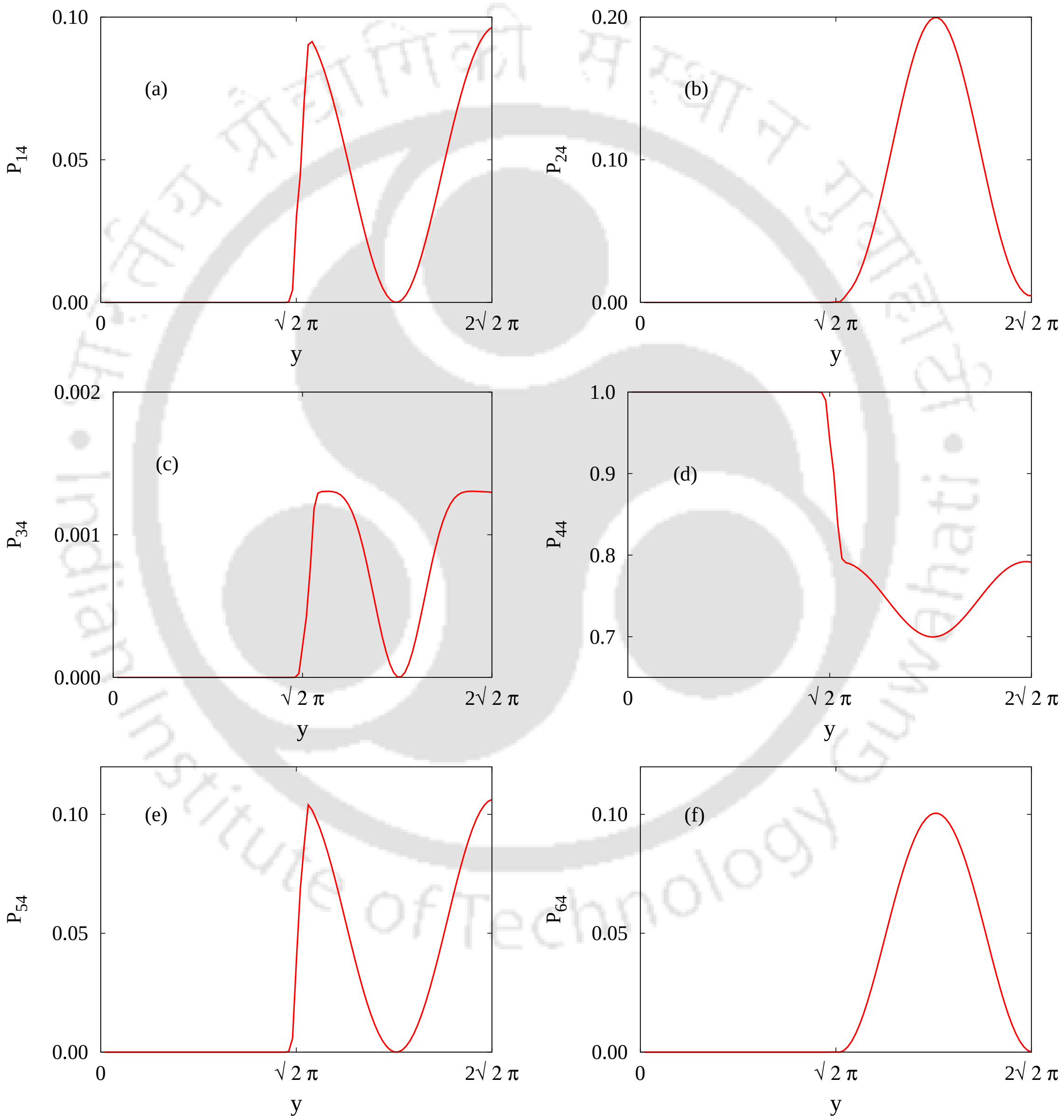

Figure 6.10: Electronic transition probabilities, $P_{k2}(y) = |\omega_{k4}(y)|^2$, as a function of y calculated along the line $\Gamma_{\phi t}$. Results are shown for j=4 (the initial state), E_0=4, $\sigma_\phi = 0.174$ rad and L=6. The curves in the panels (a)-(d) are calculated for $k = \{1, 6\}$.

6.6.3 Numerical treatment of the field-dressed NACMs

The field-dressed NAC elements are presented as three dimensional profiles. In Figs. 6.11 the norms of the $\tilde{\tau}_{12}(\phi, t)$ and $\tilde{\tau}_{12}(\phi, t)$, respectively are given as a function of ϕ and t. Since the field-free values of τ_{12} and τ_{34} are 0.5 and 1.5, respectively, it is noticed that the external field sometimes enhances these NAC terms by more than one order of magnitude.

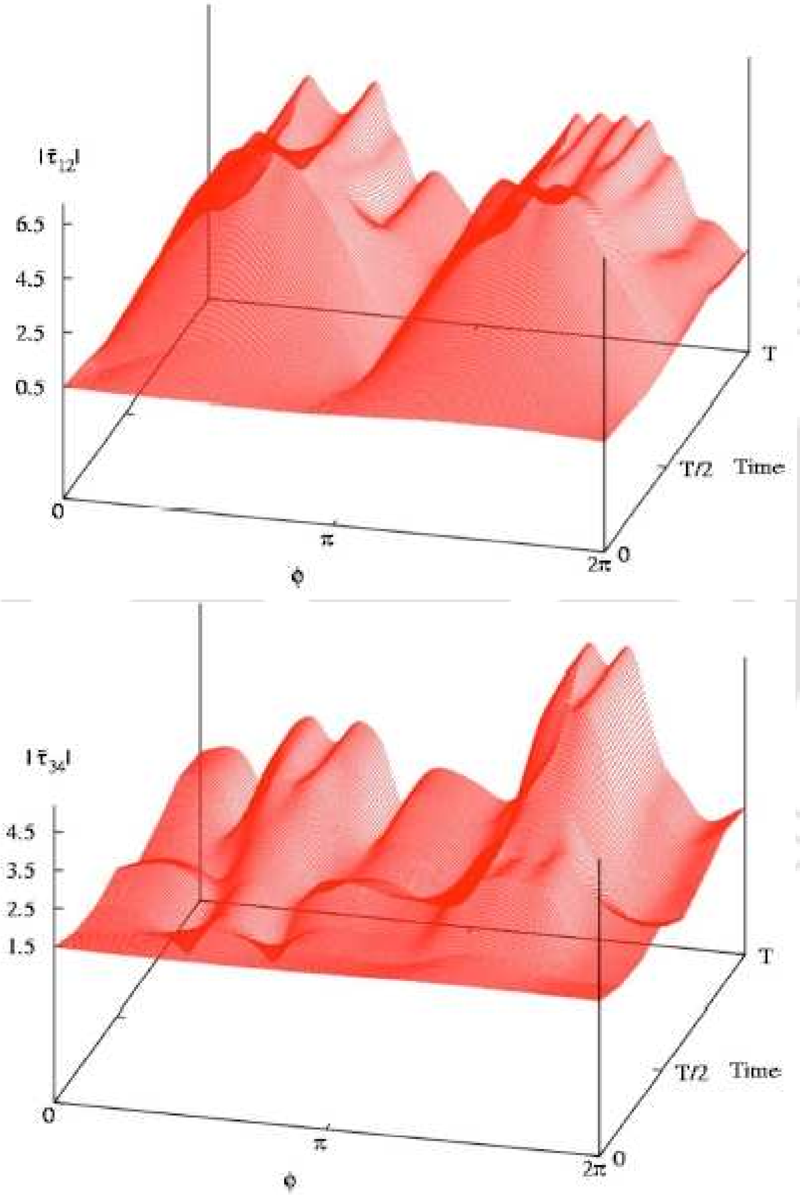

Figure 6.11: Three dimensional figures of the norms of $\tilde{\tau}_{12}(\phi, t)$ and $\tilde{\tau}_{12}(\phi, t)$, respectively, as a function of ϕ and t.

In Figs. 6.12 and 6.13 are presented the field-dressed NAC elements as calculated employing Eq. (6.12). In Fig. 6.12 absolute values of are given, i.e., as calculated for

$E_0 = 1.5$, $N = 2$, and $L = 4$, where the two curves refer to $\sigma = 0.087$ and 0.350 rad, respectively. In Fig. 6.13 , and are presented as calculated for $E_0 = 4$, $N = 4$, $L = 6$, and $\sigma = 0.087$ rad. It is important to remember that the corresponding field-free NAC elements and are ~ 0.5, ~ 0.0, and ~ 1.5 rad$^-1$, respectively. The main feature to be noticed is that the stronger the field the larger is the variations in the corresponding NAC terms.

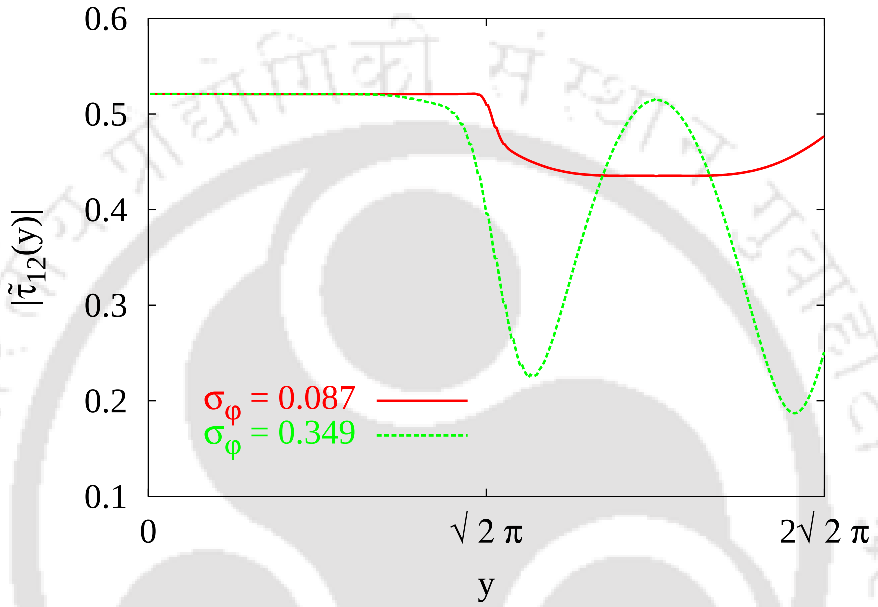

Figure 6.12: Three dimensional figures of the norms of $\tilde{\tau}_{12}(\phi, t)$ and $\tilde{\tau}_{12}(\phi, t)$, respectively, as a function of ϕ and t.

Next we consider a few elements of $\tilde{\tilde{\mathbf{H}}}$, the matrix that stands for the time component of the NAC vector. In Fig. 6.14 the three matrix elements are presented $|\tilde{\tilde{\mathbf{H}}}_{ij}(y)|; j = 1, 2, 3$ as a function of y, calculated for $E_0 = 4$, $N = 4$, $L = 6$, and $\sigma = 0.087$ rad. It is noticed that the values of these off-diagonal terms are larger than the previous spatial NACTs.

6.6.4 Numerical treatment of $\tilde{\mathrm{A}}$: The ADT field-dressed matrix

To calculate the elements of $\mathbf{D}$ matrix, we need to divide each ϕ segment and each t segment into small enough segments and diagonalize $\tilde{\tau}(\phi, t)$ and $\tilde{\mathbf{H}}_e(\phi, t)$ at a series of angular and time grid points, respectively. We present in Fig. 6.15 the fourth eigenvalues $\tilde{\tilde{\tau}}_{44}(\phi, t)$ and $\tilde{\tilde{\mathbf{H}}}_{44}(\phi, t)$ of $\tilde{\tau}(\phi, t)$ and $\tilde{\mathbf{H}}_e(\phi, t)$, respectively along Γ.

To calculate the field-dressed $\tilde{\mathbf{A}}$ matrix we use the solution of Eqs. 6.60. To perform

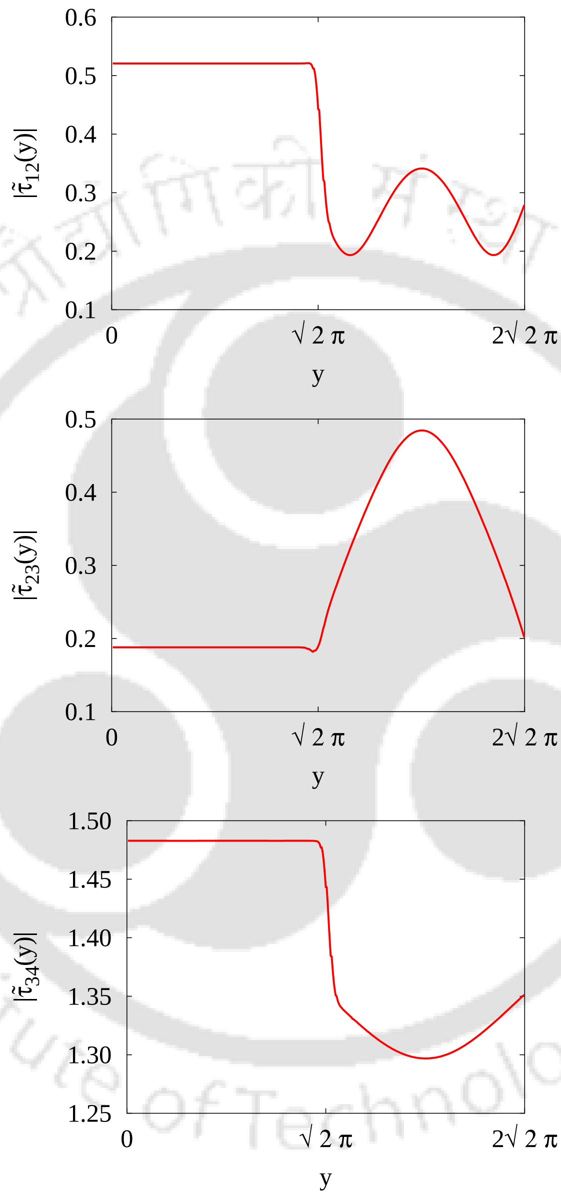

Figure 6.13: The angular dependent NAC term, $\tau_{12}^{\phi}(y)$, $\tau_{23}^{\phi}(y)$, and $\tau_{13}^{\phi}(y)$, as calculated along $\Gamma_{\phi t}$ (see Fig 6.3). In the figure the corresponding absolute values are presented.

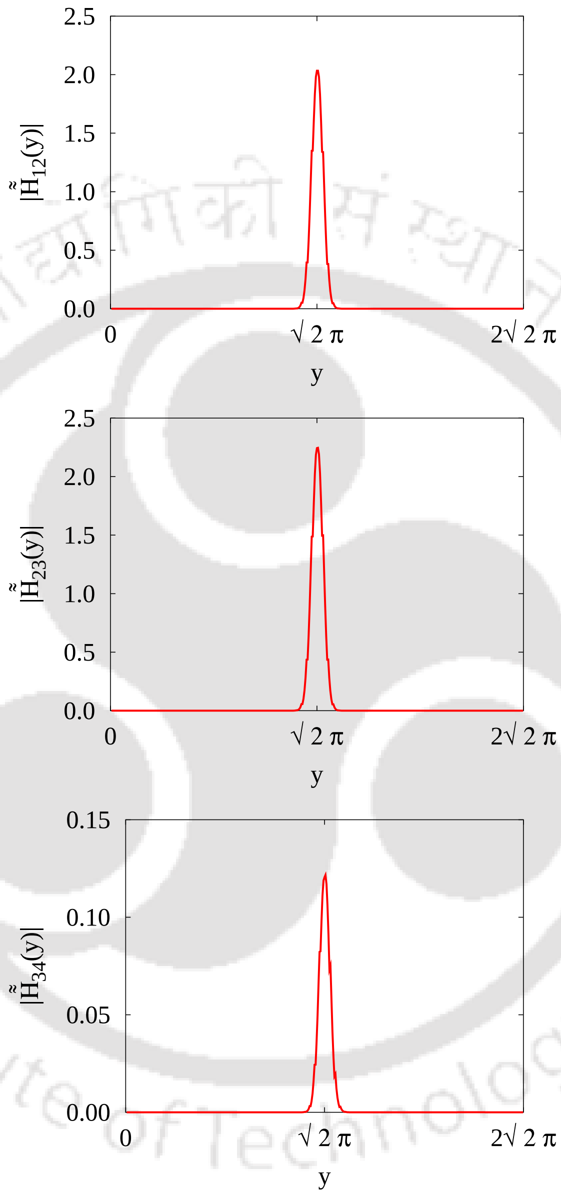

Figure 6.14: The time component of the NAC vector, $\tilde{\tilde{\mathbf{H}}}$, as calculated along $\Gamma_{\phi t}$ (see Fig 6.3) for $E_0 = 4$, $N = 4$, $L = 6$, and $\sigma = 0.087$ rad. In the figure the corresponding absolute values are presented.

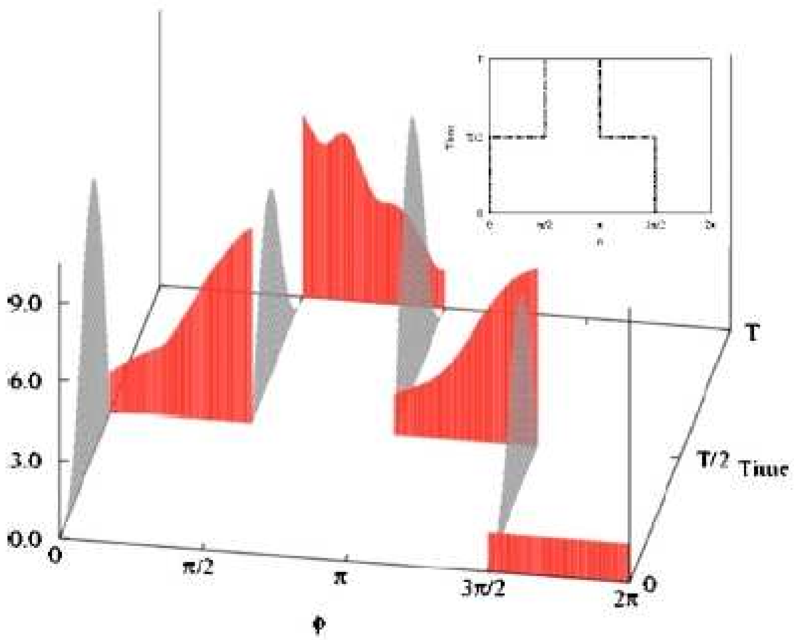

Figure 6.15: the fourth eigenvalues $\tilde{\tilde{\tau}}_{44}(\phi, t)$ and $\tilde{\tilde{\mathbf{H}}}_{44}(\phi, t)$ of $\tilde{\tau}(\phi, t)$ and $\tilde{\mathbf{H}}_e(\phi, t)$, respectively along Γ. The dark ones represent $\tilde{\tilde{\tau}}_{44}(\phi, t)$ while the grey ones $\tilde{\tilde{\mathbf{H}}}_{44}(\phi, t)$. The contour Γ is given in the insert.

the actual calculations we present the corresponding contour, $\Gamma_{\phi t}$ in terms infinitesimal small increments $\Delta\phi$ and as follows:

$$\Gamma_{\phi t} = \{(\phi = 0, t = 0) \to (\phi_1, 0) \to (\phi_1, t_1) \to \ldots \to (\phi_n, t_n) \to \ldots\} \tag{6.67}$$

where and $\phi_j = \phi_{j-1} + \Delta\phi$ and $t_j = t_{j-1} + \Delta t$. The end point along t is $(\phi = 2\pi, t = T)$. The contour $\Gamma_{\phi t}$ forms only a portion of the closed contour, $\Gamma_{\phi - t}$ and in order to close it we have to add the segment $\Gamma_t\{(\phi = 2\pi, t = T) \to (\phi = 2\pi, t = 0)\}$ (see Fig. 6.3.

In order to calculate the matrices $\tilde{\mathbf{A}}$ and $\tilde{\mathbf{D}}$ along $\Gamma_{\phi - t}(= \Gamma_{\phi t} + \Gamma_t)$ we need the corresponding elements of the two component vectorial matrix (see Figs. 6.13 - 6.14). In Figs. 6.4 - 6.6 the diagonal elements of several matrices $\tilde{\mathbf{A}}$ are presented. On the l.h.s. of each figure the diagonal elements are presented as a function of y and on the r.h.s as a function of t. The four curves in Fig. 6.4 were calculated for $E_0 = 1.5$, $L = 6$, $N = 4$, and $\sigma = 0.350$ rad, and those in Fig. 6.6 were calculated for $E_0 = 4$, $L = 8$, $N = 4$, and $\sigma = 0.087$ rad. The four curves in Fig.6.5 were calculated for $N = 2$ but for two different situations: In a the two curves were calculated for $E_0 = 1.5$, $L = 4$, and $\sigma = 0.350$ rad and in b they were calculated for $E_0 = 4$, $L = 6$, and $\sigma = 0.087$ rad. It is important to emphasize that all four cases discussed in Figs. 6.4 - 6.6 are characterized by the fact that $N < L$ in other words, none of them was calculated for $N = L$.

In all cases we start at $\phi = 0$ and $t = 0$ which corresponds to $y = 0$ with $\tilde{\mathbf{A}} = \mathbf{I}$, and in all of them we expect, at the end point $(\phi = 2\pi, t = 0)$ of $\Gamma_{\phi-t}(= \Gamma_{\phi t} + \Gamma_t)$, to have again a diagonal $\tilde{\mathbf{A}}$ matrix. Based on our time independent study, we should have $\tilde{\mathbf{A}}(\phi = 2\pi, t = 0) = -\mathbf{I}$. It is well noticed that indeed this result is, approximately, obtained in all our four cases.

We recall that by definition the $\tilde{\mathbf{A}}$ matrix at the end point of a closed contour is defined as the topological $\tilde{\mathbf{D}}$ matrix. Therefore the corresponding matrix $\tilde{\mathbf{D}}$ is expected to be equal, in all four cases, to $(-\mathbf{I})$ as indeed is the case.

6.7 Summary

In this chapter we elaborated on the connection between the field-free and the field-dressed approaches emphasizing the ADT matrices, $\mathbf{A}(s)$ and $\tilde{\mathbf{A}}(s,t)$, and the corresponding topological matrices, $\mathbf{D}(\mathrm{s})$ and $\tilde{\mathbf{D}}(\Gamma_{st})$.

The connection between these two approaches is done via the field-free to field-dressed transformation matrix $\boldsymbol{\omega}(s,t)$. The strange fact about this matrix is that it can be ignored while treating the perturbative framework (for example, the expression for the diabatic potentials does not require any reference to it), whereas it plays an important role in developing the nonperturbative framework. The importance of this matrix is due to the fact that its elements along each column are closely connected with the electronic transitions from a given state j to the various states k. In other words, magnitudes $P_{kj}(s,t) \equiv |\boldsymbol{\omega}_{kj}(s,t)|^2$ (where j is fixed and $k = \{1, L\}$) are interpreted as the probabilities to find the molecular system at time t in the kth state when at time $t = 0$ it was in the jth state.

However, there is much more to it. Having $\boldsymbol{\omega}$ (or its jth column) is crucial for determining L_j, the number of field-free states that get populated by the field in case we start with a molecule in its j state. These numbers, for the various initial states, are important for estimating the size of the system of nuclear SEs to be solved. Ignoring this information (as is usually the case within the perturbative approach) can be damaging.

Defining L as the largest L_j value may become a problem. If L is too large, performing a sensible, meaningful numerical study of such a system of SEs is not feasible. Therefore, the question to be asked is if there exists a rigorous way to reduce the number of SEs from L to N (so that $N < L$) and still maintain the contribution of the $(L-N)$ populated states.

It was shown that the necessary and sufficient condition for that to happen is that the relevant N-dimensional field-dressed topological matrix $\tilde{\mathbf{D}}(\Gamma_{st})$ is diagonal along any space-time closed contour in the space-time region of interest. Moreover, we proved analytically that whenever a group of N (not L) field-free states forms a Hilbert subspace in a given spatial region, the corresponding group of N field-dressed states forms a Hilbert subspace in any space-time region where the spatial part overlaps with the spatial region of the original field-free system.

This outcome can also be summarized as:

The necessary and sufficient condition for having a diagonal field-dressed $\tilde{\mathbf{D}}$ matrix is that the corresponding field-free $\mathbf{D}$ matrix must be diagonal. In other words, immaterial of how intense the field is or how long it acts, it cannot affect the topological features of the field-free $\mathbf{D}$ matrix.

Returning now to the crucial role played by the $\boldsymbol{\omega}$ matrix it is important to emphasize that to reach these final statements the matrix $\boldsymbol{\omega}(s,t)$ played a crucial role. Moreover, the expression for the diabatic potential explicitly contains this matrix.

We also presented a numerical backup to the theory and the following three issues are discussed.

(i) The main feature that characterizes our space-time contour approach is that it enables to distinct between two numbers, namely, L, which stands for the size of the field-free manifold, and N, which stands for the size of the field-dressed manifold, both required for achieving converged results. Consequently, before doing any attempts to solve the nuclear SE we suggest to use the probability matrix $P(s,t)$ with the aim of finding out as much information as possible about L and N and in particular, about the $L(N)$ dependence. This dependence is studied numerically in Figs. 6.8 - 6.10.

(ii) One of the more interesting features revealed in the numerical study is that we always have $L > N$ or in other words L is not likely to be equal to N. Since the $L = N$ case yields the perturbative approach , which is the common approach, this finding implies that the perturbative approach is in general not reliable for solving the nuclear time dependent SEs (unless N is very large). In other words, it seems to us that the more realistic approach is the one recommended here, namely, solving a reduced number (N) of SEs which are based on an extended number (L) of field-free eigenfunctions.

(iii) This situation leads to the third issue related to the ability to eliminate the unpleasant (singular) NAC terms namely, the diabatization process. Here the difficulty to worry about is related to the single valuedness of the calculated diabatic potentials. We derived the necessary and sufficient conditions for this to happen, in particular, when $N < L$. We also show, using a model based on the Mathieu equation, that these conditions are fully satisfied (see Figs. 6.4 to 6.6).

It is our hope that not before too long we will be able to tackle a realistic two or three atomic molecular system.

References

[1] M. Baer, A. Yahalom and R. Englman, J. Chem. Phys. **109**, 6550 (1998).

[2] R. Englman, A. Yahalom and M. Baer, Int. J. Quantum Chem. **90**, 266 (2002).

[3] T. Vertesi et al., J. Phys. Chem. A **107**, 7189 (2003).

[4] B. Sarkar, S. Adhikari and M. Baer, J. Chem. Phys. **126**, 14106 (2006).

[5] B. Sarkar, S. Adhikari and M. Baer, J. Chem. Phys. **127**, 14301 (2007).

[6] B. Sarkar, S. Adhikari and M. Baer, J. Chem. Phys. **127**, 14302 (2007).

[7] M. Bear, *Beyond Born-Oppenheimer:Conical Intersections and Electronic nonadiabatic Coupling Terms*, Wiley Interscience, Hoboken, N.J., USA, 2006.

[8] M. Baer, J. Phys. Chem. A **107**, 4724 (2003).

[9] M. Baer, J. Phys. Chem. A **110**, 6571 (2006).

[10] R. Baer, D. J. Kouri, M. Baer and D. K. Hoffman, J. Chem. Phys. **119**, 6998 (2003).

[11] M. Baer, T. Vertesi, G. J. Halasz, A. Vivok and S. Suhai, Faraday Discuss. **127**, 337 (2004).

[12] M. Baer, Phys. Rep. **358**, 75 (2002).

Appendix A

The adiabatic SE and diabatic potential matrix for any three state BO system

The explicit expression of kinetically coupled adiabatic SEs for any three state BO system in terms of electronic basis angles (α, β and γ) are:

$$
\begin{aligned}
- & \frac{\hbar^2}{2m}\nabla^2\psi_1 - \frac{\hbar^2}{2m}[-\cos^2\beta(\nabla\alpha)^2 - (\nabla\beta)^2]\psi_1 - \frac{\hbar^2}{2m}2[-\cos\beta\cos\gamma\nabla\alpha - \sin\gamma\nabla\beta]\nabla\psi_2 \\
- & \frac{\hbar^2}{2m}[\sin\beta\cos\beta\sin\gamma(\nabla\alpha)^2 + 2\cos\beta\sin\gamma\nabla\alpha\nabla\gamma - 2\cos\gamma\nabla\beta\nabla\gamma - \cos\beta\cos\gamma\nabla^2\alpha \\
- & \sin\gamma\nabla^2\beta]\psi_2 - \frac{\hbar^2}{2m}2[\cos\beta\sin\gamma\nabla\alpha - \cos\gamma\nabla\beta]\nabla\psi_3 - \frac{\hbar^2}{2m}[\sin\beta\cos\beta\cos\gamma(\nabla\alpha)^2 \\
+ & 2\sin\gamma\nabla\beta\nabla\gamma + 2\cos\beta\cos\gamma\nabla\alpha\nabla\gamma + \cos\beta\sin\gamma\nabla^2\alpha - \cos\gamma\nabla^2\beta]\psi_3 + (u_1 - E)\psi_1 = 0
\end{aligned}
\tag{A.1}
$$

$$
\begin{aligned}
- & \frac{\hbar^2}{2m}\nabla^2\psi_2 - \frac{\hbar^2}{2m}[-\sin^2\beta\sin^2\gamma(\nabla\alpha)^2 - \cos^2\gamma(\nabla\alpha)^2 - \sin^2\gamma(\nabla\beta)^2 - (\nabla\gamma)^2 \\
- & 2\cos\beta\sin\gamma\cos\gamma\nabla\alpha\nabla\beta - 2\sin\beta\nabla\alpha\nabla\gamma]\psi_2 - \frac{\hbar^2}{2m}2[\cos\beta\cos\gamma\nabla\alpha + \sin\gamma\nabla\beta]\nabla\psi_1 \\
- & \frac{\hbar^2}{2m}[\sin\beta\cos\beta\sin\gamma(\nabla\alpha)^2 - 2\sin\beta\cos\gamma\nabla\alpha\nabla\beta + \cos\beta\cos\gamma\nabla^2\alpha + \sin\gamma\nabla^2\beta]\psi_1 \\
- & \frac{\hbar^2}{2m}2[-\sin\beta\nabla\alpha - \nabla\gamma]\nabla\psi_3 - \frac{\hbar^2}{2m}[\cos^2\beta\sin\gamma\cos\gamma(\nabla\alpha)^2 - \sin\gamma\cos\gamma(\nabla\beta)^2 \\
- & 2\cos\beta\cos^2\gamma\nabla\alpha\nabla\beta - \sin\beta\nabla^2\alpha - \nabla^2\gamma]\psi_3 + (u_2 - E)\psi_2 = 0
\end{aligned}
\tag{A.2}
$$

$$
\begin{aligned}
&- \frac{\hbar^2}{2m}\nabla^2\psi_3 - \frac{\hbar^2}{2m}[-\sin^2\beta\cos^2\gamma(\nabla\alpha)^2 - \sin^2\gamma(\nabla\alpha)^2 - \cos^2\gamma(\nabla\beta)^2 - (\nabla\gamma)^2 \\
&+ 2\cos\beta\sin\gamma\cos\gamma\nabla\alpha\nabla\beta - 2\sin\beta\nabla\alpha\nabla\gamma]\psi_3 - \frac{\hbar^2}{2m}2[-\cos\beta\sin\gamma\nabla\alpha + \cos\gamma\nabla\beta]\nabla\psi_1 \\
&- \frac{\hbar^2}{2m}[\sin\beta\cos\beta\cos\gamma(\nabla\alpha)^2 + 2\sin\beta\sin\gamma\nabla\alpha\nabla\beta - \cos\beta\sin\gamma\nabla^2\alpha + \cos\gamma\nabla^2\beta]\psi_1 \\
&- \frac{\hbar^2}{2m}2[\sin\beta\nabla\alpha + \nabla\gamma]\nabla\psi_2 - \frac{\hbar^2}{2m}[\cos^2\beta\sin\gamma\cos\gamma(\nabla\alpha)^2 - \sin\gamma\cos\gamma(\nabla\beta)^2 \\
&+ 2\cos\beta\sin^2\gamma\nabla\alpha\nabla\beta + \sin\beta\nabla^2\alpha + \nabla^2\gamma]\psi_2 + (u_3 - E)\psi_3 = 0 \qquad \text{(A.3)}
\end{aligned}
$$

Since the present models are two coordinate system, $\nabla\eta_i$ are expressible in terms of x and y, where $\nabla = \vec{i}\frac{\partial}{\partial x} + \vec{j}\frac{\partial}{\partial y}$ and η_is are mixing angles, α, β, and γ.

The diabatic potential matrix elements ($W_{ij}s$) in terms of electronic basis angles (α, β, and γ) are given by:

$$
\begin{aligned}
W_{11} &= \frac{1}{4}[u_1 + \frac{3}{2}(u_2+u_3)] + \frac{1}{4}[u_1 - \frac{1}{2}(u_2+u_3)]\cos 2\alpha + \frac{1}{4}[u_1 - \frac{1}{2}(u_2+u_3)]\cos 2\beta \\
&+ \frac{1}{8}(u_2-u_3)\cos 2\gamma + \frac{1}{4}[u_1 - \frac{1}{2}(u_2-u_3)]\cos 2\alpha\cos 2\beta + \frac{1}{8}(u_2-u_3)\cos 2\beta\cos 2\gamma \\
&- \frac{3}{8}(u_2-u_3)\cos 2\alpha\cos 2\gamma - \frac{1}{8}(u_2-u_3)\cos 2\alpha\cos 2\beta\cos 2\gamma \\
&+ \frac{1}{2}(u_2-u_3)\sin 2\alpha\sin\beta\sin 2\gamma \qquad \text{(A.4)} \\
W_{22} &= \frac{1}{4}[u_1 + \frac{3}{2}(u_2+u_3)] - \frac{1}{4}[u_1 + \frac{1}{2}(u_2+u_3)]\cos 2\beta - \frac{1}{8}(u_2-u_3)\cos 2\gamma \\
&+ \frac{3}{8}(u_2-u_3)\cos 2\alpha\cos 2\gamma + \frac{1}{8}(u_2-u_3)\cos 2\beta\cos 2\gamma \\
&- \frac{1}{2}(u_2-u_3)\sin 2\alpha\sin\beta\sin 2\gamma - \frac{1}{8}(u_2-u_3)\cos 2\alpha\cos 2\beta\cos 2\gamma \qquad \text{(A.5)} \\
W_{33} &= \frac{1}{2}[u_1 + \frac{1}{2}(u_2+u_3)] - \frac{1}{2}[u_1 - \frac{1}{2}(u_2+u_3)]\cos 2\beta - \frac{1}{4}(u_2-u_3)(1+\cos 2\beta)\cos 2\gamma \\
& \qquad \text{(A.6)}
\end{aligned}
$$

$$
\begin{aligned}
W_{12} &= W_{21} = \frac{1}{4}[u_1 - \frac{1}{2}(u_2+u_3)]\sin 2\alpha + \frac{1}{4}[u_1 - \frac{1}{2}(u_2+u_3)]\sin 2\alpha\cos 2\beta \\
&- \frac{3}{8}(u_2-u_3)\sin 2\alpha\cos 2\gamma - \frac{1}{2}(u_2-u_3)\cos 2\alpha\sin\beta\sin 2\gamma \\
&+ \frac{1}{8}(u_2-u_3)\sin 2\alpha\cos 2\beta\cos 2\gamma \qquad \text{(A.7)} \\
W_{13} &= W_{31} = \frac{1}{2}[u_1 - \frac{1}{2}(u_2+u_3)]\cos\alpha\sin 2\beta - \frac{1}{2}(u_2-u_3)\sin\alpha\cos\beta\sin 2\gamma \\
&+ \frac{1}{4}(u_2-u_3)\cos\alpha\sin 2\beta\cos 2\gamma \qquad \text{(A.8)}
\end{aligned}
$$

$$W_{23} = W_{32} = \frac{1}{2}[u_1 - \frac{1}{2}(u_2 + u_3)]\sin\alpha\sin 2\beta + \frac{1}{2}(u_2 - u_3)\cos\alpha\cos\beta\sin\gamma + \frac{1}{4}(u_2 - u_3)\sin\alpha\sin 2\beta\cos 2\gamma \quad \text{(A.9)}$$

Appendix B

The NAC matrix as the product of a vector function and an ADT angle dependent scalar matrix leads to zero Curl and thereby, the eigenvalues of the NAC matrix are vector functions.

If we wish to write the NAC matrix, $\vec{\boldsymbol{\tau}}(\theta_{12}, \theta_{13}, \theta_{23}) = \vec{\nabla}\theta_{12} \cdot \boldsymbol{g}(\theta_{12}, \theta_{13}, \theta_{23})$, its' components, namely, $\tau_p(\theta_{12}, \theta_{13}, \theta_{23})$ and $\tau_q(\theta_{12}, \theta_{13}, \theta_{23})$ (for two coordinates, p and q) are given by:

$$\begin{aligned} \tau_p(\theta_{12}, \theta_{13}, \theta_{23}) &= \nabla_p\theta_{12} \cdot g(\theta_{12}, \theta_{13}, \theta_{23}) \\ \tau_q(\theta_{12}, \theta_{13}, \theta_{23}) &= \nabla_q\theta_{12} \cdot g(\theta_{12}, \theta_{13}, \theta_{23}), \end{aligned} \tag{B.1}$$

where the Curl matrix can be expressed as:

$$\text{Curl } \tau = \tau_p(\theta_{12}, \theta_{13}, \theta_{23})\tau_q(\theta_{12}, \theta_{13}, \theta_{23}) - \tau_q(\theta_{12}, \theta_{13}, \theta_{23})\tau_p(\theta_{12}, \theta_{13}, \theta_{23}) \tag{B.2}$$

or

$$\text{Curl } \tau = \nabla_q\tau_p(\theta_{12}, \theta_{13}, \theta_{23}) - \nabla_p\tau_q(\theta_{12}, \theta_{13}, \theta_{23}). \tag{B.3}$$

The equality of Eqs. (B.2) and (B.3) is called the Curl condition.

When we substitute Eq. (B.1) in Eq. (B.2) we obtain

$$\begin{aligned}\text{Curl}\,\tau &= \nabla_p\theta_{12}\cdot g(\theta_{12},\theta_{13},\theta_{23})\nabla_q\theta_{12}\cdot g(\theta_{12},\theta_{13},\theta_{23})\\ &- \nabla_q\theta_{12}\cdot g(\theta_{12},\theta_{13},\theta_{23})\nabla_p\theta_{12}\cdot g(\theta_{12},\theta_{13},\theta_{23})\\ &= g(\theta_{12},\theta_{13},\theta_{23})\cdot g(\theta_{12},\theta_{13},\theta_{23})\big[\nabla_p\theta_{12}\nabla_q\theta_{12}-\nabla_q\theta_{12}\nabla_p\theta_{12}\big]\\ &= 0.\end{aligned} \tag{B.4}$$

On the other hand if Eq. (B.1) is substituted in Eq. (B.3), it appears:

$$\text{Curl}\,\tau = \nabla_q\big[\nabla_p\theta_{12}\cdot g(\theta_{12},\theta_{13},\theta_{23})\big]-\nabla_p\big[\nabla_q\theta_{12}\cdot g(\theta_{12},\theta_{13},\theta_{23})\big] \tag{B.5}$$

with

$$\begin{aligned}\nabla_q\big[\nabla_p\theta_{12}\cdot g(\theta_{12},\theta_{13},\theta_{23})\big] &= \nabla_q\nabla_p\theta_{12}\cdot g(\theta_{12},\theta_{13},\theta_{23})+\nabla_p\theta_{12}\big[\nabla_{\theta_{12}}g(\theta_{12},\theta_{13},\theta_{23})\nabla_q\theta_{12}\\ &+ \nabla_{\theta_{13}}g(\theta_{12},\theta_{13},\theta_{23})\nabla_q\theta_{13}+\nabla_{\theta_{23}}g(\theta_{12},\theta_{13},\theta_{23})\nabla_q\theta_{23}\big]\\ \nabla_p\big[\nabla_q\theta_{12}\cdot g(\theta_{12},\theta_{13},\theta_{23})\big] &= \nabla_p\nabla_q\theta_{12}\cdot g(\theta_{12},\theta_{13},\theta_{23})+\nabla_q\theta_{12}\big[\nabla_{\theta_{12}}g(\theta_{12},\theta_{13},\theta_{23})\nabla_p\theta_{12}\\ &+ \nabla_{\theta_{13}}g(\theta_{12},\theta_{13},\theta_{23})\nabla_p\theta_{13}+\nabla_{\theta_{23}}g(\theta_{12},\theta_{13},\theta_{23})\nabla_p\theta_{23}\big]\end{aligned} \tag{B.6}$$

leading to

$$\begin{aligned}\text{Curl}\,\tau &= \big[\nabla_q\nabla_p\theta_{12}-\nabla_p\nabla_q\theta_{12}\big]g(\theta_{12},\theta_{13},\theta_{23})\\ &+ \nabla_{\theta_{12}}g(\theta_{12},\theta_{13},\theta_{23})\big[\nabla_p\theta_{12}\nabla_q\theta_{12}-\nabla_q\theta_{12}\nabla_p\theta_{12}\big]\\ &+ \nabla_{\theta_{13}}g(\theta_{12},\theta_{13},\theta_{23})\big[\nabla_p\theta_{12}\nabla_q\theta_{13}-\nabla_q\theta_{12}\nabla_p\theta_{13}\big]\\ &+ \nabla_{\theta_{23}}g(\theta_{12},\theta_{13},\theta_{23})\big[\nabla_p\theta_{12}\nabla_q\theta_{23}-\nabla_q\theta_{12}\nabla_p\theta_{23}\big].\end{aligned} \tag{B.7}$$

The first terms of the Eq. (B.6) is zero due to the analyticity of the ADT angle (θ_{12}) and the second term is automatically zero. Thus, the validity of the identities $\big[\nabla_p\theta_{12}\nabla_q\theta_{13} = \nabla_q\theta_{12}\nabla_p\theta_{13}\big]$ and $\big[\nabla_p\theta_{12}\nabla_q\theta_{23} = \nabla_q\theta_{12}\nabla_p\theta_{23}\big]$[see Eqs. (3.12a) and (3.13a) also] ensure Curl $\tau = 0$. In other words, when Curl $\tau = 0$, the components of τ matrices commute with each other, i.e., the transformation matrix, **G** diagonalize the scalar matrix g instead of $\vec{\tau}$ matrix itself and provide the eigenvalues as vector functions.

Appendix C

Parametric representation of a conical surface

A surface with a parametric representation of the form $\mathbf{r}(u, v)$ can be described by the vector equation,

$$\mathbf{r}(u, v) = \vec{i}\, X(u, v) + \vec{j}\, Y(u, v) + \vec{k}\, Z(u, v), \qquad (u, v) \in T, \tag{C.1}$$

where $X(u, v)$, $Y(u, v)$, and $Z(u, v)$ are the three equations expressing x, y, and z in terms of two parameters u and v:

$$x = X(u, v), \qquad y = Y(u, v), \qquad z = Z(u, v). \tag{C.2}$$

The point (u, v) can vary over a two - dimensional connected set T in the uv-plane, and the corresponding points (x, y, z) trace out a surface in xyz-plane.

If X, Y, and Z are differentiable on T, we consider the two vectors,

$$\begin{aligned} \frac{\partial \mathbf{r}}{\partial u} &= \vec{i}\,\frac{\partial X}{\partial u} + \vec{j}\,\frac{\partial Y}{\partial u} + \vec{k}\,\frac{\partial Z}{\partial u} \\ \text{and} \qquad \frac{\partial \mathbf{r}}{\partial v} &= \vec{i}\,\frac{\partial X}{\partial v} + \vec{j}\,\frac{\partial Y}{\partial v} + \vec{k}\,\frac{\partial Z}{\partial v}. \end{aligned}$$

The cross product of these two vectors $\frac{\partial \mathbf{r}}{\partial u} \times \frac{\partial \mathbf{r}}{\partial v}$ is the *fundamental vector product* of the representation **r**. Its components can be expressed as Jacobian determinants as follows,

$$\frac{\partial \mathbf{r}}{\partial u} \times \frac{\partial \mathbf{r}}{\partial v} = \begin{vmatrix} \vec{i} & \vec{j} & \vec{k} \\ \frac{\partial X}{\partial u} & \frac{\partial Y}{\partial u} & \frac{\partial Z}{\partial u} \\ \frac{\partial X}{\partial v} & \frac{\partial Y}{\partial v} & \frac{\partial Z}{\partial v} \end{vmatrix} = \vec{i} \begin{vmatrix} \frac{\partial Y}{\partial u} & \frac{\partial Z}{\partial u} \\ \frac{\partial Y}{\partial v} & \frac{\partial Z}{\partial v} \end{vmatrix} + \vec{j} \begin{vmatrix} \frac{\partial Z}{\partial u} & \frac{\partial X}{\partial u} \\ \frac{\partial Z}{\partial v} & \frac{\partial X}{\partial v} \end{vmatrix} + \vec{k} \begin{vmatrix} \frac{\partial X}{\partial u} & \frac{\partial Y}{\partial u} \\ \frac{\partial X}{\partial v} & \frac{\partial Y}{\partial v} \end{vmatrix} \quad \text{(C.3)}$$

$$= \vec{i} \frac{\partial(Y,Z)}{\partial(u,v)} + \vec{j} \frac{\partial(Z,X)}{\partial(u,v)} + \vec{k} \frac{\partial(X,Y)}{\partial(u,v)}. \quad \text{(C.4)}$$

If (u, v) is a point in T at which $\frac{\partial \mathbf{r}}{\partial u}$ and $\frac{\partial \mathbf{r}}{\partial v}$ are continuous and the fundamental vector product is nonzero, then the image point $\mathbf{r}(u, v)$ is a regular point of **r**. Points at which $\frac{\partial \mathbf{r}}{\partial u}$ or $\frac{\partial \mathbf{r}}{\partial v}$ fails to be continuous or $\frac{\partial \mathbf{r}}{\partial u} \times \frac{\partial \mathbf{r}}{\partial v} = 0$ are the *singular points* of **r**.

We consider the surface of a cone (see Fig. C.1) as the image of the rectangle $T = [0, 2\pi] \times [0, h]$ under the mapping,

$$\mathbf{R}(r,\theta) = \vec{i}\,(\rho\cos\delta + r\sin\alpha\cos\theta) + \vec{j}\,(\rho\sin\delta + r\sin\alpha\sin\theta) + \vec{k}\,(z_0 - r\cos\alpha) \quad \text{(C.5)}$$

The vectors $\frac{\partial \mathbf{R}}{\partial r}$ and $\frac{\partial \mathbf{R}}{\partial \theta}$ are given by,

$$\frac{\partial \mathbf{R}}{\partial r} = \vec{i}\,\sin\alpha\cos\theta + \vec{j}\,\sin\alpha\sin\theta - \vec{k}\,\cos\alpha \quad \text{(C.6)}$$

$$\frac{\partial \mathbf{R}}{\partial \theta} = -\vec{i}\,r\sin\alpha\sin\theta + \vec{j}\,r\sin\alpha\cos\theta \quad \text{(C.7)}$$

Their cross product is:

$$\frac{\partial \mathbf{R}}{\partial r} \times \frac{\partial \mathbf{R}}{\partial \theta} = \begin{vmatrix} \vec{i} & \vec{j} & \vec{k} \\ \sin\alpha\cos\theta & \sin\alpha\sin\theta & -\cos\alpha \\ -r\sin\alpha\sin\theta & r\sin\alpha\cos\theta & 0 \end{vmatrix}$$

$$= \vec{i}\,r\sin\alpha\cos\alpha\cos\theta + \vec{j}\,r\sin\alpha\cos\alpha\sin\theta + \vec{k}\,r\sin^2\alpha \quad \text{(C.8)}$$

Since $||\frac{\partial \mathbf{R}}{\partial r} \times \frac{\partial \mathbf{R}}{\partial \theta}|| = r^2\sin^2\alpha$, the only singular point of this representation occurs when $r = 0$, which is the vertex of the cone.

The Jacobian determinant as defined in the cross product [Eqs. (B3) and (B8)] vanishes when $r = 0$, but this does not affect the validity of the transformation formula because the set of points with $r = 0$ has content zero. As for example, the Jacobian determinant along the unit vector $\vec{k}$ for $r = 0$ is given by:

$$\begin{vmatrix} \frac{\partial X}{\partial r} & \frac{\partial Y}{\partial r} \\ \frac{\partial X}{\partial \theta} & \frac{\partial Y}{\partial \theta} \end{vmatrix} = r \sin^2 \alpha = 0 \tag{C.9}$$

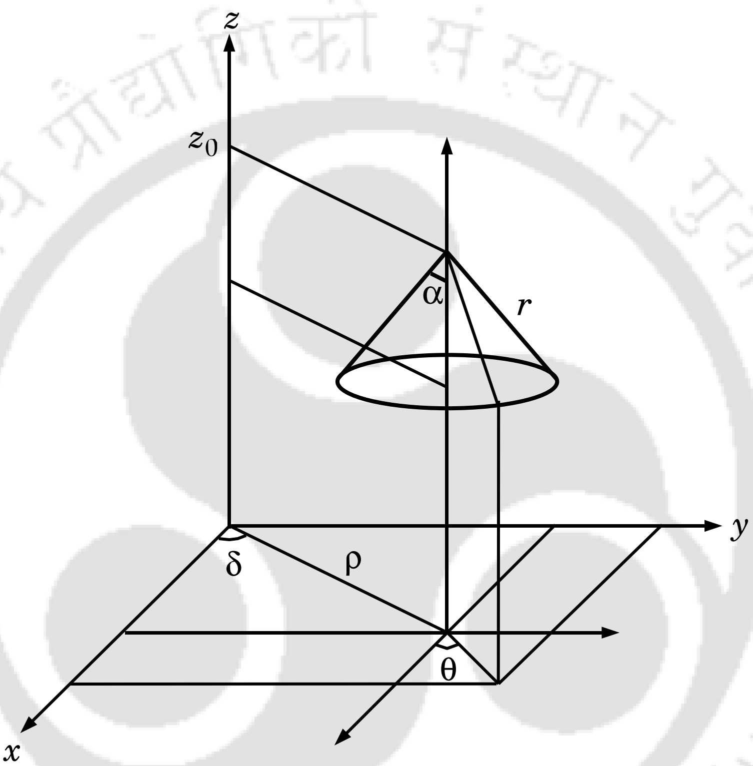

Figure C.1: Geometry of a cone in Cartesian coordinate.

Appendix D

The rigorous EBO equation for any three state BO system

When the point of CI between the first and the second state is separated by a distance from the CI between the second and the third state (**Model A**), the explicit form of rigorous EBO equation in terms of ADT/mixing angles is,

$$
\begin{aligned}
&- \frac{\hbar^2}{2m}\left(\vec{\nabla} + i\vec{\omega}_1\right)^2\phi_1 - \frac{\hbar^2}{2m}\Bigg(2\Bigg\{\frac{\sin\theta_{12}}{\cos\theta_{12}}\vec{\nabla}\theta_{12}\cdot\vec{\nabla}\phi_1 - \left(\frac{\nabla_p\theta_{23}}{\nabla_p\theta_{12}}\right)^{-1}\vec{\nabla}\left(\frac{\nabla_p\theta_{23}}{\nabla_p\theta_{12}}\right)\cdot\vec{\nabla}\phi_1 \\
&- \left[1 + \left(\frac{\nabla_p\theta_{23}}{\nabla_p\theta_{12}}\right)^2\right]^{\frac{1}{2}}\vec{\nabla}\left[1 + \left(\frac{\nabla_p\theta_{23}}{\nabla_p\theta_{12}}\right)^2\right]^{-\frac{1}{2}}\cdot\vec{\nabla}\phi_1\Bigg\} - 2\Bigg\{-\frac{\sin\theta_{12}}{\cos\theta_{12}}\vec{\nabla}\theta_{12} \\
&- \left(\frac{\nabla_p\theta_{23}}{\nabla_p\theta_{12}}\right)^{-1}\vec{\nabla}\left(\frac{\nabla_p\theta_{23}}{\nabla_p\theta_{12}}\right) - \left[1 + \left(\frac{\nabla_p\theta_{23}}{\nabla_p\theta_{12}}\right)^2\right]^{\frac{1}{2}}\vec{\nabla}\left[1 + \left(\frac{\nabla_p\theta_{23}}{\nabla_p\theta_{12}}\right)^2\right]^{-\frac{1}{2}}\Bigg\}^2\phi_1 \\
&+ \Bigg\{2(\vec{\nabla}\theta_{12})^2 + \frac{\sin\theta_{12}}{\cos\theta_{12}}\nabla^2\theta_{12} - \left(\frac{\nabla_p\theta_{23}}{\nabla_p\theta_{12}}\right)^{-1}\nabla^2\left(\frac{\nabla_p\theta_{23}}{\nabla_p\theta_{12}}\right) \\
&- \left[1 + \left(\frac{\nabla_p\theta_{23}}{\nabla_p\theta_{12}}\right)^2\right]^{\frac{1}{2}}\nabla^2\left[1 + \left(\frac{\nabla_p\theta_{23}}{\nabla_p\theta_{12}}\right)^2\right]^{-\frac{1}{2}} + 3\frac{\sin\theta_{12}}{\cos\theta_{12}}\left(\frac{\nabla_p\theta_{23}}{\nabla_p\theta_{12}}\right)^{-1}\vec{\nabla}\left(\frac{\nabla_p\theta_{23}}{\nabla_p\theta_{12}}\right)\cdot\vec{\nabla}\theta_{12} \\
&+ 3\frac{\sin\theta_{12}}{\cos\theta_{12}}\left[1 + \left(\frac{\nabla_p\theta_{23}}{\nabla_p\theta_{12}}\right)^2\right]^{\frac{1}{2}}\vec{\nabla}\left[1 + \left(\frac{\nabla_p\theta_{23}}{\nabla_p\theta_{12}}\right)^2\right]^{-\frac{1}{2}}\cdot\vec{\nabla}\theta_{12} \\
&- \frac{\sin\theta_{12}}{\cos\theta_{12}}\left(\frac{\nabla_p\theta_{23}}{\nabla_p\theta_{12}}\right)^{-1}\left[1 + \left(\frac{\nabla_p\theta_{23}}{\nabla_p\theta_{12}}\right)^2\right]^{\frac{1}{2}}\vec{\nabla}\left[1 + \left(\frac{\nabla_p\theta_{23}}{\nabla_p\theta_{12}}\right)^2\right]^{-\frac{1}{2}}\cdot\vec{\nabla}\theta_{23}\Bigg\}\phi_1 \\
&+ i\Bigg\{\frac{\sin\theta_{12}}{\cos\theta_{12}}\left[1 + \left(\frac{\nabla_p\theta_{23}}{\nabla_p\theta_{12}}\right)^2\right]^{\frac{1}{2}}(\vec{\nabla}\theta_{12})^2 - \left(\frac{\nabla_p\theta_{23}}{\nabla_p\theta_{12}}\right)^{-1}\left[1 + \left(\frac{\nabla_p\theta_{23}}{\nabla_p\theta_{12}}\right)^2\right]^{\frac{1}{2}}\vec{\nabla}\left(\frac{\nabla_p\theta_{23}}{\nabla_p\theta_{12}}\right)\cdot\vec{\nabla}\theta_{12} \\
&- \left[1 + \left(\frac{\nabla_p\theta_{23}}{\nabla_p\theta_{12}}\right)^2\right]\vec{\nabla}\left[1 + \left(\frac{\nabla_p\theta_{23}}{\nabla_p\theta_{12}}\right)^2\right]^{-\frac{1}{2}}\cdot\vec{\nabla}\theta_{12}\Bigg\}\phi_1\Bigg) + (u_1 - E)\phi_1 = 0,
\end{aligned}
$$

whereas the explicit form of the rigorous EBO for the **Model B** considering the CIs among the three BO states are at the same point:

$$
\begin{aligned}
-\; & \frac{\hbar^2}{2m}\Big(\vec{\nabla}+i\vec{\omega}_1\Big)^2\phi_1 - \frac{\hbar^2}{2m}\Bigg\{-2\Big[-\cos\theta_{12}\Big(\frac{\nabla_p\theta_{23}}{\nabla_p\theta_{12}}\Big)+\sin\theta_{12}\cos\theta_{23}\Big(\frac{\nabla_p\theta_{13}}{\nabla_p\theta_{12}}\Big)\Big]^{-1}\\
\times\; & \Big[\sin\theta_{12}\Big(\frac{\nabla_p\theta_{23}}{\nabla_p\theta_{12}}\Big)\vec{\nabla}\theta_{12}\cdot\vec{\nabla}\phi_1-\cos\theta_{12}\vec{\nabla}\Big(\frac{\nabla_p\theta_{23}}{\nabla_p\theta_{12}}\Big)\cdot\vec{\nabla}\phi_1+\cos\theta_{12}\cos\theta_{23}\Big(\frac{\nabla_p\theta_{13}}{\nabla_p\theta_{12}}\Big)\vec{\nabla}\theta_{12}\cdot\vec{\nabla}\phi_1\\
-\; & 2\Big[1+\Big(\frac{\nabla_p\theta_{13}}{\nabla_p\theta_{12}}\Big)^2+\Big(\frac{\nabla_p\theta_{23}}{\nabla_p\theta_{12}}\Big)+2\sin\theta_{23}\Big(\frac{\nabla_p\theta_{13}}{\nabla_p\theta_{12}}\Big)\Big]^{\frac{1}{2}}\\
\times\; & \vec{\nabla}\Big[1+\Big(\frac{\nabla_p\theta_{13}}{\nabla_p\theta_{12}}\Big)^2+\Big(\frac{\nabla_p\theta_{23}}{\nabla_p\theta_{12}}\Big)+2\sin\theta_{23}\Big(\frac{\nabla_p\theta_{13}}{\nabla_p\theta_{12}}\Big)\Big]^{-\frac{1}{2}}\cdot\vec{\nabla}\phi_1\\
+\; & 2\Bigg\{\Big[-\cos\theta_{12}\Big(\frac{\nabla_p\theta_{23}}{\nabla_p\theta_{12}}\Big)+\sin\theta_{12}\cos\theta_{23}\Big(\frac{\nabla_p\theta_{13}}{\nabla_p\theta_{12}}\Big)\Big]^{-1}\\
\times\; & \Big[\sin\theta_{12}\Big(\frac{\nabla_p\theta_{23}}{\nabla_p\theta_{12}}\Big)\vec{\nabla}\theta_{12}-\cos\theta_{12}\vec{\nabla}\Big(\frac{\nabla_p\theta_{23}}{\nabla_p\theta_{12}}\Big)+\cos\theta_{12}\cos\theta_{23}\Big(\frac{\nabla_p\theta_{13}}{\nabla_p\theta_{12}}\Big)\vec{\nabla}\theta_{12}\\
-\; & \sin\theta_{12}\sin\theta_{23}\Big(\frac{\nabla_p\theta_{13}}{\nabla_p\theta_{12}}\Big)\vec{\nabla}\theta_{23}+\sin\theta_{12}\cos\theta_{23}\vec{\nabla}\Big(\frac{\nabla_p\theta_{13}}{\nabla_p\theta_{12}}\Big)\Big]\\
+\; & \Big[1+\Big(\frac{\nabla_p\theta_{13}}{\nabla_p\theta_{12}}\Big)^2+\Big(\frac{\nabla_p\theta_{23}}{\nabla_p\theta_{12}}\Big)+2\sin\theta_{23}\Big(\frac{\nabla_p\theta_{13}}{\nabla_p\theta_{12}}\Big)\Big]^{\frac{1}{2}}\\
\times\; & \vec{\nabla}\Big[1+\Big(\frac{\nabla_p\theta_{13}}{\nabla_p\theta_{12}}\Big)^2+\Big(\frac{\nabla_p\theta_{23}}{\nabla_p\theta_{12}}\Big)+2\sin\theta_{23}\Big(\frac{\nabla_p\theta_{13}}{\nabla_p\theta_{12}}\Big)\Big]^{-\frac{1}{2}}\Bigg\}^2\phi_1\\
-\; & \Big[-\cos\theta_{12}\Big(\frac{\nabla_p\theta_{23}}{\nabla_p\theta_{12}}\Big)+\sin\theta_{12}\cos\theta_{23}\Big(\frac{\nabla_p\theta_{13}}{\nabla_p\theta_{12}}\Big)\Big]^{-1}\\
\times\; & \Big[\cos\theta_{12}\Big(\frac{\nabla_p\theta_{23}}{\nabla_p\theta_{12}}\Big)\big(\vec{\nabla}\theta_{12}\big)^2+2\sin\theta_{12}\vec{\nabla}\Big(\frac{\nabla_p\theta_{23}}{\nabla_p\theta_{12}}\Big)\cdot\vec{\nabla}\theta_{12}-\cos\theta_{12}\nabla^2\Big(\frac{\nabla_p\theta_{23}}{\nabla_p\theta_{12}}\Big)\\
-\; & \sin\theta_{12}\cos\theta_{23}\Big(\frac{\nabla_p\theta_{13}}{\nabla_p\theta_{12}}\Big)\big(\vec{\nabla}\theta_{12}\big)^2-2\cos\theta_{12}\sin\theta_{23}\Big(\frac{\nabla_p\theta_{13}}{\nabla_p\theta_{12}}\Big)\vec{\nabla}\theta_{12}\cdot\vec{\nabla}\theta_{23}\\
+\; & 2\cos\theta_{12}\cos\theta_{23}\vec{\nabla}\Big(\frac{\nabla_p\theta_{13}}{\nabla_p\theta_{12}}\Big)\cdot\vec{\nabla}\theta_{12}+\cos\theta_{12}\cos\theta_{23}\Big(\frac{\nabla_p\theta_{13}}{\nabla_p\theta_{12}}\Big)\nabla^2\theta_{12}\\
-\; & \sin\theta_{12}\cos\theta_{23}\Big(\frac{\nabla_p\theta_{13}}{\nabla_p\theta_{12}}\Big)\big(\vec{\nabla}\theta_{23}\big)^2-2\sin\theta_{12}\sin\theta_{23}\vec{\nabla}\Big(\frac{\nabla_p\theta_{13}}{\nabla_p\theta_{12}}\Big)\cdot\vec{\nabla}\theta_{23}\\
-\; & \sin\theta_{12}\sin\theta_{23}\Big(\frac{\nabla_p\theta_{13}}{\nabla_p\theta_{12}}\Big)\nabla^2\theta_{23}+\sin\theta_{12}\cos\theta_{23}\nabla^2\Big(\frac{\nabla_p\theta_{13}}{\nabla_p\theta_{12}}\Big)\Big]\phi_1\\
-\; & 2\Big[-\cos\theta_{12}\Big(\frac{\nabla_p\theta_{23}}{\nabla_p\theta_{12}}\Big)+\sin\theta_{12}\cos\theta_{23}\Big(\frac{\nabla_p\theta_{13}}{\nabla_p\theta_{12}}\Big)\Big]^{-1}\\
\times\; & \Big[1+\Big(\frac{\nabla_p\theta_{13}}{\nabla_p\theta_{12}}\Big)^2+\Big(\frac{\nabla_p\theta_{23}}{\nabla_p\theta_{12}}\Big)+2\sin\theta_{23}\Big(\frac{\nabla_p\theta_{13}}{\nabla_p\theta_{12}}\Big)\Big]^{\frac{1}{2}}
\end{aligned}
$$

$$
\begin{aligned}
\times\ & \left[\sin\theta_{12}\left(\frac{\nabla_p\theta_{23}}{\nabla_p\theta_{12}}\right)\vec{\nabla}\theta_{12} - \cos\theta_{12}\vec{\nabla}\left(\frac{\nabla_p\theta_{23}}{\nabla_p\theta_{12}}\right) + \cos\theta_{12}\cos\theta_{23}\left(\frac{\nabla_p\theta_{13}}{\nabla_p\theta_{12}}\right)\vec{\nabla}\theta_{12}\right. \\
-\ & \left.\sin\theta_{12}\sin\theta_{23}\left(\frac{\nabla_p\theta_{13}}{\nabla_p\theta_{12}}\right)\vec{\nabla}\theta_{23} + \sin\theta_{12}\cos\theta_{23}\vec{\nabla}\left(\frac{\nabla_p\theta_{13}}{\nabla_p\theta_{12}}\right)\right] \\
\cdot\ & \vec{\nabla}\left[1 + \left(\frac{\nabla_p\theta_{13}}{\nabla_p\theta_{12}}\right)^2 + \left(\frac{\nabla_p\theta_{23}}{\nabla_p\theta_{12}}\right) + 2\sin\theta_{23}\left(\frac{\nabla_p\theta_{13}}{\nabla_p\theta_{12}}\right)\right]^{-\frac{1}{2}}\phi_1 \\
+\ & \left[1 + \left(\frac{\nabla_p\theta_{13}}{\nabla_p\theta_{12}}\right)^2 + \left(\frac{\nabla_p\theta_{23}}{\nabla_p\theta_{12}}\right) + 2\sin\theta_{23}\left(\frac{\nabla_p\theta_{13}}{\nabla_p\theta_{12}}\right)\right]^{\frac{1}{2}} \\
\times\ & \nabla^2\left[1 + \left(\frac{\nabla_p\theta_{13}}{\nabla_p\theta_{12}}\right)^2 + \left(\frac{\nabla_p\theta_{23}}{\nabla_p\theta_{12}}\right) + 2\sin\theta_{23}\left(\frac{\nabla_p\theta_{13}}{\nabla_p\theta_{12}}\right)\right]^{-\frac{1}{2}}\phi_1 \\
-\ & i\left\{\left[-\cos\theta_{12}\left(\frac{\nabla_p\theta_{23}}{\nabla_p\theta_{12}}\right) + \sin\theta_{12}\cos\theta_{23}\left(\frac{\nabla_p\theta_{13}}{\nabla_p\theta_{12}}\right)\right]^{-1}\right. \\
\times\ & \left[1 + \left(\frac{\nabla_p\theta_{13}}{\nabla_p\theta_{12}}\right)^2 + \left(\frac{\nabla_p\theta_{23}}{\nabla_p\theta_{12}}\right) + 2\sin\theta_{23}\left(\frac{\nabla_p\theta_{13}}{\nabla_p\theta_{12}}\right)\right]^{\frac{1}{2}} \\
\times\ & \left[\sin\theta_{12}\left(\frac{\nabla_p\theta_{23}}{\nabla_p\theta_{12}}\right)(\vec{\nabla}\theta_{12})^2 - \cos\theta_{12}\vec{\nabla}\left(\frac{\nabla_p\theta_{23}}{\nabla_p\theta_{12}}\right)\cdot\vec{\nabla}\theta_{12} + \cos\theta_{12}\cos\theta_{23}\left(\frac{\nabla_p\theta_{13}}{\nabla_p\theta_{12}}\right)(\vec{\nabla}\theta_{12})^2\right. \\
-\ & \left.\sin\theta_{12}\sin\theta_{23}\left(\frac{\nabla_p\theta_{13}}{\nabla_p\theta_{12}}\right)\vec{\nabla}\theta_{12}\cdot\vec{\nabla}\theta_{23} + \sin\theta_{12}\cos\theta_{23}\vec{\nabla}\left(\frac{\nabla_p\theta_{13}}{\nabla_p\theta_{12}}\right)\cdot\vec{\nabla}\theta_{12}\right] \\
+\ & \left[1 + \left(\frac{\nabla_p\theta_{13}}{\nabla_p\theta_{12}}\right)^2 + \left(\frac{\nabla_p\theta_{23}}{\nabla_p\theta_{12}}\right) + 2\sin\theta_{23}\left(\frac{\nabla_p\theta_{13}}{\nabla_p\theta_{12}}\right)\right] \\
\times\ & \left.\vec{\nabla}\left[1 + \left(\frac{\nabla_p\theta_{13}}{\nabla_p\theta_{12}}\right)^2 + \left(\frac{\nabla_p\theta_{23}}{\nabla_p\theta_{12}}\right) + 2\sin\theta_{23}\left(\frac{\nabla_p\theta_{13}}{\nabla_p\theta_{12}}\right)\right]^{-\frac{1}{2}}\right\}\phi_1 \\
-\ & \left[-\cos\theta_{12}\left(\frac{\nabla_p\theta_{23}}{\nabla_p\theta_{12}}\right) + \sin\theta_{12}\cos\theta_{23}\left(\frac{\nabla_p\theta_{13}}{\nabla_p\theta_{12}}\right)\right]^{-1}\left[1 + \sin\theta_{23}\left(\frac{\nabla_p\theta_{13}}{\nabla_p\theta_{12}}\right)\right] \\
\times\ & \left[\cos\theta_{12}\left(\frac{\nabla_p\theta_{23}}{\nabla_p\theta_{12}}\right)(\vec{\nabla}\theta_{12})^2 + \sin\theta_{12}\vec{\nabla}\left(\frac{\nabla_p\theta_{23}}{\nabla_p\theta_{12}}\right)\cdot\vec{\nabla}\theta_{12} - \sin\theta_{12}\cos\theta_{23}\left(\frac{\nabla_p\theta_{13}}{\nabla_p\theta_{12}}\right)(\vec{\nabla}\theta_{12})^2\right. \\
-\ & \left.\cos\theta_{12}\sin\theta_{23}\left(\frac{\nabla_p\theta_{13}}{\nabla_p\theta_{12}}\right)\vec{\nabla}\theta_{12}\cdot\vec{\nabla}\theta_{23} + \cos\theta_{12}\cos\theta_{23}\vec{\nabla}\left(\frac{\nabla_p\theta_{13}}{\nabla_p\theta_{12}}\right)\cdot\vec{\nabla}\theta_{12}\right]\phi_1 \\
-\ & \cos\theta_{12}\sin\theta_{23}\left(\frac{\nabla_p\theta_{13}}{\nabla_p\theta_{12}}\right)\vec{\nabla}\theta_{12}\cdot\vec{\nabla}\theta_{23} + \cos\theta_{12}\cos\theta_{23}\vec{\nabla}\left(\frac{\nabla_p\theta_{13}}{\nabla_p\theta_{12}}\right)\cdot\vec{\nabla}\theta_{12}\Big]\phi_1 \\
+\ & \left[-\cos\theta_{12}\left(\frac{\nabla_p\theta_{23}}{\nabla_p\theta_{12}}\right) + \sin\theta_{12}\cos\theta_{23}\left(\frac{\nabla_p\theta_{13}}{\nabla_p\theta_{12}}\right)\right]^{-1} \\
\times\ & \left[\sin\theta_{23}\left(\frac{\nabla_p\theta_{23}}{\nabla_p\theta_{12}}\right) + \cos\theta_{12}\cos\theta_{23}\left(\frac{\nabla_p\theta_{13}}{\nabla_p\theta_{12}}\right)\right] \\
\times\ & \left.\left[-\cos\theta_{23}\left(\frac{\nabla_p\theta_{13}}{\nabla_p\theta_{12}}\right)\vec{\nabla}\theta_{12}\cdot\vec{\nabla}\theta_{23} - \sin\theta_{23}\vec{\nabla}\left(\frac{\nabla_p\theta_{13}}{\nabla_p\theta_{12}}\right)\cdot\vec{\nabla}\theta_{12}\right]\phi_1\right\} \\
+\ & (u_1 - E)\phi_1 = 0
\end{aligned}
$$

Appendix E

The Derivation of the $\omega(s,t)$ matrix

We start with the following equation

$$i\hbar\frac{\partial \boldsymbol{\omega}(s,t)}{\partial t} = \tilde{\mathbf{H}}(s,t)\boldsymbol{\omega}(s,t), \quad \text{(E.1)}$$

where $\tilde{\mathbf{H}}(s,t)$ are given by:

$$\tilde{\mathbf{H}}(s,t) = \mathbf{U}_{mk}(s,t) + \mathbf{u}_k(s)\delta_{mk}. \quad \text{(E.2)}$$

Writing Eq. (E.1) more explicitly we get

$$i\hbar\frac{\partial \boldsymbol{\omega}(s,t)}{\partial t} = \sum_{k=1}^{L}\big(\mathbf{U}_{mk}(s,t) + \mathbf{u}_k(s)\delta_{mk}\big)\boldsymbol{\omega}_{kj}(s,t), \qquad m = \{1, L\}, \qquad j = \{1, N\}. \quad \text{(E.3)}$$

In what follows we treat each column, namely, the jth column, separately. Each of these are solved in the same way but for a different set of initial conditions. Thus the initial values for the j column is a vector of zeros with 1 located at the jth position, namely, $(0, 0, \ldots, 1, 0, \ldots, 0)$.

To continue we perform the following transformation:

$$\boldsymbol{\omega}(s,t) = \exp\Big(-\frac{i}{\hbar}\mathbf{u}_m t\Big)\tilde{\boldsymbol{\omega}}_{mj}(s,t) \quad \text{(E.4)}$$

Substituting Eq. (E.4) in Eq. (E.3) yields the equations for the $\tilde{\boldsymbol{\omega}}$-matrix elements:

$$i\hbar\frac{\partial\tilde{\boldsymbol{\omega}}(s,t)}{\partial t} = \sum_{k=1}^{L}\mathbf{U}_{mk}(s,t)\exp\Big(-\frac{i}{\hbar}(\mathbf{u}_m-\mathbf{u}_k)t\Big)\tilde{\boldsymbol{\omega}}_{kj}(s,t), \qquad m=\{1,L\}. \tag{E.5}$$

Equation (E.5) is, in fact, the corresponding textbook set of equations.

Sometimes the diagonal elements $\mathbf{U}_{kk}(s,t)$ may become too large. Consequently, it is advisable to eliminate them while performing the following transformation:

$$\tilde{\boldsymbol{\omega}}(s,t) = \exp\Big\{\Big(-\frac{i}{\hbar}\int_0^t \mathbf{U}_{kk}(s,t)dt\Big)\Big\}\bar{\omega}_{kj}(s,t). \tag{E.6}$$

Substituting Eq. (E.6) in Eq. (E.5) yields

$$\begin{aligned}&\exp\left(-\frac{i}{\hbar}\int_0^t \mathbf{U}_{mm}(s,t)dt\right)\left(i\hbar\frac{\partial}{\partial t}+\mathbf{U}_{mm}(s,t)\right)\bar{\omega}_{mj}(s,t)\\ =&\sum_{k=1}^{L}\mathbf{U}_{mk}(s,t)\exp\left(\frac{i}{\hbar}(\mathbf{u}_m-\mathbf{u}_k)t\right)\exp\left(-\frac{i}{\hbar}\int_0^t \mathbf{U}_{kk}(s,t)dt\right)\bar{\omega}_{kj}(s,t)\delta_{jk}\end{aligned} \tag{E.7}$$

or

$$i\hbar\frac{\partial\bar{\omega}_{mj}(s,t)}{\partial t} = \sum_{k=1}^{L} Z_{mk}(s,t)\bar{\omega}_{kj}(s,t), \tag{E.8}$$

where $Z_{mk}(s,t)$ is given as

$$\begin{aligned}Z_{mk}(s,t) &= \mathbf{U}_{mk}(s,t)\Bigg[\exp\left(\frac{i}{\hbar}(\mathbf{u}_m(s)-\mathbf{u}_k(s))t\right)\\ &\times \exp\left(\frac{i}{\hbar}\int_0^t(\mathbf{U}_{mm}(s,t)-\mathbf{U}_{kk}(s,t))dt\right)-\delta_{km}\Bigg]\end{aligned} \tag{E.9}$$

or also

$$Z_{mk}(s,t) = \begin{cases}\mathbf{U}_{mk}(s,t)\exp\left(\frac{i}{\hbar}\int_0^t(\tilde{\mathbf{H}}_{mm}(s,t)-\tilde{\mathbf{H}}_{kk}(s,t))dt\right), & m\neq k\\ 0, & m=k\end{cases} \tag{E.10}$$

List of publications:

1. Quantum-classical dynamics of scattering processes in adiabatic and diabatic representations, Panchanan Puzari, Biplab Sarkar and Satrajit Adhikari, J. Chem. Phys. **121**, 707 (2004).

2. Quantum dynamics of inelastic scattering with a moving grid, Panchanan Puzari, Biplab Sarkar and Satrajit Adhikari, Int. J. Quantum Chem. **105**, 209 (2005).

3. A quantum-classical approach to the photoabsorption spectrum of pyrazine, Panchanan Puzari, R. S. Swathi, Biplab Sarkar and Satrajit Adhikari, J. Chem. Phys. **123**, 134317 (2005).

4. Matrix representation of vector potential: DVR and TDDVR formulation and dynamics, Panchanan Puzari, Biplab Sarkar and Satrajit Adhikari, Chem. Phys. **324**, 497 (2006).

5. Extended Born-Oppenheimer equation for a three-state system, Biplab Sarkar and Satrajit Adhikari, J. Chem. Phys. **124**, 014701 (2006).

6. The effect of cluster environment on a chemical reaction, Biplab Sarkar, Deepak K. S. Bhadauria, Nitin Verma and Satrajit Adhikari, Chem. Phys. **328**, 338 (2006).

7. A quantum-classical approach to the molecular dynamics of pyrazine with a realistic model Hamiltonian, Panchanan Puzari, Biplab Sarkar and Satrajit Adhikari, J. Chem. Phys. **125**, 194316 (2006).

8. Do intense electro-magnetic fields annihilate/create conical intersections? Biplab Sarkar, Satrajit Adhikari and Michael Baer, J. Chem. Phys. **126**, 014106 (2007).

9. Space-time contours to treat intense field-dressed molecular states. I. Theory, Biplab Sarkar, Satrajit Adhikari and Michael Baer, J. Chem. Phys. **127**, 014301 (2007).

10. Space-time contours to treat intense field-dressed molecular states. II. Applications, Biplab Sarkar, Satrajit Adhikari and Michael Baer, J. Chem. Phys. **127**, 014302 (2007).

11. A generalized formulation of extended Born-Oppenheimer equation for three-state system, Biplab Sarkar and Satrajit Adhikari, Int. J. Quantum Chem. (*in press*) (2008).

12. The curl equations for an induced Renner-Teller type model, Biplab Sarkar and Satrajit Adhikari, Indian J. Phys. **81**, 925 (2007).

13. Curl condition for a four-state Born-Oppenheimer system employing the Mathieu equation, Biplab Sarkar and Satrajit Adhikari, J. Phys. Chem. A DOI 10.1021/jp8029709 (2008).